

**High-Pressure Viscosity of Biodiesel, Diesel,
and Biodiesel-Diesel Blends: Experimental Data and Modeling**

By

Andrew M. Duncan

Submitted to the graduate degree program in Chemical and Petroleum Engineering and the Graduate Faculty of the University of Kansas in partial fulfillment of the requirements for the degree of Doctor of Philosophy.

Chairperson Susan M. Stagg-Williams

Kyle V. Camarda

Christopher D. Depcik

Aaron M. Scurto

Laurence R. Weatherley

Date Defended: 05/13/15

The Dissertation Committee for Andrew M. Duncan
certifies that this is the approved version of the following dissertation:

High-Pressure Viscosity of Biodiesel, Diesel,
and Biodiesel-Diesel Blends: Experimental Data and Modeling

Chairperson Susan M. Stagg-Williams

Date approved:

Abstract

Biodiesel was produced in excess of one billion gallons in the United States last year. It is sold as B100 (neat) and as a variety of blends. It is well known as a renewable fuel that reduces net carbon dioxide production, and other harmful emissions. Because much of the recent experimentation has involved biodiesel simply as a “drop in” fuel, its full, beneficial potential has not been reached. The ability to understand, model and predict important physical property behavior of current and potential fuels can lead to increased diesel engine performance, reduce harmful emissions further, and even improve fuel perception. High-pressure viscosity has been identified as one of the most important fuel properties of diesel fuel due to vehicle injectors creating pressures thousands of times greater than atmospheric. High-pressure viscosity measurements were performed for common biodiesels like those produced from soy and canola oils, but more exotic feedstocks like coconut and jatropha were also tested. Measurements were performed on dozens of fuels for temperatures between 278.15 and 373.15 K and pressures up to 131 MPa. Fuels were found to vary significantly from their ambient viscosities, and some were found to be more than 700 percent of their initial viscosity at the highest pressure tested. Blends were typically found to increase in viscosity with increasing blend fraction of biodiesel, however, this trend was shown to vary at low temperature and high pressure. Possible pressure freezing was found to occur for all biodiesel samples and for several high-percentage biodiesel blends at 283.15 K. Empirical models were developed as functions of temperature, pressure and blend percentage and were typically within the 95% confidence interval of the instrument.

Acknowledgements

I would first of all like to thank my committee members. I have had the privilege of working with each one of you either on research projects or as a GTA, and both in the case of Dr. Williams. I have been working for Dr. Williams since I was an undergraduate student, and I know that I could not have had a better mentor and example by her approach to research, teaching, and genuine care for her students.

Thanks to Dr.'s Azita Ahosseini, Ray Carter, and Karen Peltier for their help with equipment and analytical techniques. I would also like to thank undergraduate students Bah Pavlicek and Rachel Swezy for their exceptional dedication and assistance to my research.

A special thanks to Dr. Kirk Snavelly who was able to assist me, on countless occasions, with malfunctioning, broken or otherwise stubborn equipment.

I would lastly like to thank my parents for their support and wisdom over this long and sometimes arduous journey.

Additional Acknowledgements

Much of the work in several chapters has been taken directly from Energy & Fuels Published Works:

“Reprinted with permission from [Duncan, A. M.; Ahosseini, A.; McHenry, R.; Depcik, C. D.; Stagg-Williams, S. M.; Scurto, A. M., High-pressure viscosity of biodiesel from soybean, canola, and coconut oils. *Energy & Fuels* **2010**, 24, (10), 5708-5716.]. Copyright [2010] American Chemical Society

“Reprinted with permission from [Duncan, A. M.; Pavlicek, N.; Depcik, C. D.; Scurto, A. M.; Stagg-Williams, S. M., High-pressure viscosity of soybean-oil-based biodiesel blends with ultra-low-sulfur diesel fuel. *Energy & Fuels* **2012**, 26, (11), 7023-7036.]. Copyright [2012] American Chemical Society.”

Table of Contents

Title Page	i
Acceptance Page	ii
Abstract	iii
Acknowledgments	iv
Table of Contents	vi
List of Tables	xii
List of Figures	xiv
Chapter 1: Introduction	1
1.1: Overview: Biodiesel and Biodiesel Blends	1
1.2: Objectives	3
1.3: Dissertation Structure	3
References for Chapter 1	5
Chapter 2: Background	8
2.1: Biodiesel Composition	8
2.2: Biodiesel FAME Cloud Points	10
2.3: Biodiesel FAME Viscosities	12
2.4: Recent Works in High-Pressure Viscosity of Fuels	14
References for Chapter 2	17

Chapter 3: Experimental Methods	21
3.1.: Biodiesel Samples	21
3.2: Transesterification Reaction	21
3.2.1.: Lab Scale Reaction Procedure	22
3.2.2.: Five Gallon Reactions	24
3.3.: Biodiesel Characterization Methods	24
3.3.1.: FAME Composition Testing	24
3.3.2.: Kinetmatic Viscosity	25
3.3.3.: Density	25
3.3.4.: Cloud Point	26
3.3.5.: Oxidation Stability	26
3.3.6.: Higher Heating Value (Calorimetry)	27
3.4.: Diesel Samples	28
3.4.1.: Diesel Composition Testing	28
3.5.: Biodiesel Diesel Fuel Blending	29
3.6.: High-Pressure and Ambient Viscosity Measurement	29
3.6.1.: Viscometer Description	29
3.6.2.: Viscometer Experimental	31
References for Chapter 3	33
Chapter 4: High-Pressure Viscosity of Soybean, Canola, Coconut and ULSD	34
4.1.: Biodiesel Composition and ASTM Tests	35
4.2: Viscosity Correlation Method	36
4.3.: Ambient-Pressure Viscosity	38

.4.4: High-Pressure Viscosity	39
4.4.1.: Petroleum Derived Diesel	40
4.4.2.: Biodiesel from Canola Oil	44
4.4.3.: Biodiesel from Soybean Oil	50
4.4.4.: Biodiesel from Coconut Oil	52
4.4.5.: Comparison of the Diesel and Biodiesel Samples	54
4.5.: Ramifications of Data on Current and Future (Bio-)Diesel Engines and Designs	59
4.6.: Conclusions	59
References for Chapter 4	61
Chapter 5: High-Pressure Viscosity of Soybean Oil-Based Biodiesel	
Blends with Ultra Low Sulfur Diesel Fuel	63
5.1.: Viscosity Correlation Method	64
5.2: Ambient-Pressure Viscosity Results	65
5.3.: High-Pressure Viscosity	67
5.3.1.: Ultra Low Sulfur Diesel	67
5.3.2.: Soybean Biodiesel	70
5.3.3.: Biodiesel Blends	71
5.3.4.: B100 and Blends at Low Temperature	77
5.3.5.: Empirical and Extrapolated Crossover Pressures	81
5.4.: Ramifications on Current and Future (Bio-)Diesel Engines and Designs	83

5.5.: Conclusions	83
References for Chapter 5	85
Chapter 6: High-Pressure Viscosity	
of Jatropha Biodiesel and Biodiesel-Diesel Blends	87
6.1.: Biodiesel and Petroleum Diesel Samples	87
6.2.: Ambient-Pressure Viscosity	88
6.3.: High-Pressure Viscosity	89
6.3.1.: Jatropha Biodiesel and Tait-Litovitz Modeling	89
6.3.2.: Jatropha Biodiesel Comparison	92
6.3.3.: Jatropha and Soy Biodiesels	94
6.3.4.: Jatropha and Canola Biodiesels	95
6.3.5.: Normalized Viscosity of Jatropha and Other Biodiesels	98
6.4.: Jatropha Biodiesel Blends Comparison	100
6.5.: Jatropha Blends Mixing Rules	107
6.6.: Jatropha Biodiesel and Blends Cloud Point Pressures	109
6.7.: Conclusions and Ramifications	111
References for Chapter 6	112
Chapter 7: Biodiesel, Diesel and Biodiesel-Diesel Blends	
Using Normalized Viscosity Models	114
7.1.: Normalized Viscosity	114
7.2.: Biodiesel High-Pressure Viscosity Parameters	116
7.2.1.: Biodiesel Experimental-Predictive Viscosity Model Comparison	120
7.2.2.: Biodiesel Model Comparison to Literature	123
7.2.3.: Biodiesel Model Extrapolation Potential	126

7.3.: Diesel High-Pressure Parameters	128
7.3.1.: Diesel Model Comparison to Literature	130
7.4.: Biodiesel-Diesel Blends Model	133
7.4.1.: Biodiesel-Diesel Model with Known Mole Fractions and Ambient Pressure Viscosities	133
7.4.2.: Biodiesel-Diesel Blends Volume Fraction Model	135
7.4.3.: Biodiesel-Diesel Blends Volume Fraction Model Literature Comparison	136
7.4.4.: Biodiesel-Diesel Blends Volume Fraction Model At High Temperatures and Pressures	139
7.5.: Conclusions	140
References for Chapter 7	141
Chapter 8: Conclusions	143
8.1.: Biodiesel Comparisons to Diesel	143
8.2.: Biodiesel Comparisons by Feedstocks	144
8.3.: Biodiesel Blend Data Comparisons	145
8.4.: Biodiesel, Diesel and Biodiesel-Blend Modeling	146
References for Chapter 8	147
Chapter 9: Future Work and Recommendations	148
9.1.: Instrument Calibration	148
9.2.: Apparatus Additions	149
9.3.: Further Experiments with Saturated Fuels	150

Appendix A: Uncorrected High-Pressure Viscosity Data for	
Biodiesel, Diesel, and Biodiesel-Diesel Blends	151
Appendix B: High-Pressure Viscometer Consistency,	
Precision, and Comparison to Literature Data	276
Appendix C: Corrected High-Pressure Data for Biodiesel,	
Diesel and Biodiesel-Diesel Blends	322

List of Tables

- Table 2.1.** FAME compositions for several feedstocks in this dissertation.
- Table 2.2.** Recent high-pressure diesel and biodiesel viscosity works.
- Table 4.1.** Diesel and biodiesel samples and characteristic properties.
- Table 4.2.** Litovitz and Tait parameters regressed at each isotherm for diesel and biodiesel samples.
- Table 4.3.** Tait-Litovitz equation parameters and AARD%.
- Table 4.4.** Approximate cloud point pressure of the samples at 283.15 K.
- Table 5.1.** Diesel, biodiesel, and biodiesel blends physical properties.
- Table 5.2.** Litovitz and Tait parameters regressed at each isotherm for soybean biodiesel and diesel fuels.
- Table 5.3.** Tait-Litovitz equation parameters and AARD% for soybean biodiesel and diesel fuels.
- Table 5.4.** Tait-Litovitz model mixing comparison: Grunberg-Nissan and Kay's Rule AARD%.
- Table 5.5.** Mixing Rule Comparison: Grunberg-Nissan and Kay's Rule AARD%.
- Table 6.1.** Jatropha biodiesel composition.

Table 7.1. Tait parameters for biodiesel regressed for five isotherms.

Table 7.2. Biodiesel Tait linearized temperature parameters.

Table 7.3. Soybean-coconut oil biodiesel blend FAME composition.

Table 7.4. Absolute average relative deviations (AARD) and maximum deviations of all biodiesels tested.

Table 7.5. Tait 4 parameter model evaluation of soy, rape, and a soy-rape biodiesel blend from Freitas et al.

Table 7.6. Tait 4 parameter model evaluation of data from Bair.

Table 7.7. Diesel Tait linearized temperature parameters.

Table 7.8. Diesel statistics from our work using the Tait 4 parameter model.

List of Figures

Figure 2.1. Melting points for even-numbered saturated FAMES derived from Knothe and Dunn.

Figure 2.2. Melting points for cis-unsaturated C16 and C18 FAMES—derived from Knothe and Dunn.

Figure 2.3. Three parameter ambient-pressure viscosity correlations for several saturated FAMES derived from literature.

Figure 2.4. Three parameter ambient-pressure viscosity correlations derived from literature data for FAMES common to biodiesel.

Figure 3.1. Biodiesel reaction (RXN) apparatus.

Figure 4.1. Ambient-pressure viscosity with temperature for the No. 2 diesel and biodiesel samples. The lines represent the correlation from the Litovitz equation from parameters regressed from all data.

Figure 4.2. Viscosity with pressure for petroleum-based Diesel (No. 2) at four isotherms: 283.15 K, 298.15 K, 313.15 K, and 373.15 K. Lines represent Tait-Litovitz equation from temperature-dependent parameters regressed from all four isotherms.

Figure 4.3. Tait-Litovitz equation residuals from the diesel experimental data.

Figure 4.4. Viscosity with pressure for biodiesel from used canola oil at four isotherms: 283.15, 298.15K, 313.15 K, and 373.15 K and Tait-Litovitz model.

Figure 4.5. Tait-Litovitz equation residuals from the used canola oil sample.

Figure 4.6. Viscosity with pressure for biodiesel from used canola oil at 283.15 over a larger pressure range indicating a cloud point at approximately 83 MPa.

Figure 4.7. Viscosity with pressure for biodiesel from soybean oil at four isotherms: 283.15, 298.15K, 313.15 K, and 373.15 K with Tait-Litovitz model.

Figure 4.8. Viscosity with pressure for biodiesel from soybean oil and Vistive soybean oil at 313.15 K and 373.15.

Figure 4.9. Viscosity with pressure for biodiesel derived from Coconut oil at four isotherms: 283.15 K, 298.15 K, 313.15 K, and 373.15 K.

Figure 4.10. All fuels at 298.15 K.

Figure 4.11. All fuels at 373.15 K.

Figure 4.12. Comparison of viscosity with pressure for each of the samples at 283.15 K normalized to each sample's ambient-pressure viscosity with comparison to biodiesel correlation from pure sunflower oil from Robertson and Schaschke 2010.

Figure 5.1. Ambient-pressure viscosity with temperature for ULSD, B20 B60, and B100 from soybean oil at 283.15K, 298.15 K, 313.15 K, 343.15 K and 373.15 K.

Figure 5.2. Viscosity with pressure for ULSD at five isotherms: 283.15, 298.15, 313.15, 343.15, and 373.15 K.

Figure 5.3. Viscosity with pressure for B100 at five isotherms: 283.15, 298.15, 313.15, 343.15, and 373.15 K and Tait-Litovitz model.

Figure 5.4. Viscosity with pressure for ULSD, B100 and blends: B5, B10, B20, B40, B60, B80 at 298.15 K.

Figure 5.5. Viscosity with pressure for B20 at five isotherms: 283.15, 298.15, 313.15, 343.15, and 373.15 K with Tait-Litovitz model and Kay's mixing rule.

Figure 5.6. Viscosity with pressure for B80 at five isotherms: 283.15, 298.15, 313.15, 343.15, and 373.15 K with Tait-Litovitz model and Kay's mixing rule.

Figure 5.7. Normalized viscosity with pressure for soybean B20 and B100 at 283 K from this work, and literature correlations for sunflower B20 and B100 from Robertson and Schaschke.

Figure 5.8. Final viscosity measurement before possible cloud point pressure for several biodiesel blends at 283.15 K.

Figure 5.9. B0, B5, B10 and B20 at 283.15 K viscosity with pressure. Crossover pressures were found for B10 and B20 at ~69 MPa, and for B5 and B20 at ~100 MPa.

Figure 5.10. B0, B20, and B100 extrapolated (using the Tait-Litovitz model regressed for each isotherm) for pressures up to 300 MPa at 298.15 K. Several crossover pressures were identified.

Figure 6.1. Jatropha biodiesel (B100), ULSD (B0), and B20 blend viscosities at ambient pressure.

Figure 6.2. Viscosity as a function of pressure for jatropha biodiesel.

Figure 6.3. Residuals for the high-pressure viscosity of jatropha biodiesel and the Tait-Litovitz hybrid equation.

Figure 6.4. High pressure viscosity of biodiesels at 313.15 K.

Figure 6.5. High-pressure viscosity of biodiesels at 373.15 K.

Figure 6.6. High-pressure viscosity of biodiesels at 283.15 K.

Figure 6.7. High-pressure viscosity of Jatropha biodiesel and soybean biodiesels from literature at 313.15 K.

Figure 6.8. High-pressure viscosity of jatropha biodiesel and canola based biodiesels from literature at 313.15 K.

Figure 6.9. High-pressure viscosity of jatropha, canola and soy-based biodiesels at 283.15 K.

Figure 6.10. Normalized viscosity of biodiesels at 313.15 K.

Figure 6.11. Normalized viscosity of biodiesels at 373.15 K.

Figure 6.12. High-pressure viscosity of B20s at 313.15 K.

Figure 6.13. Normalized viscosity of B20s at 313.15 K.

Figure 6.14. High-pressure viscosity of B20s at 283.15 K.

Figure 6.15. Normalized viscosity of B20s at 283.15 K.

Figure 6.16. High-pressure viscosity of B5s at approximately 298 K.

Figure 6.17. Normalized viscosity of B5 blends at approximately 293 K.

Figure 6.18. High-pressure viscosity of B20 Jatropha with Kay's mixing rule.

Figure 6.19. Kay's mixing rule for jatropha B20 blend.

Figure 6.20. Grunberg-Nissan mixing rule for B20 blend.

Figure 6.21. Final viscosity measurement before possible cloud-point pressure for several biodiesel blends. The dashed lines indicate a possible parallel relationship between biodiesel feedstocks.

Figure 7.1. Normalized viscosity of alkanes at 62 MPa produced from literature.

Figure 7.2. Biodiesels and Tait model at 373.15 K using parameters from Table 7.1.

Figure 7.3. Biodiesels and Tait model at 283.15 K.

Figure 7.4. Experimental high-pressure viscosity of soy-coconut biodiesel with Tait 4 parameter model.

Figure 7.5. Normalized viscosity of literature biodiesel samples at 353.15 K with Tait 4 Parameter Model.

Figure 7.6. Normalized viscosity of literature biodiesel samples at 373.15 K with Tait 4 Parameter Model.

Figure 7.7. B100 literature data at high-pressure and temperature dashed lines are the Tait 4 parameter biodiesel model.

Figure 7.8. Normalized viscosity of the four diesels used in this work at 313.15 K with Tait 4 parameter model.

Figure 7.9. Normalized diesel model comparison to correlations from literature at 298.15 K.

Figure 7.10. Diesel fuels at 348 K with Tait 4 parameter model using parameters in Table 7.5.

Figure 7.11. High-pressure viscosity of Jatropha B20 with Tait biodiesel and diesel 4 parameter models and Kay's rule.

Figure 7.12. B5 biodiesel blends at 298 K using the overall volume model and ambient-pressure viscosity.

Figure 7.13. Palm B10 modeled with results from Eqn. 8.

Figure 7.14. Literature B20 with dashed lines using equation 9.

Chapter 1

Introduction

1.1 Overview: Biodiesel and Biodiesel Blends

According to the Energy Information Agency (EIA), the current production capacity of biodiesel in the United States is approximately 2 billion gallons per year with approximately 1.27 billion gallons of biodiesel produced in 2014¹. The increase in capacity and production are no doubt driven by the Renewable Fuels Standard Program requirements. The proposed requirement for 2015 from the EPA is 1.28 billion gallons of biomass-based diesel fuel². The majority of biodiesel, a biomass-based diesel fuel, in the United States is derived from soybean, canola, and corn oil, which comprises over 90 % of production in the United States³.

Biodiesel is produced through the transesterification reaction with methanol, usually in the presence of a base catalyst. In the course of the reaction, one triglyceride molecule, from a fat or an oil, is converted into three molecules of fuel (biodiesel) and one molecule of glycerol. Biodiesel is a mixture of fatty acid methyl esters, also known as FAMES. Biodiesel is commonly blended with petroleum diesel or used in its pure form as an alternative to petroleum diesel. Biodiesel from most feedstocks is classified as a renewable fuel and as such, significantly reduces green house gases (GHG) including carbon dioxide. The EPA performs a lifecycle analysis of potential fuels, and while most biodiesels surpass the 20% threshold of reduction⁴ palm biodiesel is a notable

exception. Palm biodiesel was estimated by the EPA to reduce green house gas emissions by only 17%, falling short in part due to the production of methane by the associated waste water⁵.

In addition to the net reduction of carbon dioxide production in biodiesel's life cycle, there are several advantages to using a biodiesel or biodiesel-diesel blend over petroleum-based diesel. The majority of harmful emissions are reduced, including sulfur dioxide, particulate matter, and various hydrocarbons⁶. Biodiesel and biodiesel blends are often used in diesel engines with relatively few modifications; however, many important fuel properties for atomization and combustion may change significantly. If injection parameters are not adjusted, fuel efficiency may decrease and unwanted emissions may increase.

An example of an increase in unwanted emissions is nitrogen oxides. NO and NO₂ otherwise known as NO_x, is often found in higher concentrations than what is produced by the combustion of diesel fuel. Part of the change in NO_x production relates to the inadvertent advancing of injection timing when using biodiesel caused by the rapid transfer of the pressure wave from the fuel injection pump to the fuel injector causing it to open earlier. While some researchers suggest that the increase in NO_x is from differences in injection timing due to the bulk modulus of the fuel⁷, others believe that it is the high-pressure viscosity that has a larger effect on atomization and combustion⁸⁻¹⁰.

Recalibration of engines based on blending of biodiesel with other fuels has resulted in the lowering of NO_x production in some studies^{11, 12}.

Diesel engine injection systems operate at high pressures, which have increased over the last few decades from an average of 80 MPa to 200 MPa found in today's vehicles¹³,¹⁴ with recent advances in common rail injection systems allowing for pressures as high as 300 MPa¹⁵. ***A detailed understanding of how the high-pressure viscosity of biodiesel and biodiesel-diesel blends compares with petroleum diesel fuel is necessary to improve engine performance and reduce harmful emissions as injection pressures increase.***

1.2 Objectives

The objectives for this work can be broken down into three main areas:

1. Accurately measure the viscosity of biodiesel, diesel and biodiesel-diesel blends for a wide range of temperatures and high pressures.
2. Identify trends and important differences between diesel and biodiesel.
3. Develop robust models for biodiesels, diesel, and their blends for a wide range of temperatures and pressures that are successfully predictive for potential fuels.

1.3 Dissertation Structure

Biodiesel compositional data, physical properties, and other relevant background information for biodiesel from several feedstocks are included in Chapter 2. Chapter 2 also includes the state of the art for high-pressure viscosity measurements of biodiesel

and biodiesel blends. The reaction methods for biodiesel production, fuel characterization, and high-pressure viscosity apparatus description and measurement procedure are contained in Chapter 3.

Chapters 4 through 6 contain the bulk of the experimental work covered in the dissertation. Chapter 4, sometimes referred to as the "*Feedstock Study*," compares biodiesels from soybean, Vistive (low-linolenic acid soybean), canola, used canola, and coconut oil to a sample of diesel fuel at four temperatures between 283.15 and 373.15 K and pressures up to 131 MPa.

Chapters 5 and 6 examine the high-pressure viscosity of soybean and jatropha biodiesel blends with diesel fuel for five temperatures between 283.15 and 373.15 K and pressures up to 131 MPa. Soybean biodiesel is one of the most widely used biodiesels in the United States; in Chapter 5 its blends: B5, B10, B20, B40, B60, and B80 are measured. While not well known in the United States, jatropha is viewed as a promising feedstock. Jatropha has a high oil yield and the ability to grow in poor conditions along with its inedible nature allow it to not directly compete with the food supply¹⁶. High-pressure viscosity measurements of jatropha biodiesel blends B5, B10, and B20 with diesel fuel are presented in Chapter 6.

Chapter 7 presents an empirical-predictive model for both pure biodiesel and biodiesel blends with petroleum diesel as a function of temperature, pressure, and blend fraction.

Additional data is presented for a soybean and coconut oil feedstock biodiesel at five temperatures between 283.15 and 373.15 K and pressures up to 131 MPa, and for palm oil biodiesel that has been blended with diesel for five temperatures between 278.15 and 298.15 K and pressures up to 131 MPa. Conclusions and recommendations for future work conclude the main body of work in Chapters 8 and 9.

The appendices follow Chapter 9 and include the raw viscosity data, and the methods used to make corrections, and the corrected data. At elevated temperatures and pressures correction factors are required for viscometer measurements. Uncorrected, referred to as *raw* viscosity, data for biodiesels, diesels, and biodiesel-diesel blends are given in Appendix A. Appendix B contains the methodology and correction factors used to calibrate the high-pressure viscometer, repeatability, and deviations from literature values for high-purity alkanes, dodecane and pentadecane. Appendix C contains the corrected data for biodiesels, diesels, and biodiesel-diesel blends.

References for Chapter 1

1. EIA, U.S. Energy Information Administration Monthly, Biodiesel Production Report. **May 2015**, Table 2.
2. EPA, EPA Proposes 2014 Renewable Fuel Standards, 2015 Biomass-Based Diesel Volume. **November 2013**, (EPA-420-F-13-048).
3. EIA, U.S. Energy Information Administration Monthly, Biodiesel Production Report. **May 2015**, Table 3.

4. Federal Register / Vol. 77, N. F., January 27, 2012 / Notices.
5. EPA, EPA Issues Notice of Data Availability Concerning Renewable Fuels Produced from Palm Oil Under the RFS Program. **December 2011**, (EPA-420-F-11-046).
6. Canakci, M.; Van Gerpen, J. H. In *The performance and emissions of a diesel engine fueled with biodiesel from yellow grease and soybean oil*, American Society of Agricultural Engineers, ASAE Annual International Meeting, Sacramento, California, USA, 2001; 2001.
7. Choi, C.; Bower, G.; Reitz, R. D. *Effects of biodiesel blended fuels and multiple injections on DI diesel engines*; SAE Technical Paper: 1997.
8. Arcoumanis, C.; Gavaises, M.; Yamanishi, M.; Oiwa, J. *Application of a FIE computer model to an in-line pump-based injection system for diesel engines*; SAE Technical Paper: 1997.
9. Rakopoulos, C.; Hountalas, D., A simulation analysis of a DI diesel engine fuel injection system fitted with a constant pressure valve. *Energy Conversion and Management* **1996**, 37, (2), 135-150.
10. Szybist, J. P.; Boehman, A. L. *Behavior of a diesel injection system with biodiesel fuel*; SAE Technical Paper: 2003.
11. Kegl, B.; Pehan, S., Influence of biodiesel on injection, fuel spray, and engine characteristics. *Thermal Science* **2008**, 12, (2), 171-182.

12. Lu, X.; Ma, J.; Ji, L.; Huang, Z., Simultaneous reduction of NO_x emission and smoke opacity of biodiesel-fueled engines by port injection of ethanol. *Fuel* **2008**, 87, (7), 1289-1296.
13. Mahr, B., Future and potential of diesel injection systems. In *Thermo-and Fluid Dynamic Processes in Diesel Engines 2*, Springer: 2004; pp 3-17.
14. Strotos, G.; Koukouvinis, P.; Theodorakakos, A.; Gavaises, M.; Bergeles, G., Transient heating effects in high pressure Diesel injector nozzles. *International Journal of Heat and Fluid Flow* **2015**, 51, 257-267.
15. Morgan, R.; Banks, A.; Auld, A.; Heikal, M. *The Benefits of High Injection Pressure on Future Heavy Duty Engine Performance*; 0148-7191; SAE Technical Paper: 2015.
16. Koh, M. Y.; Ghazi, T. I. M., A review of biodiesel production from *Jatropha curcas* L. oil. *Renewable and Sustainable Energy Reviews* **2011**, 15, (5), 2240-2251.

Chapter 2

Background

This chapter gives biodiesel composition profiles for the samples used in this work, pure component data and trends for ambient-pressure viscosities, and condensed state phase change data and trends for pure fatty acid methyl esters. Recent high-pressure viscosity data for biodiesel, diesel and biodiesel-diesel blends are also included.

2.1. Biodiesel Composition

Biodiesel is produced via the transesterification of fats and oils with methanol. The composition of the fat or oil feedstock determines the fatty acid methyl ester (FAME) profile and ultimately the chemical and physical properties of the resulting biodiesel. Only around a dozen FAMEs are typically found in significant quantities in all vegetal sources used to produce biodiesels. The majority of fatty acid chains are either saturated or unsaturated and between 6 and 22 carbons long, odd-numbered FAMEs are not often found in the feedstocks studied. A biodiesel from a single feedstock typically would not have significant amounts of more than ten FAMEs. The notation given in Table 2.1 is of the form CXX:Y, where XX is the number of carbon atoms in the fatty acid chain, and Y is the number of carbon-carbon double bonds in the fatty acid chain.

Table 2.1. FAME compositions for several feedstocks in this dissertation. Compositions were similar to what was found in a comprehensive review¹.

Sample	Coconut	Soybean	Vistive	Canola	Used Canola	Jatropha	Palm
FAME Composition by wt%.							
C6:0	0.3	-	-	-	-	-	-
C8:0	8.6	-	-	-	-	-	-
C10:0	6.3	-	-	-	-	-	-
C12:0	49.9	-	-	-	-	-	-
C14:0	17.9	0.2	-	-	-	-	-
C16:0	8.0	10.7	10.2	4.4	6.6	13.0	39.1
C16:1	-	-	-	-	-	0.5	-
C18:0	2.2	4.1	3.9	1.9	2.4	7.4	1.7
C18:1	5.4	21.4	23.7	63.5	53.4	43.9	50.2
C18:2	1.3	55.5	58.8	20.7	27.7	34.1	8.9
C18:3	-	8.0	2.8	8.5	8.9	-	-
C20:0	-	0.2	0.2	0.5	-	-	-
C22:0	-	-	0.2	0.2	-	-	-

The carbon number does not include the methyl group, for example, methyl oleate (C18:1), which is the primary FAME in canola oil (sometimes referred to as rapeseed oil) biodiesel has a single double bond in the chain, and 19 carbons with molecular formula $C_{19}H_{36}O_2$. Biodiesel produced from soybean and canola oils typically contains methyl ester profiles rich in oleate (C18:1) and linoleate (C18:2). Vegetal sources that are grown in warmer climates can have higher saturated fatty acid compositions (higher energy storage than unsaturated) as those compounds are still mobile at the plant's ambient conditions². Biodiesels from coconut oil, palm oil and jatropha oil have the highest amounts of saturated fatty acids. These differences in compositions affect all properties, most importantly cloud point and viscosity³⁻⁵.

2.2. Biodiesel FAME Cloud Points

Though biodiesel can be substituted for petroleum diesel in engines, biodiesel typically clouds at temperatures 10 to 15 degrees (K) higher than petroleum diesel^{6, 7}, and crystals that develop due to freezing of the fuel may cause problems with a vehicle's fuel filters and fuel lines⁸. Pure FAME melting point data from literature is given in Figure 2.1 and Figure 2.2. Figure 2.1 shows saturated FAMEs, of which C16:0 and C18:0 are the most common saturated FAMEs in soybean and canola oil.

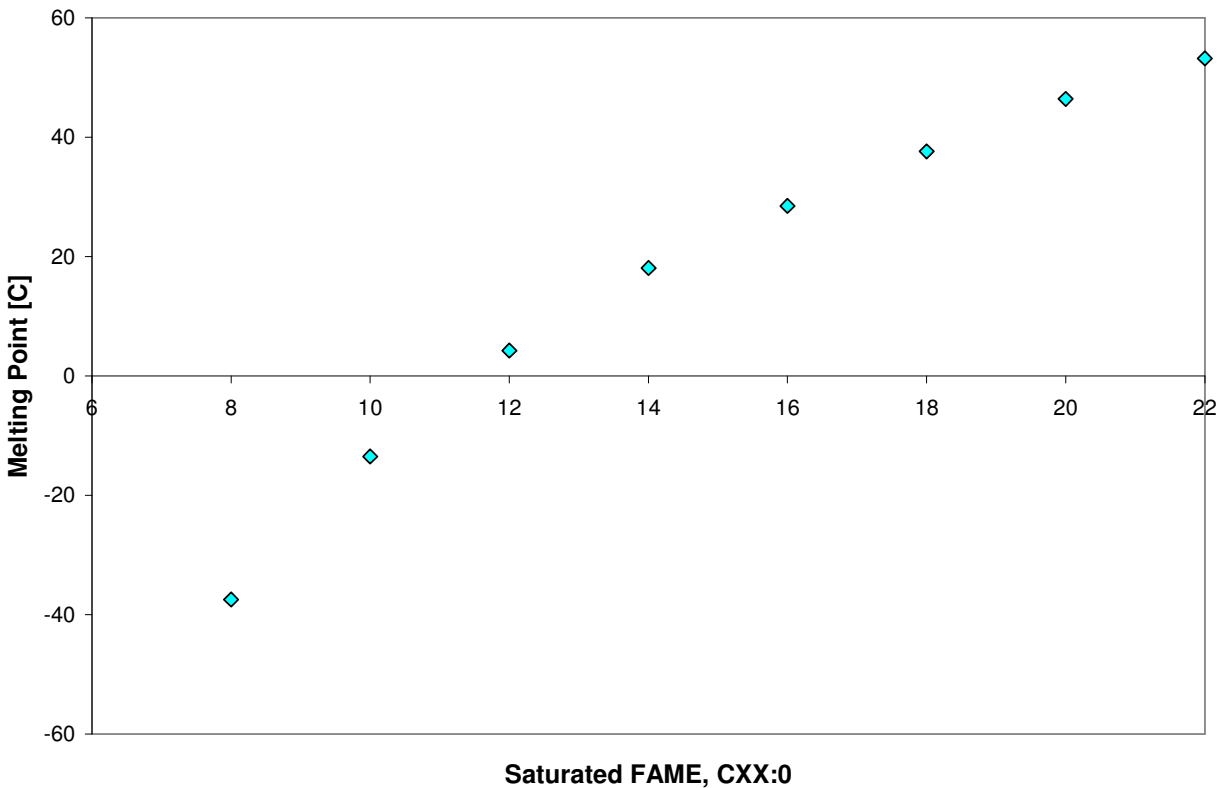


Figure 2.1. Melting points for even-numbered saturated FAMEs derived from Knothe and Dunn⁹.

Figure 2.2 shows that while there is an effective decrease in melting point with increasing chain length, one or two double bonds in the FAME chain has a greater effect.

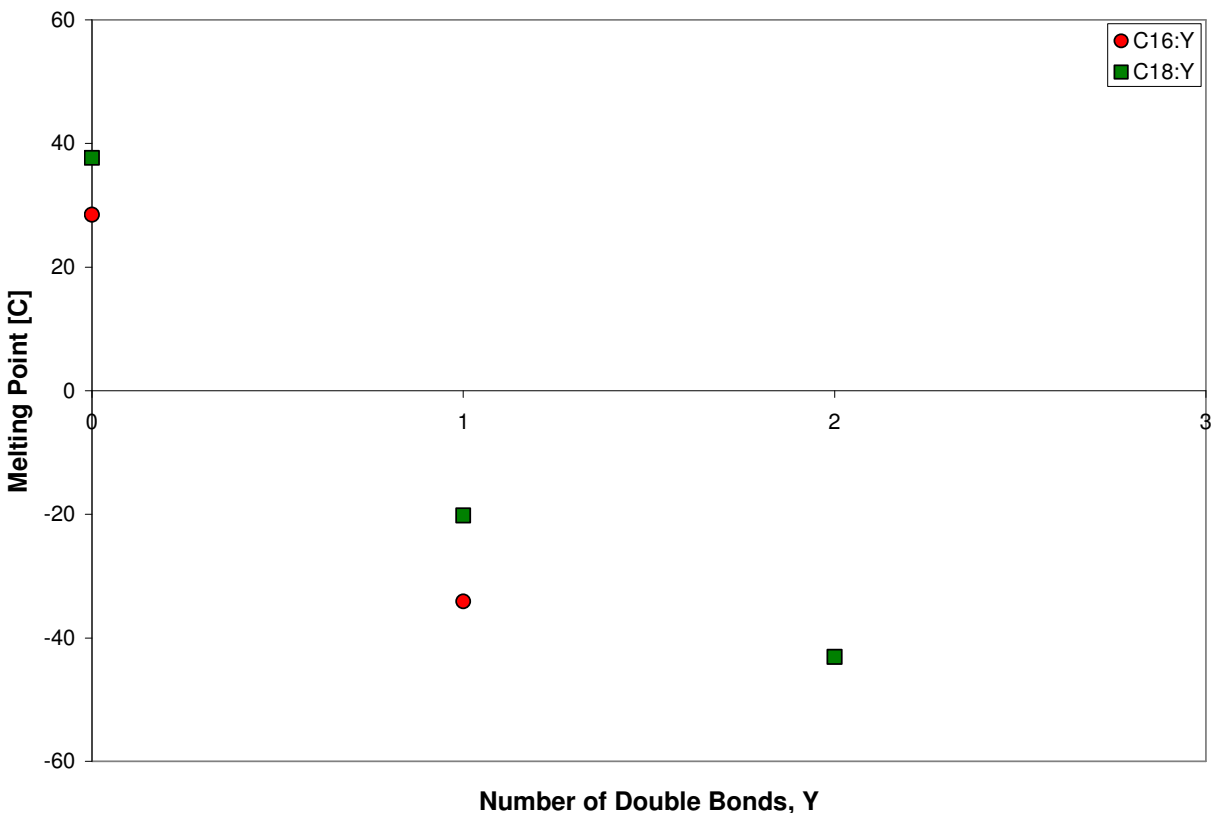


Figure 2.2. Melting points for cis-unsaturated C16 and C18 FAMEs—derived from Knothe and Dunn⁹.

Work from Imahara¹⁰ has shown that only small amounts of these long-chained, saturated FAMEs have a significant impact on cloud point. In a binary system containing methyl oleate (C18:1) and methyl stearate (C18:0) with an only 10% mole fraction of the saturated methyl stearate, the cloud point of the mostly unsaturated mixture was found to increase to approximately 283 K approximately 30 degrees higher than methyl oleate's melting point¹⁰. In this same work from Imahara, eutectic points were identified for saturated FAME mixtures and

unsaturated FAME mixtures, but in binary systems of one saturated and one unsaturated FAME there were no measurable eutectic points.

2.3. Biodiesel FAME Viscosities

Viscosity ordering among FAMEs is primarily affected by two types of molecular characteristics at ambient pressure. The first is chain length. Figure 2.3 gives even-numbered saturated FAMEs, which are common in biodiesels. Throughout the temperature range, *as chain length increases, so does viscosity*.

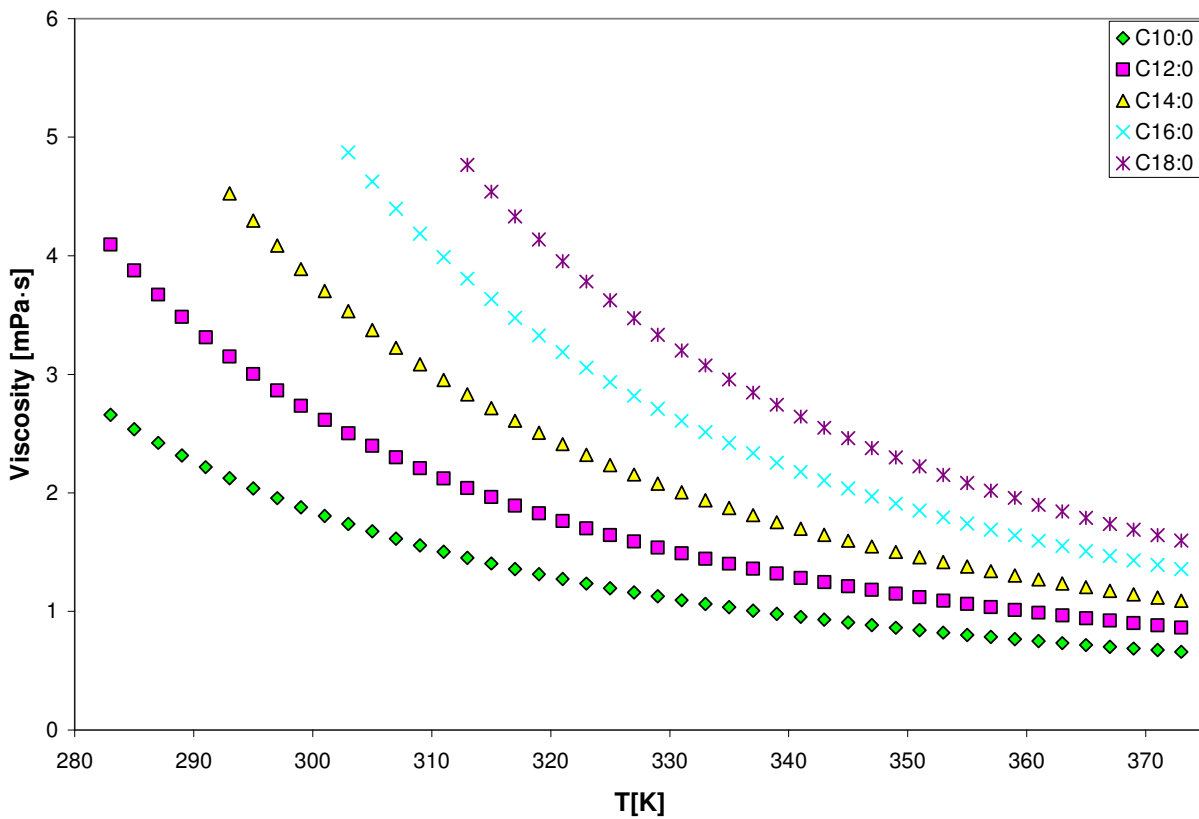


Figure 2.3. Three parameter ambient-pressure viscosity correlations for several saturated FAMEs derived from literature¹¹⁻¹⁸.

The second characteristic of FAMES that influence viscosity is the degree of unsaturation. Unsaturated fatty acids are in either cis or trans conformations. Transfats are the well known product of the partial hydrogenation used in food processing. Transfats were found only in very low quantities in GC/MS analysis for the samples used in this dissertation. Therefore, discussion of unsaturated FAMES if not specified will refer to cis isomers. In the components common to biodiesel *as the degree of unsaturation increases, the FAME viscosity decreases when chain length is held constant* as seen in Figure 2.4.

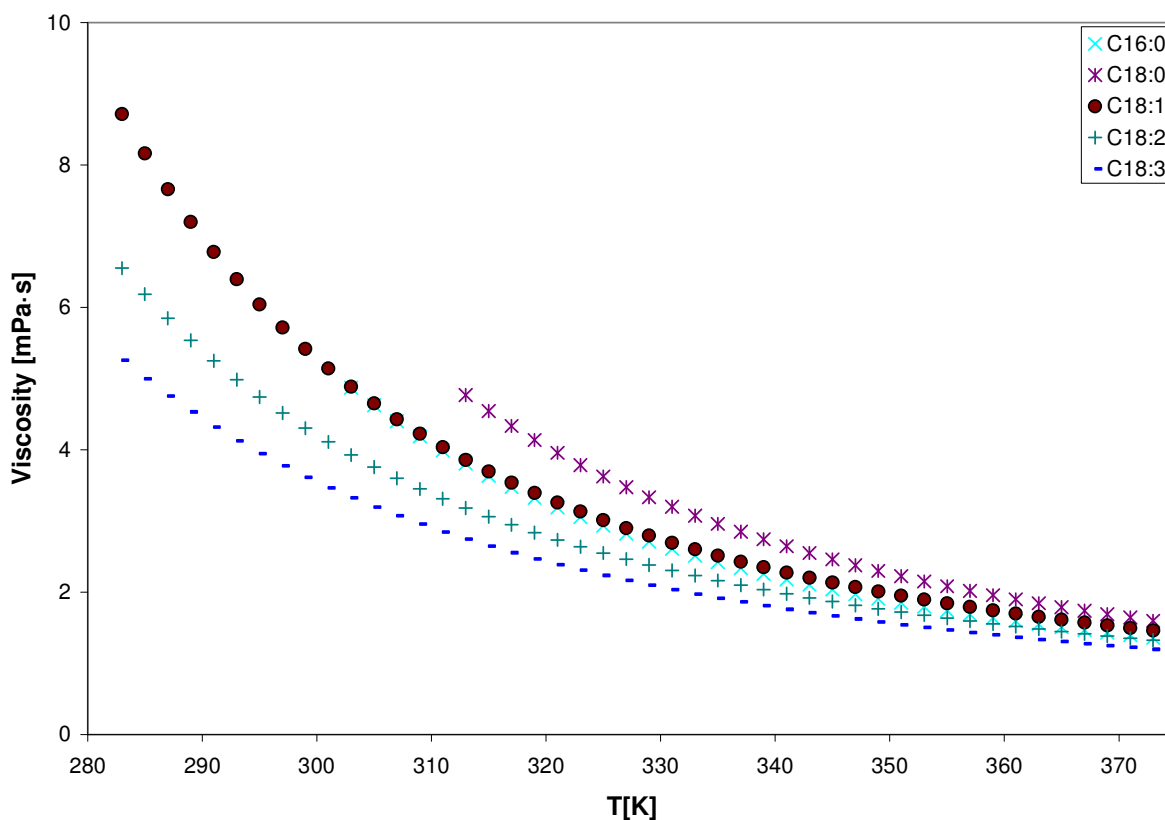


Figure 2.4. Three parameter ambient-pressure viscosity correlations derived from literature data¹¹⁻¹⁸ for FAMES common to biodiesel.

Interestingly, palmitic acid methyl ester, (C16:0), has a nearly equivalent pure component viscosity to methyl oleate, (C18:1) for much of the temperature range making one unsaturated site equivalent to the shorter FAME. This trend was not found to continue.

Most models find that ideal mixing rules are adequate when describing ambient-pressure viscosity of biodiesels at low pressure¹⁹. The contribution of a single FAME in low concentration does not have the same effect on viscosity as it can on cold flow behavior.

2.4. Recent Works in High-Pressure Viscosity of Fuels

The first high-pressure viscosity works in biodiesel and biodiesel blends was performed by Schaschke and coworkers²⁰⁻²². The method used required accurate knowledge of the high-pressure density of a liquid sample to compute the viscosity. The high-pressure density data for biodiesel was unavailable so using estimated critical properties and the Peng-Robinson equation of state, the density was calculated. Predicting accurate liquid densities from cubic equations of state is often difficult for long-chained hydrocarbons²³, and this may be the cause for the significant difference in the normalized biodiesel viscosity found in these initial works and ours and work from others²⁴⁻²⁶. The method by Schaschke and coworkers has since been improved, with the addition of a micro-pVT device used to determine density and higher a pressure range²⁷.

During the course of the work, and after the publication of our first two works^{25, 26}, additional authors have measured diesel and biodiesels in high-pressure systems. A summary of recent

works is given in Table 2.2. Comparisons to the more recent works are given in Chapters 6 and 7.

Table 2.2. Recent high-pressure diesel and biodiesel viscosity works.

Samples	Temperature Range	Pressure	Viscometer Type	Year	1st Author
Biodiesels from waste cooking oil, vegetable oil and petroleum diesel	293.15 K	up to 140 MPa	Falling sinker	2009	Paton ²⁰
Sunflower biodiesel, B20 blend	273-294 K	up to 153 MPa	Falling sinker	2010	Robertson ²¹
Canola, Jatropa, and Soapnut biodiesels	273-573 K	up to 7 MPa	Torsional oscillation resonance	2012	Chhetri ²⁸
Four diesels and B5 blend	298-373 K	up to 500 MPa	Falling sinker	2013	Schaschke ²⁷
Soybean, Rapeseed, and Soy/Rape blend biodiesels	293.15-393.15 K	up to 140 MPa	Vibrating wire	2014	Freitas ²⁹
Two diesels, Soybean biodiesel and B20 blend	313.15-433.15 K	up to 350 MPa	Falling cylinder	2014	Bair ²⁴
Methyl and Ethyl decanoate	293.15-353.15 K	up to 200 Mpa	Falling sinker & quartz resonator	2015	Habrioux ³⁰

References for Chapter 2

1. Hoekman, S. K.; Broch, A.; Robbins, C.; Cenicerros, E.; Natarajan, M., Review of biodiesel composition, properties, and specifications. *Renewable and Sustainable Energy Reviews* 2012, 16, (1), 143-169.
2. Haas, M. J., Animal fats. *Bailey's industrial oil and fat products* 2005.
3. Rodrigues, J.; Cardoso, F.; Lachter, E.; Estevão, L.; Lima, E.; Nascimento, R., Correlating chemical structure and physical properties of vegetable oil esters. *Journal of the American Oil Chemists' Society* 2006, 83, (4), 353-357.
4. Ramos, M.; Fernandez, C.; Casas, A.; Rodriguez, L.; Perez, A., Influence of fatty acid composition of raw materials on biodiesel properties. *Bioresource Technology* 2009, 100, (1), 261-268.
5. Knothe, G., Dependence of biodiesel fuel properties on the structure of fatty acid alkyl esters. *Fuel processing technology* 2005, 86, (10), 1059-1070.
6. Chandler, J. E.; Horneck, F. G. *The effect of cold flow additives on low temperature operability of diesel fuels*; Society of Automotive Engineers, 400 Commonwealth Dr, Warrendale, PA, 15096, USA: 1992.
7. McMillan, M.; Barry, E. *Fuel and Vehicle Effects on Low-Temperature Operation of Diesel Vehicles- the 1981 CRC Field Test*; Society of Automotive Engineers, 400 Commonwealth Dr, Warrendale, PA, 15096, USA: 1983.
8. Dunn, R.; Shockley, M.; Bagby, M., Improving the low-temperature properties of alternative diesel fuels: vegetable oil-derived methyl esters. *Journal of the American Oil Chemists' Society* 1996, 73, (12), 1719-1728.

9. Knothe, G.; Dunn, R. O., A comprehensive evaluation of the melting points of fatty acids and esters determined by differential scanning calorimetry. *Journal of the American Oil Chemists' Society* 2009, 86, (9), 843-856.
10. Imahara, H.; Minami, E.; Saka, S., Thermodynamic study on cloud point of biodiesel with its fatty acid composition. *Fuel* 2006, 85, (12), 1666-1670.
11. Allen, C. A.; Watts, K.; Ackman, R.; Pegg, M., Predicting the viscosity of biodiesel fuels from their fatty acid ester composition. *Fuel* 1999, 78, (11), 1319-1326.
12. Gros, A. T.; Feuge, R., Surface and interfacial tensions, viscosities, and other physical properties of some n-aliphatic acids and their methyl and ethyl esters. *Journal of the American Oil Chemists Society* 1952, 29, (8), 313-317.
13. Knothe, G.; Steidley, K. R., Kinematic viscosity of biodiesel components (fatty acid alkyl esters) and related compounds at low temperatures. *Fuel* 2007, 86, (16), 2560-2567.
14. Ceriani, R.; Gonçalves, C. B.; Rabelo, J.; Caruso, M.; Cunha, A. C.; Cavaleri, F. W.; Batista, E. A.; Meirelles, A. J., Group contribution model for predicting viscosity of fatty compounds. *Journal of Chemical & Engineering Data* 2007, 52, (3), 965-972.
15. Gouw, T.; Vlugter, J.; Roelands, C., Physical properties of fatty acid methyl esters. VI. Viscosity. *Journal of the American Oil Chemists' Society* 1966, 43, (7), 433-434.
16. Liew, K.; Seng, C.; Oh, L., Viscosities and densities of the methyl esters of some n-alkanoic acids. *Journal of the American Oil Chemists' Society* 1992, 69, (2), 155-158.
17. Bonhorst, C. W.; Althouse, P. M.; Triebold, H. O., Esters of naturally occurring fatty acids-physical properties of methyl, propyl, and isopropyl esters of C6 to C18 saturated fatty acids. *Industrial & Engineering Chemistry* 1948, 40, (12), 2379-2384.

18. Gouw, T.; Vlugter, J., Physical properties of fatty acid methyl esters. I. Density and molar volume. *Journal of the American Oil Chemists' Society* 1964, 41, (2), 142-145.
19. Freitas, S. V.; Pratas, M. J.; Ceriani, R.; Lima, A. S.; Coutinho, J. A., Evaluation of predictive models for the viscosity of biodiesel. *Energy & Fuels* 2010, 25, (1), 352-358.
20. Paton, J.; Schaschke, C., Viscosity measurement of biodiesel at high pressure with a falling sinker viscometer. *Chemical Engineering Research and Design* 2009, 87, (11), 1520-1526.
21. Robertson, L.; Schaschke, C., Combined high pressure and low temperature viscosity measurement of biodiesel. *Energy & Fuels* 2009, 24, (2), 1293-1297.
22. Schaschke, C.; Abid, S.; Heslop, M., High-pressure viscosity measurement of fatty acids and oils. *High Pressure Research* 2007, 27, (1), 33-37.
23. Mulero, A.; Cachadina, I., Liquid saturation density from simple equations of state. *International Journal of Thermophysics* 2007, 28, (1), 279-298.
24. Bair, S., The pressure and temperature dependence of volume and viscosity of four Diesel fuels. *Fuel* 2014, 135, 112-119.
25. Duncan, A. M.; Ahosseini, A.; McHenry, R.; Depcik, C. D.; Stagg-Williams, S. M.; Scurto, A. M., High-pressure viscosity of biodiesel from soybean, canola, and coconut oils. *Energy & Fuels* 2010, 24, (10), 5708-5716.
26. Duncan, A. M.; Pavlicek, N.; Depcik, C. D.; Scurto, A. M.; Stagg-Williams, S. M., High-pressure viscosity of soybean-oil-based biodiesel blends with ultra-low-sulfur diesel fuel. *Energy & Fuels* 2012, 26, (11), 7023-7036.

27. Schaschke, C.; Fletcher, I.; Glen, N., Density and viscosity measurement of diesel fuels at combined high pressure and elevated temperature. *Processes* 2013, 1, (2), 30-48.
28. Chhetri, A.; Watts, K., Densities of canola, jatropha and soapnut biodiesel at elevated temperatures and pressures. *Fuel* 2012, 99, 210-216.
29. Freitas, S. V.; Segovia, J. J.; Martín, M. C.; Zambrano, J.; Oliveira, M. B.; Lima, Á. S.; Coutinho, J. A., Measurement and prediction of high-pressure viscosities of biodiesel fuels. *Fuel* 2014, 122, 223-228.
30. Habrioux, M.; Bazile, J.-P.; Galliero, G.; Daridon, J. L., Viscosities of Fatty Acid Methyl and Ethyl Esters under High Pressure: Methyl Caprate and Ethyl Caprate. *Journal of Chemical & Engineering Data* 2015.

Chapter 3

Experimental Methods

The structure of this chapter is chronological. Oil or diesel sample description, biodiesel production methods, molecular composition techniques, ASTM standards and characterization methods, and finally high-pressure viscosity methodology are described.

3.1. Biodiesel Samples

All biodiesels used in this work were produced and tested at the University of Kansas. Both traditional soybean oils were Wesson Pure Natural Vegetable oil, the canola oil was Crisco Pure brand, and the Vistive low-linolenic soybean oil was ordered directly from Monsanto. The coconut oil was produced by Wilderness Family Naturals. The used canola oil was acquired from an on-campus dining facility and was filtered prior to the transesterification reaction in order to remove particulates. The soybean oil and coconut oil used for the equal mass blend were Wesson brand and Lou Ana respectively. The palm oil was ordered from Bulk Naturals, the jatropha oil was from AgroenhSA, Honduras, and the beef tallow was from Cargill Meat Solutions.

3.2. *Transesterification Reaction*

The biodiesel reactions were performed in two types of experiments. Lab scale reactions where typically, 250 mL vessels were used in the biodiesels produced in Chapters 4 and 5, as well as the soy-coconut blend presented in Chapter 7. In the soy-coconut blend a 1000 mL reactor was used, but with the same set up. Larger volume reactions were performed in a 5

gallon jacketed reactor from ChemGlass to produce the palm, jatropha, and beef tallow biodiesels.

3.2.1. Lab Scale Reaction Procedure

Soybean oil was reacted with 1% weight sodium methoxide catalyst and a 6:1 molar ratio of methanol. The methanol was from Fischer Scientific and was of 99% purity. A liquid catalyst used in reactions was 25% wt sodium methoxide in methanol from Sigma Aldrich. The reaction vessel was placed in a mineral oil bath with a magnetic stir bar to maintain homogenous mixing and temperature. As shown in Figure 3.1, the vessel and condenser setup was held in place using a ring stand and clamps. The mineral oil bath was placed on one of two types of magnetically stirred/hot plates.

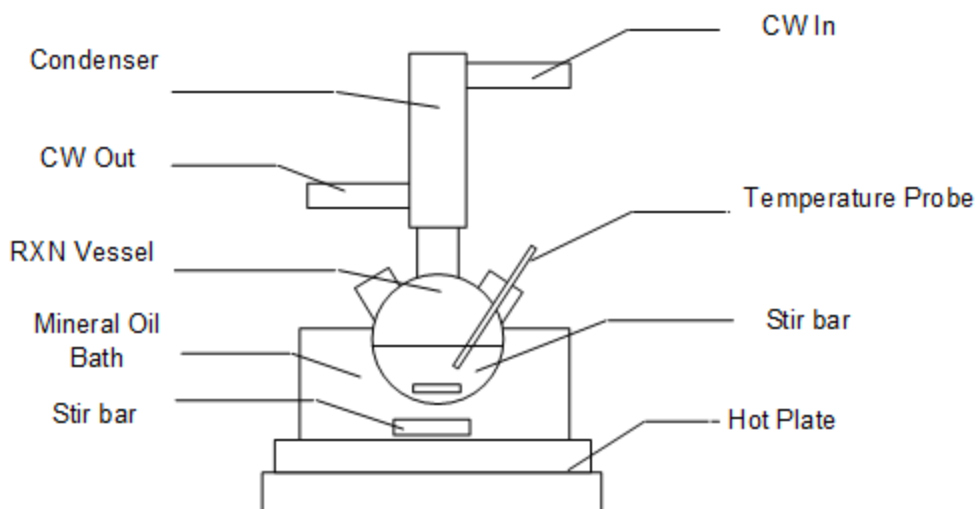


Figure 3.1. Biodiesel reaction (RXN) apparatus.

The majority of reactions involved the use of either a Thermo Scientific Super Nuova, or a Barnstead/Thermolyne Super Nuova controlled hot plate/magnetically stirred plate. The Super Nuova adjusted the hot plate temperature based on the set point and probe temperature. Other experiments were performed using a Barnstead/Thermodyne Cimarec hot/magnetic stir plate where the temperature was not controlled, but instead, adjusted manually. The hot/stir plates allowed for a variety of stir speeds. Stirring speeds in this study were typically 600 rpm to provide vigorous mixing of the multiple liquid phases. While stir bar size, vessel dimensions, molar ratio of methanol to oil and other factors will affect mass transfer, a study with similar apparatus dimensions found that 600 rpm would prevent the reaction from being mass-transfer limited¹. Oil was added to the reaction vessel, and allowed to reach the reaction temperature of 65 C before the addition of methanol and catalyst. The methanol and catalyst addition was either consecutive or concurrent. Reactions were 2 hours long for all samples except for the soy-coconut biodiesel reaction, which required 4 hours to allow for possible inadequate mixing due to the larger vessel size. After the transesterification reaction, the products from the reaction were poured from the reaction vessel into a separatory funnel. The products, primarily biodiesel and glycerol, were allowed to settle and separate for a minimum of 12 hours. Approximately 40 to 50 mL of deionized water was used to wash the biodiesel. The water was added through the top of the separatory funnel. With the top back on, the contents of the separatory funnel were mixed by quickly turning the funnel right-side up and upside-down between 5-15 times. The biodiesel and aqueous phases were allowed to settle for at least an hour, before the removal of the more-dense aqueous phase. The number of washes varied between 5 and 10 times. Wash steps were generally performed until the aqueous layer

was completely clear. Since water has some solubility in biodiesel, any remaining water in the biodiesel needs to be removed. To remove the remaining water, the biodiesel was added back to the reaction vessel and heated to 338.15 K. The condenser set up was removed and the only covered port was for the thermometer or temperature probe. Drying times were between 2 and 4 hours, at 600 rpm. The biodiesel was added back to a clean separatory funnel before samples were collected.

3.2.2. Five Gallon Reactions

Two types of reactions were performed in the 5 gallon reactor. Because of the high amount of free fatty acids in the jatropha oil, an esterification with methanol and an acid catalyst was performed prior to the transesterification reaction with the solid KOH catalyst. The jatropha oil was reacted for 2 hours with one percent weight sulfuric acid, based on the mass of oil, using a methanol oil ratio of 9:1 at 60 C. Jatropha, palm and tallow oils were reacted using sodium hydroxide solid catalyst at one percent weight based on the mass of oil. After glycerol removal, the biodiesel was washed with deionized water until the pH was approximately 7. The palm and tallow fuels were then dried at 105 C for 50 minutes. The jatropha biodiesel was dried at 65 C for two hours.

3.3. Biodiesel Characterization Methods

3.3.1. FAME Composition Testing

The FAME composition was determined using an Agilent 6890 Series GC system and a 5973 Network Mass Selective Detector and with MSD ChemStation Data Analysis Application

software. The column was an Agilent model 19091N-231 HP-INNOWax polyethylene glycol capillary column, which was capable of separating out methyl esters ranging from methyl hexanoate (C6:0) to lignoceric methyl ester (C24:0). Peaks were confirmed by comparison with FAME standards C6 (PN# 21599-1mL-F from Sigma-Aldrich), and FAME C8-C24 standards (#18918-1AMP, from Supelco). Ethyl stearate (PN# S8269-56 from Sigma-Aldrich) was used as an internal standard for determining the density of the methyl ester composition. However, once response factors were determined, the internal standard was not required to determine FAME weight percentage. Samples were run in triplicate, although data seldom varied by more than 1% composition among runs for a particular fuel.

3.3.2. Kinematic Viscosity

The kinematic viscosity of the samples at 313.15 K and atmospheric pressure was measured with a calibrated capillary viscometer using a Koehler KV4000 series kinematic viscosity bath according to ASTM Test Method D445. The calibration of the glass viscometers were periodically checked with calibration fluids. Experiments were typically performed in duplicate.

3.3.3. Density

Density measurements in Chapters 4 and 5 were found using an Anton Paar densitometer DMA 4500 with an uncertainty of $\pm 0.0001 \text{ g.cm}^{-3}$. Density measurements for all other work was performed using an Anton Paar DMA 5000 M with an improved uncertainty of $0.000005 \text{ g.cm}^{-3}$. The combination of accurate density and accurate mass measurements were vital to obtaining accurate blend fractions.

3.3.4. Cloud Point

Cloud point tests were performed in two ways, manually, and with an automated system. The cloud point test was performed according to ASTM standard D 2500-05 using a Koehler 5000 unit. Biodiesel samples of approximately 40 mL were required for each test. The biodiesel sample was poured into a glass cylinder before being sealed with a cork. A thermometer was placed through the center of the cork and to the bottom of the cylinder just above the glass. The sample was then placed in an ethanol bath that was kept at 0 C. Once the sample reached 9 C it was transferred to another ethanol bath kept at -18 C. The sample was checked for no more than 2-3 seconds to determine if a cloud had started to form. In general, crystals formed near the bottom of the test tube. The temperature at which a cloud was first seen was rounded to the nearest integer and recorded. The automated test was performed with a PAC CPP5Gs. While the automation was time-saving and often useful, samples that were very clear would often be cooled well below their cloud point, so visual inspection was required.

3.3.5. Oxidation Stability

The oxygenated nature of the compounds in biodiesel and exposure to air can lead to degradation and polymerization of biodiesel over time, effectively creating a shelf life for the fuel. Real time testing of a fuel's shelf life is impractical in a production-type setting. In order to approximate real-time fuel storage conditions, an oxidation stability test is performed to increase the rate at which the fuel breaks down. Oxidation stability testing is used to determine if adequate shelf life for a fuel will be attained. ASTM standard D6751 requires that an induction period of at least 3 hours be reached for biodiesel. Oxidation stability tests were performed using a Metrohm 873 Biodiesel Rancimat, in accordance with EN 14112. Tests were performed shortly after the transesterification reaction to give the best reading possible.

3.3.6. Higher Heating Value (Calorimetry)

The higher heating value (HHV) was measured using a Parr 6200 calorimeter. Sample amounts between 0.4 and 0.8 grams were added to a crucible, which was placed inside a Parr 1108 oxygen combustion bomb. The fuel was combusted and the heat was transferred from the bomb to a Parr 6510 Water Handling System that measured the increase in temperature for a specific volume of water. The change in water temperature was correlated to the higher heating value after being calibrated using solid benzoic acid pellets as a standard. After calibration, ten samples of the standard were tested. The average HHV was less than 0.1 Btu/lb from the benzoic acid standard of 11373 Btu/lb, with a standard deviation of 11.4 Btu/lb.

3.4. Diesel Samples

Diesel samples used in Chapters 4 and 5 (diesel 1 and diesel 2) were both No. 2 diesel with 15 ppm sulfur content (No. 2-D S15), and collected from a local gas station. Both samples were collected after the ASTM standard made it acceptable to add biodiesel to diesel without explicitly notifying the consumer in 2008². It is not known whether those samples contained biodiesel at less than 5%. Samples collected for later work, diesel 3 and diesel 4, were collected from a different local gas station, however, the supplier was contacted to verify that the ULSD did not contain any biodiesel.

3.4.1. Diesel Composition Testing

A simulated distillation (SIMDIS) method described by Stadler and Deo³ was used to determine the composition and average molecular weight of the ULSD. A Varian 3800 GC was used with a Restek MXT-2997 10 m, 2.65 μ m, 0.53 mm column and analyzed using Varian StarWS software. A sample volume of 1 μ L was injected using a Varian CP8410 auto-sampler and helium was used as the carrier gas. A flame ionization detector was used to detect the material eluted from the column. The detector temperature was set to 623.15 K while the injector temperature was set to 603.15 K. The initial oven temperature was 303.15 K and was held for two minutes before being increased at a rate of 15 K/min to 603.15 K. The oven temperature was held at 603.15 K for 18 minutes. N-tetradecane, n-pentadecane, n-hexadecane, and n-heptadecane from Supelco were used as internal standards.

3.5. Biodiesel Diesel Fuel Blending

Fuel blends were produced by combining biodiesel and ULSD by mass, which yields better precision than volumetric measurements. Because biodiesel-diesel blends are designated by volume fraction (for example B5 indicates five percent biodiesel by volume), the mass required for each blend was calculated using the densities of biodiesel and ULSD at 298.15 K. Fuels B5, B10, B20, B40, B60, B80, were blended in 500 mL glass Pyrex bottles.

3.6. High-Pressure and Ambient Viscosity Measurement

3.6.1. Viscometer Description

A Cambridge Applied Systems (currently Cambridge Viscosity, Inc. of PAC, L.P.) high-pressure viscometer was used for these measurements (ViscoPro 2000 System 4- SPL-440 with Viscolab software). This viscometer has been used in several published works in multiple laboratories^{4, 5}. The apparatus has been described in high detail in Ahosseini and Scurto including a detailed schematic⁶.

A series of electromagnets inside of the viscometer apply a force to the piston, which oscillates the piston in the viscometer chamber. The piston is situated at a 45 degree angle to prevent bubbles from collecting in the chamber. The viscometer uses the principles of annular flow around an axially oscillating piston⁷ and has been given an ASTM certification⁸. The sensor is capable of measurements from 0.2 to 10,000 mPa·s, at a maximum pressure of 137.9 MPa and in a temperature range of 233.15 K to 463.15 K. The digital display gives instantaneous readings for the piston's travel time up the chamber, and the piston's travel time down the chamber.

Based on the piston size, travel time, calibration drive level (CDL), and drive level (DL), a viscosity measurement is computed. A second menu screen gives the average viscosity of the previous 20 measurements and a value for standard deviation along with temperature and temperature deviation. A pressure gauge with units in PSI was mounted above the viscometer oven. The nominal uncertainty of the pressure gauge is 0.07% full-scale (FS=206.8 MPa); but the NIST-traceable calibration was accurate to 0.0084% full-scale. The maximum temperature for the pressure transducer was listed as 95 F, and a small fan was added for high-temperature runs.

The apparatus consists of a temperature-controlled oven (± 0.1 K) that houses the high-pressure viscometer sensor, a precision pressure transducer (PT), and a resistance temperature detector (RTD) (± 0.05 K). The viscometer is connected to a manual high-pressure syringe pump purchased from High Pressure Equipment Company (HIP) (Model No. 50-575-30; 30,000 psi, capacity of 18 cm^3 per stroke (with PolyPak) to pressurize the samples.

At ambient temperature and pressure, the diameter of the inner chamber is 0.314 inches. Three piston sizes are used according to the nominal viscosity range suggested by the manufacturer: 0.25-5 cP (0.3085 inch diameter), 1-20 cP (0.3055 inch diameter), and 2.5-50 cP (0.3025 inch diameter). The dimensions between the pistons and the inside of the viscometer cylinder, i.e. the annular flow geometry, vary with both temperature and pressure and are corrected by modified factory calibration algorithms for each piston. Significant work was performed to improve these corrections. Factory corrections attempted to account for changes

in temperature and pressure to the apparatus annulus, but assumed they were independent of each other. Through a wide range of temperature and pressure measurements using alkanes and calibration fluids, more accurate corrections were developed. The raw data, which does not include any corrections is given in Appendix A, the methodology, instrument repeatability, and comparisons to literature can be found in Appendix B, and the corrected data is found in Appendix C. Based on a repeatability investigation and comparison to literature, presented in Appendix B, the uncertainty of the instrument is estimated to be 3.3%.

3.6.2. Viscometer Experimental

Viscosities were recorded manually after allowing the standard deviation of 20 measurements to reach a steady measurement. This manually recorded data is the “raw data” in Appendix A. The raw data given in Appendix A gives the piston used for each sample, but typically the 5 cP was used for 373.15 K, the 20 cP piston was used for 313.15 and 343.15 K, and the 50 cP piston was used for 278.15, 283.15, and 298.15 K. Over 99% of data taken had a standard deviation equal to or less than 0.3% of the displayed viscosity measurement. Those data with standard deviations greater than 0.3% are specified in both Appendix A and Appendix C.

Pressure was increased by 1000 psi (~6.9 MPa) increments; a new value would typically take 5 minutes to be reached. Increasing viscosity was associated with increasing piston travel time, and some measurements would take as much as 30 to 60 minutes to reach the required 0.3% standard deviation.

Isotherms greater than ambient temperature (313.15, 343.15, and 373.15) were controlled by the oven, however, the oven set point was sensitive to one degree, so temperature needed to be constantly adjusted manually. For example, for data at 373.15 K, the oven temperature needs to be at 100 C for 7 minutes and 101 C for 3 minutes to maintain 100.0 C on the viscometer readout. Typically, two to three hours were required to reach the desired temperature for testing.

A Fisher Isotemp chiller was used for samples at ambient temperature and below. Plastic tubing with a water / antifreeze mixture flowing through it was wrapped around the entirety of the viscometer body and then covered with several layers of Parafilm to act as an insulator. During operation, the chiller temperature was set below the required viscometer operation temperature. A lower chiller set point was required due to losses to the environment and because the viscometer itself produces heat during operation. The chiller was set to approximately 22 C for measurements of 25 C, 2 C for measurements of 10 C, and -8 C for 5 C isotherms. The required chiller temperature would vary only slightly with laboratory temperature. Additional work should be performed to verify the uncertainty of viscosity measurements at low temperatures due to the increased temperature gradient.

Prior to testing a new sample, approximately 100 mL of sample would be sent through to purge the high-pressure circuit, approximately five times the system volume. After significant testing, this procedure was found to give reliable results to remove any residual solvent or sample that had been used previously. Samples were removed from the system by flowing 2 or 3 times the

system volume of acetone through, followed by the operation of a vacuum pump to remove the high-volatility solvent. The high-pressure generator was operated manually. Pressure was increased or decreased at a rate no greater than 1000 psi / min to prevent damage to the apparatus.

References for Chapter 3

1. Zhao, L., Novel solid base catalysts for the production of biodiesel from lipids. **2010**.
2. Testing, A. S. f.; Materials, ASTM D975, Standard Specification for Diesel Fuel Oils. In ASTM International West Conshohocken, PA: 2011.
3. Stadler, M.; Deo, M. In *Crude Oil Characterization Using Gas Chromatography and Supercritical Fluid Chromatography*, 1993; 1993.
4. Laesecke, A.; Cousins, D. S., Wide-Ranging Viscosity Measurements of Rocket Propellant RP-2. *Journal of Propulsion and Power* **2013**, 29, (6), 1323-1327.
5. Rajagopal, K.; Andrade, L. L.; Paredes, M. L., High-Pressure Viscosity Measurements for the Binary System Cyclohexane+ n-Hexadecane in the Temperature Range of (318.15 to 413.15) K[†]. *Journal of Chemical & Engineering Data* **2009**, 54, (10), 2967-2970.
6. Ahosseini, A.; Scurto, A. M., Viscosity of Imidazolium-Based Ionic Liquids at Elevated Pressures: Cation and Anion Effects. *Int. J. Thermophys.* **2008**, 29, 1222-1243.
7. Bird, R. B.; Stewart, W. E.; Lightfoot, E. N., *Transport Phenomena*. John Wiley & Sons, Inc.: New York, NY, 1960.
8. *ASTM D7483 - 08 Determination of Dynamic and Kinematic Viscosity of Liquids by Oscillating Piston Viscometer.*; 2008.

Chapter 4

High-Pressure Viscosity of Soybean, Canola, Coconut and ULSD

In this Chapter, we attempt to quantify how the vegetal oil source and resultant fatty-acid methyl ester (FAME) profile affects the ultimate biodiesel high-pressure viscosity. The viscosity for five different types of biodiesel has been measured under high pressures (up to 131 MPa) and at four temperatures (283.15 K, 298.15 K, 313.15 K, and 373.15 K). The five biodiesel samples were derived from a variety of sources including: two types of soybean oil; fresh (unused) canola oil and from canola oil that was used as a cooking oil; and coconut oil. The soybean samples are from oils of both common soybeans and Vistive, which is Monsanto's soybean variety that is lower in linolenic acid. In addition, the viscosity of No. 2 petroleum diesel (No. 2-D S15) under pressure was measured for comparison to the biodiesel samples. The Litovitz equation combined with the Tait equation^{1, 2} were used to describe the viscosity of biodiesel as a function of pressure and temperature. The Figures and Tables have been changed from the published version to reflect the newest and best calibration. The average correction was 1.04%, with the most significant correction applied to the 5 cP piston, resulting in an 8% change in viscosity for the maximum pressure tested at 373.15 K.

4.1 Biodiesel Composition and ASTM Tests

As seen from the properties listed in Table 4.1, the biodiesel samples had FAME profiles similar to what was expected based on typical soybean³, canola³, and coconut oil⁴ feedstocks.

Table 4.1. Diesel and Biodiesels samples and characteristic properties.

Sample	Coconut	Soybean	Vistive	Canola	Used Canola	No. 2 Diesel
Kinematic Viscosity						
at 313.15 K [cSt]	4.02	2.61	4.47	4.12	4.47	2.52
Density at 313.15 K [g/cm ³]	0.8674	0.8554	0.8649	0.8665	0.8663	0.8278
Cloud Point [K]	270.15	275.15	273.15	273.15	272.15	-
Composition						
% Methyl Esters:						
C6:0	0.3	-	-	-	-	-
C8:0	8.6	-	-	-	-	-
C10:0	6.3	-	-	-	-	-
C12:0	49.9	-	-	-	-	-
C14:0	17.9	0.2	-	-	-	-
C16:0	8.0	10.7	10.2	4.4	6.6	-
C18:0	2.2	4.1	3.9	1.9	2.4	-
C18:1	5.4	21.4	23.7	63.5	53.4	-
C18:2	1.3	55.5	58.8	20.7	27.7	-
C18:3	-	8.0	2.8	8.5	8.9	-
C20:0	-	0.2	0.2	0.5	-	-
C22:0	-	-	0.2	0.2	-	-

The soybean oils were highest in linoleic with moderate amounts of oleic acid. The Vistive soybean oil biodiesel contained approximately 3% linolenic methyl ester compared to about 8% linolenic methyl ester in traditional soybean oil feedstock biodiesel. The two canola oils had similar compositions, but varied slightly in the composition of oleic acid methyl ester and

linoleic acid methyl ester, with the used oil sample having slightly less oleic and slightly more linoleic acid methyl ester.

The acceptable range for kinematic viscosity of biodiesel at 313.15 K based on ASTM D 6751 is between 1.9 and 6 cSt. The kinematic viscosities for all biodiesels tested were within this acceptable range. ASTM standard D975 for viscosity of No. 2 diesel is between 1.9 and 4.1 cSt. The diesel used in these experiments is within this specification. ASTM D 6751 for cloud point specifies only that the value be reported.

4.2 Viscosity Correlation Method

Various theoretical models and empirical expressions can be found in the literature to represent the viscosity of liquids (η) as functions of pressure and temperature. Litovitz^{5, 6} has suggested an empirical equation, which has been used at a single pressure over wide temperature ranges:

$$\eta = A \exp(B / RT^3) \quad \text{Eqn. [1]}$$

where R is the gas constant and A and B are fitted parameters. The Tait equation is well-known to represent the pressure-volume-temperature relationship of many liquids^{1, 2}. Tammann modified the Tait equation¹ to:

$$\frac{(V_0 - V)}{V_0} = C \log\left(\frac{B + P}{B + 0.1}\right) \quad \text{Eqn. [2]}$$

where \underline{V}_0 and \underline{V} represent the molar volume at ambient pressure and under pressure P ; C and B are adjustable constants. The modified equation has become widely accepted to represent high-pressure density data for liquids and liquid mixtures.

In a similar manner, the Tait equation has been used to correlate the pressure dependence of viscosity²:

$$\ln\left(\frac{\eta_p}{\eta_o}\right) = E \ln\left(\frac{D+P}{D+0.1}\right) \quad \text{Eqn. [3]}$$

where η_p and η_o are the viscosities at a pressure P and at 0.1 MPa, respectively. This equation contains only two fitted parameters and has yielded good correlation with experimental data as shown by Kashiwagi and Makita² for aromatic hydrocarbons and cyclohexane up to 110 MPa.

This investigation will use a hybrid Tait-Litovitz equation at elevated pressures for the viscosity data for a series of biodiesels:

$$\eta_p = A \exp(B'/T^3) ((D+P)/(D+0.1))^E$$

$$B' = B/R \quad \text{Eqn. [4]}$$

The Litovitz parameters are fit to the relatively easy to obtain ambient-pressure viscosity data. Then, the Tait parameters are fit to the high-pressure data. The aforementioned equation has the advantages of containing fewer fitting parameters (A , B , D , E) than other models and simplicity of data analysis. This equation has successfully modeled high-pressure viscosity data of imidazolium ionic liquids⁷. Data regression was performed using a Gauss-Newton non-linear method. Athena Visual Studio, using non-linear least squares or Bayesian estimation, was used to fit the temperature-linearized models, which required additional parameters.

4.3 Ambient-Pressure Viscosity

The ambient-pressure viscosity of the five biodiesel samples and one petroleum diesel sample were measured with a Cambridge Viscosity, Inc. viscometer described in Chapter 3. The data are tabulated in Tables C.1 through C.6 in Appendix C. Figure 4.1 illustrates the exponential decrease of viscosity with temperature for diesel, and biodiesels from soybean, canola, and coconut oil in a manner consistent with Litovitz behavior.

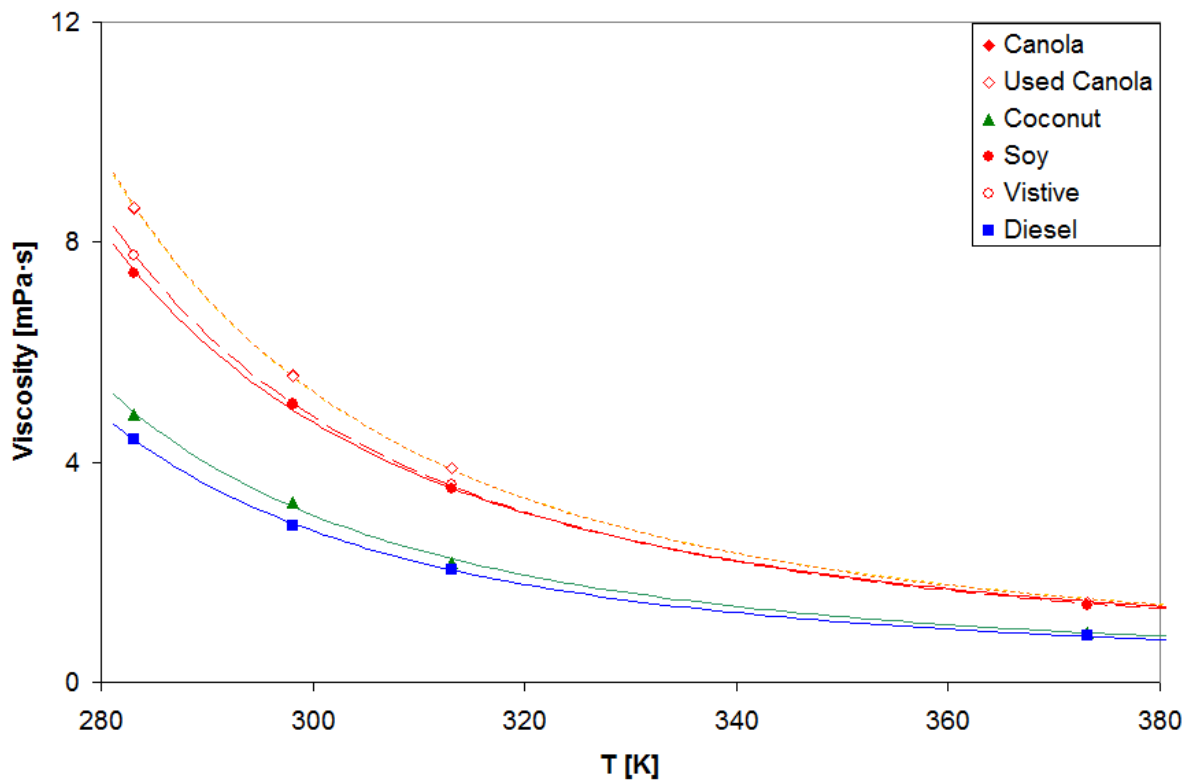


Figure 4.1. Ambient-pressure viscosity with temperature for the No. 2 diesel and biodiesel samples. The lines represent the correlation from the Litovitz equation from parameters regressed from all data.

In general, the viscosity of the various samples at higher temperatures falls into two groups. No. 2 diesel and biodiesel from coconut oil become very similar with their lower viscosity compared to the second group comprised of all of the other biodiesel samples. The ambient-pressure trends for all isotherms are generally, in the order of increasing viscosity: diesel < coconut < soybean < vistic < canola ~ used canola. This is in close agreement with Allen⁸ who had similar trends at 313.15 K for soybean, canola, and coconut derived biodiesels, and Tate who saw similar behavior for soybean and canola over a 293.15 to 573.15 K range⁹. The slight difference between Vistic low-linolenic and traditional soybean derived biodiesels can be explained by the additional linolenic FAMES in the soy, which was found by Rodrigues to decrease viscosity compared to oleic FAMES¹⁰. The Litovitz parameters (A and B' from Eqn. 1) were fit to the data for each sample and are listed in Table 4.2.

The Litovitz fit to all of the data was good with a percent average absolute relative deviation (%AARD) of 1.5 % for all of the ambient pressure viscosity data.

4.4 High-Pressure Viscosity

The high-pressure viscosity of each of the samples was measured at four temperatures (283.15 K, 298.15 K, 313.15 K, and 373.15 K) and pressures to 131 MPa and the results are found in Table 4.2. For comparison, the high-pressure viscosity of petroleum-derived diesel (No. 2) was also measured and shown in Figure 4.2.

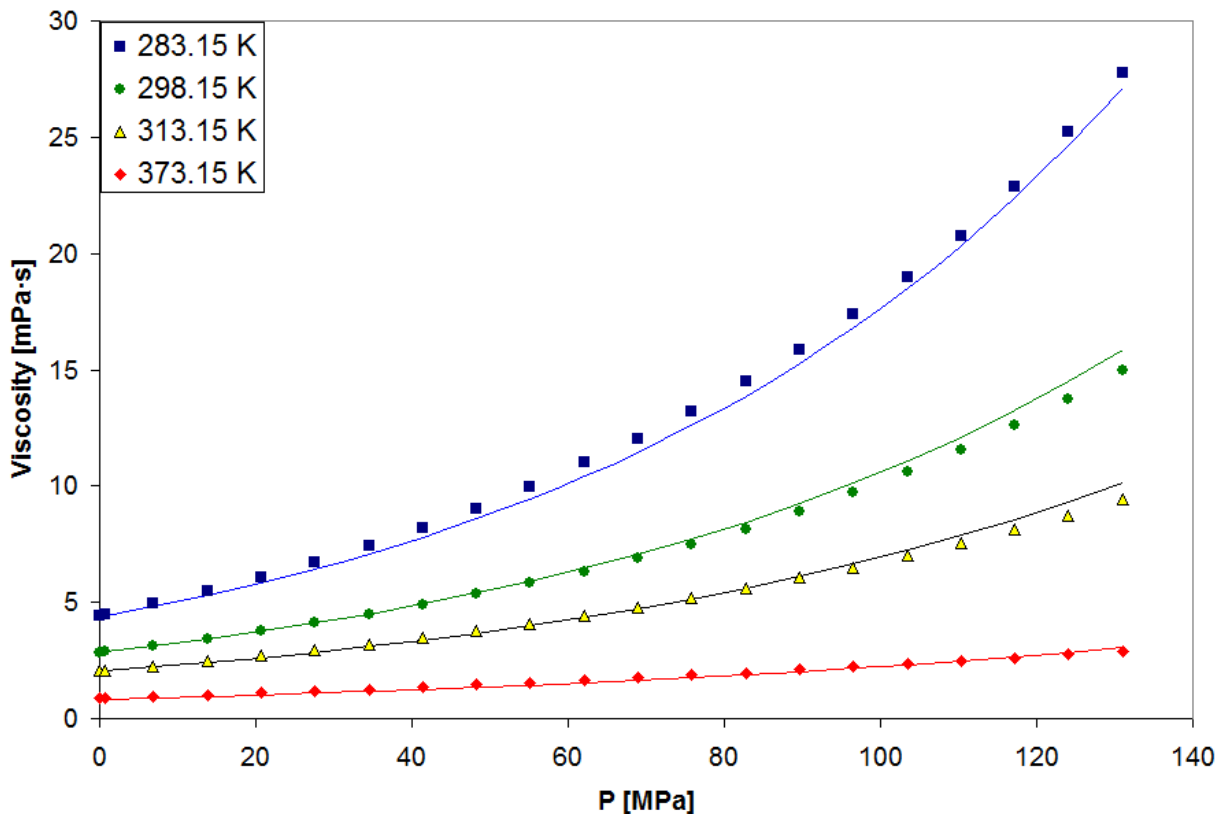


Figure 4.2. Viscosity with pressure for petroleum-based Diesel (No. 2) at four isotherms: 283.15 K, 298.15 K, 313.15 K, and 373.15 K. Lines represent Tait-Litovitz equation from temperature-dependent parameters regressed from all four isotherms (Table 4.3), here and all subsequent Figures.

4.4.1 Petroleum Derived Diesel

The viscosity of diesel with pressure trend is mostly linear to approximately 35 MPa at all temperatures, after which the viscosity begins to experience a larger nonlinear increase with pressure. The viscosity of diesel at the lower temperatures is more largely affected by pressure, than at the higher temperatures. For instance, the increase over ambient-pressure

viscosity is approximately 330% at 103MPa and 283.15K, while at 373.15K the increase is approximately 175% at the same pressure.

The viscosity of the diesel sample as a function of temperature and pressure is correlated with the Tait-Litovitz model as discussed above. Table 4.2 lists the Litovitz and Tait equation parameters (Eqn. 4) regressed at each of the four different temperatures.

Table 4.2. Litovitz and Tait parameters regressed at each isotherm.									
	Litovitz		283.15 K			298.15 K			
<i>Sample</i>	<i>A</i>	<i>B' × 10⁻⁶</i>	<i>D</i>	<i>E</i>	% <i>AARD</i>	<i>D</i>	<i>E</i>	% <i>AARD</i>	
	[mPa·s]	[K ³]	[MPa]	-		[MPa]	-		
Diesel	0.229348	67.0591	338.028	5.43227	1.15%	2726.779	35.06155	0.42%	
Soybean	0.416463	65.5699	236.999	3.00830	0.16%	216.004	2.68289	0.70%	
Vistive	0.387597	68.0733	237.870	3.00204	0.05%	235.690	2.87354	0.35%	
Canola	0.395625	69.9619	346.916	4.38558	0.31%	238.687	2.95454	0.57%	
Used Canola	0.390917	70.3139	355.045	4.42122	0.18%	260.009	3.15483	0.15%	
Coconut	0.242083	68.2777	265.921	3.18697	0.17%	165.211	2.12181	0.99%	
	313.15 K			373.15 K					
<i>Sample</i>	<i>D</i>	<i>E</i>	% <i>AARD</i>	<i>D</i>	<i>E</i>	% <i>AARD</i>			
	[MPa]	-		[MPa]	-				
Diesel	383.471	5.19615	0.46%	142.359	1.90287	0.90%			
Soybean	430.479	4.60283	0.43%	797.490	6.74964	1.25%			
Vistive	317.529	3.60852	0.89%	451.728	4.14914	0.76%			
Canola	219.450	2.61684	0.51%	742.391	6.54252	1.23%			
Used Canola	208.829	2.53150	0.51%	582.545	5.28072	0.84%			
Coconut	317.958	3.42682	0.27%	109.905	1.37088	1.00%			

The AARD% for all of the viscosity data was 0.6 %.

However, these Tait parameters (D and E) can be fit to linear functions of temperature in the following manner:

$$E = a + bT [K]$$

$$\frac{D}{E} = c + dT [K]$$

The E parameter was fit first to a linear expression of temperature, followed by fitting the ratio of D to E to a linear function. This was done as it produced markedly better fits compared to simply fitting a linear expression to both D and E directly, while retaining the same number of fitting parameters. The resulting coefficients for these expressions are listed in Table 4.3.

Table 4.3. Tait-Litovitz equation parameters and AARD% ^a .							
	$\eta_0 = A \exp(B'/(T^3))$		$E = a + bT$		$D/E = c + dT$		
Sample	A	$B' \times 10^{-6}$	a	b	c	d	AARD ^a
	[mPa·s]	[K ³]		[K ⁻¹]	[MPa]	[MPa·K ⁻¹]	[%]
Diesel	0.229348	67.0591	20860890	-21022.2	-18.6209	0.319835	3.27%
Soybean	0.416463	65.5699	-5.90922	0.03106	-45.6774	0.43601	0.86%
Vistive	0.387597	68.0733	-10.3749	0.04457	-38.5534	0.40475	0.70%
Canola	0.395625	69.9619	-1.93125	0.01643	-33.1103	0.38248	0.81%
Used Canola	0.390917	70.3139	-2.98560	0.01995	-26.8126	0.36258	0.64%
Coconut	0.242083	68.2777	4.82942	-0.00825	61.3565	0.06911	1.62%

a.

$$\% \text{ AARD} = \frac{100}{N} \sum_{i=1}^N \left| \frac{\eta_i^{\text{pred}} - \eta_i^{\text{exp}}}{\eta_i^{\text{exp}}} \right|$$

Table 4.3 indicates that despite the linearization procedure, the model exhibits good correlation to the data. This form of Tait-Litovitz model with temperature linearized parameters will be used in all of the subsequent figures. The %AARD for all of the viscosity data for No. 2 diesel was 3.27%, significantly higher than the biodiesel models. Figure 4.3 illustrates the residuals between the model and experimental data at each pressure for the four temperatures.

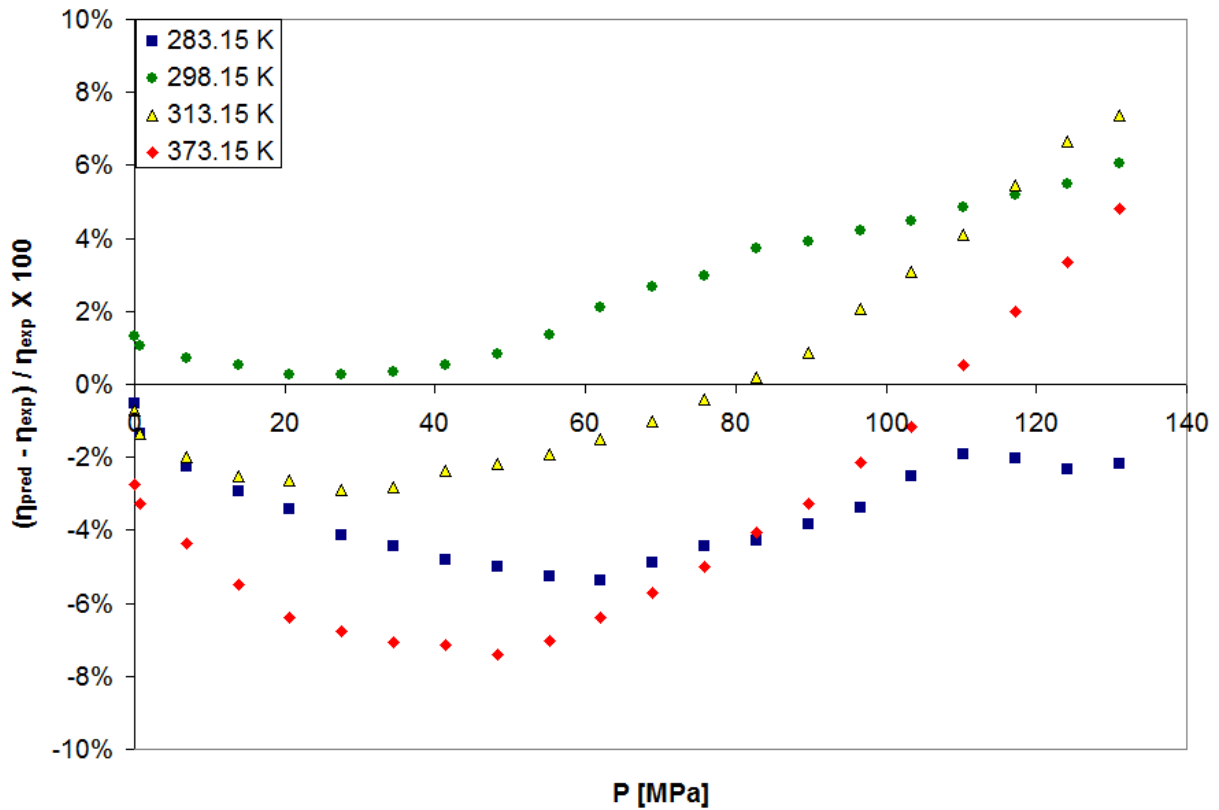


Figure 4.3. Tait-Litovitz equation residuals from the diesel experimental data.

The isotherms at 283.15 K and 373.15 K have a negative bias (under prediction) for most of the pressure range, while at 298.15 K there is an over prediction throughout. When fitting the Tait parameters (D and E) at each individual isotherm (Table 4.2), the residuals are evenly distributed between over- and under-prediction. However, upon fitting these parameters to

temperature dependence (Table 4.3), certain biases develop. These biases are temperature dependent and oscillate with increasing pressure. As shown, the maximum deviations occur for the 373.15 K isotherm at ~50 MPa at 7.4 %. However, the overall %AARD for the fit for all biodiesel and diesel data and all isotherms is approximately 1.3%, which is relatively good considering the span of 90 K and 131 MPa of the data.

4.4.2 Biodiesel from Canola Oil

The high-pressure viscosity of two types of diesel from canola oil has been measured and is listed in Appendix C, Tables C.1 through C.2. Figure 4.4 illustrates the high-pressure behavior of the biodiesel sample synthesized from recycled canola oil that was used in cooking and frying (waste cooking oil: WCO).

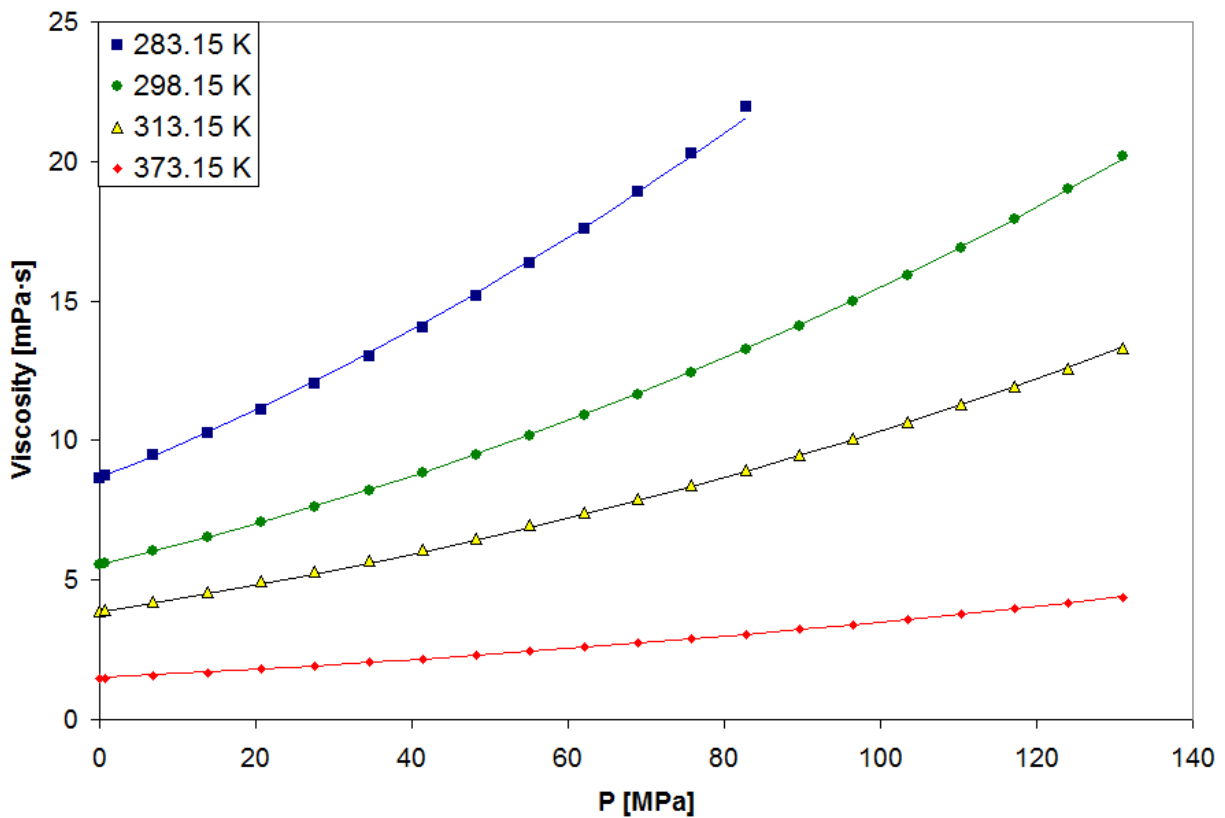


Figure 4.4. Viscosity with pressure for biodiesel from used canola oil at four isotherms: 283.15, 298.15K, 313.15 K, and 373.15 K and Tait-Litovitz model.

The viscosity increases significantly over the large pressure range studied. For instance at 298.15 K, the viscosity increases approximately 180+% at 100 MPa over the viscosity at 0.1 MPa. The rate of viscosity increase with pressure is approximately 0.1 mPa·s per MPa at 298.15 K. For all of the isotherms, the viscosity is relatively linear with pressure until approximately 35 to 40 MPa, after which it becomes steeper and more nonlinear.

Overall a good correlation was obtained with the linearized (temperature dependent) form and the residuals for the 4 isotherms are found in Figure 4.5 with a maximum deviation for all isotherms of approximately 4.7 % and a %AARD for all canola data at all isotherms of 0.7 %.

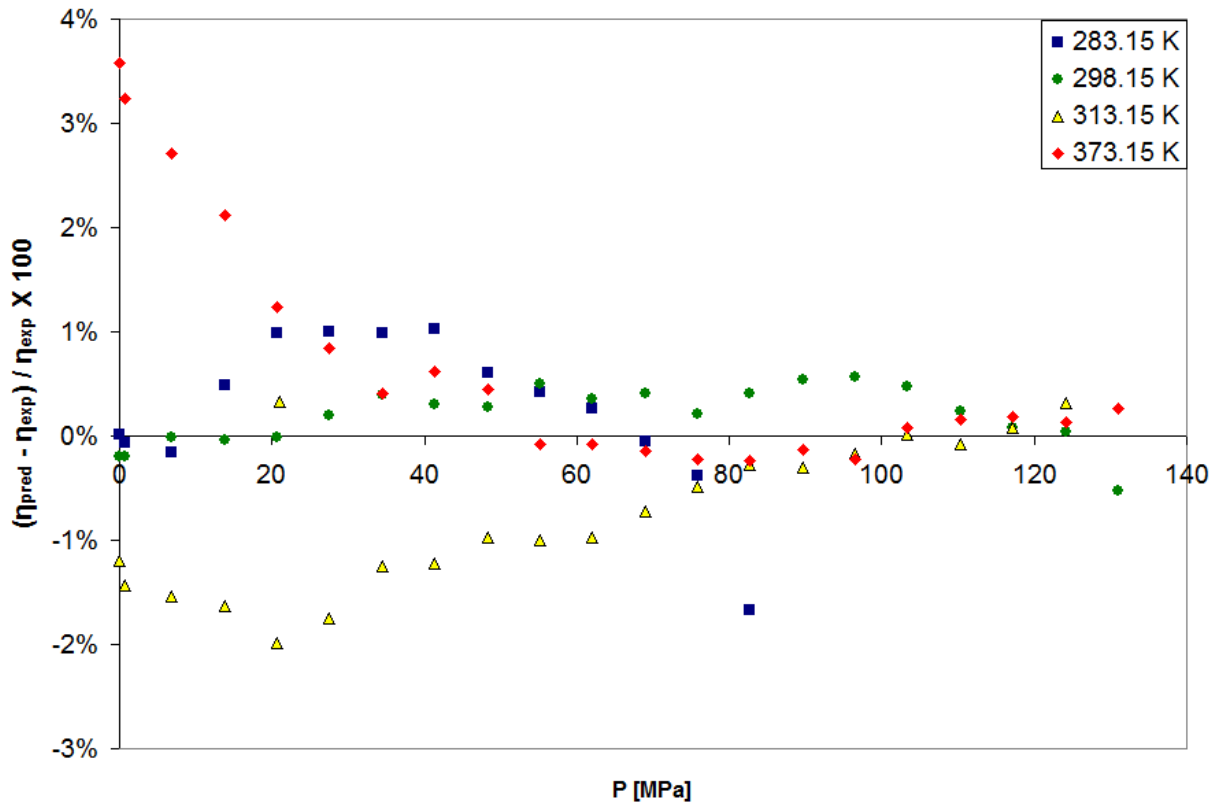


Figure 4.5. Tait-Litovitz equation residuals from the used canola oil sample.

The low AARD confirms the ability of the model to account for both the temperature and pressure effects on the viscosity of both petroleum- and bio-diesel. The power of this format is to accurately correlate and predict (interpolate and reasonably extrapolate, see also Chapters 6 and 7) to other pressures and temperatures than those measured here. We have found that even if the parameters are regressed to only three of the four isotherms that a good prediction is found; for instance, a %AARD of 3.5% was obtained by regressing data at 298.15K, 313.15 K, and 373.15 K and extrapolating to the isotherm at 283.15 K. The extrapolation potential of this model at higher temperatures and pressures is explored further in Chapter 7.

Figure 4.6 illustrates the viscosity behavior at 283.15 K, but now over a larger pressure range than in Figure 4.4.

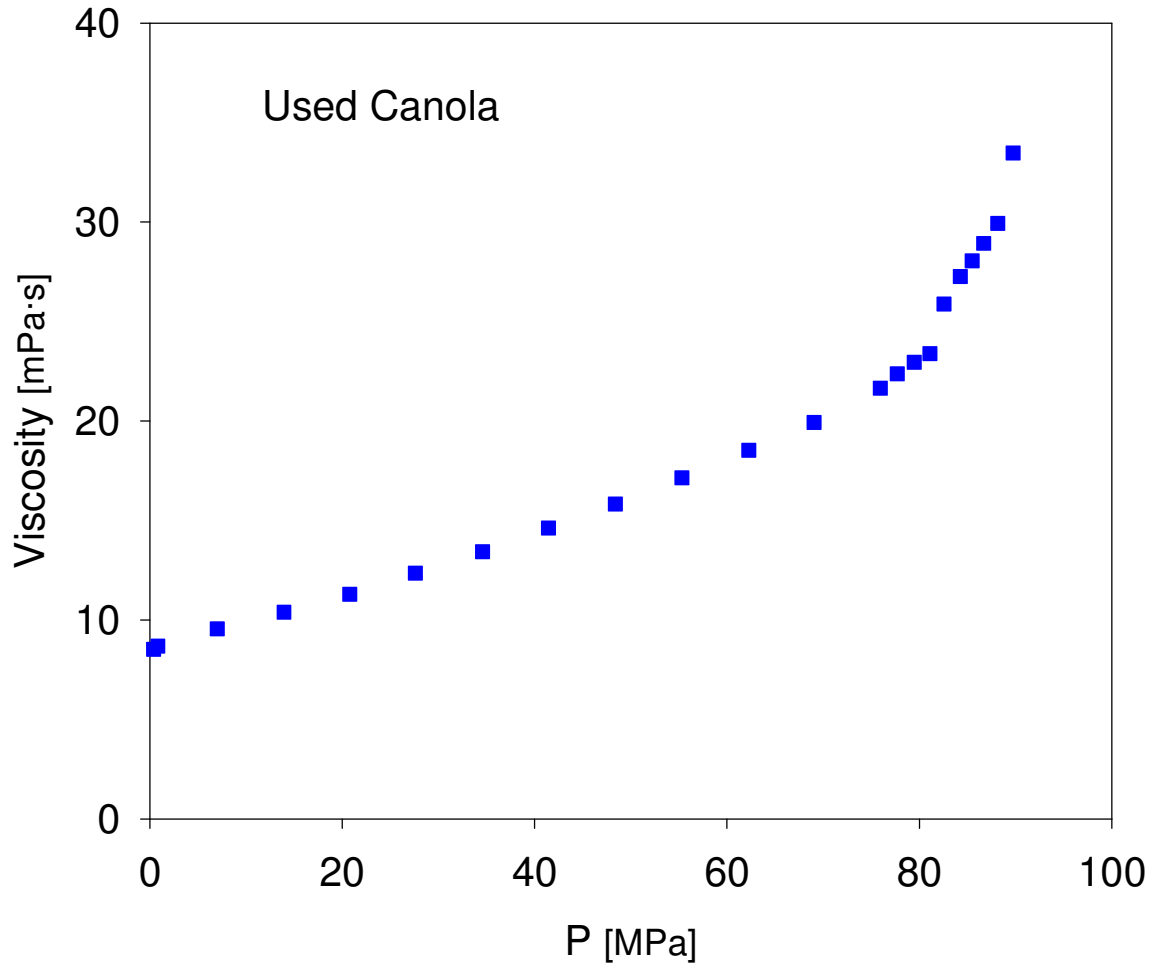


Figure 4.6. Viscosity with pressure for biodiesel from used canola oil at 283.15 over a larger pressure range indicating a cloud point at approximately 83 MPa.

As seen in Figure 4.6, the slope of the viscosity versus pressure curve experiences a change in functional form (piece-wise continuous) at approximately 83 MPa (Table 4.4).

Table 4.4 Approximate cloud point pressure of the samples at 283.15 K.	
Sample	Cloud Point Pressure [MPa]
Diesel	>130 ^a
Soybean	69
Vistive	73
Canola	83
Used Canola	83
Coconut	100
a) was not observed under conditions investigated	

This indicates that a second order phase transition is occurring, which we believe to be the cloud point or the thermodynamic solid-liquid equilibrium line, where the formation of a suspension of the solids in the liquid becomes more gel-like. Beyond the final data point in Figure 4.6, it was not possible to collect additional data, as the viscometer no longer functioned. It is possible that at this point a solid phase became significant enough to disrupt the oscillating motion or path of the piston within the viscometer chamber. The cloud point at ambient pressure for used canola has been measured to be 272.15 K (Table 4.1). Thus, we can very roughly approximate the cloud point temperature (T_{cpt}) of the biodiesel from used canola as a function of pressure as $T_{cpt} [K]=272.15 K + 0.133 \times P[MPa]$. At the higher temperature

isotherms, this behavior is not observed as the cloud point pressure will increase beyond the experimental pressure limit. After the cloud point temperature and pressure, non-Newtonian behavior is usually observed as the mixture often becomes a suspension¹¹. The cloud point for petroleum diesel was not observed under any of the conditions investigated. The high-pressure cloud point is an important parameter to quantify in order to properly operate diesel engines. Simply operating just above the ambient pressure cloud point, may not circumvent gelling of the fuel in the lines and injector at higher pressures. For all isotherms where this was observed, only the continuous data before this point is reported and modeled.

The high-pressure viscosity of biodiesel synthesized from pure (unused) canola oil was measured at the four isotherms. The plots for the pure and *used* canola oil are nearly indistinguishable even at elevated pressure (see Appendix C, Tables C.1 through C.2).

From the FAME compositional analysis of each sample (Table 4.1), the biodiesel from used cooking oil has measurable increases in methyl palmitate (C16:0) and methyl linoleate (C18:2) and decreases in methyl oleate (C18:1) over the biodiesel from unused canola oil. However as shown from the data, these differences, which amount to less than a 10% difference, do not significantly affect the ambient and high-pressure data. The Tait-Litovitz equation was used to correlate the data at all isotherms. Overall a good correlation was obtained and the %AARD for the unused canola oil for all isotherms was 0.6 %.

4.4.3 Biodiesel from Soybean Oil

The high-pressure viscosity of two types of diesel from soybean oil have been measured. Store-bought unused soybean oil and Vistive soybean oil. The high-pressure viscosity for the unused soybean is given in Figure 4.7.

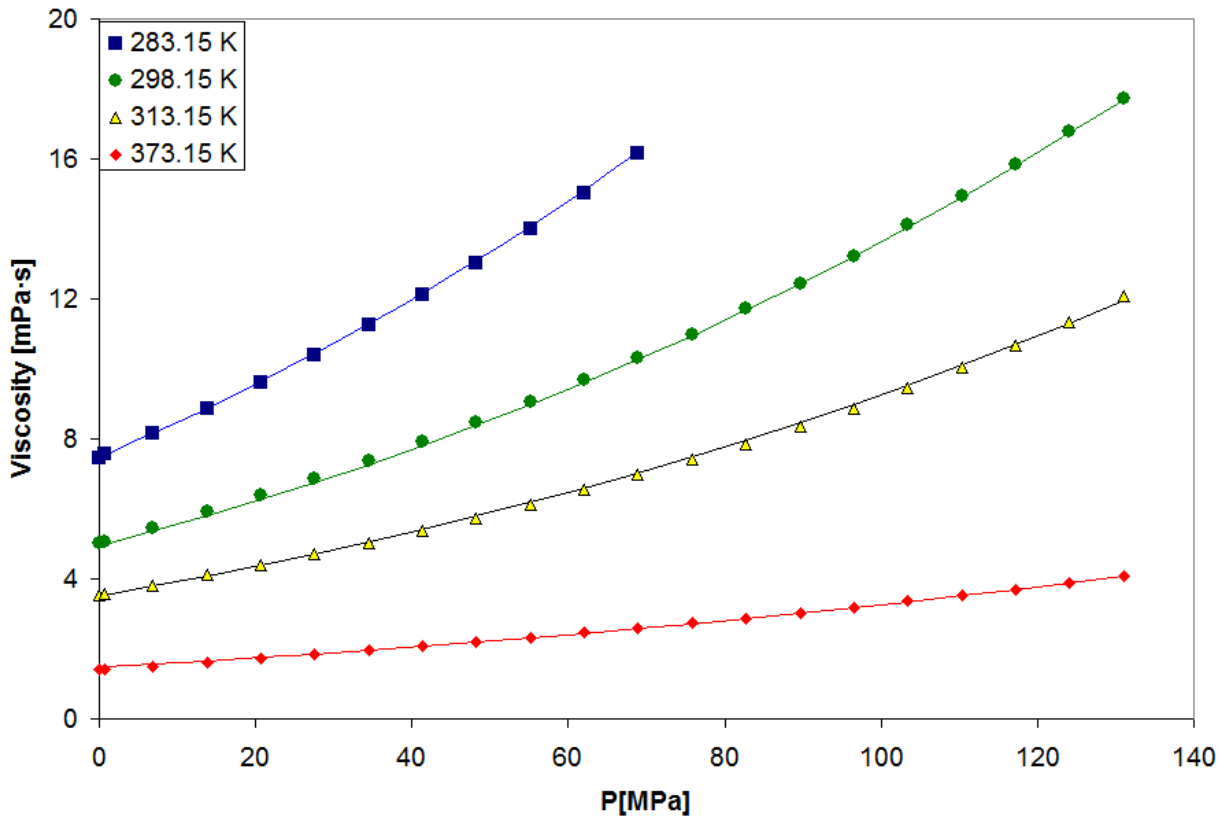


Figure 4.7. Viscosity with pressure for biodiesel from soybean oil at four isotherms: 283.15, 298.15K, 313.15 K, and 373.15 K with Tait-Litovitz model.

The Vistive sample is derived from oil produced from Monsanto's low linolenic acid soybean variety. The viscosity with temperature and pressure profiles is similar to the canola biodiesels. At approximately 100 MPa, each sample demonstrates a viscosity increase over ambient pressure of approximately 183, 172, and 142% at 298.15, 313.15, and 373.15 K, respectively. At

313.15 K, the difference between the ambient-pressure viscosity between the Vistive and regular soybean samples is only 2% as shown in Figure 4.8. At 100 MPa, the Vistive sample is roughly 3% greater than the regular soybean sample. At 373.15 K, the difference between the samples at both ambient pressure and 100 MPa is <1% and almost indistinguishable in Figure 4.8.

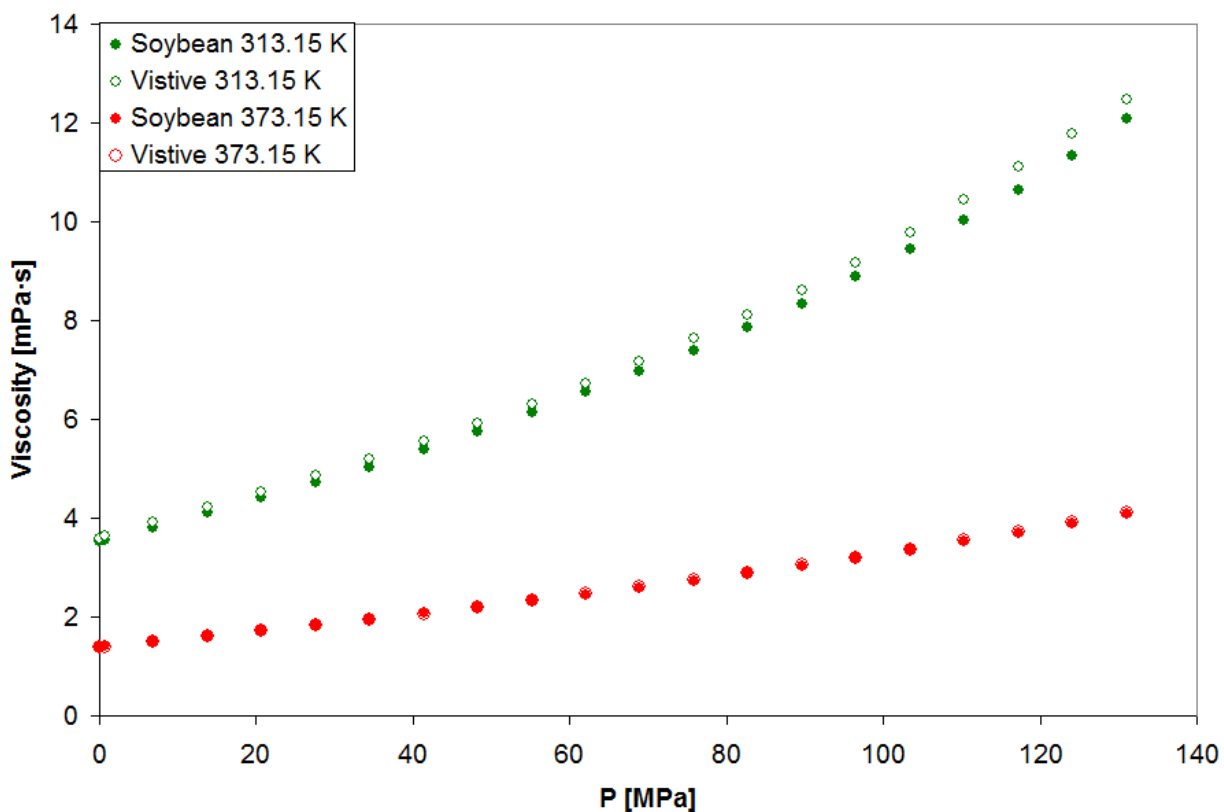


Figure 4.8. Viscosity with pressure for biodiesel from soybean oil and Vistive soybean oil at 313.15 K and 373.15.

The similar FAME profiles between the two fuels yield similar viscosities through the span of temperatures and pressures tested. The higher amount of linolenic FAME in the soybean biodiesel gives this fuel a slightly lower viscosity than the Vistive. Overall, a good correlation

with the T-L model was obtained, and the AARD for all isotherms was 0.9 and 0.7% for the soybean and Vistive samples, respectively.

4.4.4 Biodiesel from Coconut Oil

The high-pressure viscosity of diesel made from coconut oil has been measured and shown in Figure 4.9.

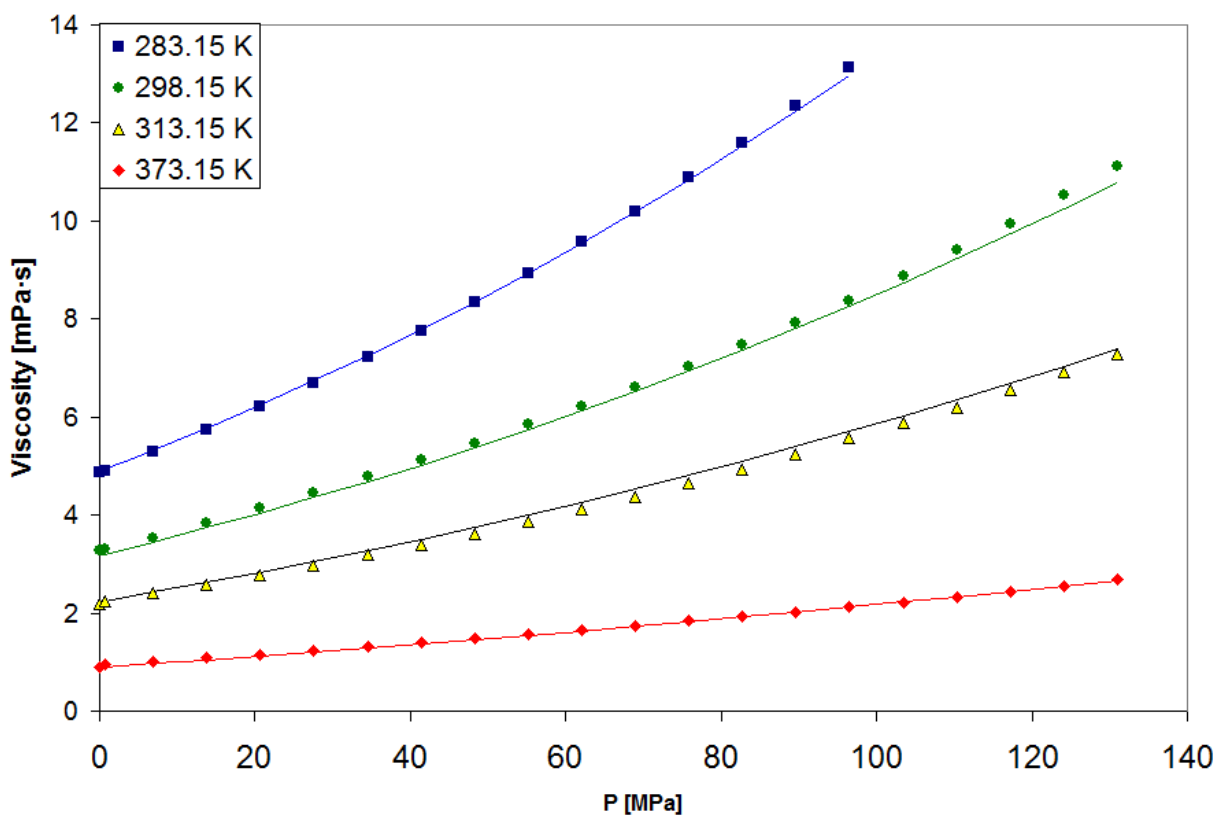


Figure 4.9. Viscosity with pressure for biodiesel derived from Coconut oil at four isotherms: 283.15 K, 298.15 K, 313.15 K, and 373.15 K.

The behavior with pressure is similar to the other biodiesel samples, but with lower viscosity magnitude. Coconut biodiesel is composed of FAMES, which are shorter on average than the

other fuels, and whose pure component viscosities are less than the pure component viscosities of the FAMEs in the other feedstocks tested.

The cloud point pressure in coconut biodiesel also deviated from the other fuels. At 283.15 K, the range of data is to nearly 100 MPa, which is well beyond the pressure induced cloud points of the other biodiesel samples (Table 4.4). Overall, the %AARD for all coconut biodiesel isotherms was 1.6 %.

4.4.5 Comparison of the Diesel and Biodiesel Samples

Figures 4.10 and 4.11 compare the high-pressure viscosity of the petroleum diesel and biodiesel samples at 298.15 and 373.15 K, respectively. As discussed above, the ambient-pressure trends are generally, in the order of increasing viscosity: diesel < coconut < soybean < vistic < canola ~ used canola. For all of the biodiesel data, the order of viscosity among the samples at ambient pressure (Figure 4.1) is maintained at higher pressure.

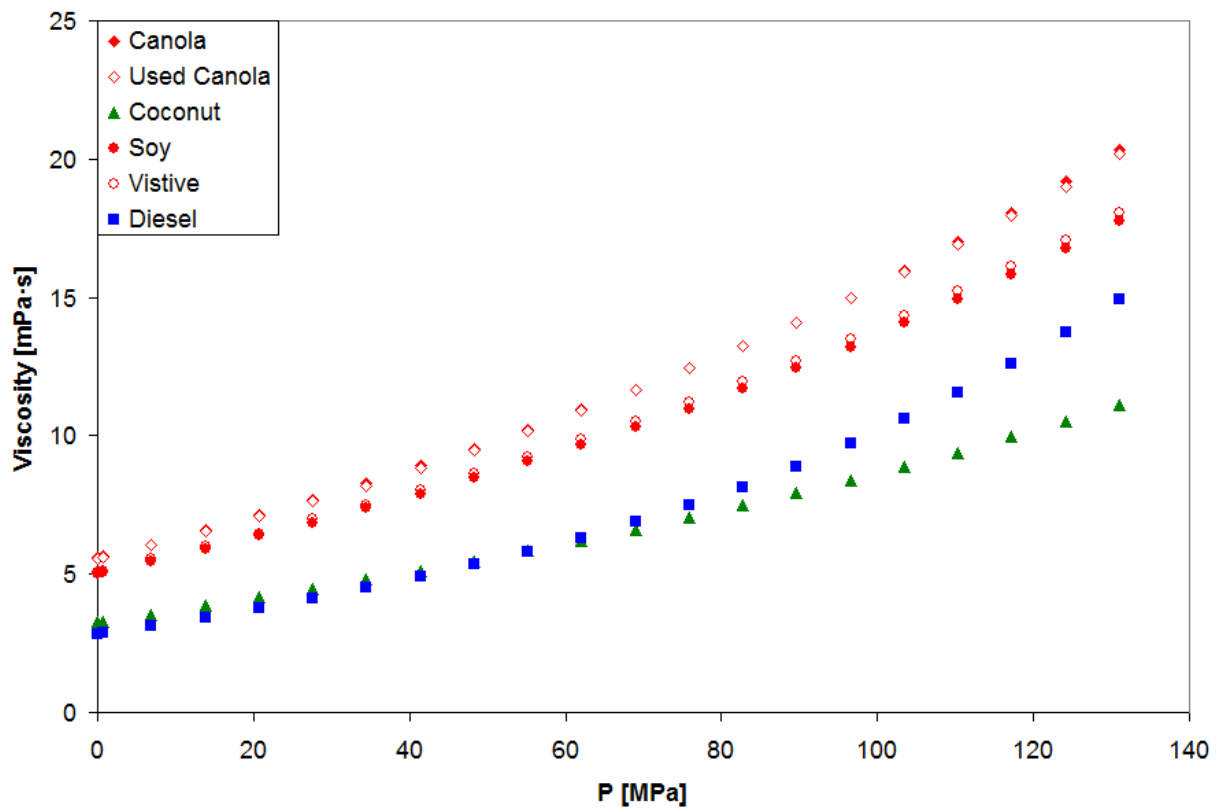


Figure 4.10. All fuels at 298.15 K.

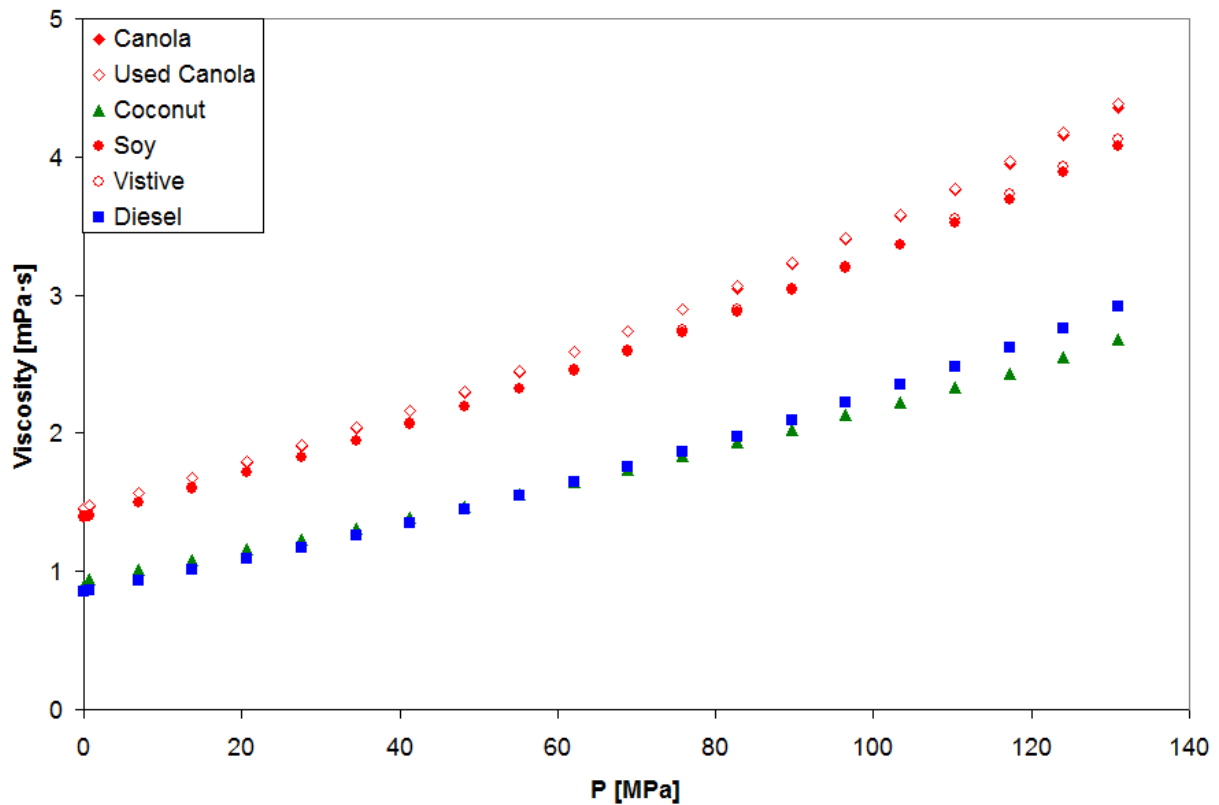


Figure 4.11. All fuels at 373.15 K.

However, for the petroleum diesel and the coconut biodiesel samples, diesel has a lower viscosity than the coconut biodiesel at ambient pressure, but, at certain higher pressures, the trend switches and the diesel sample becomes more viscous than the coconut biodiesel sample. At 283.15 K, this point is approximately 27 MPa and, at 373.15 K, the change occurs at approximately 62 MPa.

Among the biodiesel samples, the percentage difference in viscosity from each sample does not change substantially with pressure, except at the lower temperature data. For instance at 373.15 K, the percent difference between the Vistive and coconut biodiesel at ambient

pressure and 131 MPa were approximately 56 % and 54% respectively (Figure 4.11). However, at 298.15 K (Figure 4.10), the differences at ambient pressure and 131 MPa were 55% and 63% respectively. This is shown more clearly in Figure 4.12 for the data at 283.15 K, by normalizing each sample by its ambient pressure viscosity (η/η_0). As shown, each of the biodiesel samples measured have very similar normalized viscosity changes with pressure except at the highest pressure ranges, which are near the cloud points. Only the diesel sample has a significantly different trend. Fernandez and coworkers^{12, 13} have shown that hydrocarbons (such as in petroleum diesel) have a stronger viscosity/pressure dependence than esters (such as in biodiesel). The normalized viscosity with pressure data at the higher temperatures (not shown) is even more consistent. Additional thoughts regarding the trend differences are included in Chapter 7.

The only *previous* literature data for high-pressure viscosity of a biodiesel sample measured at similar conditions, are those by Robertson and Schaschke¹¹ for biodiesel from sunflower oil at 283.15 K; while the raw data was not tabulated in their report an empirical expression was given relating viscosity with pressure.

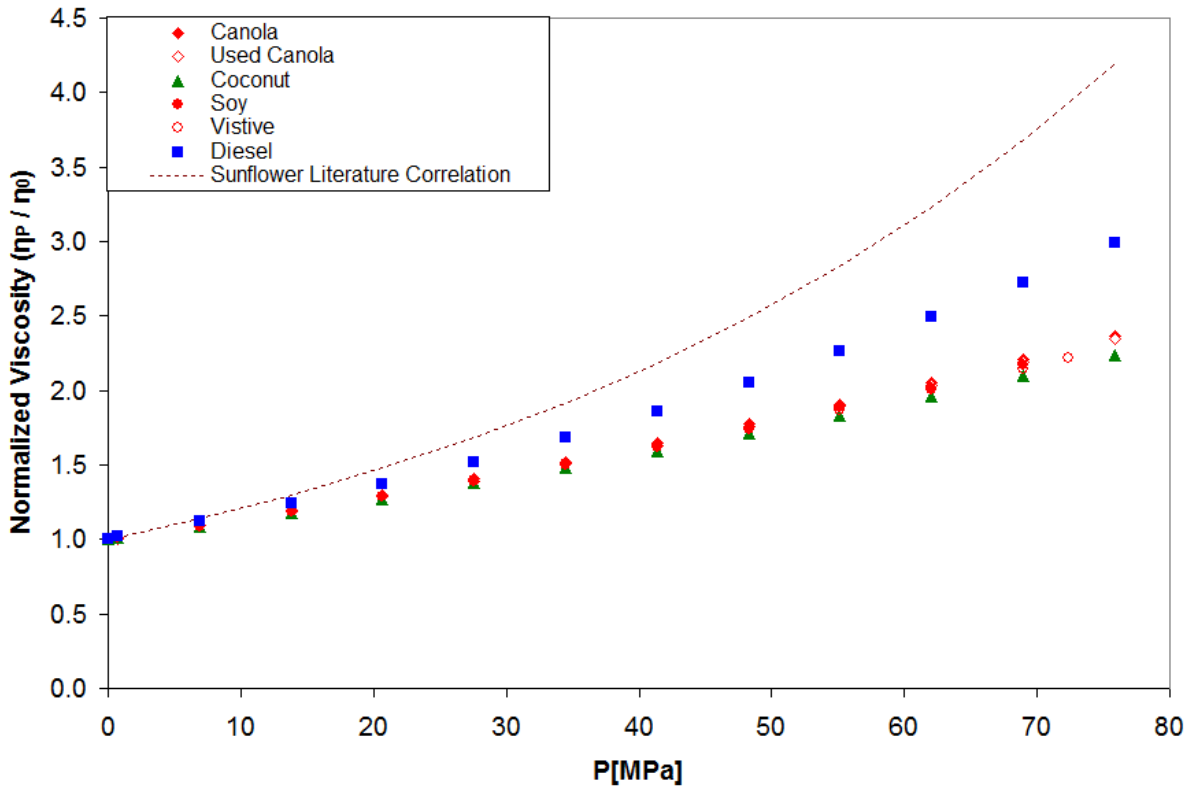


Figure 4.12. Comparison of viscosity with pressure for each of the samples at 283.15 K normalized to each sample's ambient-pressure viscosity with comparison to biodiesel correlation from pure sunflower oil from Robertson and Schaschke 2010.

As shown in Figure 4.12, normalizing this data has much different behavior than the biodiesel samples and the diesel sample. The reason for this discrepancy is not clear as the FAME composition of biodiesels from sunflower oil and soybean oil are relatively similar, i.e. high linoleate and oleate. Their method to compute the viscosity requires accurate density of the compressed sample, which are unavailable, so they predicted the densities using the Peng-Robinson equation of state from estimated critical properties. Accurate *liquid* density

predictions from cubic equations of state are often difficult especially for long-chained hydrocarbons¹⁴ and this may account for the difference in relative viscosity at high pressure.

The approximate pressure-induced cloud point at 283.15 K seems to only roughly correlate with the ambient pressure cloud point measurements. Among biodiesels, coconut derived biodiesel has the lowest cloud point temperature at ambient pressure and has an approximate cloud point pressure that is the highest at 283.15 K, while the reverse is true for soybean biodiesel. Soybean biodiesel has the highest cloud point temperature at ambient pressure, and the lowest approximate cloud point pressure at 283.15 K. The other biodiesel cloud points do not correlate as well to the approximate cloud point pressure at 283.15 K, however, in these samples, if fuel 1 has a cloud point temperature lower than fuel 2, fuel 2 *will not* have an approximate cloud point pressure that is greater than fuel 1 at 283.15 K. The trend, in order of increasing cloud point pressure, is soybean<Vistive<used canola<canola<coconut<<diesel. However, these are *approximate* cloud point pressures and we are planning further studies into the high-pressure thermodynamic transition of biodiesels.

4.5 Ramifications of Data on Current and Future (Bio-)Diesel Engines and Designs

By having a better understanding of the viscosity of the fuel at high pressure, engine designers can properly correct for changes in line dynamics and the impact on fuel injection timing and amount in the engine. An increased understanding will allow engines to become more robust in their designs and allow for higher blends of biodiesel to be utilized without ramifications on performance or emissions. These benefits can occur through on-board resetting of the fuel injection timing or new injector designs that offer flexibility across many different types of biodiesel fuels. Since not all feedstock is created the same, viscosity data across a wide array of different biodiesels may help engine designers formulate a universal injector suited for temperature, pressure and fuel conditions. Moreover, understanding the pressure induced cloud points would have significant impact on the startup of engines using biodiesel and help lead to a wider implementation in colder climates.

4.6 Conclusions

The viscosity of five biodiesels from various bio-renewable sources was measured to determine the effect of high pressures (up to 131 MPa) and temperatures from 283.15 to 373.15 K. ***These data are the first to explore comprehensively, the effect of temperature, pressure, and vegetal source on the viscosity of biodiesel.*** The viscosity change that a biodiesel would experience in a fuel injector would be up to several hundred percent greater than the ambient pressure viscosity. While differences in ambient pressure viscosity exist among the different biodiesels, the effect of pressure is relatively similar. At 283.15 K, pressure induced cloud points were observed for all of the biodiesel samples, which was up to 13 K above their ambient

pressure cloud points. The viscosity data have been correlated with a hybrid Tait-Litovitz equation with average absolute relative deviation percentages (AARD%) for biodiesels from 0.6 % for used canola derived biodiesel to 1.6 % for coconut derived biodiesel and 3.3% for petroleum diesel. The correlation could be used for a wide range of simulation and design scenarios.

References for Chapter 4

1. Dymond, J. H.; Malhotra, R., The Tait equation: 100 years on. *International Journal of Thermophysics* **1988**, 9, (6), 941-951.
2. Kashiwagi, H.; Makita, T., Viscosity of Twelve Hydrocarbon Liquids in the Temperature Range 298-348 K at Pressures up to 110 MPa. *International Journal of Thermophysics* **1982**, 3, (4), 289-305.
3. Knothe, G., Improving biodiesel fuel properties by modifying fatty ester composition. *Energy & Environmental Science* **2009**, 2, (7), 759-766.
4. Krisnangkura, K.; Yimsuwan, T.; Pairintra, R., An empirical approach in predicting biodiesel viscosity at various temperatures. *Fuel* **2006**, 85, (1), 107-113.
5. Litovitz, T. A., Temperature Dependence of the Viscosity of Associated Liquids. *The Journal of Chemical Physics* **1952**, 20, 1088-1089.
6. Litovitz, T. A., Temperature Dependence of the Viscosity of Associated Liquids. *The Journal of Chemical Physics* **1952**, 20, 1980.
7. Ahosseini, A.; Scurto, A. M., Viscosity of Imidazolium-Based Ionic Liquids at Elevated Pressures: Cation and Anion Effects. *Int. J. Thermophys.* **2008**, 29, 1222-1243.
8. Allen, C.; Watts, K.; Ackman, R.; Pegg, M., Predicting the viscosity of biodiesel fuels from their fatty acid ester composition. *Fuel* **1999**, 78, (11), 1319-1326.
9. Tate, R.; Watts, K.; Allen, C.; Wilkie, K., The viscosities of three biodiesel fuels at temperatures up to 300 C. *Fuel* **2006**, 85, (7), 1010-1015.

10. Rodrigues, J.; Cardoso, F.; Lachter, E.; Estevão, L.; Lima, E.; Nascimento, R., Correlating chemical structure and physical properties of vegetable oil esters. *Journal of the American Oil Chemists' Society* **2006**, 83, (4), 353-357.
11. Robertson, L. X.; Schaschke, C. J., Combined High Pressure and Low Temperature Viscosity Measurement of Biodiesel. *Energy Fuels* **2010**, In Press.
12. Lugo, L.; Canet, X.; Comuñas, M. J. P.; Pensado, A. S.; Fernández, J., Dynamic Viscosity under Pressure for Mixtures of Pentaerythritol Ester Lubricants with 32 Viscosity Grade: Measurements and Modeling. *Industrial & Engineering Chemistry Research* **2007**, 46, (6), 1826-1835.
13. Pensado, A. S.; Comuñas, M. J. P.; Lugo, L.; Fernández, J., High-Pressure Characterization of Dynamic Viscosity and Derived Properties for Squalane and Two Pentaerythritol Ester Lubricants: Pentaerythritol Tetra-2-ethylhexanoate and Pentaerythritol Tetranonanoate. *Industrial & Engineering Chemistry Research* **2006**, 45, (7), 2394-2404.
14. Mulero, A.; Cachadiña, I., Liquid saturation density from Simple Equations of State. *Int. J. Thermophys.* **2007**, 28, (1), 279-298.

Chapter 5

High-Pressure Viscosity of Soybean Oil-Based Biodiesel Blends with Ultra Low Sulfur Diesel Fuel

There is little literature that examines the dynamic viscosity of biodiesel/ultra-low sulfur diesel (ULSD) blends and none that studies the combination of temperature, pressure, and blend fraction for a significant range. In this contribution, we quantify how the biodiesel blend percentage affects the high-pressure viscosity of the fuel. The viscosity of eight blends of soybean biodiesel and diesel has been measured under high pressures (up to 131 MPa) and at five temperatures (283.15 K, 298.15 K, 313.15 K, 343.15 K and 373.15 K). The fuel samples were blended from a biodiesel feedstock of store-bought soybean oil and ULSD. The high-pressure viscosity of the pure biodiesel and diesel samples was also measured. The Litovitz equation combined with the Tait equation^{1,2} was used to describe the viscosity of biodiesel and diesel fuels as a function of temperature and pressure. The blended fuel samples were described using mixing rules, which weighted the biodiesel and diesel viscosities according to mole fraction. Ambient property data for biodiesel, diesel and their blends is given in Table 5.1.

Table 5.1. Diesel, biodiesel, and biodiesel blends physical properties.								
Sample	B0	B5	B10	B20	B40	B60	B80	B100
Kinematic Viscosity at 313.15 K [cSt]	2.407	2.466	2.527	2.639	2.950	3.285	3.666	4.084
Density at 298.15 K [g/cm ³]	0.8372	0.8392	0.8412	0.8434	0.8531	0.8615	0.8700	0.8784
Density at 313.15 K [g/cm ³]	0.8266	0.8286	0.8305	0.8327	0.8423	0.8506	0.8591	0.8674
Average MW [g/mol]	203	206	210	217	232	249	269	292
Soybean biodiesel (B100) methyl ester composition, wt %.								
C16:0	C18:0		C18:1		C18:2		C18:3	
10.4%	4.1%		21.8%		56.0%		7.8%	

The data, Figures, and Tables have been changed from the published version³ to reflect the newest and best calibration. The average correction was 2.57%, with the most significant corrections being applied to the 50 cP piston, resulting in a 10.2% change in viscosity for the maximum pressure tested at 283.15 K.

5.1 Viscosity Correlation Method

Various theoretical models and empirical expressions can be found in the literature that can be used to represent the viscosity of liquids (η) as functions of pressure and temperature. Our previous contribution describes some of the more often used methods for high pressure⁴. We have found the hybrid Tait-Litovitz model given in Eqn. 1 to provide highly accurate correlations to the high-pressure viscosity data.

$$\eta_p = A \exp(B'/T^3) \left[(D+P)/(D+0.1) \right]^E \quad \text{Eqn. [1]}$$

$$B' = B/R$$

Data regression was performed using a Gauss-Newton method.

The biodiesel blend viscosity is predicted using both Kay's mixing rule:

$$\eta_{Blend} = x_{Diesel}\eta_{Diesel} + x_{Biodiesel}\eta_{Biodiesel} \quad Eqn. [2]$$

and the Grunberg-Nissan mixing rule:

$$\ln(\eta_{Blend}) = x_{Diesel} \ln(\eta_{Diesel}) + x_{Biodiesel} \ln(\eta_{Biodiesel}) \quad Eqn.[3]$$

where x_{Diesel} and $x_{Biodiesel}$ are the lumped mole fractions based on the average molecular weights of diesel and biodiesel in the blended fuel and η_{Diesel} and $\eta_{Biodiesel}$ are the dynamic viscosities of pure diesel and biodiesel at the same temperature and pressure as the blend viscosity η_{Blend} .

5.2. Ambient-Pressure Viscosity Results

The ambient-pressure viscosity of the biodiesel, diesel and six blended samples were measured at 283.15 K, 298.15 K, 313.15 K, 343.15 K and 373.15 K. The data are tabulated in Appendix C, Tables C.7 through C.14. Figure 5.1 illustrates the exponential decrease of viscosity with temperature for diesel and biodiesel in a manner consistent with Litovitz behavior. The lines for B0 and B100 represent the Litovitz equation from parameters regressed from all isotherms. The lines for B20 and B60 represent the application of Kay's mixing rule using the Litovitz equations for B0 and B100.

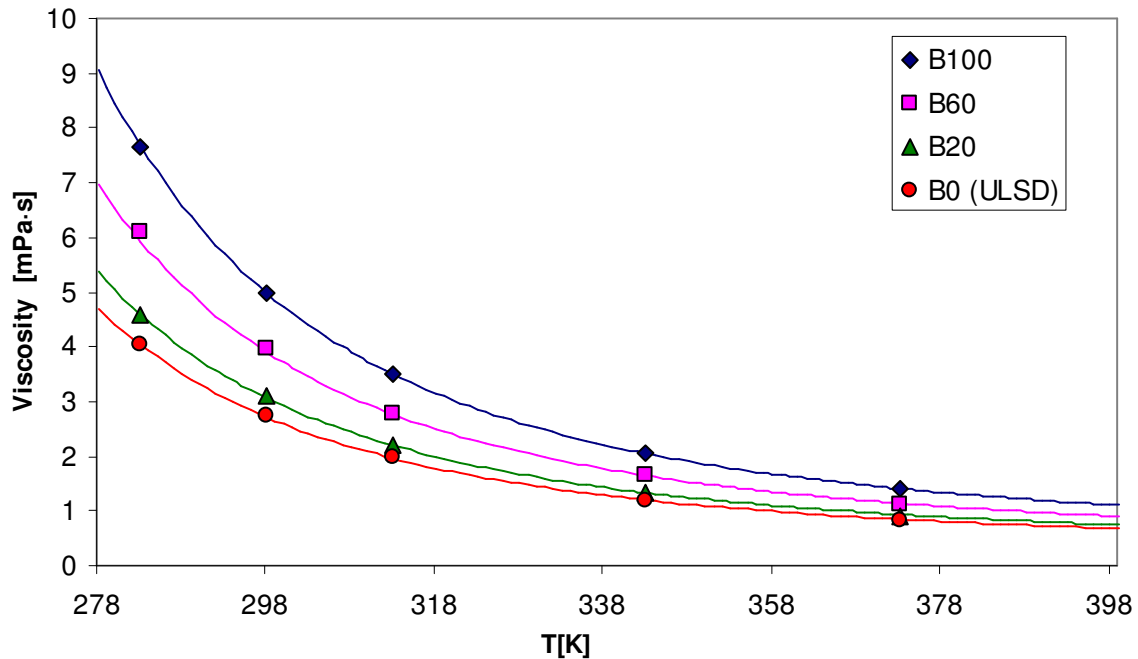


Figure 5.1. Ambient-pressure viscosity with temperature for ULSD, B20 B60, and B100 from soybean oil at 283.15K, 298.15 K, 313.15 K, 343.15 K and 373.15 K.

The ambient-pressure trends for all isotherms are, in the order of increasing viscosity: B0 (ULSD)<B5<B10<B20<B40<B60<B80<B100 (biodiesel). The ambient-pressure trend is in close agreement with Tate⁵ who saw similar behavior for soybean over a 293.15 to 573.15 K range, and for others who performed ambient-pressure viscosity blend studies⁶⁻⁸. The Litovitz parameters (A and B' from Eqn. 1) were fit to the data for diesel and biodiesel and are listed in Table 5.2. The Litovitz fit to the data had a percent average absolute relative deviation (AARD%) of 0.74% for the biodiesel and diesel ambient-pressure viscosity data.

5.3. High-Pressure Viscosity

The high-pressure viscosity of each of the samples was measured at five temperatures (283.15 K, 298.15 K, 313.15 K, 343.15 K and 373.15 K) and pressures to 131 MPa in approximately 7 MPa increments. The results are found in Appendix C, Tables C.7 through C.14.

5.3.1. Ultra Low Sulfur Diesel

The viscosity of the ULSD in this work was compared with the sample used in our previous study ⁴. The AARD% of the two fuels was 6.81% for the shared isotherms: 283.15, 298.15, 313.15, and 373.15 K; the largest deviations were found at the 283.15K isotherm. While the sample was obtained from the same local company as before, it is likely to have a different formulation, as the previous batch was obtained in winter and the ULSD in this study was obtained in summer. Despite the average difference between samples, the normalized (viscosity at pressure/viscosity at ambient pressure) was fairly low, with an average normalized maximum deviation of 2.22%--this value does not include the ambient-pressure viscosities which are equivalent when normalized.

The viscosity of the ULSD sample as a function of temperature and pressure was correlated with the Tait-Litovitz model as discussed above. To reiterate, the Litovitz parameters for the temperature effect were obtained at ambient pressure. Tait parameters were regressed using the high-pressure data. Table 5.2 lists the Litovitz and Tait equation parameters (Eqn. 4) regressed at each of the five different temperatures for ULSD and B100.

Table 5.2. Litovitz and Tait parameters regressed at each isotherm.									
	Litovitz			283.15 K			298.15 K		
Sample	<i>A</i>	<i>B'</i> × 10 ⁻⁶		<i>D</i>	<i>E</i>	% <i>AARD</i>	<i>D</i>	<i>E</i>	% <i>AARD</i>
	[mPa·s]	[K ³]		[MPa]	-		[MPa]	-	
Diesel	0.256007	62.7532		585.614	8.68769	0.29%	415.605	5.80283	0.47%
Soybean	0.380140	68.2831		266.767	3.27430	0.10%	288.516	3.35814	0.23%
	313.15 K			343.15 K			373.15 K		
Sample	<i>D</i>	<i>E</i>	% <i>AARD</i>	<i>D</i>	<i>E</i>	% <i>AARD</i>	<i>D</i>	<i>E</i>	% <i>AARD</i>
	[MPa]	-		[MPa]	-		[MPa]	-	
Diesel	400.146	5.28328	0.48%	482.805	5.57339	0.12%	318.198	3.41566	0.54%
Soybean	513.374	5.32301	0.30%	303.797	3.13280	0.22%	318.680	3.05608	0.24%

The AARD% for all of the viscosity data was 0.23%.

Each isotherm has different Tait parameters (*D* and *E*), however, these parameters can be fit to linear functions of temperature in the following manner:

$$E = a + bT [K]$$

$$\frac{D}{E} = c + dT [K]$$

The *E* parameter was fit first to a linear expression of temperature, followed by fitting the ratio of *D* to *E* to a linear function. This was done as it produced markedly better fits compared to simply fitting a linear expression to both *D* and *E* directly, while retaining the same number of fitting parameters. This method allows the data to be accurately modeled as a function of temperature and pressure, while remaining a simple method of calculation with few required parameters. The temperature dependent Tait parameters yield an AARD% of 0.68% (Table 5.3) for all ULSD isotherms (Figure 5.2), with a maximum deviation of 3.59% at the highest pressure of the 283.15 K isotherm.

Table 5.3. Tait-Litovitz equation parameters and %AARD ^a .							
	$\eta_0 = A \exp(B'/(T^3))$		$E = a + bT$		$D/E = c + dT$		
Sample	A	$B' \times 10^{-6}$	a	b	c	d	AARD ^a
	[mPa·s]	[K ³]		[K ⁻¹]	[MPa]	[MPa·K ⁻¹]	[%]
Diesel	0.256007	62.7532	13.7606	-0.024917	-28.2556	0.334324	0.68%
Soybean	0.380140	68.2831	3.93894	-0.001403	10.6969	0.255848	0.53%

a.

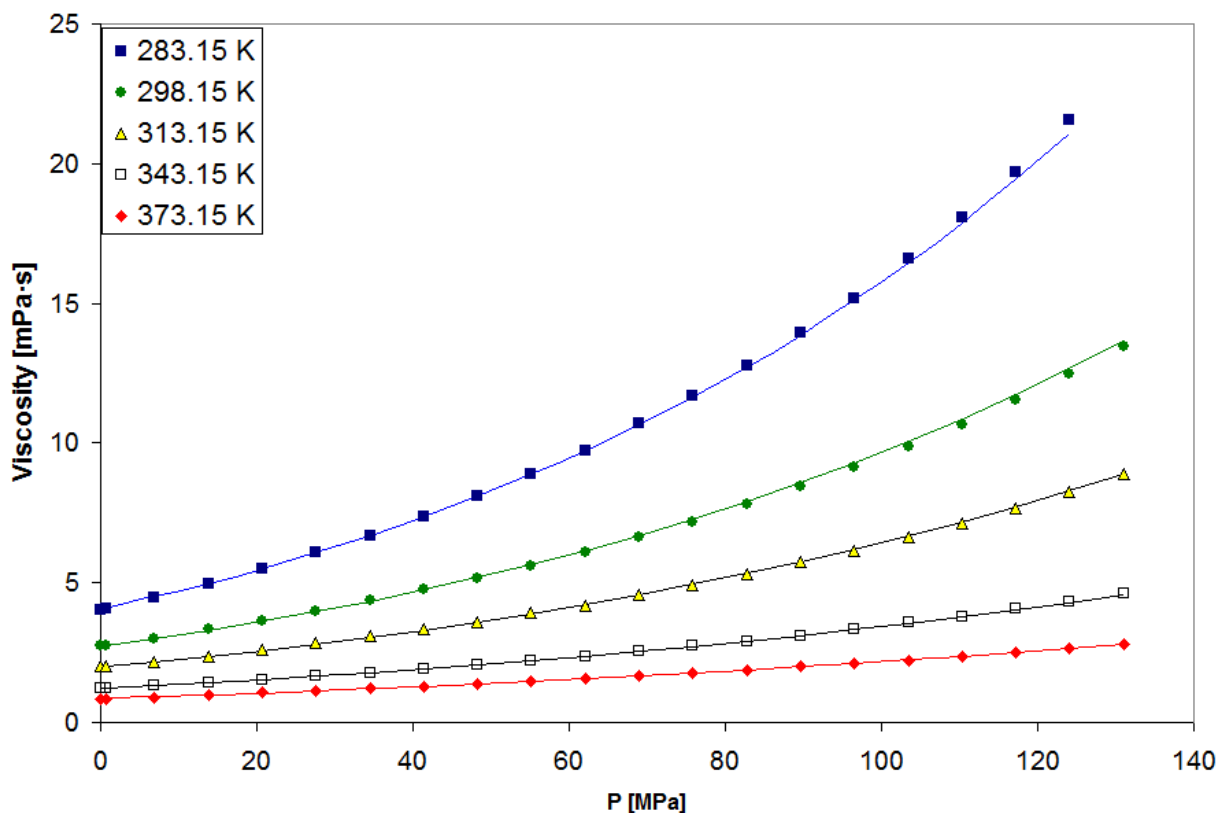
$$\% AARD = \frac{100}{N} \sum_{i=1}^N \left| \frac{\eta_i^{pred} - \eta_i^{exp}}{\eta_i^{exp}} \right|$$


Figure 5.2. Viscosity with pressure for ULSD at five isotherms: 283.15, 298.15, 313.15, 343.15, and 373.15 K.

5.3.2. Soybean Biodiesel

The viscosity of the soybean biodiesel increases appreciably over the large pressure range studied. At 298.15 K, the viscosity increases ~170% at 100 MPa over the viscosity at 0.1 MPa. For all of the isotherms, the viscosity is relatively linear with pressure until approximately 35 to 40 MPa, after which it becomes steeper and more nonlinear. The soybean biodiesel in this work had viscosity measurements that were well within the mutual uncertainty of the data from our previous work with an AARD% of 1.07% for all of the shared isotherms: 283.15, 298.15, 313.15 and 373.15 K. The small differences could also be partly explained by the slight difference in composition from the different soybean oil feedstock. The viscosity of the B100 sample as a function of temperature and pressure is well-correlated with the Tait-Litovitz model. The temperature dependent Tait parameters yield an AARD% of 0.53% (Table 5.3) for all B100 isotherms (Figure 5.3), with a maximum deviation of 1.99%.

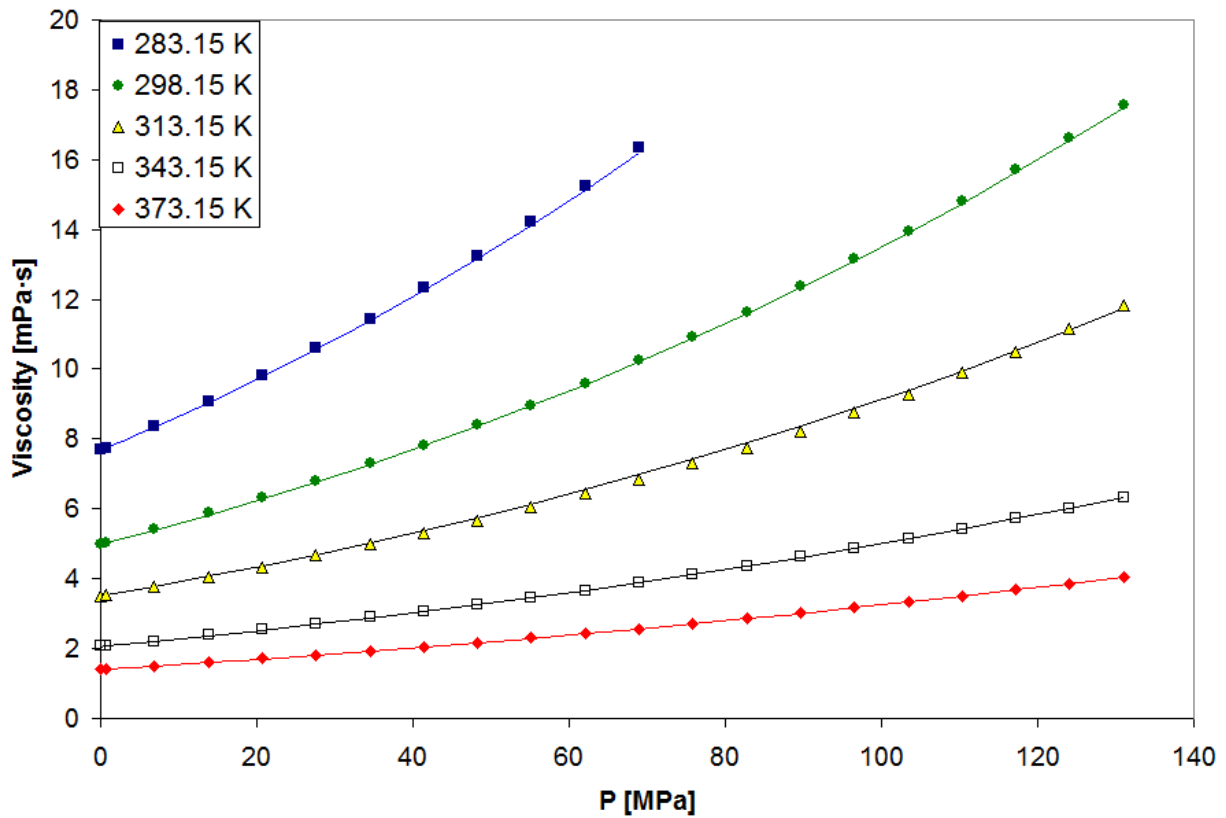


Figure 5.3. Viscosity with pressure for B100 at five isotherms: 283.15, 298.15, 313.15, 343.15, and 373.15 K and Tait-Litovitz model.

5.3.3. Biodiesel Blends

The viscosity of the biodiesel blends B5, B10, B20, B40, B60, and B80 was found to increase with increasing biodiesel blend fraction. The differences among the blends with the smallest amounts of biodiesel (e.g. B0, B5, B10, etc.) were very small, but the viscosity order $B_0 < B_5 < B_{10} < B_{20} < B_{40} < B_{60} < B_{80} < B_{100}$, was generally constant as seen in Figure 5.4.

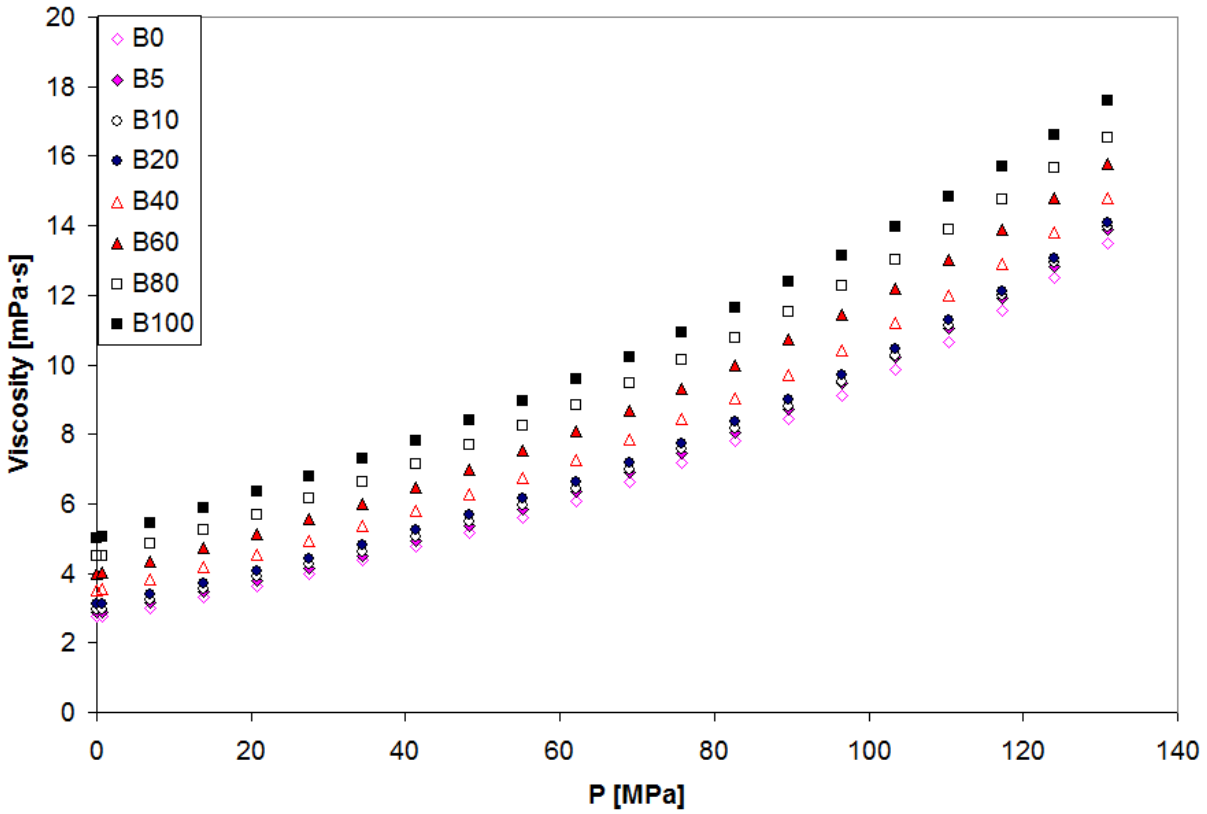


Figure 5.4. Viscosity with pressure for ULSD, B100 and blends: B5, B10, B20, B40, B60, B80 at 298.15 K.

The biodiesel blends in this work are predicted using two common mixing rules, Kay's mixing rule (Eqn. 5) and the Grunberg-Nissan mixing rule (Eqn. 6) described previously. The biodiesel blend viscosity was calculated using the ULSD and B100 Tait-Litovitz models to calculate the viscosities for ULSD and B100; those viscosities would then be used with the mixing rules described in Eqns. 5 and 6.

The biodiesel blend viscosity predictions using Tait-Litovitz models to calculate viscosities for each biodiesel blend at every isotherm can be found in Table 5.4 (the cloud point pressure measurement for B80 and 283.15 K was not included in calculations used for Table 5.4).

	283.15 K		298.15 K		313.15 K		343.15 K		373.15 K	
<i>Sample</i>	<i>G-N</i>	<i>Kay</i>	<i>G-N</i>	<i>Kay</i>	<i>G-N</i>	<i>Kay</i>	<i>G-N</i>	<i>Kay</i>	<i>G-N</i>	<i>Kay</i>
	AARD, %									
B5	4.09%	3.66%	1.37%	0.95%	0.59%	0.60%	0.52%	0.41%	2.55%	0.78%
B10	4.82%	4.01%	1.43%	0.87%	0.96%	0.51%	3.01%	2.26%	2.31%	1.71%
B20	1.84%	0.45%	1.64%	0.98%	1.33%	1.01%	1.77%	0.46%	1.99%	1.19%
B40	5.25%	2.90%	2.36%	0.83%	1.54%	1.15%	3.06%	0.87%	3.35%	1.31%
B60	6.62%	3.88%	4.01%	1.60%	4.14%	1.78%	4.92%	2.62%	2.49%	0.85%
B80	3.72%	1.49%	3.07%	1.33%	3.57%	1.88%	4.30%	2.65%	2.67%	1.03%
Total	4.37%	2.77%	2.31%	1.09%	2.02%	1.16%	2.93%	1.54%	2.56%	1.15%

Kay's mixing rule predicted the viscosity for every isotherm more accurately than the Grunberg-Nissan (G-N) mixing rule. B20 is a widely accepted biodiesel blend, and being able to predict its high-pressure viscosity behavior simply from the biodiesel and the diesel fuel it is derived from would be highly useful. B20's viscosity using Kay's mixing rule predictions are given in Figure 5.5.

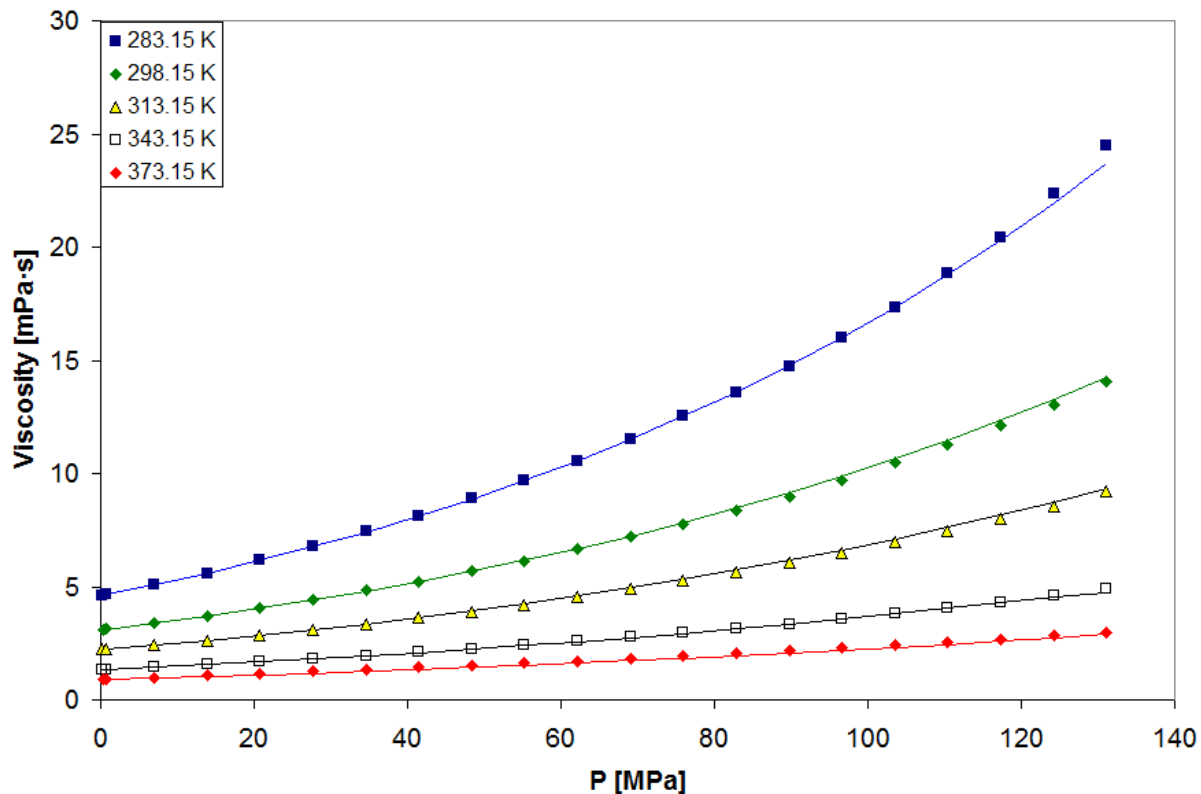


Figure 5.5. Viscosity with pressure for B20 at five isotherms: 283.15, 298.15, 313.15, 343.15, and 373.15 K with Tait-Litovitz model and Kay’s mixing rule.

The AARD% for all B20 data using Kay’s mixing rule was found to be 0.82%, and the maximum deviation for any single data point was found to be 3.55% at 0.1 MPa for the 373.15 K isotherm.

While higher percentage blends of biodiesel are less often used than low percentage blends, the success of a model throughout the entire biodiesel blend range may bring confidence to the methodology and be useful at a future time. The highest blend percentage of biodiesel tested was B80, with viscosities and model shown in Figure 5.6.

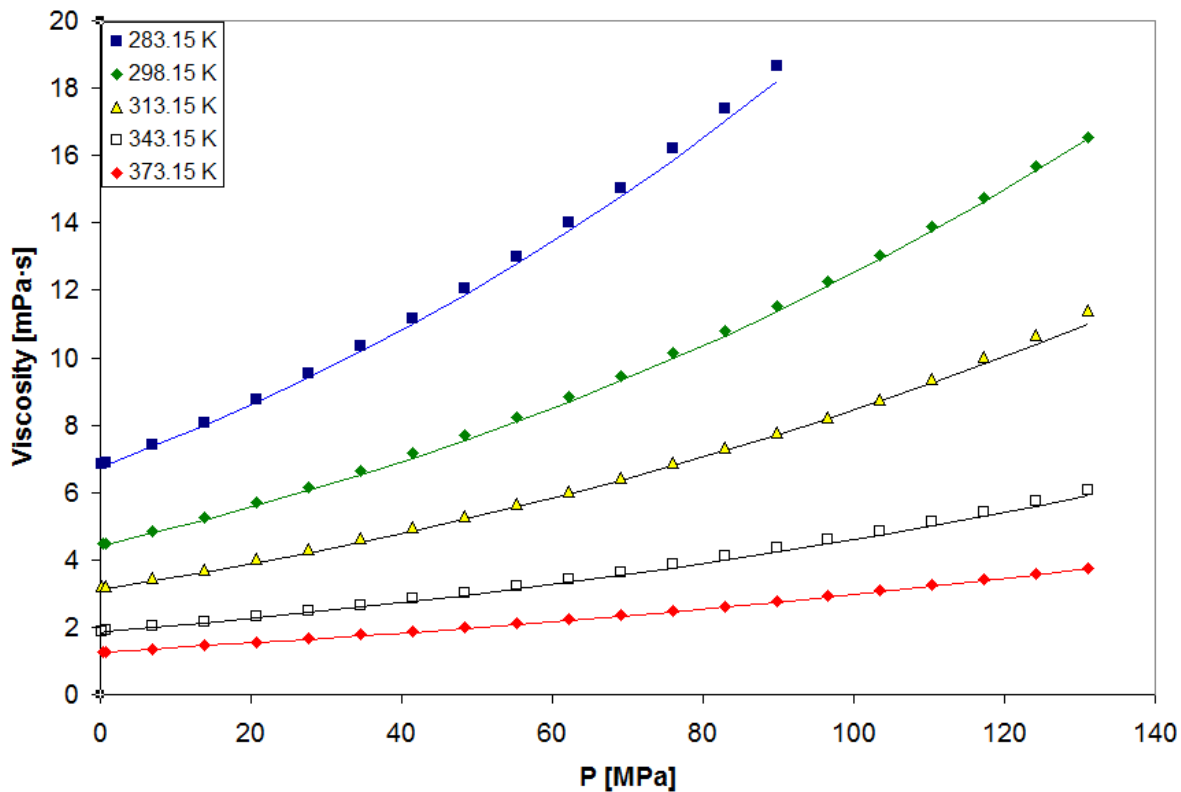


Figure 5.6. Viscosity with pressure for B80 at five isotherms: 283.15, 298.15, 313.15, 343.15, and 373.15 K with Tait-Litovitz model and Kay's mixing rule.

The prediction of all B80 viscosities using the Tait-Litovitz model approach along with Kay's mixing rule was found to yield an AARD% of 1.66%. The maximum error at any point was found to be 3.32% at 131 MPa for the 313.15 K isotherm.

The AARD% for the Tait-Litovitz model/Kay's mixing rule for all data was 1.51%, with a maximum deviation for any isotherm of 8.25%. The AARD% for G-N mixing rule for all data was 2.77% with a maximum deviation for any isotherm of 8.09%, both of which occur at 283.15 K and 131.1 MPa for B10. The biodiesel blend viscosity was also predicted at each point using the

ULSD and B100 data to verify that the error in the Tait-Litovitz model did not change the favorability of one mixing rule over the other. An overall comparison of both the data and the Tait-Litovitz based mixing rule can be found in Table 5.5. The viscosity calculated directly from data finds Kay's mixing rule superior to the Grunberg-Nissan mixing rule while yielding only slightly more accurate results than the Tait-Litovitz model-based viscosities.

Table 5.5. Mixing Rule Comparison: G-N (Grunberg-Nissan) and Kay (Kay's Rule) AARD %				
<i>Sample</i>	Data		T-L Models	
	<i>G-N</i>	<i>Kay</i>	<i>G-N</i>	<i>Kay</i>
AARD, %				
B5	1.55%	0.99%	1.82%	1.28%
B10	2.30%	1.50%	2.51%	1.87%
B20	1.54%	0.45%	1.71%	0.82%
B40	2.64%	0.97%	3.11%	1.41%
B60	4.33%	1.90%	4.37%	2.09%
B80	3.27%	1.60%	3.56%	1.73%
Total	2.60%	1.24%	2.77%	1.51%

The accuracies of the mixing rules seemed to have three different pressure regimes of performance. Separating the viscosity measurements into low, moderate, and high-pressure regions, the mixing rules are compared in Table 5.6.

Table 5.6. Empirical Mixing Comparison: Grunberg-Nissan (G-N) and Kay's Rule (K) AARD for Different Pressure Ranges						
	low pressure		moderate pressure		high pressure	
	0.1-34.5 MPa		41.5-82.8 MPa		89.7-131.1 MPa	
T[K]	G-N	K	G-N	K	G-N	K
283.15	4.6%	2.0%	3.8%	2.2%		
298.15	3.3%	0.9%	2.7%	1.2%	1.5%	1.0%
313.15	2.7%	1.3%	2.2%	1.3%	1.3%	1.2%
343.15	3.0%	1.3%	2.8%	1.4%	2.2%	1.3%
373.15	2.9%	1.2%	2.7%	1.3%	1.9%	0.8%
Total	3.3%	1.3%	2.8%	1.4%	1.8%	1.1%

While Kay's mixing rule appears to be fairly consistent regardless of pressure region, the Grunberg-Nissan mixing rule decreases in AARD% as the pressure increases, from 3.3% at low pressure to 1.8% for the high-pressure region. Kay's mixing rule has a lower AARD% at the high-pressure region than Grunberg-Nissan, it is possible that for pressures far outside of the testing range, the Grunberg-Nissan mixing rule might become more accurate if the trend were to continue--it has been observed in other works that viscosity mixing behavior varies with increasing pressure⁹.

5.3.4 B100 and Blends at Low Temperature

Robertson and Schaschke¹⁰ provide literature data for the viscosity of sunflower biodiesel and blends at high pressures. Robertson and Schaschke's work was the only other work that examined biodiesel blends at high pressures prior to this study. While no tabulated data are given, equations were provided for B20 and B100 derived from sunflower oil. The only common isotherm between Robertson and Schaschke's work and this work is at ~283.15 K. To compare the data more easily, the data are normalized to their ambient pressure viscosity at the given temperature (η_p / η_0). Figure 5.7 shows the normalized B100 and B20 viscosities from our data compared with the correlations given in the literature.

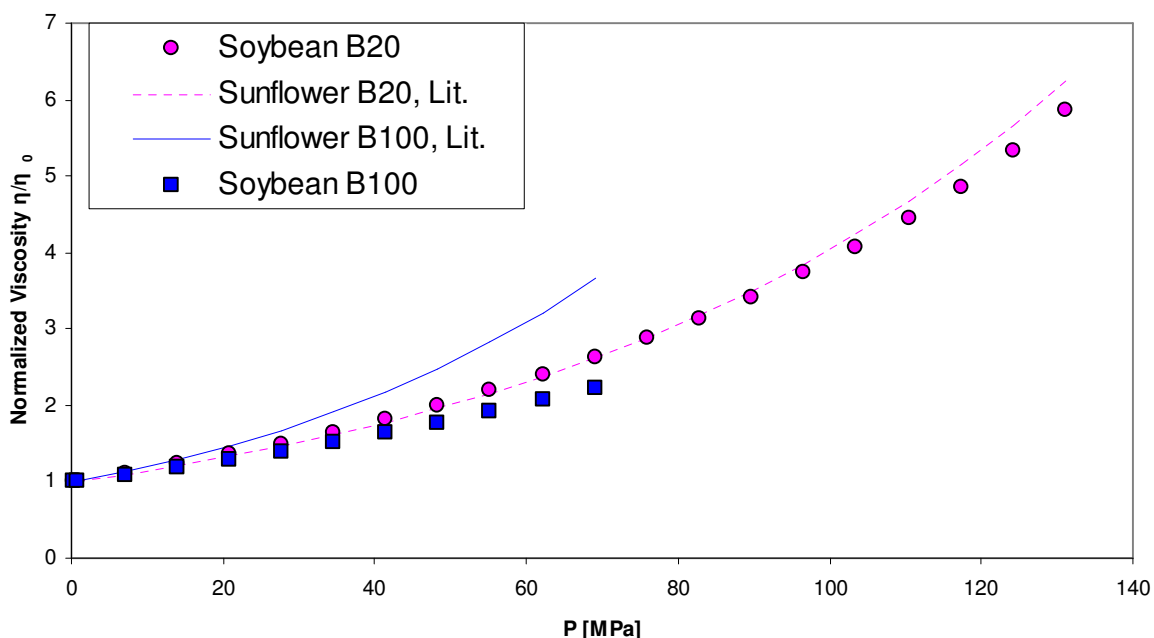


Figure 5.7. Normalized viscosity with pressure for soybean B20 and B100 at 283 K from this work, and literature correlations for sunflower B20 and B100 from Robertson and Schaschke.

The normalized B100 correlation found in Robertson and Schaschke's work indicates a significantly higher pressure effect with sunflower B100 viscosity compared to the soybean biodiesel in this work; whereas, the normalized correlation and data for the B20 isotherms appear to be more congruous. In our previous contribution⁴, we had measured the high-pressure viscosity of biodiesels derived from two types of soybean oil, new and used canola oil, and coconut oil. While the biodiesel samples had a wide range of ambient pressure viscosities, their normalized viscosity were very similar even at the highest pressures. This large deviation between our soybean oil biodiesel and the literature sunflower oil may be an artifact of the indirect method in which the sunflower biodiesel viscosity was measured in the literature report. This method requires the density of the high-pressure diesel and biodiesel samples

which are not available or measured. The Peng-Robinson equation of state was used to determine the liquid-phase density assuming that the density of methyl oleate was equal to the sunflower biodiesel. Cubic equations of state can be problematic when evaluating the liquid density of long-chained hydrocarbons¹¹ and this may be the reason for such a large different difference.

One of the benefits of using biodiesel in blends with diesel fuel alluded to in Chapter 2 is to effectively lower the cloud point of the fuel, allowing the fuel to be used in lower temperature environments. Biodiesel pressure-induced phase change was documented in our previous work for several vegetal feedstock sources at 283.15 K⁴, but not for the petroleum-based diesel fuel tested. Others in the literature also discuss this phase change; for example, Robertson and Schaschke¹⁰ suggests a phase change occurs within a sunflower B20 biodiesel blend at temperatures of 283 K and at successive lower temperatures at higher pressures. The approximate freezing points reported for fuels B100, B80, B60 and B40 for the 283.15 K isotherms are found in Figure 5.8.

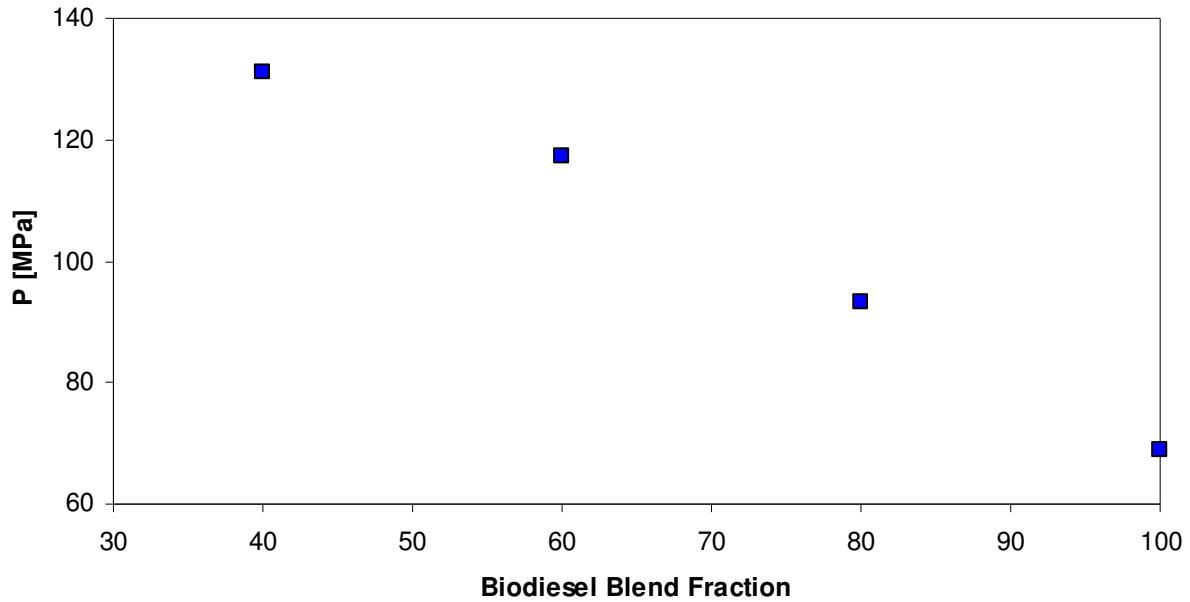


Figure 5.8. Final viscosity measurement before possible cloud point pressure for several biodiesel blends at 283.15 K.

The cloud point pressure increases, almost linearly, with decreasing biodiesel blend fraction. Further investigation into this phenomenon may yield possible optimum biodiesel blend fractions relative to environmental conditions, engine injection pressure, etc. to help widen biodiesel usage.

5.3.5. Empirical and Extrapolated Crossover Pressures

Biodiesel blend ambient viscosity increases with increasing biodiesel fraction for all temperatures examined. However, at elevated pressures the viscosity of the blends with higher amounts of biodiesel would actually have lower viscosity than lower amounts of biodiesel. Figure 5.9 indicates the crossover pressures at 283.15K at ~69 MPa for B10 and B20 and at ~100 MPa for B5 and B20.

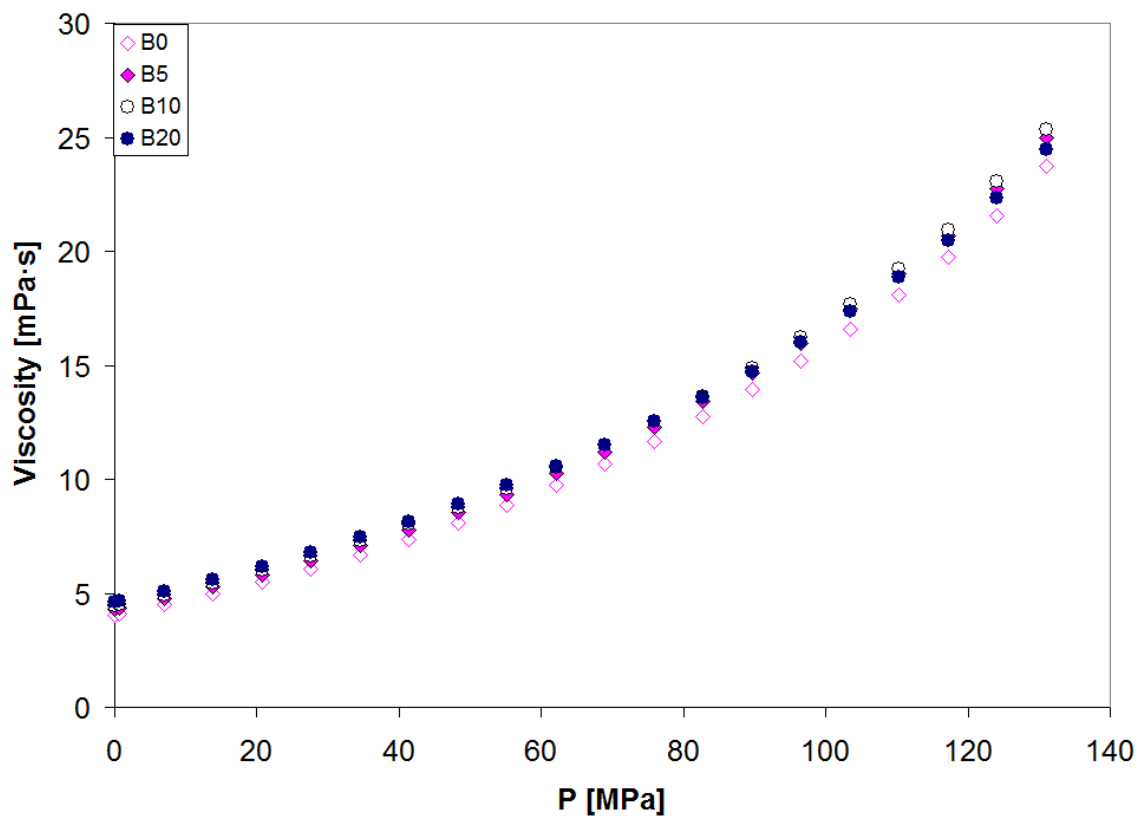


Figure 5.9. B0, B5, B10 and B20 at 283.15 K viscosity with pressure. Crossover pressures were found for B10 and B20 at ~69 MPa, and for B5 and B20 at ~100 MPa.

The crossover pressure indicates a point where, despite different blend composition, the same viscosity is found. While no other crossover pressures were found in the experimental data in

this work, when the data are extrapolated to pressures proposed in future engine designs, crossover pressures occur for most fuels. Figure 5.10 illustrates the predicted crossover phenomena for B0, B20, and B100 at 298.15 K at extrapolated pressures—pressures beyond the 131 MPa tested using the Tait-Litovitz hybrid equation.

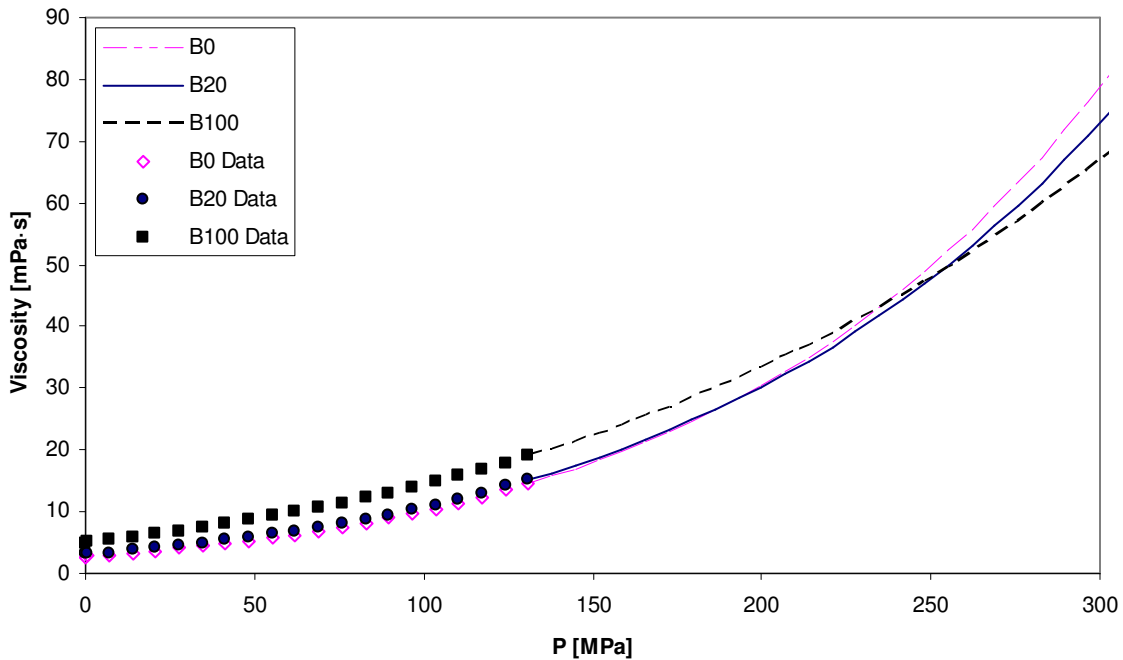


Figure 5.10. B0, B20, and B100 extrapolated (using the Tait-Litovitz model regressed for each isotherm) for pressures up to 300 MPa at 298.15 K. Several crossover pressures were identified.

The extrapolated data predicts crossover pressures of ~190 MPa for B20 and B0, ~235 MPa for B100 and B0, and ~250 MPa for B100 and B20. While these are merely extrapolated predictions well beyond the experimental range, they do, however, allude to the possibility that biodiesel may in actuality, reduce the viscosity of petroleum-based diesel at pressures anticipated for current and future injector pressure ranges.

5.4 Ramifications on Current and Future (Bio-)Diesel Engines and Designs

Viscosity plays a significant role in both the injection and combustion process of a compression ignition engine. Moreover, biodiesel feedstocks have different properties and a wide variation of viscosity exists among blends and neat options. As a result, when the consumer fills up at the pump with an unknown biofuel, the Engine Control Unit (ECU) must react dynamically in order to adjust injection timing appropriately ensuring that performance is not lost while emissions do not exceed regulatory standards. By better understanding biodiesel and biodiesel blend properties, fuel sensors for thermal conductivity¹² and density¹³ can be employed in the fuel system in order to indicate the percentage and type of biodiesel feedstock. Then, by embedding the viscosity models developed in this paper within the ECU, adjustments to fuel injection timing and rate shaping can occur immediately. This guarantees that the consumer retains maximum fuel economy and performance (e.g. acceleration) when running on any blend of biodiesel. The result is a more widespread acceptance of biodiesel at the pump along with subsequently increasing the likelihood of meeting RFS2 targets.

5.5. Conclusions

The viscosity of soybean biodiesel (B100), ultra low sulfur diesel (ULSD), and several biodiesel/diesel blends were measured to determine the effect of high-pressures (up to 131 MPa) for a large temperature range, 283.15-373.15 K. B100 and ULSD behavior was modeled well with a Tait-Litovitz hybrid equation. Biodiesel blends were found to be well-predicted using mixing rules assuming a pseudo-binary system. The overall AARD% was 1.51% using Kay's mixing rule and 2.77% using the Grunberg-Nissan mixing rule, with the Tait-Litovitz hybrid equation. Pressure-induced cloud points were found at 283.15 K for biodiesel blends as low as

B40 at the highest pressures tested. Blend percentage usage may be tailored based on environmental temperature constraints in conjunction with the state of injection technology to optimize the use of biodiesel as a fuel in new high-pressure systems.

References for Chapter 5

1. Dymond, J.; Malhotra, R., The Tait equation: 100 years on. *International Journal of Thermophysics* **1988**, 9, (6), 941-951.
2. Kashiwagi, H.; Makita, T., Viscosity of twelve hydrocarbon liquids in the temperature range 298–348 K at pressures up to 110 MPa. *International Journal of Thermophysics* **1982**, 3, (4), 289-305.
3. Duncan, A. M.; Pavlicek, N.; Depcik, C. D.; Scurto, A. M.; Stagg-Williams, S. M., High-pressure viscosity of soybean-oil-based biodiesel blends with ultra-low-sulfur diesel fuel. *Energy & Fuels* **2012**, 26, (11), 7023-7036.
4. Duncan, A. M.; Ahosseini, A.; McHenry, R.; Depcik, C. D.; Stagg-Williams, S. M.; Scurto, A. M., High-Pressure Viscosity of Biodiesel from Soybean, Canola, and Coconut Oils. *Energy & Fuels* **2010**, 24, (10), 5708-5716.
5. Tate, R.; Watts, K.; Allen, C.; Wilkie, K., The viscosities of three biodiesel fuels at temperatures up to 300 C. *Fuel* **2006**, 85, (7), 1010-1015.
6. Aksoy, F.; Baydir, Ş.; Bayrakçeken, H., The viscosity at different temperatures of soybean and sunflower biodiesels and diesel fuel blends. *Energy Sources, Part A: Recovery, Utilization, and Environmental Effects* **2009**, 32, (2), 148-156.
7. Yoon, S. H.; Park, S. H.; Lee, C. S., Experimental investigation on the fuel properties of biodiesel and its blends at various temperatures. *Energy & Fuels* **2007**, 22, (1), 652-656.
8. Tat, M. E.; Van Gerpen, J. H., The kinematic viscosity of biodiesel and its blends with diesel fuel. *Journal of the American Oil Chemists' Society* **1999**, 76, (12), 1511-1513.
9. Bair, S., The high pressure rheology of mixtures. *Journal of tribology* **2004**, 126, (4), 697-702.

10. Robertson, L.; Schaschke, C., Combined high pressure and low temperature viscosity measurement of biodiesel. *Energy & Fuels* **2009**, 24, (2), 1293-1297.
11. Mulero, A.; Cachadina, I., Liquid saturation density from simple equations of state. *International Journal of Thermophysics* **2007**, 28, (1), 279-298.
12. Hofmann, T.; Beckmann, F.; Michaelis, S.; Zacheja, J.; Binder, J.; Tagliante, S., Comparison of a conventional with an advanced micromachined flexible-fuel sensor. *Sensors and Actuators A: Physical* **1997**, 61, (1-3), 319-322.
13. Integrated Sensing Systems ISSYS' New Density Sensor for Fuel Applications.
http://www.mems-issys.com/pdf/whitepaper-ISSYS_fuel_quality_sensor.pdf

Chapter 6

High-Pressure Viscosity of *Jatropha* Biodiesel and Biodiesel-Diesel Blends

One of the more promising feedstocks for biodiesel production is oil derived from the *Jatropha curcas* plant. *Jatropha curcas* (*Jatropha*) is a small tree grown in and near equatorial regions known for its medicinal properties and oil producing capability¹. Unlike many other seeds and seed oils used in biodiesel production, the seeds of the *Jatropha* plant are poisonous to both humans and most animals¹, and therefore *Jatropha* does not directly interfere with food production, giving the possibility of a more viable feedstock. ***This is the first work to report the viscosity of *Jatropha* biodiesel and *Jatropha* biodiesel-diesel blends above 7 MPa.***

6.1 Biodiesel and Petroleum Diesel Samples

The *Jatropha* oil was acquired from Agroenhsa SA, Honduras and produced as described in Chapter 2. The composition of *Jatropha* biodiesel is found in Table 6.1. The average molecular weight of the *Jatropha* biodiesel was calculated from Table 6.1 to be 278 g/mol.

Table 6.1 <i>Jatropha</i> Biodiesel				
FAME Composition by wt %.				
C16:0	C16:1	C18:0	C18:1	C18:2
13.0	0.5	7.4	43.9	34.1

The diesel fuel was ultra low sulfur diesel (ULSD) and came from a local gas station. Gas stations in the United States are allowed to sell diesel fuel with biodiesel content of five percent or less by volume without identification². Carter Energy, the supplier to the local gas station verified that the diesel collected did not contain biodiesel. The average molecular weight of the diesel fuel was found to be 207 g/mol using the methodology presented in Chapter 2.

6.2 Ambient-Pressure Viscosity

An exponential decrease in viscosity with increasing temperature was found for all fuels. The Litovitz correlation presented in earlier chapters was used to model the ambient-pressure viscosity of biodiesel and ULSD as shown in Figure 6.1.

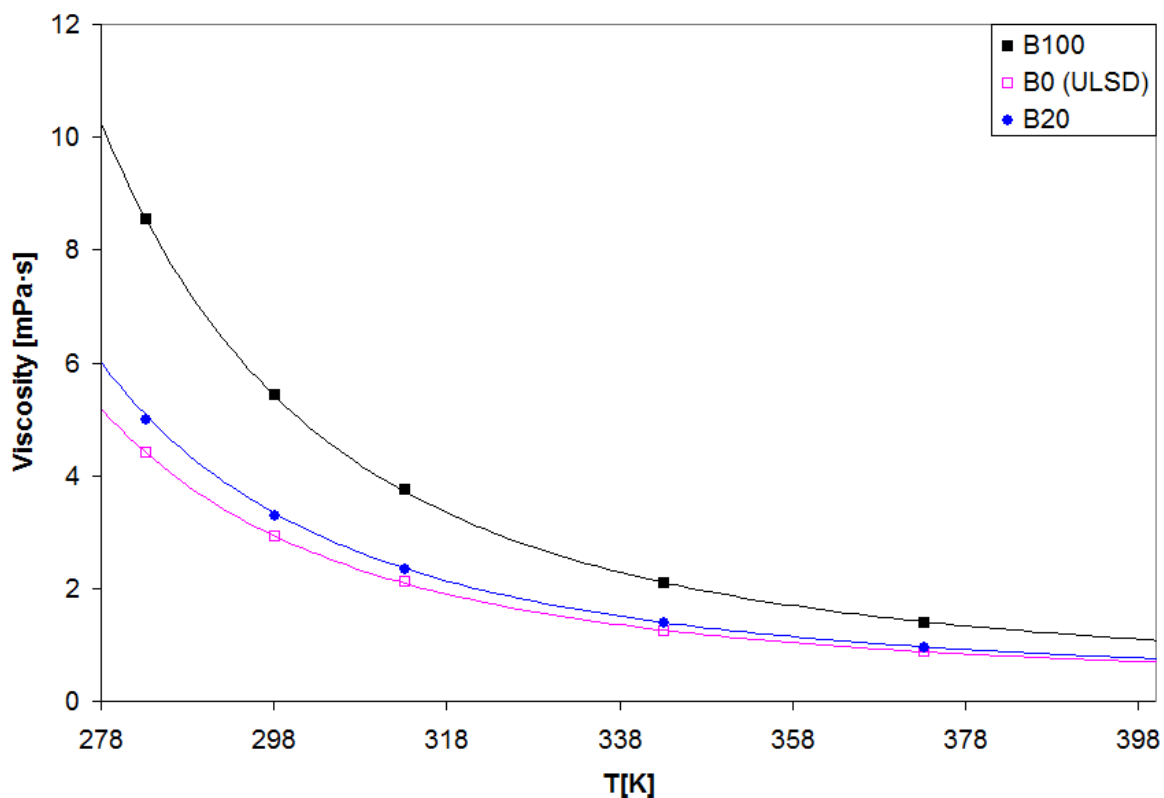


Figure 6.1. Jatropha biodiesel (B100), ULSD (B0), and B20 blend viscosities at ambient pressure.

The empirical data are given as symbols. The Litovitz model for B100 and B0 are given as lines, and Kay's mixing rule was used to generate the line for B20. The absolute average relative deviation (AARD) for biodiesel was 0.85% with the largest deviation of 2.03% at 373.15 K, and the AARD of ULSD was 0.68% with the maximum deviation of 1.67% also at the highest

temperature tested, 373.15 K. Blends with lower concentrations of biodiesel, B5 and B10, are not included for visual clarity as those data are found between B0 and B20.

6.3 High-Pressure Viscosity

As with the soybean biodiesel blends work³, isotherms of 283.15, 298.15, 313.15, 343.15 and 373.15 K were measured for all fuels: ULSD (B0), B5, B10, B20 and jatropha biodiesel (B100) at pressure increments of 7 MPa from atmospheric pressure to 131 MPa. The high-pressure viscosity data can be found in Tables C.15 to C.19 in Appendix C.

6.3.1 Jatropha Biodiesel and Tait-Litovitz Modeling

The Tait-Litovitz (T-L) model with temperature-linearized Tait parameters was used to accurately model the jatropha biodiesel. All five isotherms are shown in Figure 6.2. The empirical data is given as symbols while the T-L model is represented with solid lines.

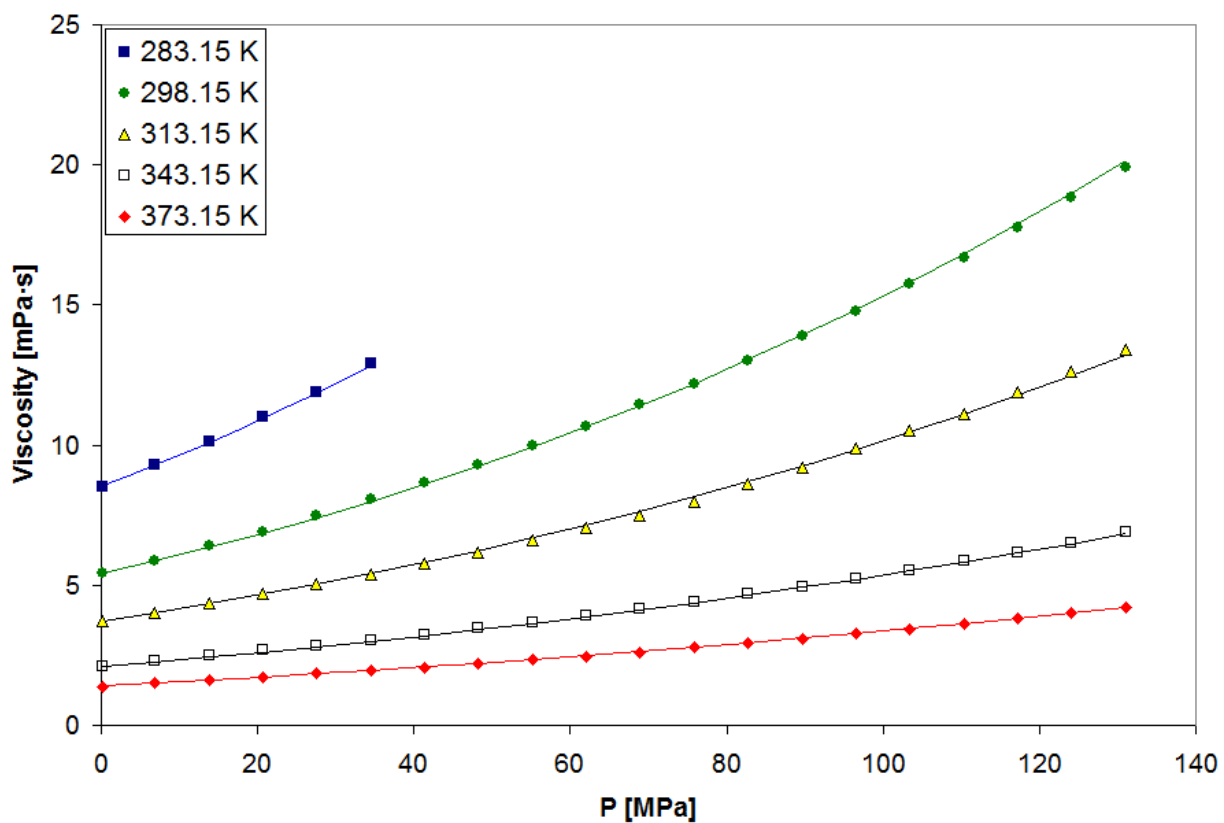


Figure 6.2. Viscosity as a function of pressure for jatropha biodiesel.

The AARD for the entire data set was 0.81 % while the maximum deviation was 2.66% as seen in Figure 6.3. The maximum deviation of the model was within the stated uncertainty of the instrument.

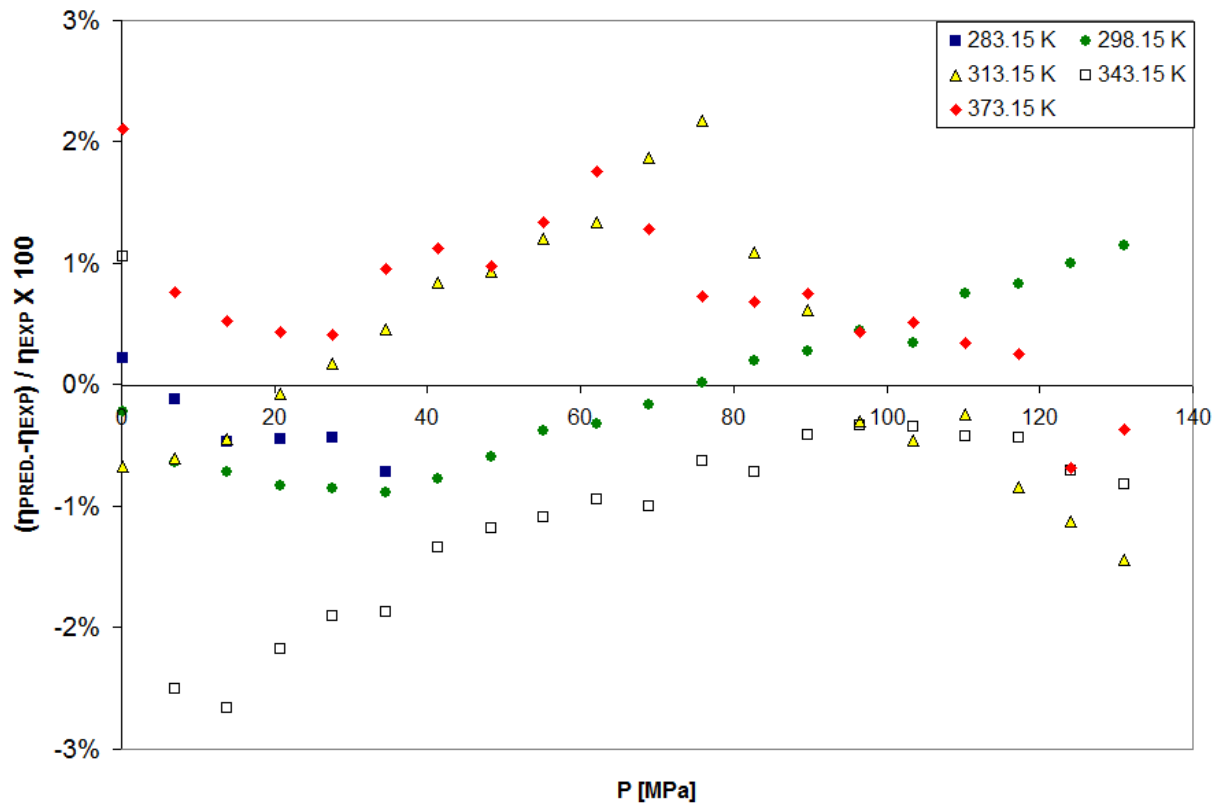


Figure 6.3. Residuals for the high-pressure viscosity of jatropha biodiesel and the Tait-Litovitz hybrid equation.

There is an initial bias for all isotherms due to the Litovitz parameters being used for ambient viscosity. The largest initial deviation is in the 343.15 K isotherm, but overall the model represents the data well.

6.3.2 Jatropha Biodiesel Comparisons

The jatropha biodiesel viscosity showed similar trends with pressure as those biodiesels studied in Chapters 4 and 5. The biodiesel viscosities were found to vary significantly with feedstock. Figure 6.4 includes biodiesels from Chapters 4 and 5 and from recent literature^{4, 5}. At a maximum pressure of 131 MPa, coconut oil biodiesel, composed mostly of shorter-chained FAMES, has the lowest viscosity. In our works, jatropha biodiesel had the highest viscosity at 131 MPa and 313.15 K among all fuels, though it was very similar to both canola samples.

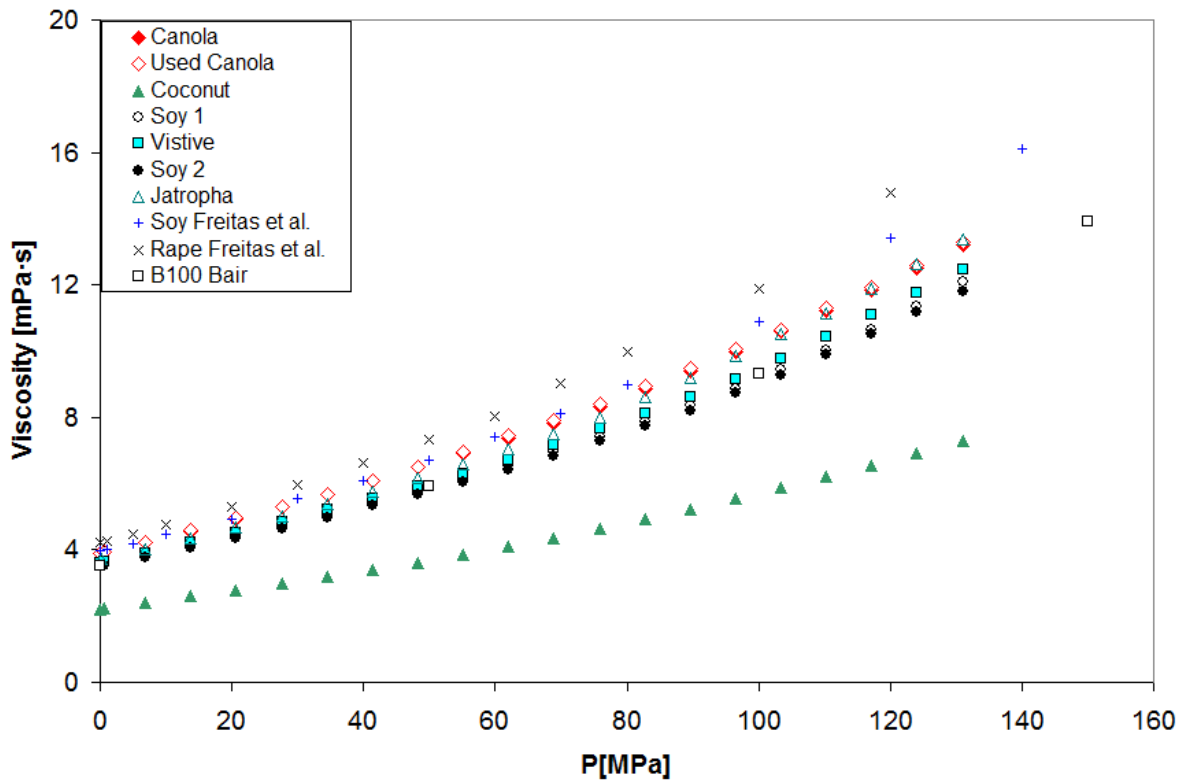


Figure 6.4. High pressure viscosity of biodiesels at 313.15 K.

The soy and canola samples from Freitas et al. had the highest viscosities, of all biodiesels, but maintained the trend observed in our work, where the canola biodiesel maintained greater viscosity relative to soybean biodiesel.

At the highest temperature tested, given in Figure 6.5, the overall trends were very similar to data at 313.15 K. However, jatropha biodiesel was found to have a viscosity at the maximum pressure tested that was slightly less than the canola samples, though still greater than the soy samples.

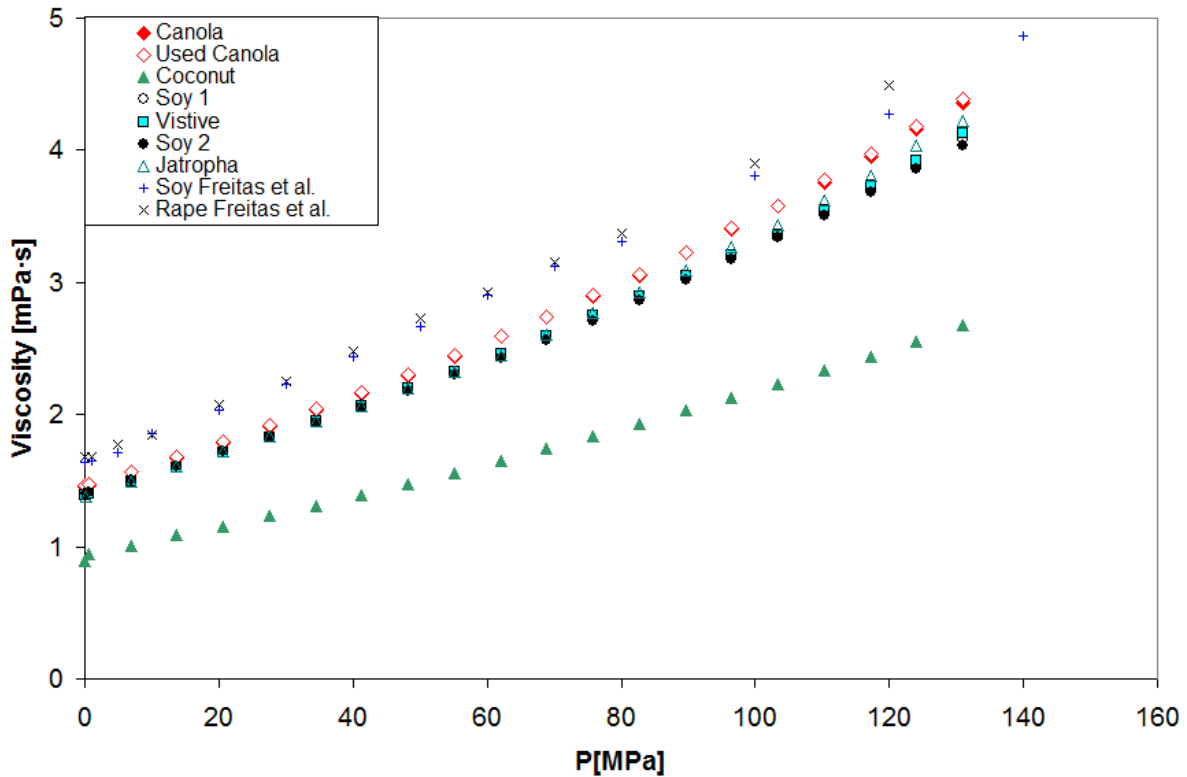


Figure 6.5. High-pressure viscosity of biodiesels at 373.15 K.

Figure 6.6 compares jatropha and other biodiesel samples from our work to literature data⁶ at 283.15 K. The difference in trend between the literature data and our biodiesels is likely due to Robertson and Schaschke's assumptions used to calculate density which was necessary for their method of viscosity determination. Accurate density data was required, but unavailable.

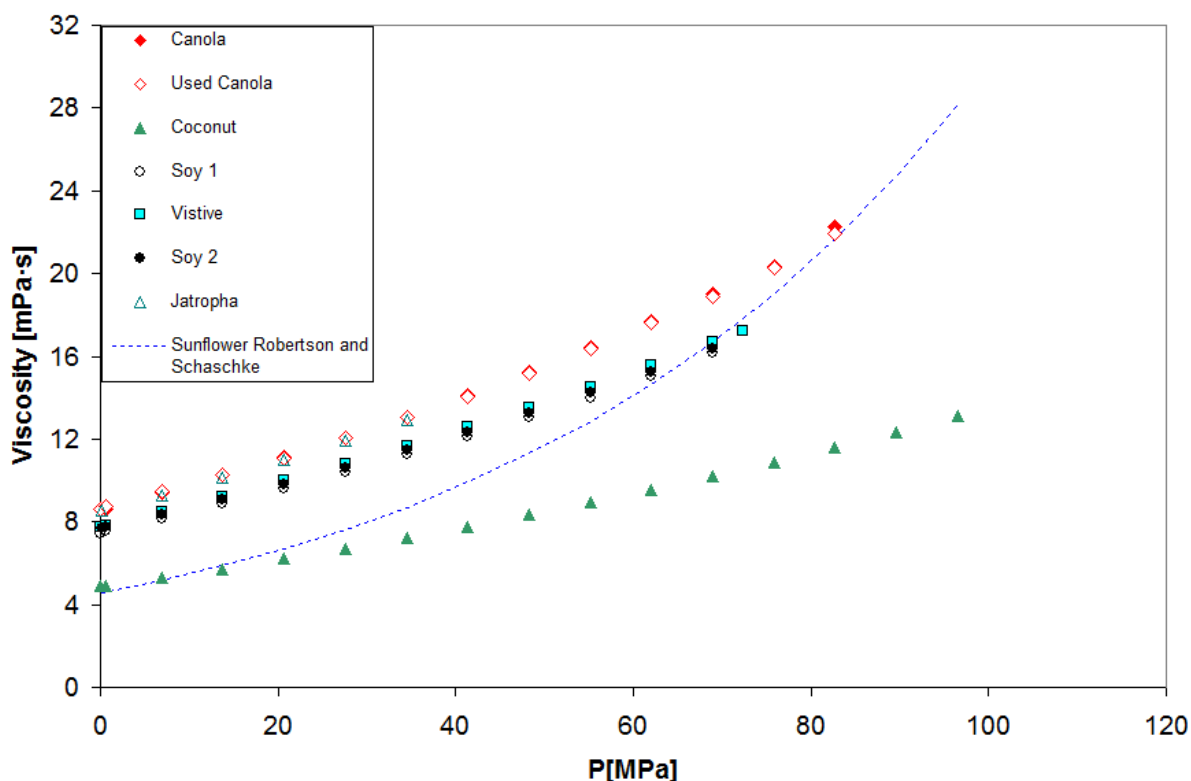


Figure 6.6. High-pressure viscosity of biodiesels at 283.15 K.

6.3.3 Jatropha and Soy Biodiesels

The soybean biodiesel from our two previous works is very similar to the soybean biodiesel of Bair⁵, and when interpolated, these samples (not including Vistive low-linolenic soy) were found to have an AARD of less than 2% for both fuels. Jatropha biodiesel has a viscosity that is greater than the soybean biodiesels from our previous works and the work of Bair, but less than the

works of Freitas et al., as shown in Figure 6.7. The greater viscosity of jatropha biodiesel is likely due to the higher amounts of methyl oleate (C18:1) compared to the soybean biodiesels, which are richer in methyl linoleate (C18:2).

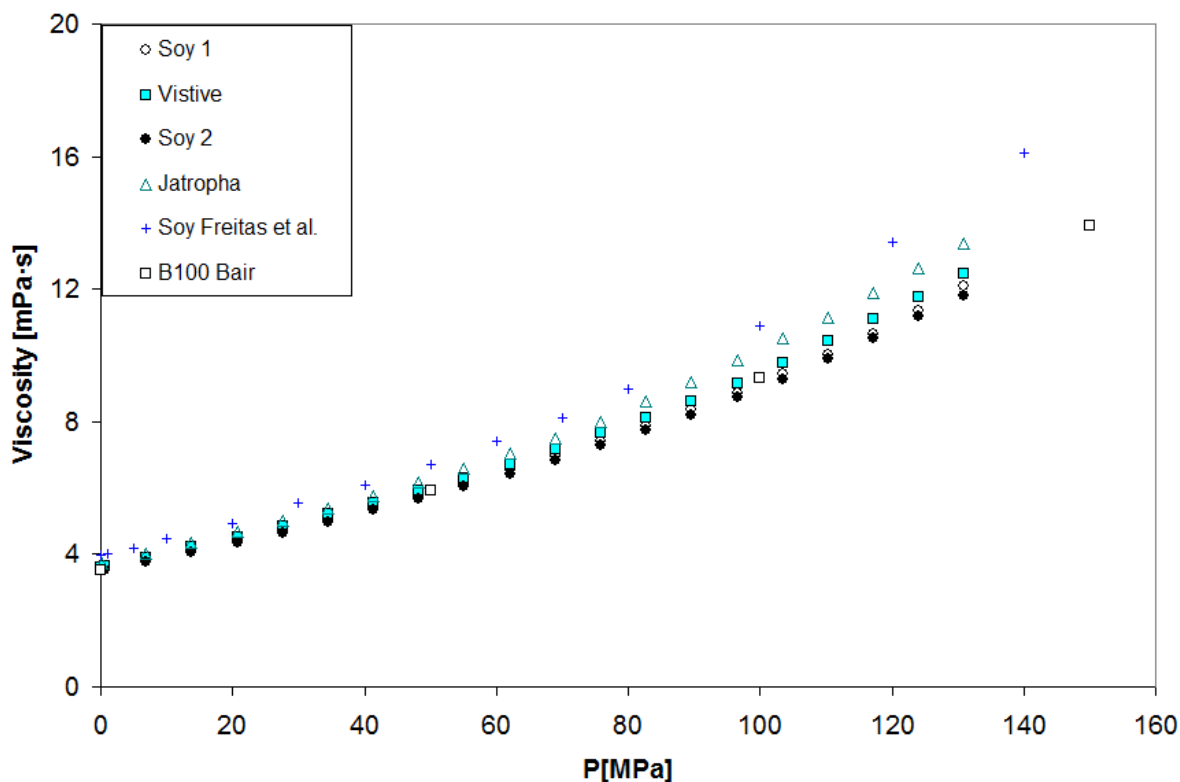


Figure 6.7. High-pressure viscosity of Jatropha biodiesel and soybean biodiesels from literature at 313.15 K.

6.3.4 Jatropha and Canola Biodiesels

The viscosity of jatropha biodiesel trended most similarly to the canola oil-based biodiesels⁷. Recent works have measured the high-pressure viscosity of soybean and rapeseed (canola), biodiesels⁴ given in Figure 6.8. Jatropha biodiesel has a composition which is fairly similar to canola. The amount of methyl oleate composition was found to be 10 to 20% less in jatropha,

but the methyl palmitate (C16:0) composition was approximately 10% greater than canola oil. Figure 2.4 showed how C16:0 and C18:1 had nearly equivalent viscosities for much of the temperature range at ambient pressure, in essence, the sum of these two components in each fuel results in an equivalent viscosity contribution for both fuels.

Figure 6.8 also indicates that a cross-over pressure between jatropha and canola is occurring. While a true cross-over pressure is possible due to their difference in composition, at the 313.15 K isotherm the fuels used different pistons. An overlap was observed in a viscosity standard given in Appendix B with a similar bias. The bias was small and within the uncertainty of the instrument.

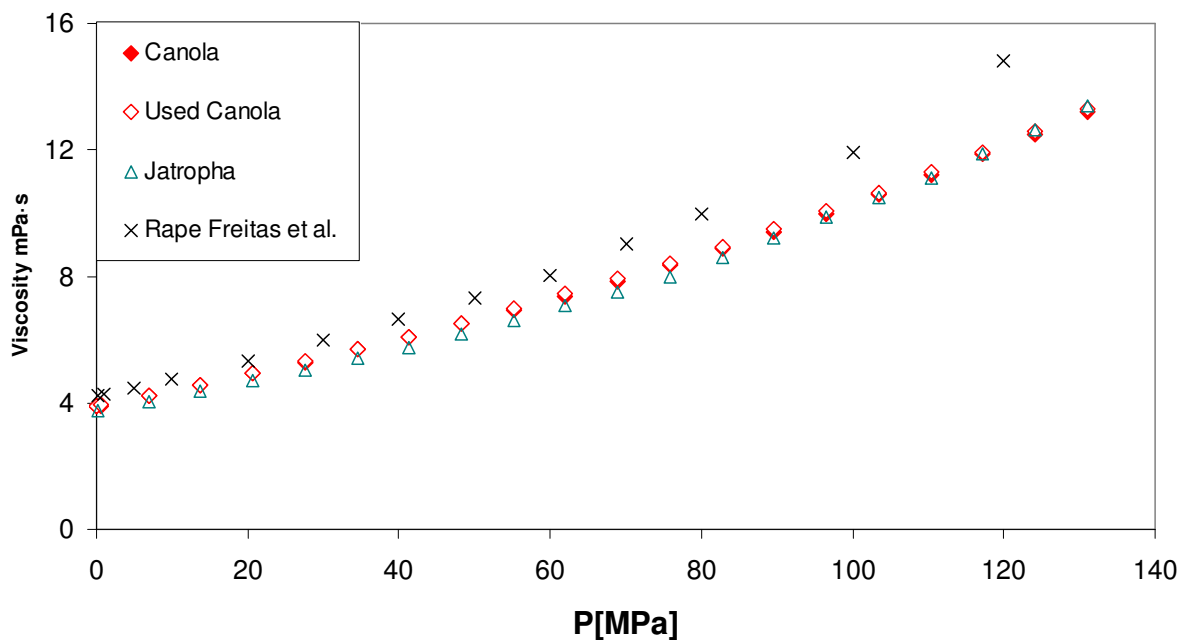


Figure 6.8. High-pressure viscosity of jatropha biodiesel and canola based biodiesels from literature at 313.15 K.

Figure 6.9 gives the high-pressure viscosity of biodiesels including the last data point prior to their approximate cloud point pressure at 283.15 K. Jatropha has the lowest pressure at which this occurs at approximately 35 MPa.

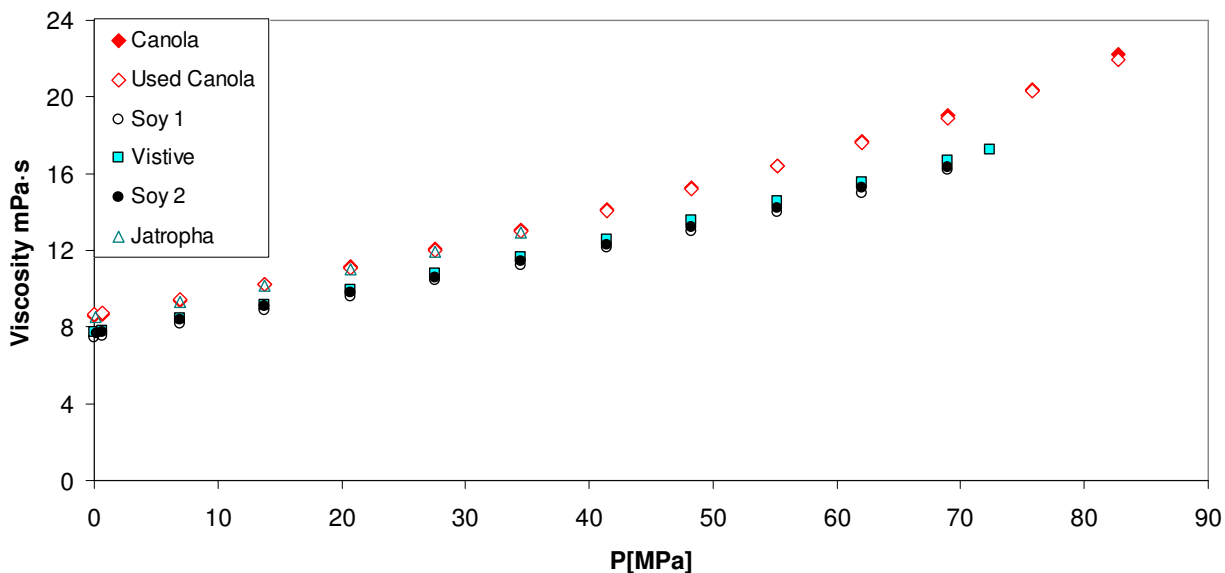


Figure 6.9. High-pressure viscosity of jatropha, canola and soy-based biodiesels at 283.15 K.

The 20% long-chained saturated FAMES of jatropha, given in Table 6.1, are likely the cause for this significant difference. The order of increasing cloud point pressure of the fuels was observed to be jatropha < soy < canola, which corresponds to the decreasing level of long-chained saturated FAMES in each feedstock which are in order of increasing amounts: canola < soy < jatropha. At extremely high pressures (250-1000 MPa), additive amounts of a particular component have been shown to have a significant affect on viscosity, decreasing some samples by as much as 60% at 1000 MPa⁸. In the pressure range examined in this work, the viscosity appears to *mostly* be an approximate sum of pure component viscosities and quantities, while

the cloud point pressure appears almost entirely effected by the percent composition of long-chained saturated FAMES.

6.3.5 Normalized Viscosity of Jatropha and Other Biodiesels

Chapter 4 showed that despite the wide range of viscosity, the relative percent increase among biodiesels was fairly similar, as seen in the normalized viscosity plot in Figure 6.10. This phenomenon will be analyzed further in Chapter 7.

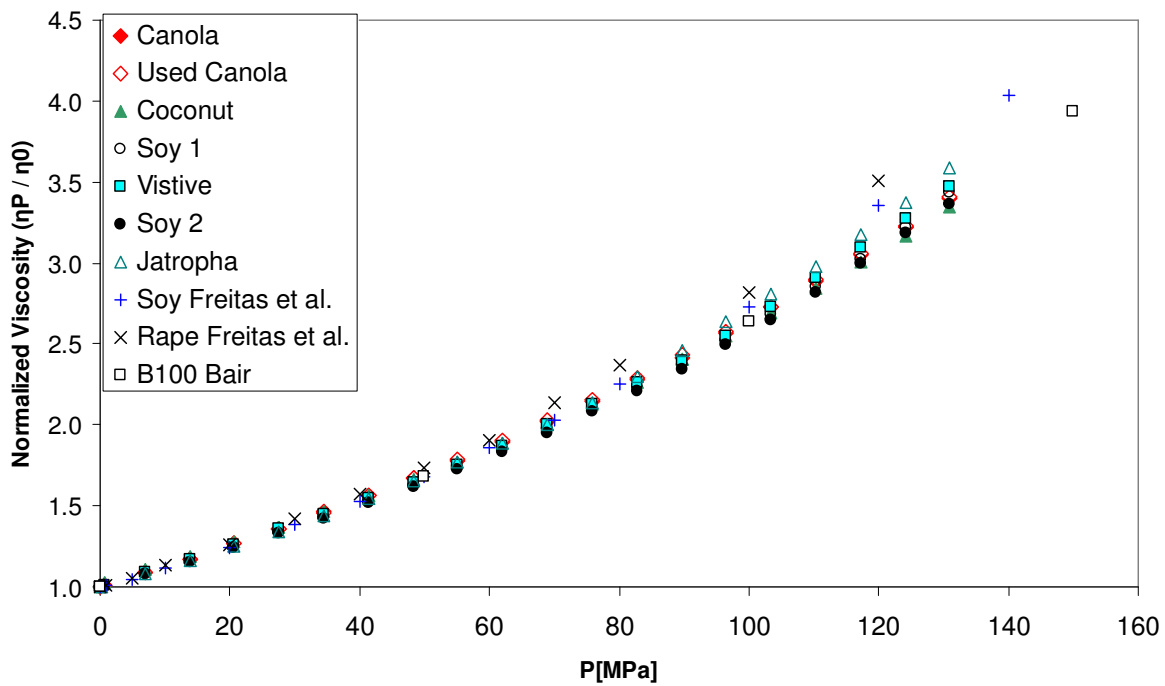


Figure 6.10. Normalized viscosity of biodiesels at 313.15 K.

Jatropha biodiesel's normalized viscosity is very similar to the other fuels studied, although its increase with pressure is slightly greater. I would suggest that it is the decreased mobility of

the saturated components at higher densities that are responsible for this slightly greater increase.

Data from Freitas et al., had a similar normalized viscosity profile as fuels in this dissertation and that in Bair's work until approximately 70 MPa, at which point the viscosity increased at a much faster rate. The trend with Freitas et al.'s work is reversed at high temperature, and the normalized viscosity of biodiesels differentiates themselves at approximately 110 MPa, with a slightly smaller percent viscosity increase as shown in Figure 6.11.

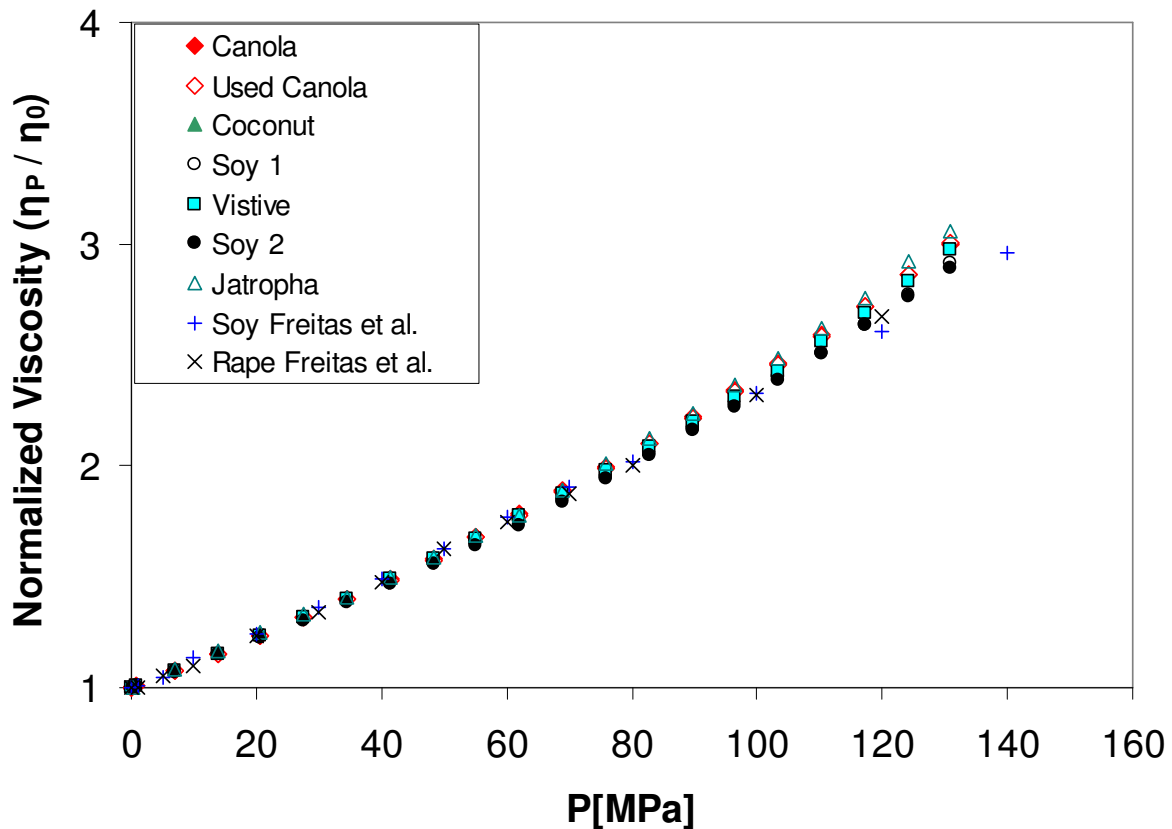


Figure 6.11. Normalized viscosity of biodiesels at 373.15 K.

While Freitas's soy and canola samples at 313.15 and 373.15 K have viscosities that are greater than all of our biodiesel samples, the change with temperature of the normalized-viscosity trend is surprising. Further work would be needed to understand the difference.

6.4 Jatropha Biodiesel Blends Comparison

Each isothermal data set was collected with the same piston, so any small differences among pistons due to their calibration with the pressure or temperature correction factors will not affect mixing rule agreement. After the publication of the soybean biodiesel blend work, multiple works of diesel and diesel blend data sets have been produced^{5, 9}. Overlapping data sets with works from outside authors include B20 blend of sunflower biodiesel at 283.15 K⁶, B5 blend of rape (canola) biodiesel and petroleum diesel at 298.15 K⁹, and a B20 blend of an unknown biodiesel with petroleum diesel (from Chevron Phillips) at 313.15 K⁵. Figure 6.12 gives the viscosity of B20 blends with pressure.

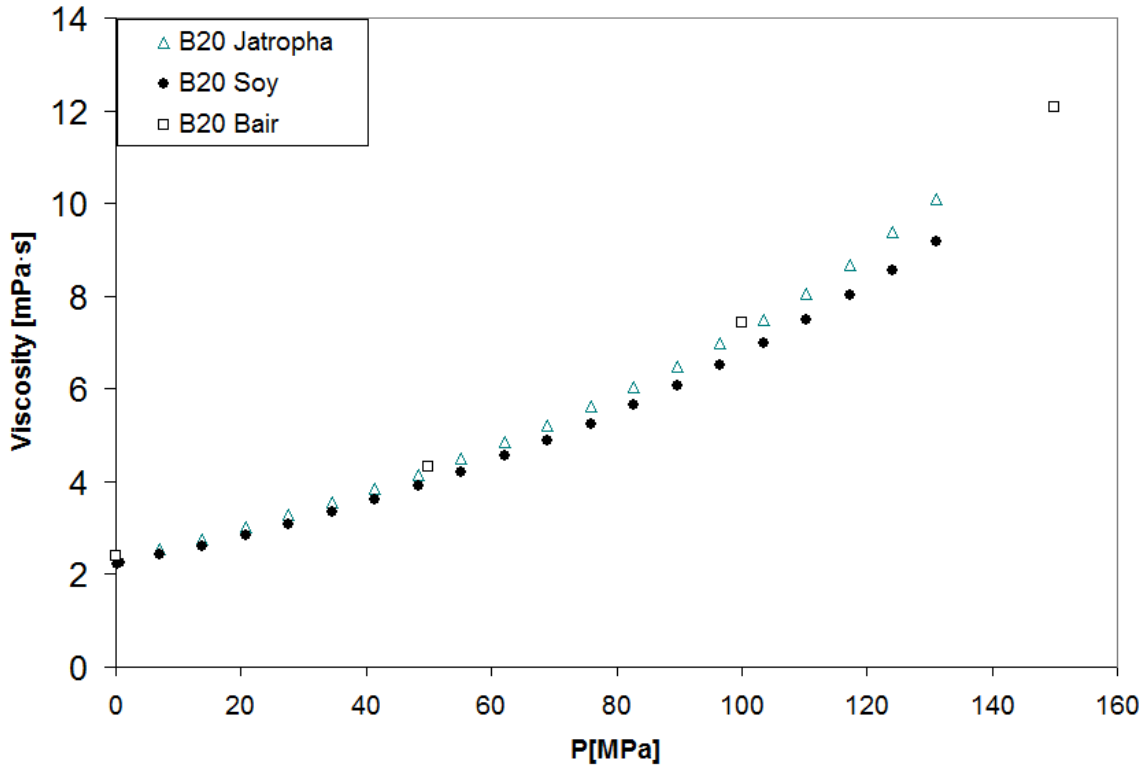


Figure 6.12. High-pressure viscosity of B20s at 313.15 K.

The jatropha B20 blend has a viscosity that is comparable to both the B20 soy blend and the B20 blend produced commercially. While the biodiesel source in the B20 blend in Bair's work is not identified, we might suspect that it is a fuel with a viscosity that is very similar to jatropha, possibly canola biodiesel, which is produced widely in the United States. The normalized behavior shown in Figure 6.13 among the three blends is nearly identical to the results in Figure 6.10 with the jatropha blend appearing to be slightly more effected by pressure.

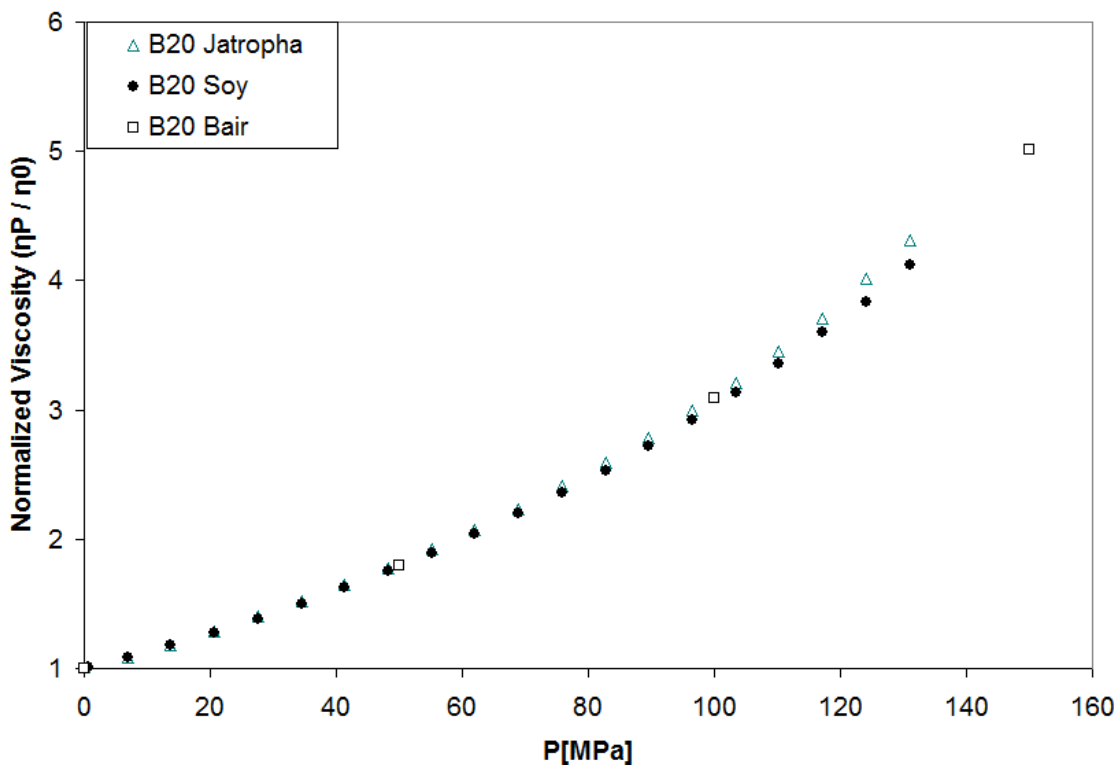


Figure 6.13. Normalized viscosity of B20s at 313.15 K.

While the two diesel samples used to blend soy B20 and jatropha B20 were different, the normalized rate of viscosity increase in these blends is consistent with Figure 6.10, with the jatropha sample having a slightly greater rate of increase in viscosity than soybean biodiesel blends from Chapter 5 and from literature. *At lower temperatures, the effect of biodiesel source on the blend intensifies.* Figure 6.14 indicates that at 283.15 K, **Jatropha B20 has a potential cloud point pressure** near the end of the pressure range as indicated by a significant increase in viscosity followed by the inability to collect data at even higher pressures.

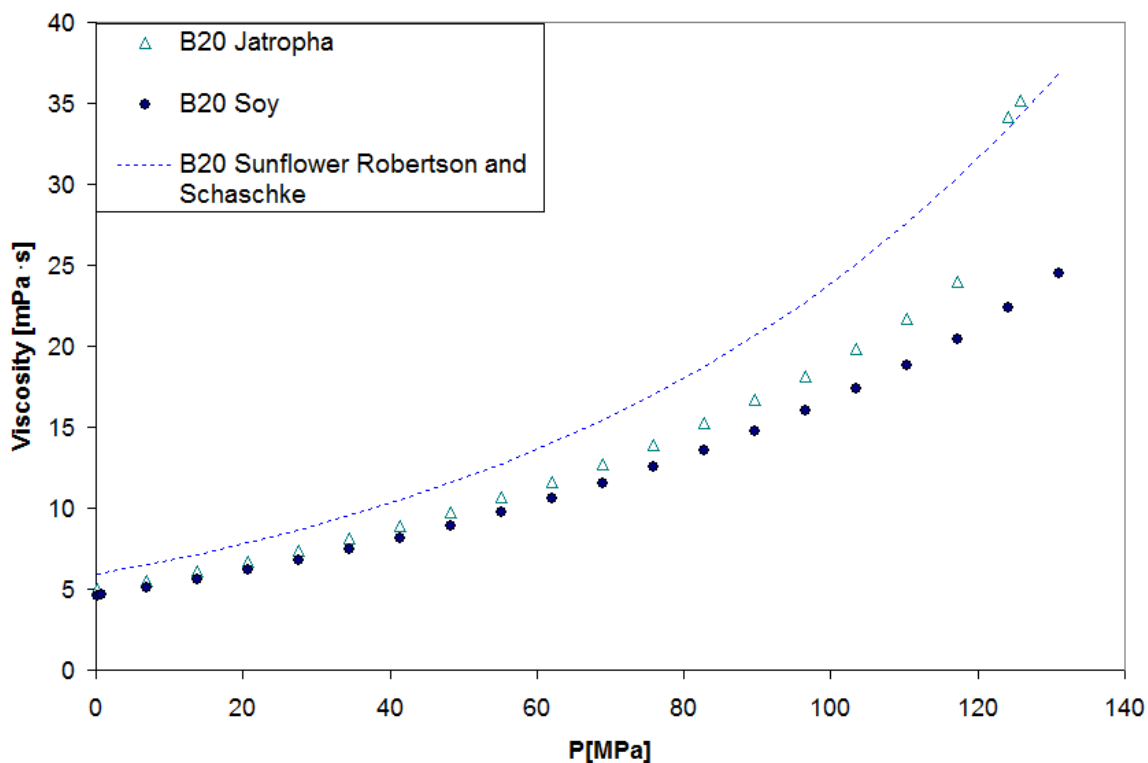


Figure 6.14. High-pressure viscosity of B20s at 283.15 K.

Jatropha has the lowest approximate cloud point pressure among all feedstocks investigated—most likely due to its greater amount of high melting temperature FAMES. The viscosity appears to be affected not only near the end of the pressure range, but the B20 jatropha differentiates much earlier from the B20 soybean blend sample. This is a very important observation, as it is thought that no modifications need to be made for engines when using biodiesel blends B20 and below.

The literature B20 sample in Figure 6.14 has a much greater viscosity than both of the fuels from our work, but when the data is normalized in Figure 6.15, the fuel viscosity profiles

become very similar. The sunflower B20 sample appears to increase at a faster rate at approximately 70 MPa, however, the dashed line is not representative of data, but of a (rough) correlation.

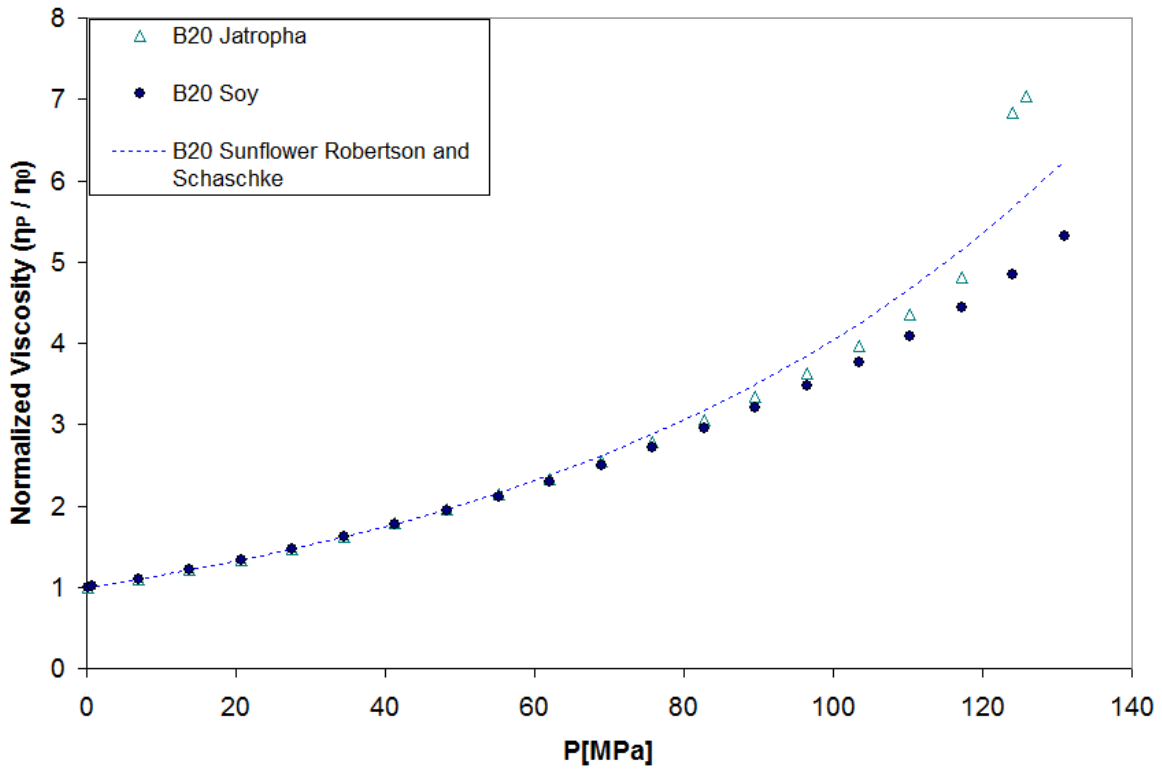


Figure 6.15. Normalized viscosity of B20s at 283.15 K.

The B5 blends were more similar in magnitude as shown in Figure 6.16, and in their normalized behavior in Figure 6.17 than the higher percentage B20 blends.

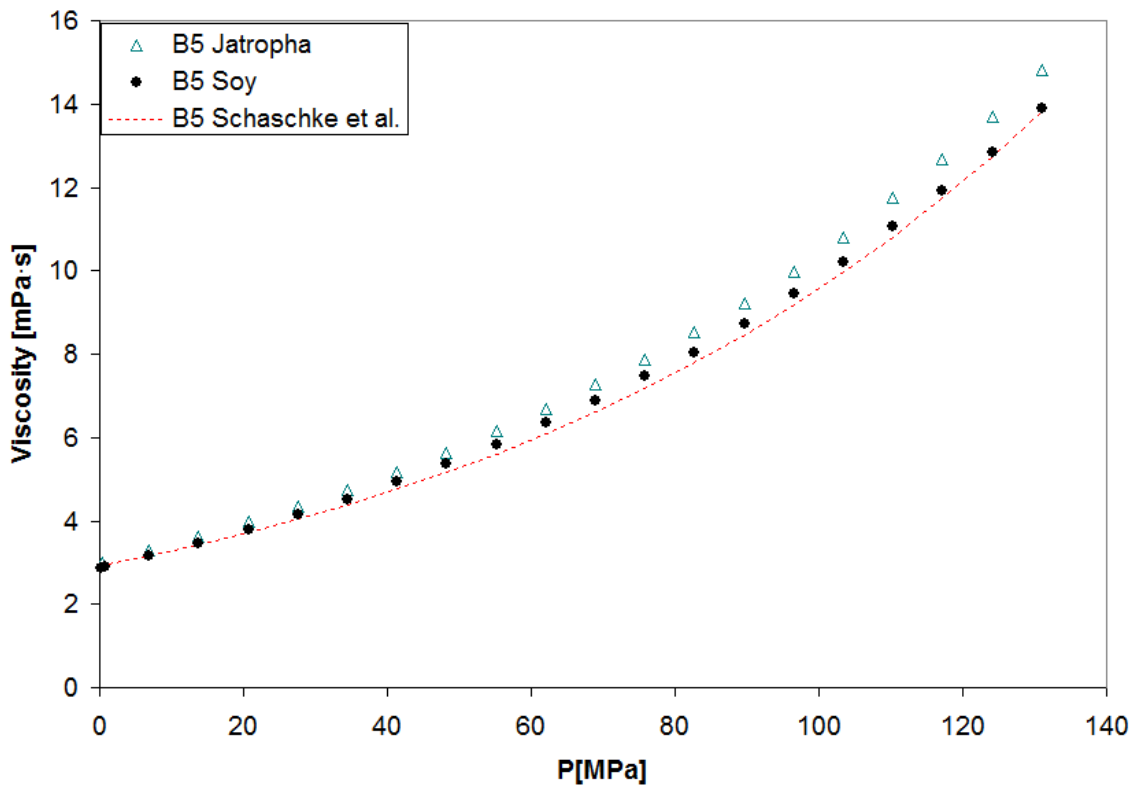


Figure 6.16. High-pressure viscosity of B5s at approximately 298 K.

The soy B5 and rape B5 (from literature) are very similar throughout the entirety of the pressure range, while the jatropha B5 is slightly more viscous. However, this appears to be an effect of the initial ambient viscosity. The normalized viscosity in Figure 6.17 show very similar rates of increase with pressure.

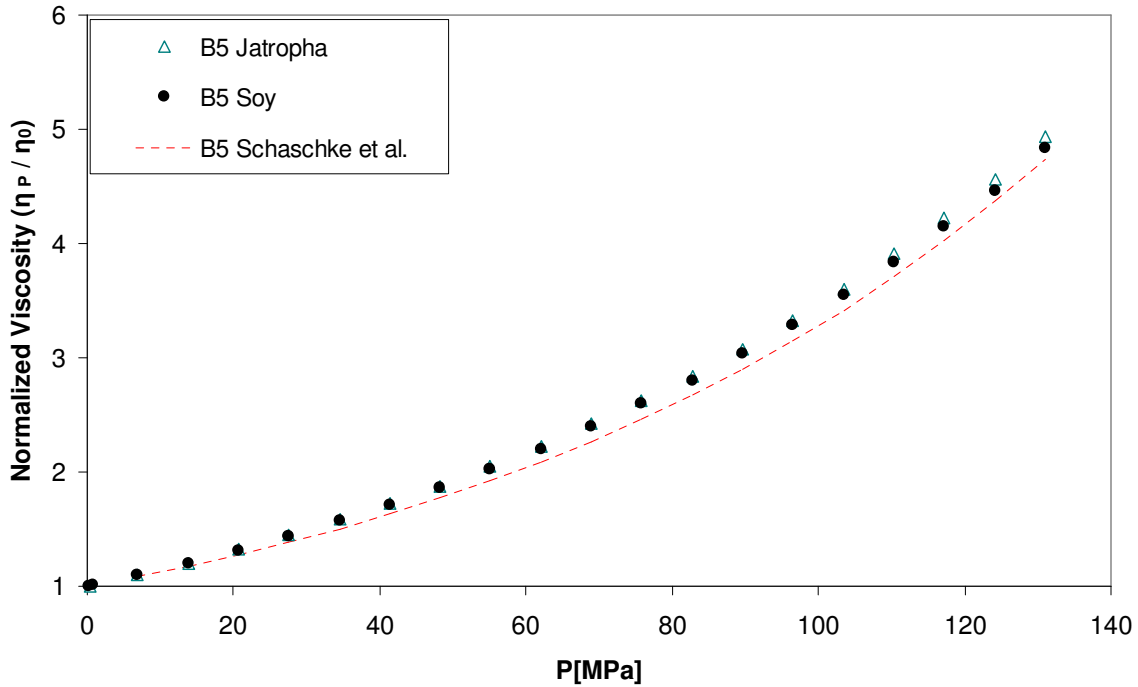


Figure 6.17. Normalized viscosity of B5 blends at approximately 293 K.

At low blend percentages, it is expected that the effect of the biodiesel component on the entire fuel would be reduced as the polar compounds approach dilution in the nonpolar diesel, at least at the pressure range and fuel types investigated here. At significantly higher pressures, or in biodiesels composed almost entirely of long chained saturated FAMES, differences among feedstocks in low percentage blends will likely be visible. Again, it is important to keep in mind that these fuels contained 80 or 95% diesel by volume, and the blends are therefore not truly directly comparable because the diesel was not taken from the same source.

6.5 Jatropha Blends Mixing Rules

Similarly to the soybean biodiesel blends in Chapter 5, both Kay's and the idealized Grunberg-Nissan mixing rules modeled blend data. On average, the mixing rules predicted viscosities that were less than the uncertainty of the instrument. However, in this work, the idealized Grunberg-Nissan (G-N) equation gave slightly better predictions than Kay's rule. The less accurate of the two models used is shown in Figure 6.18 for B20.

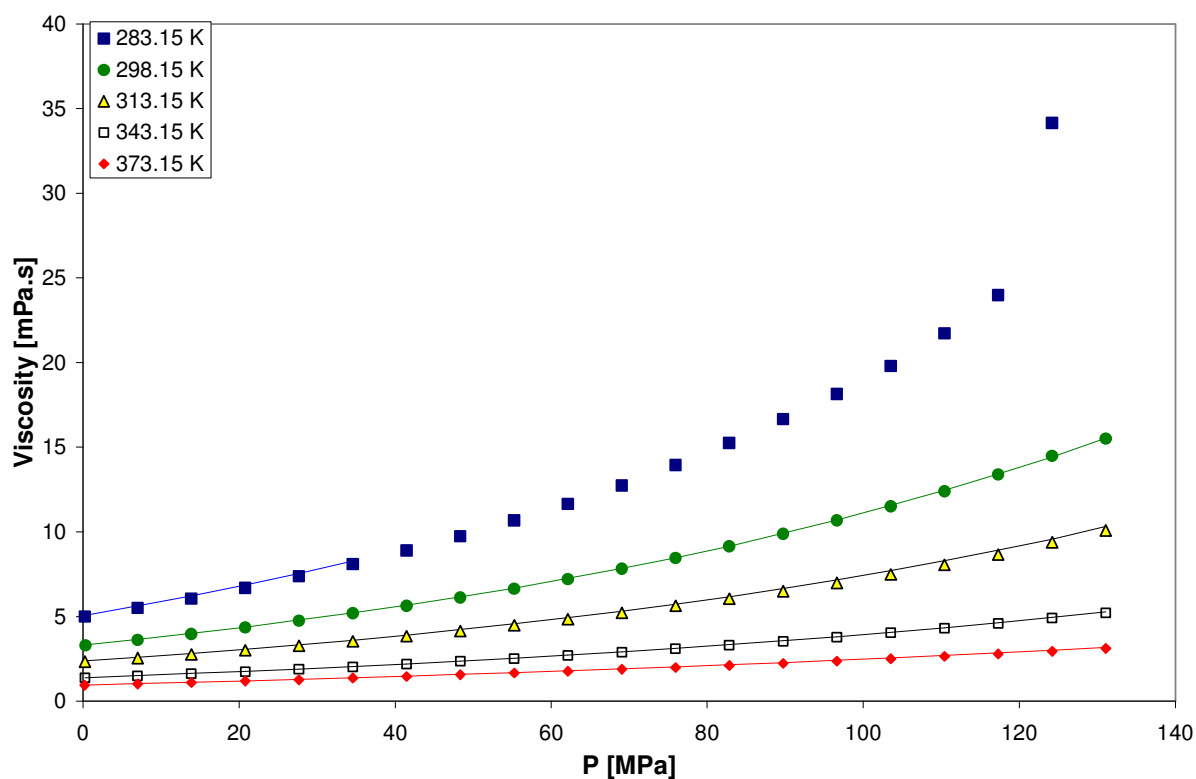


Figure 6.18. High-pressure viscosity of B20 Jatropha with Kay's mixing rule.

The solid lines representing the predicted viscosity are very similar to the empirical data—notice that for 283.15 K the model only covers part of the pressure range. This is due to jatropha's cloud point pressure.

Kay's rule typically showed over-prediction; residuals for each B20 are shown in Figures 6.19 and 6.20. Overall, the G-N equation predicted viscosities with an AARD of approximately 1%.

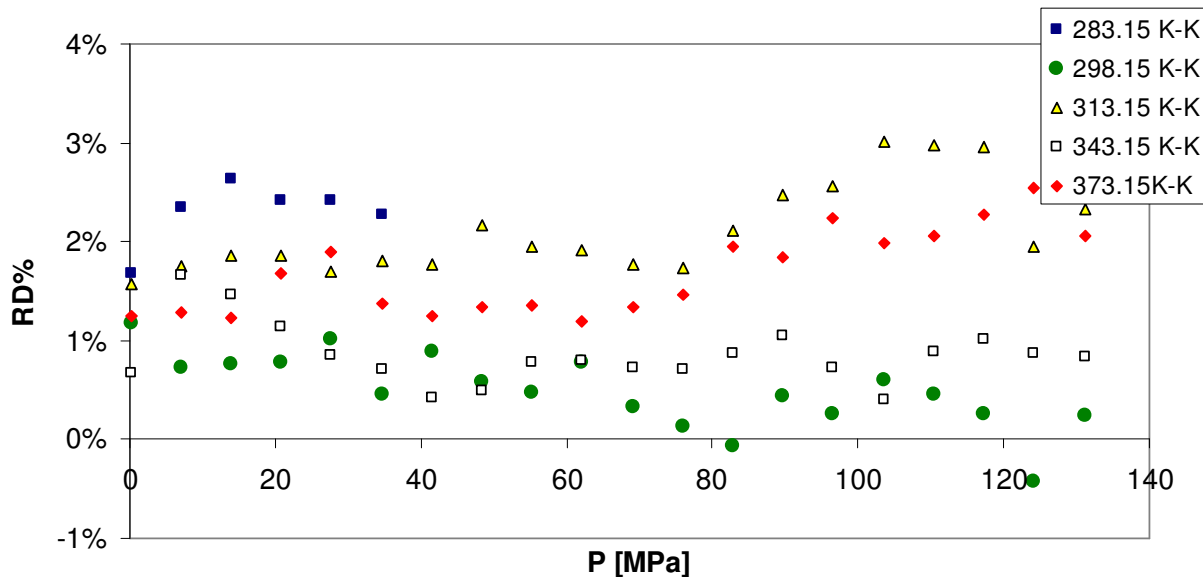


Figure 6.19. Kay's mixing rule for jatropha B20 blend.

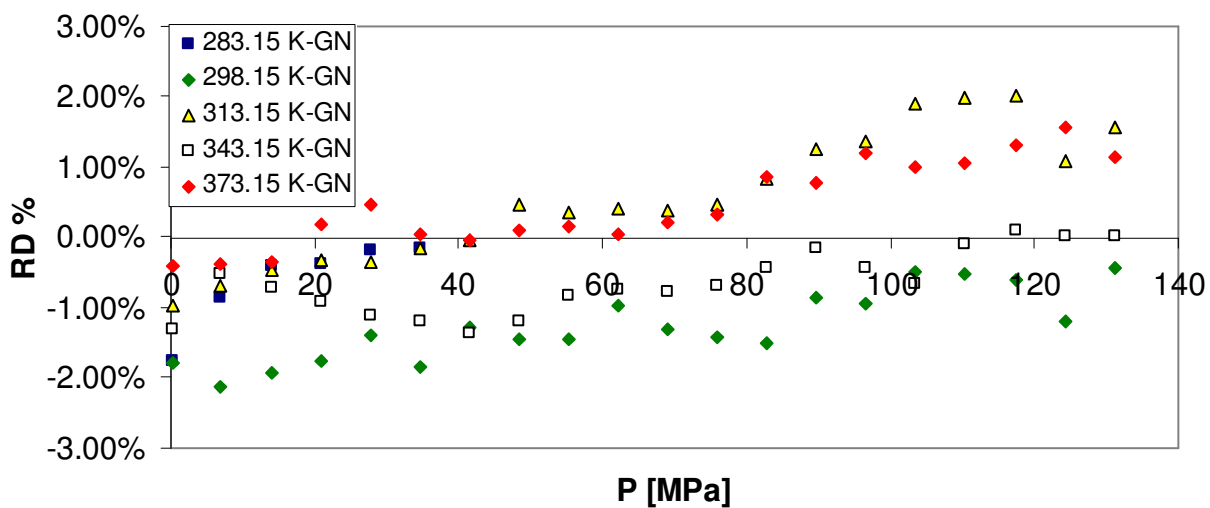


Figure 6.20. Grunberg-Nissan mixing rule for B20 blend.

The usefulness of a particular mixing rule is related to the interaction among molecules. One such thermodynamic property that can be used to estimate viscous changes with mixing is the excess molar volume. One suggested method predicts that if the excess molar volume of a system at a particular composition is positive, the viscosity will be lower than the prediction of an ideal mixture, resulting in a positive bias¹⁰. The ideal Grunberg-Nissan mixing rule used in this dissertation will always under-predict Kay's calculated values. Likewise, a negative excess molar volume would suggest the possibility of a greater than ideal viscosity^{10, 11}. The excess molar volume of soybean, sunflower, and fish oil biodiesel and diesel was found to be positive and very small^{12, 13} while for coconut biodiesel and diesel fuel the excess molar volume was mostly negative for the composition range¹⁴. A difference in diesel composition, and biodiesel FAME composition may yield varying results in the excess molar volume, which may suggest that it cannot be assumed that the G-N mixing rule will always be preferential for jatropha blends, nor may Kay's rule be more accurate to soybean blends. Additional work should be performed to clarify these trends.

6.6 Jatropha Biodiesel and Blends Cloud Point Pressures

Approximate cloud point pressures for the jatropha biodiesel and the jatropha B20 blend, along with soybean biodiesel blends, are given in Figure 6.21. The slopes between approximate cloud point pressures among blends were found to be very similar. Additional low temperature high-pressure measurements could be taken, possibly to develop an additional freezing-point pressure biodiesel blend heuristic that is developed using multiple temperatures.

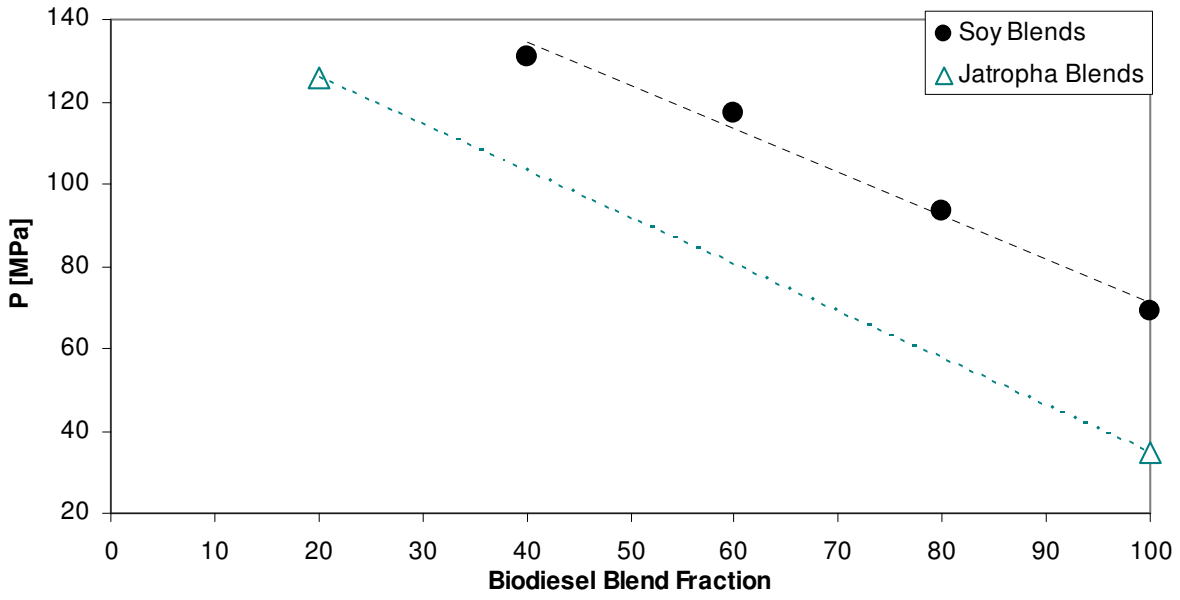


Figure 6.21. Final viscosity measurement before possible cloud-point pressure for several biodiesel blends. The dashed lines indicate a possible parallel relationship between biodiesel feedstocks.

6.7 Conclusions and Ramifications

High-pressure viscosity was measured for jatropha biodiesel, diesel and its blends B5, B10, and B20. The jatropha biodiesel and the diesel fuel were modeled with the Tait-Litovitz equation using Tait temperature-linearized pressure parameters. The ideal Grunberg-Nissan mixing rules gave better results than Kay's rule for the B5, B10 and B20 jatropha blends. Jatropha biodiesel was found to have a viscosity that compared very closely with canola oil samples from previous work, and was more viscous than the soybean biodiesels previously tested.

The increase in viscosity of jatropha biodiesel from ambient pressure to a higher pressure, referred to here as "normalized viscosity" was similar to all the other feedstocks studied in this dissertation as well as recent literature data. Compared to other biodiesels studied by the author, jatropha biodiesel had a slightly higher pressure response than did the other feedstocks.

Jatropha biodiesel was found to have a lower approximate cloud point pressure at 283.15 K than all other biodiesels previously tested as well as an approximate cloud point pressure at 283.15 K for its B20 blend. This potential cloud point pressure represents a significant difference in jatropha biodiesel blends when compared to the soy and canola blends typically used. The increased percentage of long chained saturated FAMES, namely stearic and palmitic acid methyl esters, is likely the cause.

References for Chapter 6

1. Gübitz, G. M.; Mittelbach, M.; Trabi, M., Exploitation of the tropical oil seed plant *Jatropha curcas* L. *Bioresource Technology* **1999**, 67, (1), 73-82.
2. Testing, A. S. f.; Materials, ASTM D975, Standard Specification for Diesel Fuel Oils. In ASTM International West Conshohocken, PA: 2011.
3. Duncan, A. M.; Pavlicek, N.; Depcik, C. D.; Scurto, A. M.; Stagg-Williams, S. M., High-pressure viscosity of soybean-oil-based biodiesel blends with ultra-low-sulfur diesel fuel. *Energy & Fuels* **2012**, 26, (11), 7023-7036.
4. Freitas, S. V.; Segovia, J. J.; Martín, M. C.; Zambrano, J.; Oliveira, M. B.; Lima, Á. S.; Coutinho, J. A., Measurement and prediction of high-pressure viscosities of biodiesel fuels. *Fuel* **2014**, 122, 223-228.
5. Bair, S., The pressure and temperature dependence of volume and viscosity of four Diesel fuels. *Fuel* **2014**, 135, 112-119.
6. Robertson, L.; Schaschke, C., Combined high pressure and low temperature viscosity measurement of biodiesel. *Energy & Fuels* **2009**, 24, (2), 1293-1297.
7. Duncan, A. M.; Ahosseini, A.; McHenry, R.; Depcik, C. D.; Stagg-Williams, S. M.; Scurto, A. M., High-pressure viscosity of biodiesel from soybean, canola, and coconut oils. *Energy & Fuels* **2010**, 24, (10), 5708-5716.
8. Bair, S. S., *High pressure rheology for quantitative elastohydrodynamics*. Elsevier: 2007; Vol. 54, p. 91-92.
9. Schaschke, C.; Fletcher, I.; Glen, N., Density and viscosity measurement of diesel fuels at combined high pressure and elevated temperature. *Processes* **2013**, 1, (2), 30-48.
10. Mamagakis, N.; Panayiotou, C., Excess volume and dynamic viscosity of ternary liquid mixtures. *Zeitschrift für Physikalische Chemie* **1989**, 162, (Part_1), 57-72.

11. Bair, S. S., *High pressure rheology for quantitative elastohydrodynamics*. Elsevier: 2007; Vol. 54, p. 126-128.
12. Mesquita, F. M.; Feitosa, F. X.; Santiago, R. S.; de Sant'Ana, H. B., Density, excess volumes, and partial volumes of binary mixtures of soybean biodiesel+ diesel and soybean biodiesel+ n-hexadecane at different temperatures and atmospheric pressure. *Journal of Chemical & Engineering Data* **2010**, 56, (1), 153-157.
13. Parente, R. C.; Nogueira Jr, C. A.; Carmo, F. R.; Lima, L. P.; Fernandes, F. A.; Santiago-Aguiar, R. S.; Sant'Ana, H. B., Excess Volumes and deviations of viscosities of binary blends of sunflower biodiesel+ diesel and fish oil biodiesel+ diesel at various temperatures. *Journal of Chemical & Engineering Data* **2011**, 56, (7), 3061-3067.
14. Mesquita, F.; Feitosa, F.; de Santiago-Aguiar, R.; de Sant'Ana, H., Experimental density data and excess molar volumes of coconut biodiesel+ n-hexadecane and coconut biodiesel+ diesel at different temperatures. *Brazilian Journal of Chemical Engineering* **2014**, 31, (2), 543-551.

Chapter 7

Biodiesel, Diesel and Biodiesel-Diesel Blends Using Normalized Viscosity Models

Parameters for the Tait-Litovitz linearized temperature model were developed for individual fuels in Chapters 4, 5 and 6. In Chapter 5, ideal mixing rules were presented and in Chapters 5 and 6 they were compared for soybean and jatropha biodiesel-diesel blends. Both Kay's and the ideal Grunberg-Nissan mixing rules were typically found to predict the viscosity of biodiesel blends within the estimated uncertainty of the instrument, 3.3%. In this chapter, the Tait linearized temperature model, a four parameter model, is presented with parameters that enable the prediction of the viscosity of biodiesel, diesel, and biodiesel-diesel blends as a function of temperature, pressure, blend fraction, and the ambient viscosity of the fuel. The fuel's ambient viscosity may be either empirical or predicted using ambient-viscosity literature models.

7.1. Normalized Viscosity

It was observed that biodiesels from different feedstocks have similar percent increases in viscosity with increasing pressure at constant temperature. This percent increase can be described by the normalized viscosity (NV). The (NV) given in Eqn. [1] is a function of the viscosity of a sample at high pressure, η_p , and the viscosity at atmospheric pressure, η_0 , at constant temperature.

$$(NV) = (\eta_p / \eta_0) \quad \text{Eqn. [1]}$$

The similar percent increase is likely due to biodiesel's homogenous nature—it consists entirely of fatty acid methyl esters (FAMES). The FAMES found in biodiesel are similar in chain length and structure for the majority of feedstocks. While the concentration of mono- and poly-unsaturated FAMES result in significant differences among biodiesel ambient-pressure viscosities, their contribution as a function of the pressures investigated in this work appear to be minimal. The density of FAMES found in biodiesel is greater than equivalent molecular weight hydrocarbons, so as density increases with pressure, molecular rearrangement is less likely to yield conformations that increase viscosity as rapidly as an equivalently sized homogenous hydrocarbon.

Diesel viscosities were found to increase with pressure at a greater rate than biodiesel fuels. While the average molecular weight of diesel fuel is approximately the molar mass of hexadecane—significantly less than biodiesel, much of its composition is made up of components that are greater in size, with molecules that have as many as 25-30 carbons, and molecules that are more complex than linear alkanes. Figure 7.1 shows that as linear alkanes increase in molecular weight their viscous response to pressure increases, with the greatest increases coming at lower temperatures.

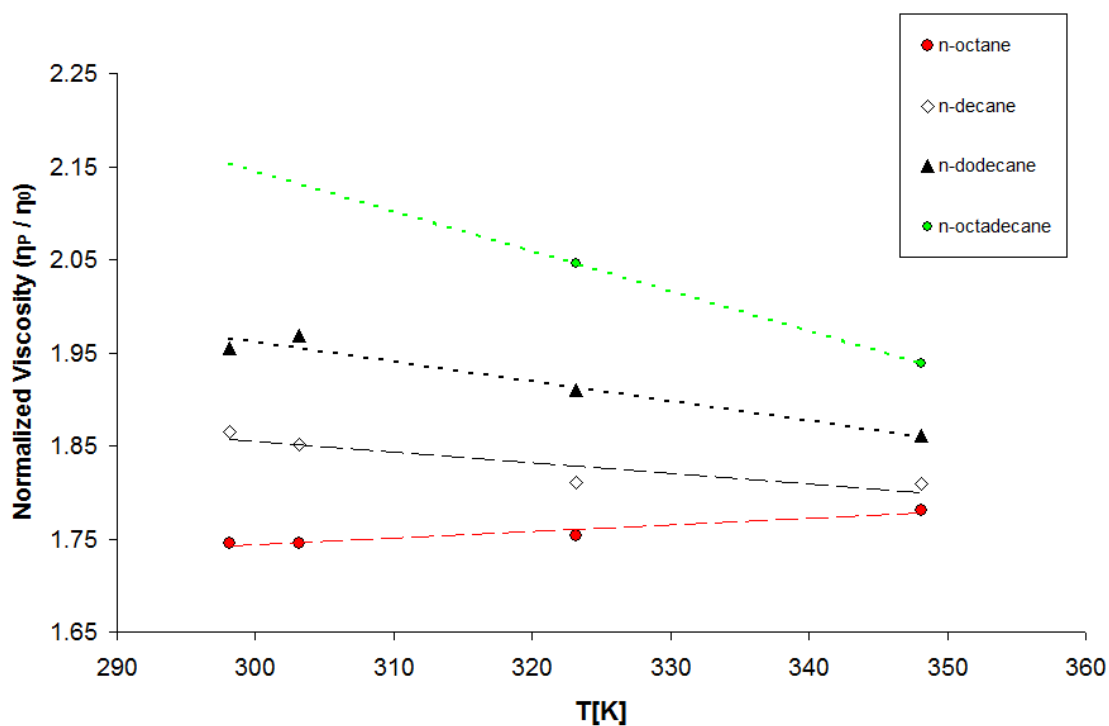


Figure 7.1. Normalized viscosity of alkanes at 62 MPa produced from literature^{1, 2}.

Functional group type has also been found to have a large influence on pressure's affect on viscosity. For example, with increased branching (which is common in fossil fuels) and overall molecular complexity of dodecane isomers, a larger viscous response to pressure was observed³.

7.2. Biodiesel High-Pressure Viscosity Parameters

The normalized viscosities were similar for all temperatures tested. Figure 7.2 shows the biodiesels from Chapters 4, 5, and 6 at 373.15 K. At the highest temperature tested

biodiesels are shown to increase to approximately 300% of their ambient pressure viscosities.

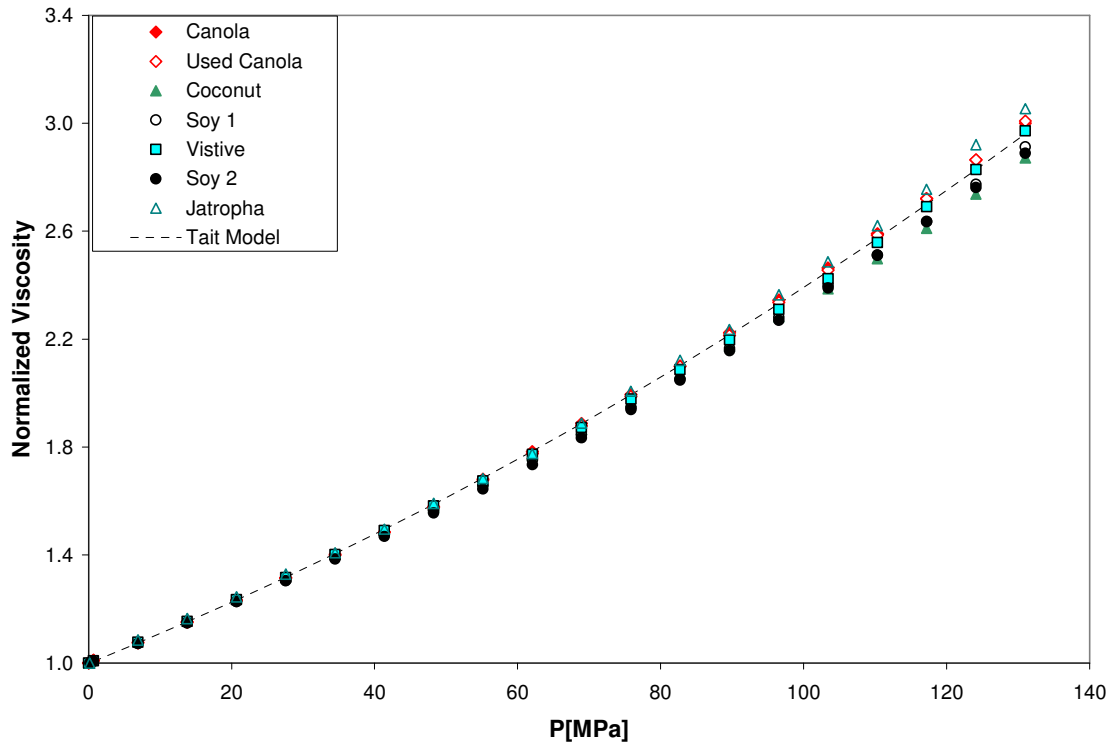


Figure 7.2. Biodiesels and Tait model at 373.15 K using parameters from Table 7.1.

Coconut biodiesel, composed of mostly shorter chained FAMES, has the lowest response to pressure at 131 MPa. The modified Tait equation with pressure parameters D and E is included for each normalized data set, with parameters given in Table 7.1.

Table 7.1. Tait parameters for biodiesel regressed for five isotherms.

Temp	D	E	AARD	MAX ARD
K	[MPa]	--	%	%
283.15	202.316	2.60493	0.8%	3.3%
298.15	262.261	3.13013	1.1%	4.3%
313.15	328.587	3.65981	1.0%	4.8%
343.15	244.007	2.68089	2.7%	4.4%
373.15	209.939	2.24063	1.3%	5.5%

The absolute average relative deviation (AARD) using individual pressure parameters for each isotherm yields an AARD well within the uncertainty of the instrument. Jatropha and soybean biodiesel are the only feedstocks for which measurements were taken at 343.15 K.

At the lowest temperature tested, 283.15 K given in Figure 7.3, the biodiesel normalized viscosities are similar to each other until approximately 70 MPa. As the canola biodiesels approach their cloud point pressures, significant differentiation is observed between them and the coconut biodiesel, which much reach a pressure 14 MPa greater before it experiences similar change of phase.

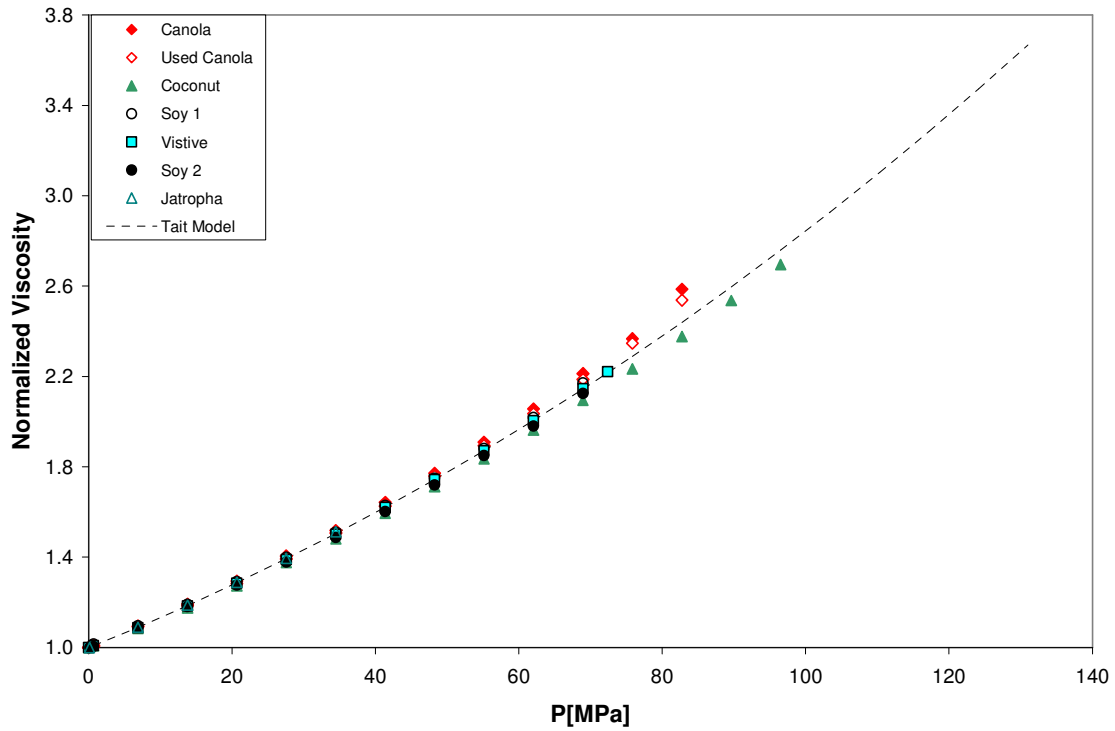


Figure 7.3. Biodiesels and Tait model at 283.15 K.

In our earlier work⁴, presented in Chapter 4, the Tait isothermal pressure parameters, D and E, were modeled simply and with great accuracy as functions of temperature. The values in Table 7.1 were developed in VBA/Excel using the Gauss-Newton non-linear regression method⁵. These values were used as an initial guess for the parameters given in Table 7.2, which were found using *Athena* chemical engineering software, to give locally optimum results.

Table 7.2. Biodiesel Tait linearized temperature parameters.

Parameters for Biodiesel Tait Equation			
E, a+b·T		D/E, c+d·T	
a	b	c	d
--	[K ⁻¹]	[MPa]	[MPaK ⁻¹]
4.539671	-0.005249	30.112160	0.178110

These parameters are used to evaluate a 50-50 mass blend of soybean-coconut biodiesel.

7.2.1. Biodiesel Experimental-Predictive Viscosity Model Comparison

A biodiesel blend with a FAME profile not found in the biodiesels used in the model development was used to test the model's predictive ability. Equal masses of soybean oil and coconut oil were added to a single vessel and then reacted with sodium methoxide and methanol and then processed as described in Chapter 3. The biodiesel FAME composition is presented in Table 7.3.

Table 7.3. Soybean-coconut oil biodiesel blend FAME composition.

Soybean-Coconut methyl ester composition (wt%)									
C6:0	C8:0	C10:0	C12:0	C14:0	C16:0	C18:0	C18:1	C18:2	C18:3
0.2%	3.8%	2.9%	22.4%	8.5%	9.8%	3.5%	15.1%	29.8%	4.0%

The high-pressure viscosity of this fuel was measured in increments of approximately 14 MPa, and then at pressure increments of approximately 7 MPa as the fuel approached its estimated cloud point pressure isothermally at 283.15 K. Each isothermal high-

pressure data set was taken in duplicate. The 373.15 K isothermal high-pressure data sets were taken consecutively, all others were alternated.

Multiplying the normalized viscosity by the ambient viscosity at the same temperature will yield the high-pressure viscosity. There are several methods that can predict ambient-pressure biodiesel viscosity to within a few percent as functions of temperature and FAME composition. A review of several methods was performed by Freitas et al. ⁶. The viscosity was calculated by the rearrangement of Eqn. [1]:

$$\eta_{p,B100} = \eta_{0, B100} \cdot (NV)_{B100} \quad \text{Eqn. [2]}$$

Where the normalized biodiesel viscosity is determined by Eqn. [3]:

$$(NV)_{B100} = ((D + P) / (D + 0.1))^E \quad \text{Eqn. [3]}$$

and ambient biodiesel viscosity, $\eta_{0, B100}$, which in this case was experimental. The average relative deviations for all temperatures and pressures were low, with the largest deviation occurring at 283.15 K. The experimental data and model data for the soy-coconut biodiesel are shown in Figure 7.4.

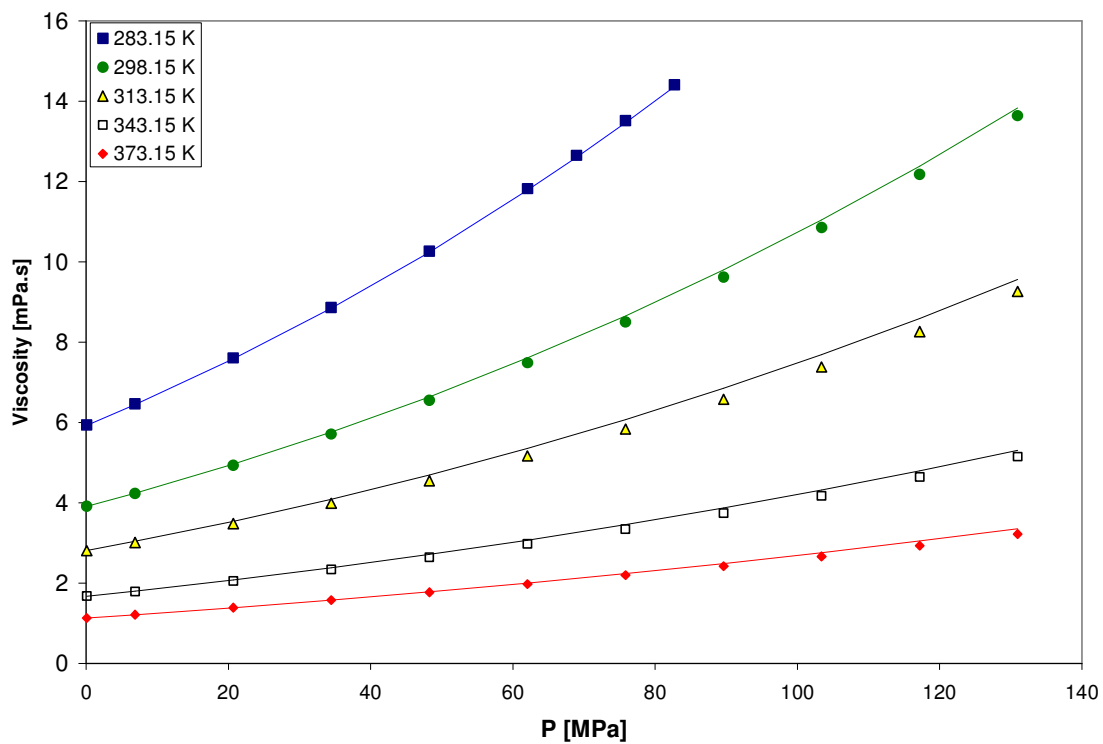


Figure 7.4. Experimental high-pressure viscosity of soy-coconut biodiesel with Tait 4 parameter model.

The model predicted the high-pressure viscosity of the soy-coconut blend with an AARD of 1.7% and a maximum deviation of 4.1%. These results are comparable to what was found for the fuels used in the model development, and with percent deviations between the two soybean biodiesels and coconut biodiesel as seen in Table 7.4.

Table 7.4. Absolute average relative deviations (AARD) and maximum deviations of all biodiesels tested using Eqn. [3] and parameters given in Table 7.2.

Overall Model, Biodiesels												
Biodiesel	283.15		298.15		313.15		343.15		373.15		Overall	
Sample	AARD	MAX ARD	AARD	MAX ARD	AARD	MAX ARD	AARD	MAX ARD	AARD	MAX ARD	AARD	MAX ARD
Canola	2.3%	6.4%	1.0%	3.0%	0.4%	0.8%	--	--	0.5%	1.0%	0.94%	6.38%
Used Canola	1.6%	4.6%	1.0%	2.8%	0.2%	0.8%	--	--	0.4%	1.2%	0.73%	4.59%
Coconut	0.9%	1.9%	2.0%	3.9%	1.2%	2.0%	--	--	3.7%	5.9%	2.02%	5.87%
Soy1	1.2%	2.2%	0.6%	1.3%	1.5%	2.8%	--	--	1.2%	2.5%	1.1%	2.78%
Vistive	0.7%	1.1%	0.5%	1.0%	1.0%	2.0%	--	--	0.4%	0.9%	0.62%	2.02%
Soy2	0.2%	0.4%	0.9%	1.7%	2.4%	4.1%	2.6%	3.9%	1.5%	2.9%	1.66%	4.10%
Jatropha	0.7%	1.5%	1.8%	4.0%	1.6%	5.1%	2.8%	4.2%	1.3%	2.9%	1.79%	5.07%
Soy/Coconut	0.2%	0.4%	1.2%	1.9%	2.9%	4.1%	2.4%	3.5%	1.7%	4.0%	1.74%	4.13%

7.2.2. Biodiesel Model Comparison to Literature

Chapter 6 compared both normalized and dynamic viscosities of biodiesels from our work to those of recent literature. Biodiesel from Bair⁷ was found to be very similar and within the uncertainty of the instrument, while those biodiesels from Freitas et al.⁸ were found to be more viscous, but similar to our biodiesels when normalized. We can see a more detailed analysis of the Tait 4 parameter model and its effectiveness in outside literature sources in Figures 7.5 and 7.6 and Tables 7.5 and 7.6.

Overall, the AARD was 3.0% for both sets of literature data and less than 2% for data between 1 and 80 MPa. The most significant variations were at low temperature and high pressure. Our work has shown a significant increase in viscosity within 10-15 MPa of the point at which further measurements are no longer obtainable due to phase change. Thus, the fact that several measurements were not given for the lowest temperature isotherm suggests phase transition.

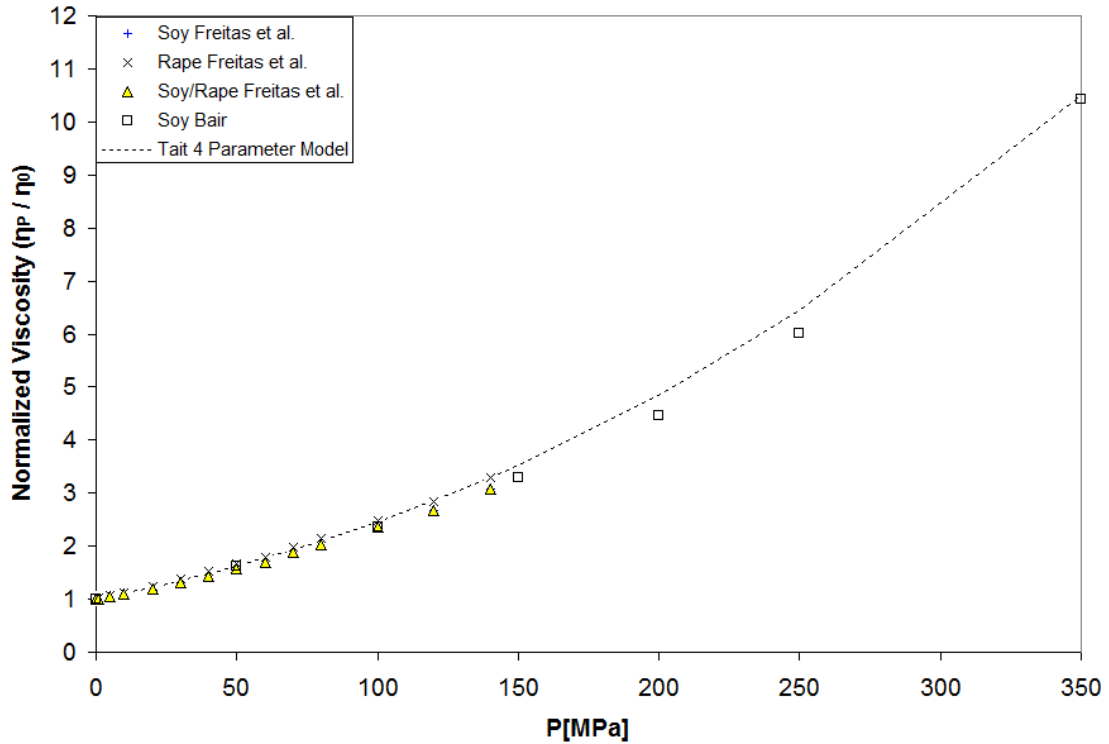


Figure 7.5. Normalized viscosity of literature biodiesel samples at 353.15 K with Tait 4 Parameter Model.

Figure 7.5 gives an extended look at the data by including pressures up to 350 MPa. While there is slight over prediction of the data the trends are very similar.

At higher temperatures, the model over-predicted Freitas et al.'s samples (see Table 7.5) at sufficient pressure, while at lower temperatures, the model under-predicted the work. The lowest maximum deviation at high pressure was found to be 5.7% in the middle of their temperature range—333.15 K as seen in Table 7.5.

Table 7.5. Tait 4 parameter model evaluation of soy, rape, and a soy-rape biodiesel blend from Freitas et al⁸.

		T[K]					
Pressure Range		293.15	313.15	333.15	353.15	373.15	393.15
1-30 MPa	AARD	1.2%	0.7%	0.8%	1.6%	0.9%	1.5%
	MAX ARD	5.2%	2.0%	2.3%	2.6%	2.5%	2.7%
40-80 MPa	AARD	7.4%	1.6%	2.1%	2.5%	1.5%	1.7%
	MAX ARD	18.1%	5.4%	4.0%	4.9%	3.9%	4.4%
100-140 MPa	AARD	25.8%	6.6%	3.0%	4.4%	5.7%	6.4%
	MAX ARD	30.6%	10.9%	5.7%	7.4%	9.5%	14.7%

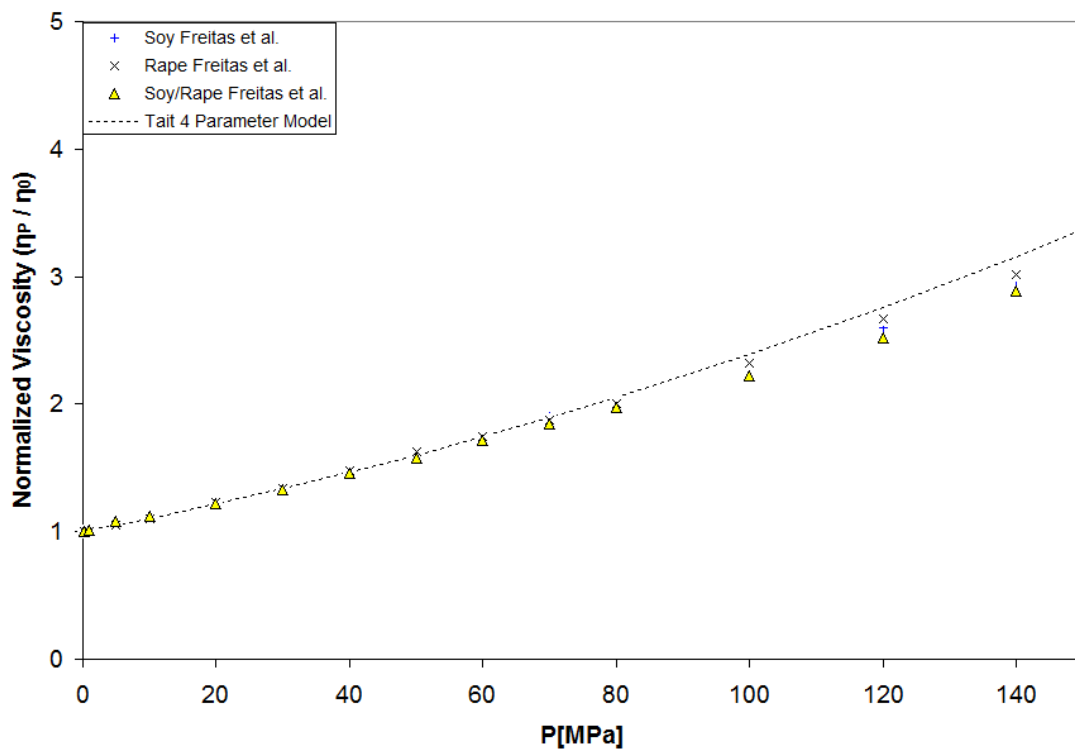


Figure 7.6. Normalized viscosity of literature biodiesel samples at 373.15 K with Tait 4 Parameter Model.

7.2.3. Biodiesel Model Extrapolation Potential

The work from Bair used a viscometer setup that was able to reach pressures beyond the capability of the apparatus used in this work, and temperatures that were higher than those included in the data set. Model evaluation for temperature and pressure range is given in Table 7.6. Figure 7.7 shows the empirical literature data as discrete points and the biodiesel Tait 4 parameter model is given as dashed lines.

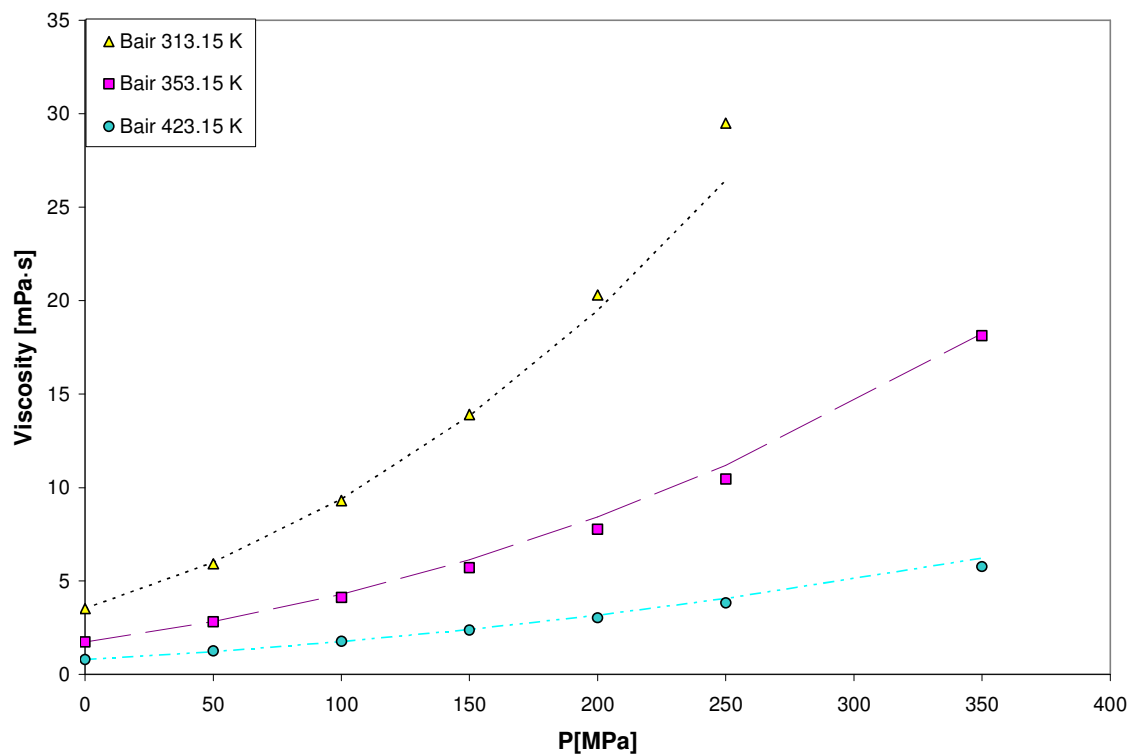


Figure 7.7. B100 literature data at high-pressure and temperature⁷ dashed lines are the Tait 4 parameter biodiesel model.

The largest deviation occurred at 313.15 K. Higher pressure measurements in Bair's work were not possible for B100 at 313.15 K because the sample essentially froze at 350 MPa and did not melt until 290 MPa. A sudden and significant rate of increase in viscosity was found frequently in our 283.15 K data sets and may also be present in the low temperature high-pressure sets from Freitas et al., as discussed in the previous section. A comparison of Bair's data using the Tait 4 parameter model for biodiesel is given in Table 7.6.

Table 7.6. Tait 4 parameter model evaluation of data from Bair⁷.

		T[K]		
Pressure Range		313.15	353.15	423.15
50 MPa	ARD	1.2%	0.8%	2.6%
100-150 MPa	AARD	0.7%	2.4%	1.6%
	MAX ARD	1.2%	4.0%	2.6%
200-350 MPa	AARD	7.2%	5.4%	6.2%
	MAX ARD	10.4%	8.5%	7.8%

The AARD, (not including ambient-pressure data, which when not using a predictive method is 0%), for pressures 150 MPa and less was 2.20 %, and the AARD for the entire data set was 4.02%. When the data set is considered without the final data point of the 313.15 K isotherm, the last data point collected by the author prior to high-pressure phase change, the AARD is reduced to 3.4%. The Tait 4 parameter model slightly over-predicted higher temperature isotherms, and under-predicted high-pressure viscosities for the 313.15 K isotherm.

7.3. Diesel High-Pressure Parameters

The viscosities of the four diesel fuels used in this dissertation were significantly different. However, as with biodiesels, the normalized viscosities of the diesel fuels were found to be similar to each other. The Tait 4 parameter model with parameters given in Table 7.7, was developed from the four diesel samples given in Tables C.6, C.8, C.16, and C.20 in Appendix C.

Table 7.7. Diesel Tait linearized temperature parameters.

Parameters for Diesel Tait Equation			
E, $a+b\cdot T$		D/E, $c+d\cdot T$	
a	b	c	d
--	[K ⁻¹]	[MPa]	[MPaK ⁻¹]
13.464330	-0.020595	-30.716640	0.341333

Figure 7.8 shows the normalized viscosity of the diesels increases to approximately 450% of their initial value at 313.15 K compared to approximately 340% for biodiesels at the same temperature.

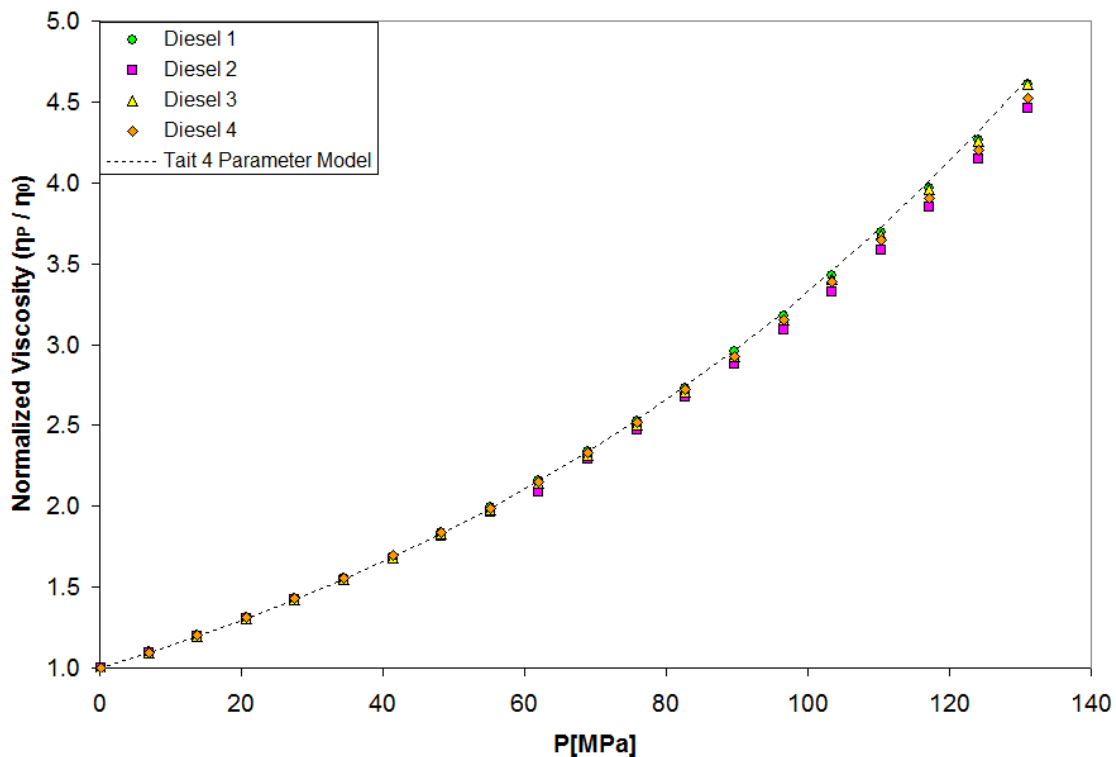


Figure 7.8. Normalized viscosity of the four diesels used in this work at 313.15 K with Tait 4 parameter model.

The 4 parameter diesel model was a poor fit at pressures above 103 MPa at 278.15 K with the model significantly under-predicting and a maximum error of ~15% at 131 MPa as seen in Table 7.8. However, only one diesel fuel was tested at this temperature, Diesel 4, found in Table C.20 in Appendix C.

Table 7.8. Diesel statistics from our work using the Tait 4 parameter model.

		Diesel 1	Diesel 2	Diesel 3	Diesel 4	Overall
278.15	AARD	--	--	--	2.9%	2.9%
	MAX ARD	--	--	--	15.5%	15.5%
283.15	AARD	2.8%	0.8%	2.3%	0.4%	1.6%
	MAX ARD	7.1%	1.5%	15.7%	2.4%	15.7%
298.15	AARD	1.3%	2.9%	1.6%	2.9%	2.2%
	MAX ARD	2.5%	5.6%	3.1%	5.5%	5.6%
313.15	AARD	0.6%	2.2%	0.8%	1.1%	1.2%
	MAX ARD	1.3%	1.3%	1.3%	1.3%	4.3%
343.15	AARD	--	0.8%	1.0%	1.0%	1.0%
	MAX ARD	--	1.8%	1.7%	2.4%	2.4%
373.15	AARD	3.3%	2.4%	3.4%	1.7%	2.7%
	MAX ARD	4.9%	3.9%	4.6%	3.3%	4.9%
Overall	AARD	2.0%	1.8%	1.8%	1.4%	1.8%
	MAX ARD	7.1%	5.6%	15.7%	15.5%	15.7%

Aside from the two or three points in the set, the overall AARD for the entire data set is approximately 1.8%.

7.3.1. Diesel Model Comparison to Literature

The Tait 4 parameter model was applied to compare to diesel fuels from a single literature source from Schaschke et al.⁹ Fuel 1 had no performance or handling additives, while Fuels 2 and 3 did, and Fuel 5 was listed as commercially available. While raw data was not available, correlations for viscosity were given for each fuel at each isotherm tested. Figure 7.9 plots the data at 298 K.

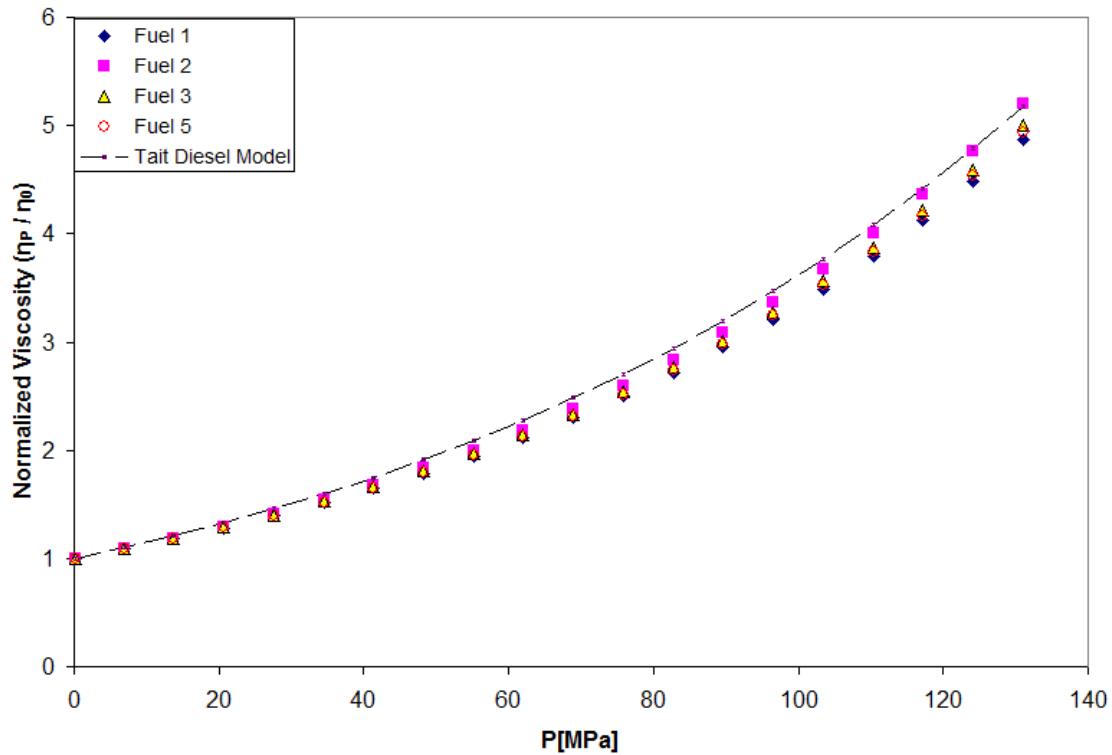


Figure 7.9. Normalized diesel model comparison to correlations from literature⁹ at 298.15 K.

At 298.15 K between 6.9 and 131 MP at 7 MPa increments, all fuels had an AARD of 5.0% with a maximum deviation of 8.3%. Interestingly, the maximum deviation occurred between 60 and 90 MPa for all fuels—not at the highest pressure tested. At the other isotherms compared the maximum difference occurs at 131 MPa.

There are significant differences at higher temperatures, not only between the fuels and the Tait linearized temperature model, but among the fuels tested in the work by Schaschke et al. as shown in Figure 7.10.

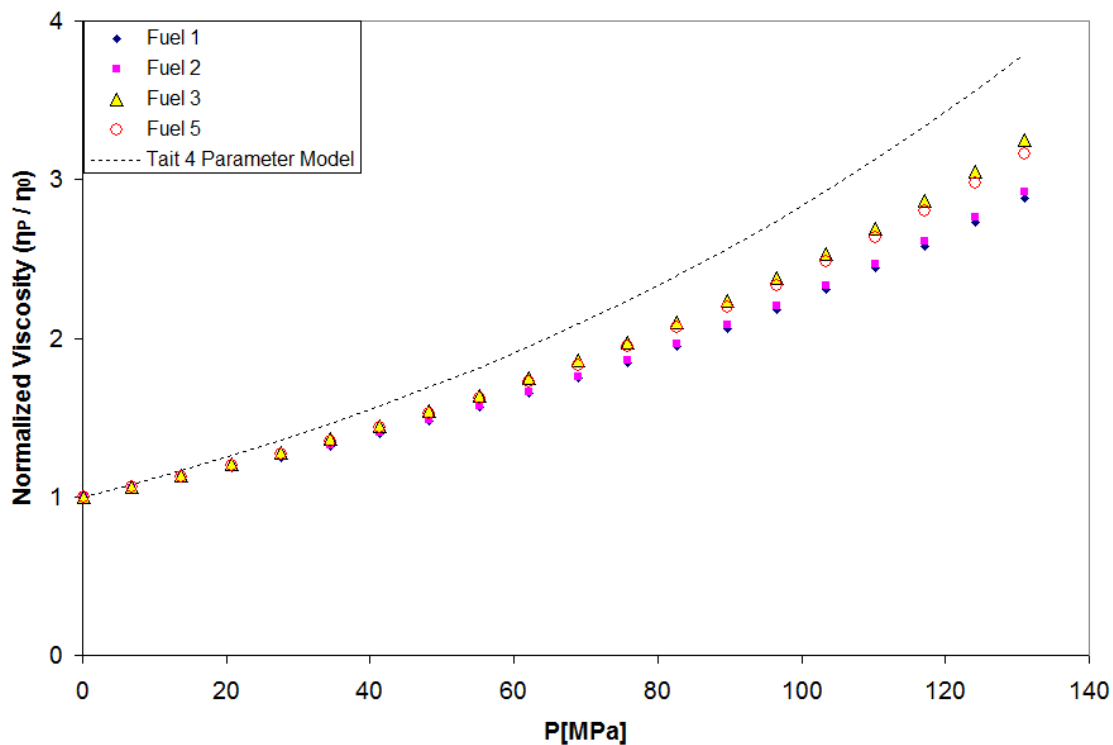


Figure 7.10. Diesel fuels at 348 K with Tait 4 parameter model using parameters in Table 7.5.

Typically, differences become smaller as temperature increases. The fuels are described as summer diesels, so perhaps the difference in composition causes differences at high temperature. At significantly high pressures (greater than 250 MPa), additive-sized quantities of components have been shown to significantly decrease viscosity³. However, the viscosity of Fuel 1, which does not contain additives, is very similar to Fuel 2, which does. Another possibility is that the correlation used by Schaschke et al. does not accurately represent their data at low pressures and is better suited at higher pressure—many of their correlations model the data to 500 MPa.

7.4. Biodiesel-Diesel Blends Model

In Chapters 5 and 6, mixing rules were used to predict the high-pressure viscosity of biodiesel blends using both empirical data and the model equations of pure biodiesel and pure diesel fuel. Using the biodiesel and diesel Tait linearized temperature models (Tait 4 parameter model), which rely on ambient viscosity, the soybean and jatropha biodiesel-diesel blends are evaluated. In some cases, empirical ambient-pressure viscosity data is unavailable or impossible to get for biodiesel at a biodiesel-diesel blend temperature of interest. These cases are more likely to occur in long-chained saturated FAME feedstocks like palm biodiesel, which has a relatively high cloud point. An approach that does not require empirical data is especially useful in this case.

7.4.1. Biodiesel-Diesel Blends Model with Known Mole Fractions and Ambient Pressure Viscosities

The simplest ideal mixing rule, which was proposed in Chapter 5, considers biodiesel and diesel as a binary mixture where the viscosity at ambient pressure for a blend is given by Eqn. [4]

$$\eta_{o,Blend} = x_{B100} \cdot \eta_{o,B100} + x_{B0} \cdot \eta_{o,B0} \quad Eqn. [4]$$

where x represents the mole fraction, and similarly, the high-pressure viscosity is given by Eqn. [5]:

$$\eta_{p,Blend} = x_{B100} \cdot \eta_{p,B100} + x_{B0} \cdot \eta_{p,B0} \quad Eqn. [5]$$

Combining Eqn.s [4] and [5] gives Eqn. [6]:

$$(NV)_{\text{Blend}} = x_{\text{B100}} \cdot (NV)_{\text{B100}} \cdot \eta_{0, \text{B100}} / \eta_{0, \text{Blend}} + x_{\text{B0}} \cdot (NV)_{\text{B0}} \cdot \eta_{0, \text{B0}} / \eta_{0, \text{Blend}} \quad \text{Eqn. [6]}$$

Applying Eqn. [6] to Jatropha biodiesel blends finds the Grunberg-Nissan and Kay's ideal mixing rules (both presented in Chapters 5 and 6) comparable at approximately 2% AARD. High-temperature viscosities at 343.15 and 373.15 K were under-predicted while the 298.15 and 313.15 K isotherms were over-predicted. The 283.15 K isotherm predicted with low deviation until approximately 100 MPa where a significant under-prediction occurred. This is especially evident prior to the approximate cloud point pressure for the jatropha B20 sample shown in Figure 7.11.

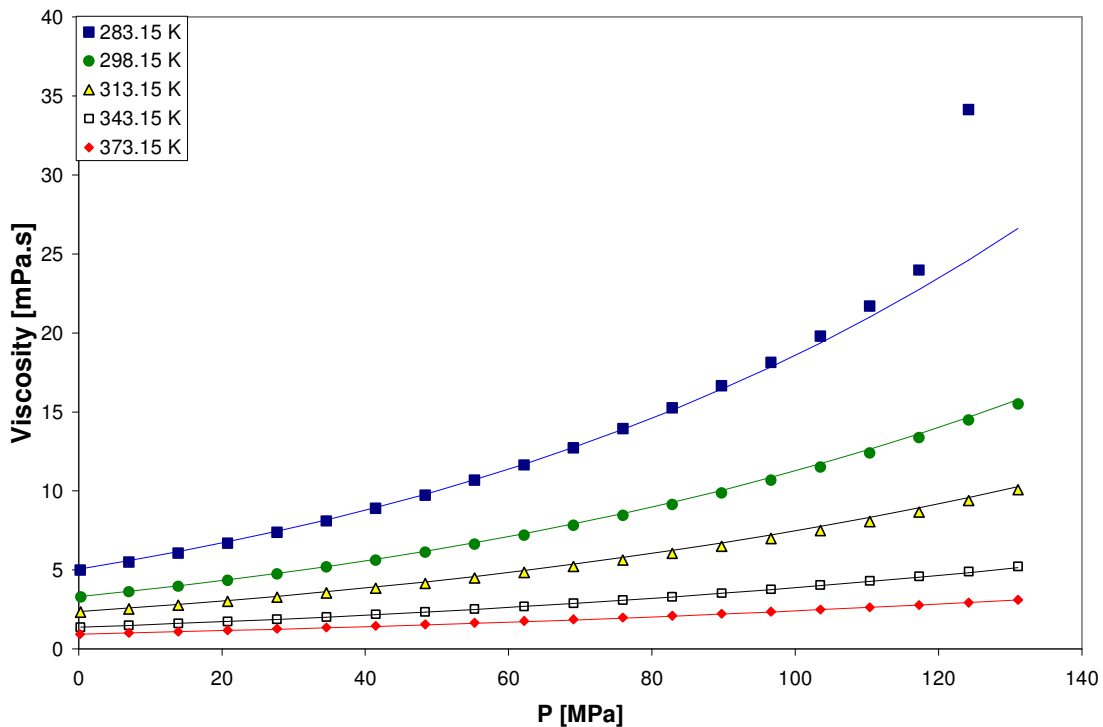


Figure 7.11. High-pressure viscosity of Jatropha B20 with Tait biodiesel and diesel 4 parameter models and Kay's rule.

7.4.2. Biodiesel-Diesel Blends Volume Fraction Model

In those cases where detailed compositional data or pure component ambient viscosity is not available, we simplify Eqn. [6], and replace the viscosity ratio and mole fractions with volume fraction, ϕ , also known as the blend percentage.

$$\phi_{B100} \approx x_{B100} \cdot \eta_{0, B100} / \eta_{0, Blend} \quad \text{Eqn. [7]}$$

and similarly

$$\phi_{B0} \approx x_{B0} \cdot \eta_{0, B0} / \eta_{0, Blend} \quad \text{Eqn. [8]}$$

At ambient pressure, the biodiesel-diesel blend ambient viscosity will be between diesel, B0, and biodiesel, B100, ambient viscosity. A blend-fraction approach *using data from our work presented in Chapter 5¹⁰* was performed by Freitas et al.⁸ using the Grunberg-Nissan ideal mixing rule.

Because of the density/MW relationship, the mole fraction of biodiesel will have a lower value than its blend fraction. When examining Eqn. [7], the ambient-viscosity ratio will be greater than one and the mole fraction of biodiesel will be less than the corresponding volume fraction. Similarly, in Eqn. [8], the ambient viscosity ratio will be less than one, while the mole fraction of diesel fuel will be greater than the corresponding volume fraction giving the pseudo Eqns. [7] and [8] greater validity.

The normalized blend viscosity becomes:

$$(NV)_{Blend} = \phi_{B100} (NV)_{B100} + \phi_{B0} (NV)_{B0} \quad \text{Eqn. [9]}$$

And the blend viscosity at high pressure is calculated using Eqn. 10:

$$\eta_{p,\text{Blend}} = \eta_{0,\text{Blend}} \cdot (NV)_{\text{Blend}} \quad \text{Eqn. [10]}$$

The left and right side of Eqns. [7] and [8] were calculated using experimental blend viscosities, pure component viscosities, and molecular weights from soybean and jatropha blends presented earlier. It was found that biodiesel has a lower contribution than the mole fraction model Eqn. [6], and diesel a higher contribution. Due to their differences in normalized viscosities, this contribution disparity suggests over-prediction is likely for a fuel when Eqn. [6] is accurate, and even greater over-prediction at lower temperatures where normalized differences are more pronounced.

7.4.3. Biodiesel-Diesel Blends Volume Fraction Model Literature Comparison

The model using Eqn.s [9] and [10] over-predicts the viscosity of all B5 blends (low blend fraction) and 298 K, both from our work and from literature^{7,9} given in Figure 7.12.

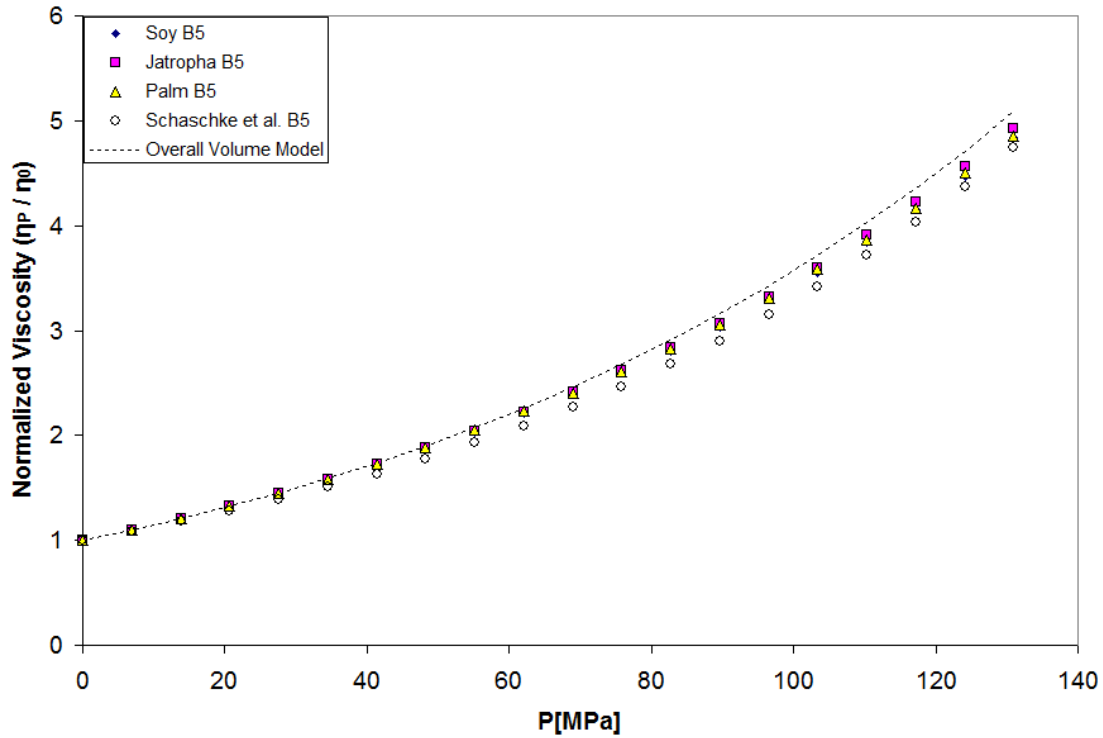


Figure 7.12. B5 biodiesel blends at 298 K using the overall volume model and ambient-pressure viscosity.

Palm biodiesel, B100, was found to cloud at 283.15 K. Using Eqn. [6] is not possible without using some sort of prediction method to find the ambient-pressure viscosity of the palm biodiesel. Applying the more robust Eqn.s [9] and [10] allows for viscosity prediction.

The AARD for all palm blends (B5, B10 and B20) tested was 1.65%, the maximum relative deviation occurred in sample B10 in Figure 7.13, just prior to the approximate cloud point pressure at 278.15 K.

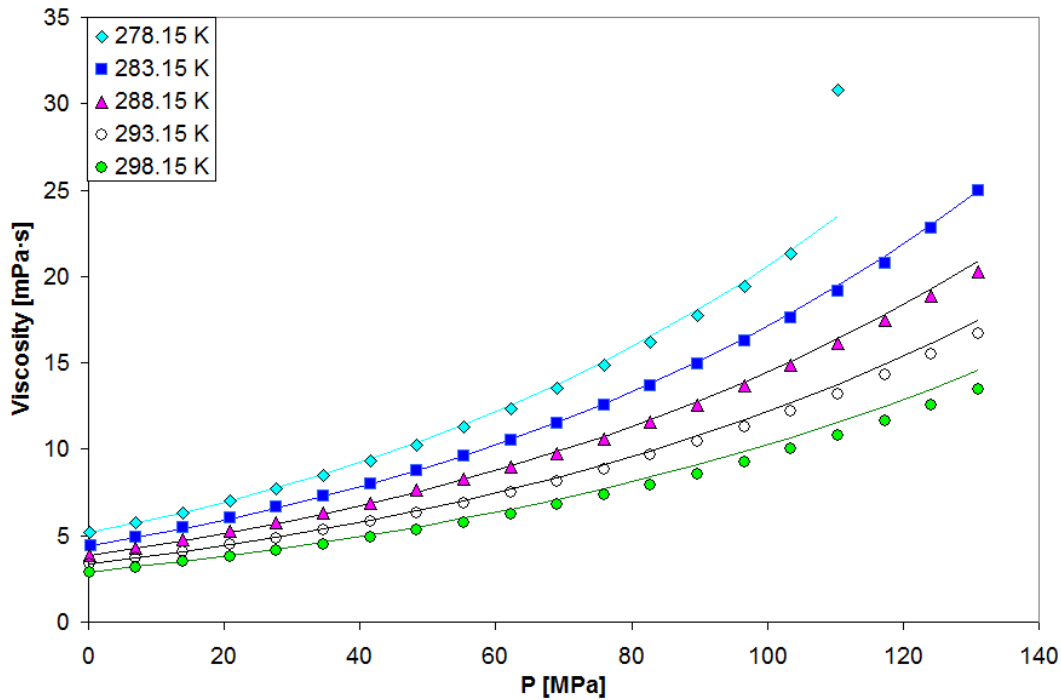


Figure 7.13. Palm B10 modeled with results from Eqn. 8.

Possible considerations to explain why this model performed well for palm biodiesel blends at low temperature:

1. Palm biodiesel has a lower molecular weight than soy and jatropha biodiesels, therefore, the relative bias in contribution when using volume fractions is changed.
2. The highly saturated nature of palm biodiesel may lead to different normalized viscosity increases. Jatropha biodiesel was shown in Figure 7.2 and Figure 7.3 earlier to have a greater normalized viscosity than the other biodiesels tested, it had an approximately 20% long chained saturated FAMES—palm biodiesel has twice that percentage.

7.4.4. Biodiesel-Diesel Blends Volume Fraction Model at High Temperatures and Pressures

The volume-fraction model given in Eqn.s [9] and [10] was applied to high pressures and temperatures beyond the parameters used in the model development. Figure 7.14 shows high temperature and high pressure data. The robust model gives reasonable estimates simply based on blend fraction and ambient viscosity of the blend. The AARD was approximately 5.5% for the entire range and approximately 4.3 % for pressures up to 150 MPa when compared to Bair's B20 sample.

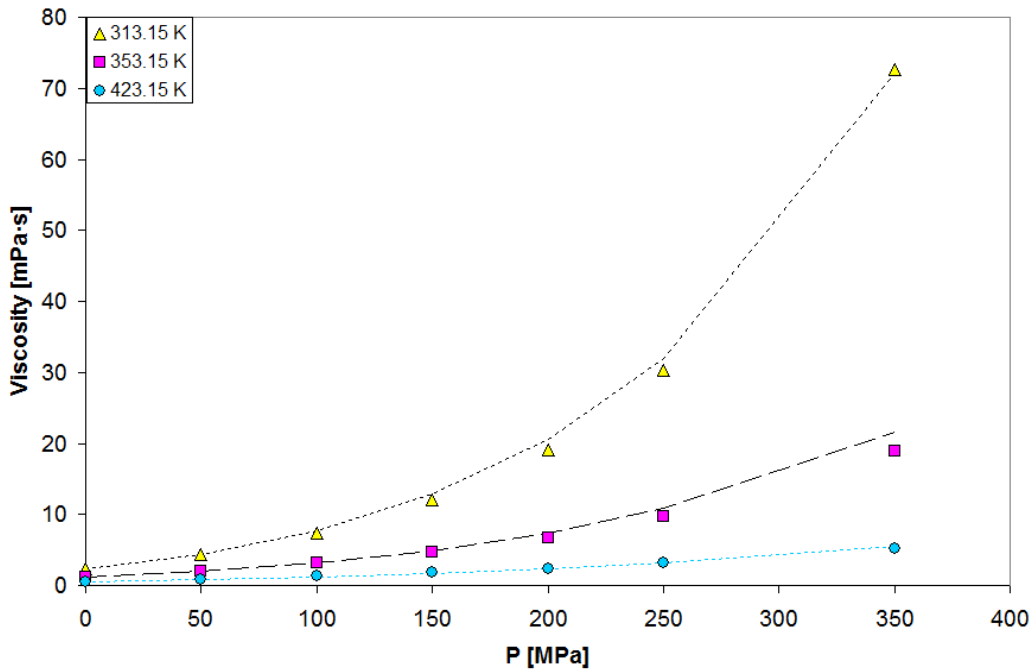


Figure 7.14. Literature B20⁷ with dashed lines using equation 9.

7.5. Conclusions

Biodiesel, diesel, and biodiesel-diesel blend models are presented, which give a potential user the flexibility to predict viscosities using a significant amount of information or with very little information, without having to sacrifice much accuracy. The majority of the models presented are not fit for predicting viscosity that is very close (10 to 15 MPa) to a possible freezing point pressure phase change. Otherwise, the models presented provide accurate values in the pressure range investigated and were found to be reasonable when extrapolated to pressures of 350 MPa when compared to literature data. When more data is available for highly-saturated compounds, it is likely that a parameter used to account for the degree of saturation or chain length may be added to increase the predictive ability of the model without additional rigorous calculations.

References for Chapter 7

1. Caudwell, D.; Trusler, J.; Vesovic, V.; Wakeham, W., The viscosity and density of n-dodecane and n-octadecane at pressures up to 200 MPa and temperatures up to 473 K. *International Journal of Thermophysics* **2004**, 25, (5), 1339-1352.
2. Kashiwagi, H.; Makita, T., Viscosity of twelve hydrocarbon liquids in the temperature range 298–348 K at pressures up to 110 MPa. *International Journal of Thermophysics* **1982**, 3, (4), 289-305.
3. Bair, S. S., *High pressure rheology for quantitative elastohydrodynamics*. Elsevier: 2007; Vol. 54, p. 91-92.
4. Duncan, A. M.; Ahosseini, A.; McHenry, R.; Depcik, C. D.; Stagg-Williams, S. M.; Scurto, A. M., High-pressure viscosity of biodiesel from soybean, canola, and coconut oils. *Energy & Fuels* **2010**, 24, (10), 5708-5716.
5. Chapra, S. C.; Canale, R. P., *Numerical methods for engineers*. McGraw-Hill College: 1988.
6. Freitas, S. V.; Pratas, M. J.; Ceriani, R.; Lima, A. S.; Coutinho, J. A., Evaluation of predictive models for the viscosity of biodiesel. *Energy & Fuels* **2010**, 25, (1), 352-358.
7. Bair, S., The pressure and temperature dependence of volume and viscosity of four Diesel fuels. *Fuel* **2014**, 135, 112-119.
8. Freitas, S. V.; Segovia, J. J.; Martín, M. C.; Zambrano, J.; Oliveira, M. B.; Lima, Á. S.; Coutinho, J. A., Measurement and prediction of high-pressure viscosities of biodiesel fuels. *Fuel* **2014**, 122, 223-228.

9. Schaschke, C.; Fletcher, I.; Glen, N., Density and viscosity measurement of diesel fuels at combined high pressure and elevated temperature. *Processes* **2013**, 1, (2), 30-48.
10. Duncan, A. M.; Pavlicek, N.; Depcik, C. D.; Scurto, A. M.; Stagg-Williams, S. M., High-pressure viscosity of soybean-oil-based biodiesel blends with ultra-low-sulfur diesel fuel. *Energy & Fuels* **2012**, 26, (11), 7023-7036.

Chapter 8

Conclusions

High-pressure viscosities of biodiesels from several feedstocks, diesel fuels, and biodiesel-diesel blends with soybean, jatropha, and palm biodiesel were measured for temperatures between 278.15 and 373.15 K and pressures up to 131 MPa. The data was fit successfully with empirical models and ideal mixing rules. Important takeaways are enumerated below.

8.1 Biodiesel Comparisons to Diesel

1. Diesel fuel at ambient pressure has viscosity that is lower than biodiesel for every feedstock and temperature tested. ***The diesel fuels maintained lower viscosity than all biodiesels, save coconut biodiesel, through the entirety of the temperature and pressure range.*** The coconut biodiesel had cross-over pressures with ULSD fuel for all isotherms tested, between 30 MPa at 283.15 K, and 62.1 MPa at 373.15 K. Coconut biodiesel is composed of FAMEs with chain lengths that are shorter on average than all other tested feedstocks, resulting in a lower ambient pressure viscosity than other biodiesels. The coconut biodiesel is still more viscous at low pressures than the diesel fuels tested, but the normalized viscosity increase found in FAMEs was less than the normalized viscosity increase for the non-polar components found in diesel, resulting in a higher diesel viscosity given sufficient pressure.

2. ***The percent increase from ambient viscosity to viscosity at high pressures was greater for all diesel fuels tested than biodiesels, and similar among diesel fuels.*** The percent increase from ambient pressure viscosity was greater for all fuels with decreasing temperature and increasing pressure. To clarify, diesel 4, (Table C20) at 278.15 K and 131 MPa has a viscosity 720% of its viscosity at 278.15 K and 0.1 MPa, and at 373.15 K and 131 MPa diesel 4 has a viscosity 327% of its viscosity at 373.15 K and 0.1 MPa.
3. All biodiesels tested had possible freezing point pressures at 283.15 K. None of the diesel samples had this property.

8.2 Biodiesel Comparisons by Feedstock

1. Generally, viscosity from least to most viscous: Coconut < soy-coconut blend < soy < low-linolenic soy < jatropha < canola oils. The soybean and low-linolenic soy biodiesels were very similar, as was the jatropha to the canola biodiesels.
2. Possible pressure freezing at 283.15 K from lowest to highest pressure: Jatropha < soy < low-linolenic soy < canola oils / soy-coconut blend < coconut oils. ***The higher the percentage of long-chained (C16:0 / C18:0) saturated FAMES, the lower pressure at which this would occur.***
3. Biodiesels all had very similar viscosity increases for the isotherms tested, as mentioned above. The percent increase from ambient pressure viscosity was

greatest for jatropha biodiesels, followed by canola oils, low-linolenic soy, soy and finally coconut biodiesel.

8.3 Biodiesel Blend Data Comparisons

1. Low-volume fraction biodiesel blends have viscosities that are similar to diesel fuel.
2. The general trend for viscosity order is that the higher the blend percentage of biodiesel, the greater the viscosity for comparable conditions.
3. Cross-over pressures are numerous among the low-percentage biodiesel-diesel blends, and are more likely at low temperature under the pressure range studied. ***At significantly higher pressures (250-350 MPa) cross-over pressures between neat biodiesels and low blend fraction blends or petroleum diesels are expected.*** This prediction has recently been proven to be correct in a work by Bair¹.
4. Biodiesel blend viscosities can be predicted using the ideal Grunberg-Nissan (GN) and Kay's mixing rules, assuming a pseudo binary. Kay's rule yielded better results for soy biodiesel-diesel blends while GN mixing rule yielded better results for Jatropha biodiesel-diesel blends.
5. Potential freezing point pressures were found for high-percentage (B40 and greater) biodiesel blends, as well as jatropha and palm biodiesel-diesel blends at a volume fraction of B20. No potential freezing point pressures were observed for any B5 or B10 percentage blends at 283.15 K.

8.4 Biodiesel, Diesel and Biodiesel-Blend Modeling

1. Individual fuels were modeled in Chapters 4, 5 and 6 with a Tait-Litovitz linearized temperature model. This is a six parameters model that is a function of temperature and pressure for a specific fuel. ***The absolute average relative deviation, given equal weighting, for the ten fuels for which this method was used was 1.1% with the maximum fuel average of 3.3% for the diesel presented in Chapter 3. The average absolute relative deviation is slightly less than the average repeatability presented in Appendix B.***
2. The neat biodiesels and diesels tested were normalized by dividing the viscosity at high pressure by the ambient pressure viscosity for a particular isotherm. The seven biodiesels and 566 data points had an AARD of 1.27%. Typical weakness in this model was for high-pressure low temperature prior to potential freezing pressures. ***The biodiesel Tait linearized-temperature parameters was able to extrapolate to pressures over 250% greater than those used in the model development with an average relative deviation of 4.25% at 350 MPa for literature data.***
3. A robust model using the biodiesel and diesel Tait linearized temperature parameters, biodiesel volume fraction, and ambient pressure viscosity of the blend was developed. The model worked well for low-temperature palm-diesel blends, jatropha blends, and soybean blends. The model would begin

to over-predict with increasing biodiesel blend fractions at high pressure, but gave average relative deviations less than 3%.

References Chapter 8

1. Bair, S., The pressure and temperature dependence of volume and viscosity of four Diesel fuels. *Fuel* **2014**, 135, 112-119.

Chapter 9

Future Work and Recommendations

The recommendations for future work consist of three main areas. The first, and most important suggested area of investigation, is the continued apparatus calibration. While extensive work has been performed to improve the accuracy and precision of the viscometer, additional steps can be taken to further the usefulness of the apparatus. The second proposed area of investigation is the addition of modular-type equipment to the high-pressure setup. Combined with high-pressure viscosity data, high-pressure density and phase change observations will aid investigators in answering many of the questions posed in this work. The third area of further investigation is a study on the effect of highly saturated renewable fuels on normalized viscosity increase and phase change conditions.

9.1 Instrument Calibration

1. Ambient-pressure temperature calibrations were found down to 293.15 K. Further work on cold temperature areas to verify corrections that have been extrapolated is recommended.
2. A fundamental adjustment to the high-pressure and ambient temperature corrections is recommended. Currently, an empirical correction has been developed based on observation. A physics-based working equation should

be investigated, and developed based on the instrument's fundamental operation.

9.2 Apparatus Additions

1. The addition of a view cell—either in line or as a modular unit that could be added or removed from the high-pressure circuit would allow for better understanding of the phase behavior which is thought to be occurring at low temperatures and high pressure for all biodiesel samples and many biodiesel blends.
2. A highly accurate densitometer, either in line or again, as a modular unit would allow for some of the more rigorous modeling methods to be used, and would be useful for not just biodiesel samples, but for many other investigations that require high-pressure fluid characterization.
3. Much of the pressure range of the normal pentadecane was unable to be reached due to tubing, which was located in the pressure circuit, but outside of the oven. Palm biodiesel, a highly-saturated fuel also experienced this problem, where at 313.15 K and approximately half of the possible pressure profile, pressure freezing occurred. The addition of an adequate length of heating rope coupled with insulation would be able to significantly increase the pressure range for many samples. An attempt was made with a 6 ft heating rope, and was found to increase the accessible pressure range of pentadecane at 373.15 K by approximately 2,000 psi up to a maximum pressure of ~11,600 psi. This maximum pressure was well short of the

20,000 psi capable of being reached by the apparatus, and pressures reached in other works. Modifications or corrections may be required for the pressure sensor during high temperature measurements where lab temperature pressure freezing might otherwise occur. Another possibility to help with this issue would be the addition of a fluid in the pressure circuit that is both immiscible with the sample being tested, and has a high pressure freezing point at room temperature.

9.3 Further Experiments with Saturated Fuels

1. Preliminary data has been taken for tallow biodiesel blends and palm biodiesel diesel blends, and can be found in their entirety in the appendices. However, a full study may yield a more complete picture. Jatropha biodiesel has approximately 20% saturated FAMES and experienced slight, but observable variations in normalized viscosity increase when compared to biodiesels with lower saturated FAME compositions. ***As saturated FAME percentages increase, additional important nuances may become apparent.***
2. Further testing is recommended not just for B100 palm and B100 tallow, but also green diesels and other potential fuels derived from highly-saturated renewable sources. A fundamental study on chain length and saturation with pure components is one suggested approach. Ideally, these studies would include high-pressure density and high-pressure view cell experiments as well.

Appendix A

Uncorrected High-Pressure Viscosity Data for Biodiesel, Diesel, and Biodiesel-Diesel Blends

All experimental high-pressure viscosity data was recorded manually. Those raw measurements, including temperature in Celsius, the standard deviation of the recorded temperature, pressure in psi, the average viscosity in cP of 20 measurements and standard deviation of those 20 measurements, as well as the piston and piston cdl used are included. ***These data must be corrected for temperature and elevated pressure. The methodology and corrections are given in Appendix B. The corrected viscosity measurements are given in Appendix C.*** Table A.0 below gives the page number for the beginning of each fuel's raw data table included in this appendix. Data included in Tables A.24 and A.25 are preliminary.

Table A.0 Table of Contents for Appendix A								
Table	Sample	Page #	Table	Sample	Page #	Table	Sample	Page #
A.1	Canola	152	A.10	Soy B10	188	A.19	Jatropha B20	234
A.2	Used Canola	156	A.11	Soy B20	193	A.20	Diesel4	240
A.3	Coconut	160	A.12	Soy B40	198	A.21	Palm B5	247
A.4	Soy1	164	A.13	Soy B60	203	A.22	Palm B10	252
A.5	Vistive	167	A.14	Soy B80	208	A.23	Palm B20	257
A.6	Diesel1	170	A.15	Jatropha	213	A.24	Tallow B5	261
A.7	Soy2	174	A.16	Diesel3	217	A.25	Tallow B20	267
A.8	Diesel2	178	A.17	Jatropha B5	222	A.26	Soy-Coconut	271
A.9	Soy B5	183	A.18	Jatropha B10	228			

Table A.1.1 Canola Oil Based Biodiesel, Raw, Uncorrected High Pressure Viscosity Experimental Data at 10 C.					
Canola Oil Based Biodiesel / 10 Celsius / 50 cP Piston / cdl 473					
Sample	P	T	dT	Raw Viscosity	SD
Name	[psi]	[C]	[C]	[cP]	%
Canola Oil Based Biodiesel	0	10.0	0.01	8.312	0.2
	100	10.0	0.01	8.351	0.3
	1000	10.0	0.02	9.016	0.3
	2000	10.0	0.02	9.769	0.1
	3000	10.0	0.02	10.53	0.1
	4000	10.0	0.01	11.36	0.2
	5000	10.0	0.01	12.19	0.2
	6000	10.0	0.01	13.11	0.2
	7000	10.0	0.01	14.05	0.2
	8000	10.0	0.01	15.05	0.1
	9000	10.0	0.02	16.12	0.1
	10000	10.0	0.02	17.25	0.2
	11000	10.0	0.01	18.35	0.2
	12000	10.0	0.03	19.95	0.3

Table A.1.2. Canola Oil Based Biodiesel, Raw, Uncorrected High Pressure Viscosity Experimental Data at 25 C.					
Canola Oil Based Biodiesel / 25 Celsius / 50 cP Piston / cdl 473					
Sample	P	T	dT	Raw Viscosity	SD
Name	[psi]	[C]	[C]	[cP]	%
Canola Oil Based Biodiesel	0	25.0	0.04	5.403	0.1
	100	25.0	0.04	5.444	0.1
	1000	25.0	0.04	5.825	0.1
	2000	25.0	0.02	6.280	0.3
	3000	25.0	0.02	6.737	0.3
	4000	25.0	0.02	7.219	0.2
	5000	25.0	0.03	7.720	0.2
	6000	25.0	0.02	8.230	0.3
	7000	25.0	0.02	8.758	0.1
	8000	25.0	0.02	9.329	0.2
	9000	25.0	0.01	9.904	0.1
	10000	25.0	0.02	10.48	0.1
	11000	25.0	0.02	11.12	0.2
	12000	25.0	0.02	11.76	0.1
	13000	25.0	0.01	12.46	0.2
	14000	25.0	0.01	13.18	0.1
	15000	25.0	0.02	13.98	0.2
	16000	25.0	0.01	14.78	0.1
17000	25.0	0.01	15.63	0.2	
18000	25.0	0.01	16.53	0.2	
19000	25.0	0.01	17.44	0.1	

Table A.1.3. Canola Oil Based Biodiesel, Raw, Uncorrected High Pressure Viscosity Experimental Data at 40 C.					
Canola Oil Based Biodiesel / 40 Celsius / 50 cP Piston / cdl 473					
Sample	P	T	dT	Raw Viscosity	SD
Name	[psi]	[C]	[C]	[cP]	%
Canola Oil Based Biodiesel	0	40.0	0.05	3.758	0.2
	100	40.0	0.05	3.785	0.2
	1000	40.0	0.03	4.041	0.1
	2000	40.0	0.03	4.333	0.2
	3000	40.0	0.05	4.636	0.3
	4000	40.0	0.04	4.945	0.3
	5000	40.0	0.03	5.267	0.3
	6000	40.0	0.04	5.600	0.2
	7000	40.0	0.04	5.927	0.3
	8000	40.0	0.03	6.262	0.3
	9000	40.0	0.03	6.625	0.3
	10000	40.0	0.04	6.999	0.1
	11000	40.0	0.03	7.395	0.3
	12000	40.0	0.02	7.800	0.2
	13000	40.0	0.03	8.211	0.1
	14000	40.0	0.03	8.664	0.1
	15000	40.0	0.03	9.142	0.3
	16000	40.0	0.03	9.625	0.1
	17000	40.0	0.02	10.13	0.3
	18000	40.0	0.02	10.62	0.1
19000	40.0	0.02	11.16	0.2	

Table A.1.4. Canola Oil Based Biodiesel, Raw, Uncorrected High Pressure Viscosity Experimental Data at 100 C.					
Canola Oil Based Biodiesel / 100 Celsius / 20 cP Piston / cdl 470					
Sample	P	T	dT	Raw Viscosity	SD
Name	[psi]	[C]	[C]	[cP]	%
Canola Oil Based Biodiesel	0	100.0	0.04	1.335	0.2
	100	100.0	0.04	1.347	0.2
	1000	100.0	0.03	1.426	0.2
	2000	100.0	0.03	1.513	0.2
	3000	100.0	0.03	1.602	0.2
	4000	100.0	0.05	1.697	0.3
	5000	100.0	0.03	1.789	0.3
	6000	100.0	0.03	1.882	0.2
	7000	100.0	0.04	1.980	0.2
	8000	100.0	0.04	2.086	0.2
	9000	100.0	0.02	2.190	0.2
	10000	100.0	0.03	2.294	0.3
	11000	100.0	0.03	2.397	0.2
	12000	100.0	0.03	2.496	0.2
	13000	100.0	0.03	2.613	0.2
	14000	100.0	0.03	2.723	0.3
	15000	100.0	0.03	2.827	0.1
	16000	100.0	0.03	2.937	0.2
	17000	100.0	0.03	3.048	0.2
18000	100.0	0.02	3.168	0.2	
19000	100.0	0.02	3.277	0.1	

Table A.2.1 Used Canola Oil Based Biodiesel, Raw, Uncorrected High Pressure Viscosity Experimental Data at 10 C.

Used Canola Oil Based Biodiesel / 10 Celsius / 50 cP Piston / cdl 473					
Sample	P	T	dT	Raw Viscosity	SD
Name	[psi]	[C]	[C]	[cP]	%
Used Canola Oil Based Biodiesel	0	10.0	0.02	8.356	0.2
	100	10.0	0.02	8.432	0.2
	1000	10.0	0.02	9.085	0.3
	2000	10.0	0.02	9.772	0.2
	3000	10.0	0.01	10.50	0.1
	4000	10.0	0.02	11.31	0.2
	5000	10.0	0.01	12.16	0.2
	6000	10.0	0.01	13.04	0.2
	7000	10.0	0.01	14.02	0.3
	8000	10.0	0.01	15.01	0.1
	9000	10.0	0.01	16.04	0.2
	10000	10.0	0.02	17.14	0.2
	11000	10.0	0.01	18.29	0.2
12000	10.0	0.01	19.68	0.2	

Table A.2.2 Used Canola Oil Based Biodiesel, Raw, Uncorrected High Pressure Viscosity Experimental Data at 25 C.

Used Canola Oil Based Biodiesel / 25 Celsius / 50 cP Piston / cdl 473					
Sample	P	T	dT	Raw Viscosity	SD
Name	[psi]	[C]	[C]	[cP]	%
Used Canola Oil Based Biodiesel	0	25.0	0.03	5.371	0.1
	100	25.0	0.03	5.412	0.3
	1000	25.0	0.03	5.781	0.3
	2000	25.0	0.03	6.223	0.1
	3000	25.0	0.02	6.681	0.2
	4000	25.0	0.02	7.148	0.2
	5000	25.0	0.02	7.634	0.1
	6000	25.0	0.02	8.164	0.2
	7000	25.0	0.02	8.711	0.1
	8000	25.0	0.02	9.258	0.1
	9000	25.0	0.02	9.861	0.2
	10000	25.0	0.02	10.47	0.2
	11000	25.0	0.02	11.13	0.2
	12000	25.0	0.03	11.77	0.2
	13000	25.0	0.01	12.44	0.2
	14000	25.0	0.02	13.15	0.3
	15000	25.0	0.01	13.90	0.2
	16000	25.0	0.01	14.70	0.2
	17000	25.0	0.01	15.52	0.2
18000	25.0	0.01	16.35	0.2	
19000	25.0	0.02	17.30	0.3	

Table A.2.3 Used Canola Oil Based Biodiesel, Raw, Uncorrected High Pressure Viscosity Experimental Data at 40 C.

Used Canola Oil Based Biodiesel / 40 Celsius / 50 cP Piston / cdl 473

Sample	P	T	dT	Raw Viscosity	SD
Name	[psi]	[C]	[C]	[cP]	%
Used Canola Oil Based Biodiesel	0	40.0	0.05	3.774	0.2
	100	40.0	0.03	3.810	0.2
	1000	40.0	0.05	4.060	0.1
	2000	40.0	0.04	4.349	0.3
	3000	40.0	0.03	4.664	0.4
	4000	40.0	0.02	4.965	0.1
	5000	40.0	0.01	5.264	0.2
	6000	40.0	0.03	5.600	0.3
	7000	40.0	0.03	5.937	0.2
	8000	40.0	0.02	6.304	0.1
	9000	40.0	0.02	6.682	0.2
	10000	40.0	0.02	7.060	0.2
	11000	40.0	0.01	7.451	0.2
	12000	40.0	0.02	7.859	0.2
	13000	40.0	0.02	8.301	0.3
	14000	40.0	0.02	8.746	0.2
	15000	40.0	0.02	9.202	0.2
	16000	40.0	0.02	9.700	0.3
17000	40.0	0.02	10.19	0.1	
18000	40.0	0.02	10.69	0.2	
19000	40.0	0.02	11.23	0.1	

Table A.2.4 Used Canola Oil Based Biodiesel, Raw, Uncorrected High Pressure Viscosity Experimental Data at 100 C.

Used Canola Oil Based Biodiesel / 100 Celsius / 20 cP Piston / cdl 470					
Sample	P	T	dT	Raw Viscosity	SD
Name	[psi]	[C]	[C]	[cP]	%
Used Canola Oil Based Biodiesel	0	100.0	0.03	1.342	0.2
	100	100.0	0.05	1.354	0.4
	1000	100.0	0.04	1.430	0.2
	2000	100.0	0.04	1.518	0.2
	3000	100.0	0.04	1.614	0.1
	4000	100.0	0.02	1.706	0.3
	5000	100.0	0.04	1.802	0.2
	6000	100.0	0.03	1.889	0.3
	7000	100.0	0.02	1.986	0.2
	8000	100.0	0.03	2.093	0.3
	9000	100.0	0.02	2.192	0.2
	10000	100.0	0.02	2.295	0.1
	11000	100.0	0.03	2.401	0.3
	12000	100.0	0.02	2.508	0.2
	13000	100.0	0.02	2.614	0.2
	14000	100.0	0.03	2.728	0.2
	15000	100.0	0.02	2.833	0.2
	16000	100.0	0.04	2.946	0.1
	17000	100.0	0.02	3.063	0.1
18000	100.0	0.02	3.185	0.3	
19000	100.0	0.02	3.303	0.3	

Table A.3.1 Coconut Oil Based Biodiesel, Raw, Uncorrected High Pressure Viscosity Experimental Data at 10 C.					
Coconut Oil Based Biodiesel / 10 Celsius / 50 cP Piston / cdl 473					
Sample	P	T	dT	Raw Viscosity	SD
Name	[psi]	[C]	[C]	[cP]	%
Coconut Oil Based Biodiesel	0	10.0	0.03	4.711	0.1
	100	10.0	0.05	4.747	0.1
	1000	10.0	0.02	5.073	0.2
	2000	10.0	0.04	5.458	0.2
	3000	10.0	0.02	5.874	0.3
	4000	10.0	0.02	6.302	0.2
	5000	10.0	0.03	6.739	0.1
	6000	10.0	0.02	7.206	0.1
	7000	10.0	0.03	7.693	0.3
	8000	10.0	0.02	8.195	0.3
	9000	10.0	0.02	8.718	0.2
	10000	10.0	0.02	9.252	0.2
	11000	10.0	0.02	9.813	0.3
	12000	10.0	0.02	10.39	0.1
	13000	10.0	0.01	11.03	0.2
14000	10.0	0.02	11.67	0.2	

Table A.3.2 Coconut Oil Based Biodiesel, Raw, Uncorrected High Pressure Viscosity Experimental Data at 25 C.					
Coconut Oil Based Biodiesel / 25 Celsius / 50 cP Piston / cdl 473					
Sample	P	T	dT	Raw Viscosity	SD
Name	[psi]	[C]	[C]	[cP]	%
Coconut Oil Based Biodiesel	0	25.0	0.03	3.160	0.1
	100	25.0	0.05	3.180	0.2
	1000	25.0	0.03	3.395	0.3
	2000	25.0	0.03	3.660	0.2
	3000	25.0	0.03	3.912	0.4
	4000	25.0	0.04	4.176	0.1
	5000	25.0	0.05	4.454	0.3
	6000	25.0	0.04	4.723	0.3
	7000	25.0	0.04	5.011	0.1
	8000	25.0	0.03	5.320	0.1
	9000	25.0	0.04	5.622	0.4
	10000	25.0	0.04	5.941	0.1
	11000	25.0	0.01	6.288	0.4
	12000	25.0	0.03	6.640	0.3
	13000	25.0	0.02	6.995	0.3
	14000	25.0	0.02	7.358	0.1
	15000	25.0	0.03	7.759	0.1
	16000	25.0	0.02	8.174	0.3
	17000	25.0	0.02	8.614	0.2
18000	25.0	0.02	9.059	0.2	
19000	25.0	0.02	9.531	0.2	

Table A.3.3 Coconut Oil Based Biodiesel, Raw, Uncorrected High Pressure Viscosity Experimental Data at 40 C.					
Coconut Oil Based Biodiesel / 40 Celsius / 20 cP Piston / cdl 484					
Sample	P	T	dT	Raw Viscosity	SD
Name	[psi]	[C]	[C]	[cP]	%
Coconut Oil Based Biodiesel	0	40.1	0.02	2.093	0.3
	100	40.1	0.04	2.145	0.2
	1000	40.1	0.03	2.288	0.4
	2000	40.0	0.03	2.442	0.2
	3000	40.1	0.03	2.597	0.2
	4000	40.1	0.02	2.754	0.2
	5000	40.0	0.04	2.926	0.3
	6000	40.1	0.03	3.092	0.3
	7000	40.1	0.02	3.259	0.2
	8000	40.0	0.03	3.447	0.2
	9000	40.0	0.01	3.636	0.1
	10000	40.0	0.03	3.829	0.1
	11000	40.1	0.01	4.035	0.3
	12000	40.1	0.02	4.247	0.3
	13000	40.0	0.03	4.461	0.2
	14000	39.9	0.01	4.696	0.2
	15000	40.0	0.02	4.910	0.2
	16000	40.1	0.02	5.131	0.2
	17000	40.1	0.01	5.367	0.1
18000	40.1	0.02	5.615	0.2	
19000	40.1	0.02	5.870	0.3	

Table A.3.4 Coconut Oil Based Biodiesel, Raw, Uncorrected High Pressure Viscosity Experimental Data at 100 C.					
Coconut Oil Based Biodiesel / 100 Celsius / 5 cP Piston / cdl 470					
Sample	P	T	dT	Raw Viscosity	SD
Name	[psi]	[C]	[C]	[cP]	%
Coconut Oil Based Biodiesel	0	100.0	0.03	0.797	0.2
	100	100.0	0.01	0.842	0.2
	1000	99.9	0.04	0.887	0.1
	2000	99.9	0.01	0.932	0.2
	3000	99.9	0.03	0.973	0.2
	4000	100.0	0.02	1.016	0.2
	5000	100.0	0.01	1.059	0.2
	6000	99.9	0.02	1.102	0.2
	7000	100.0	0.02	1.141	0.1
	8000	100.1	0.02	1.185	0.2
	9000	100.1	0.02	1.228	0.2
	10000	100.1	0.02	1.270	0.1
	11000	100.1	0.02	1.314	0.2
	12000	100.0	0.01	1.357	0.2
	13000	100.0	0.01	1.397	0.1
	14000	100.0	0.01	1.438	0.2
	15000	100.1	0.02	1.475	0.1
	16000	100.2	0.02	1.515	0.2
17000	100.2	0.02	1.554	0.2	
18000	100.0	0.04	1.599	0.2	
19000	100.0	0.01	1.646	0.2	

Table A.4.1 Soybean Oil Based Biodiesel, Raw, Uncorrected High Pressure Viscosity Experimental Data at 10 C.					
Soybean Oil Based Biodiesel / 10 Celsius / 50 cP Piston / cdl 473					
Sample	P	T	dT	Raw Viscosity	SD
Name	[psi]	[C]	[C]	[cP]	%
Soybean Oil Based Biodiesel	0	10.0	0.02	7.193	0.3
	100	10.0	0.03	7.301	0.4
	1000	10.0	0.02	7.832	0.3
	2000	10.0	0.02	8.448	0.2
	3000	10.0	0.02	9.100	0.2
	4000	10.0	0.02	9.786	0.2
	5000	10.0	0.02	10.50	0.2
	6000	10.0	0.01	11.25	0.2
	7000	10.0	0.01	12.01	0.1
	8000	10.0	0.01	12.84	0.1
	9000	10.0	0.01	13.69	0.2
10000	10.0	0.01	14.65	0.2	

Table A.4.2 Soybean Oil Based Biodiesel, Raw, Uncorrected High Pressure Viscosity Experimental Data at 25 C.					
Soybean Oil Based Biodiesel / 25 Celsius / 50 cP Piston / cdl 473					
Sample	P	T	dT	Raw Viscosity	SD
Name	[psi]	[C]	[C]	[cP]	%
Soybean Oil Based Biodiesel	0	25.0	0.02	4.864	0.1
	100	25.0	0.03	4.901	0.1
	1000	25.0	0.02	5.243	0.2
	2000	25.0	0.01	5.622	0.2
	3000	25.0	0.01	6.024	0.2
	4000	25.0	0.02	6.435	0.2
	5000	25.0	0.01	6.875	0.4
	6000	25.0	0.02	7.299	0.2
	7000	25.0	0.02	7.772	0.4
	8000	25.0	0.02	8.264	0.2
	9000	25.0	0.01	8.768	0.2
	10000	25.0	0.01	9.292	0.2
	11000	25.0	0.02	9.823	0.1
	12000	25.0	0.02	10.42	0.2
	13000	25.0	0.01	11.00	0.2
	14000	25.0	0.01	11.61	0.2
	15000	25.0	0.02	12.33	0.2
	16000	25.0	0.01	13.00	0.2
	17000	25.0	0.02	13.70	0.1
18000	25.0	0.01	14.46	0.1	
19000	25.0	0.01	15.21	0.3	

Table A.4.3 Soybean Oil Based Biodiesel, Raw, Uncorrected High Pressure Viscosity Experimental Data at 40 C.					
Soybean Oil Based Biodiesel / 40 Celsius / 20 cP Piston / cdl 484					
Sample	P	T	dT	Raw Viscosity	SD
Name	[psi]	[C]	[C]	[cP]	%
Soybean Oil Based Biodiesel	0	40.0	0.04	3.380	0.2
	100	40.1	0.02	3.415	0.1
	1000	40.0	0.02	3.626	0.2
	2000	39.9	0.02	3.879	0.2
	3000	39.9	0.02	4.119	0.1
	4000	40.0	0.02	4.373	0.2
	5000	40.1	0.02	4.619	0.2
	6000	40.1	0.01	4.890	0.2
	7000	40.1	0.02	5.171	0.2
	8000	40.0	0.02	5.478	0.1
	9000	40.0	0.02	5.794	0.2
	10000	40.1	0.02	6.104	0.2
	11000	40.1	0.01	6.421	0.2
	12000	40.1	0.03	6.760	0.2
	13000	40.0	0.03	7.112	0.2
	14000	39.9	0.01	7.494	0.1
	15000	40.0	0.03	7.906	0.1
	16000	40.1	0.02	8.314	0.2
	17000	40.1	0.01	8.741	0.1
18000	40.0	0.02	9.217	0.1	
19000	40.0	0.02	9.726	0.2	

Table A.4.4 Soybean Oil Based Biodiesel, Raw, Uncorrected High Pressure Viscosity Experimental Data at 100 C.					
Soybean Oil Based Biodiesel / 100 Celsius / 20 cP Piston / cdl 484					
Sample	P	T	dT	Raw Viscosity	SD
Name	[psi]	[C]	[C]	[cP]	%
Soybean Oil Based Biodiesel	0	100.0	0.05	1.288	0.2
	100	100.0	0.05	1.294	0.2
	1000	100.0	0.05	1.369	0.2
	2000	99.9	0.03	1.455	0.2
	3000	99.8	0.05	1.542	0.2
	4000	99.9	0.05	1.626	0.2
	5000	100.0	0.05	1.713	0.2
	6000	99.9	0.04	1.806	0.2
	7000	99.9	0.03	1.895	0.2
	8000	100.0	0.03	1.988	0.2
	9000	100.1	0.03	2.077	0.4
	10000	100.1	0.05	2.164	0.3
	11000	99.9	0.05	2.257	0.4
	12000	99.9	0.05	2.354	0.3
	13000	99.9	0.02	2.455	0.3
	14000	100.0	0.02	2.555	0.3
	15000	100.0	0.03	2.656	0.2
	16000	100.1	0.02	2.747	0.2
	17000	100.1	0.02	2.849	0.1
18000	100.1	0.03	2.960	0.2	
19000	100.0	0.04	3.069	0.2	

Table A.5.1 Vistive Oil Based Biodiesel, Raw, Uncorrected High Pressure Viscosity Experimental Data at 10 C.					
Vistive Oil Based Biodiesel / 10 Celsius / 50 cP Piston / cdl 473					
Sample	P	T	dT	Raw Viscosity	SD
Name	[psi]	[C]	[C]	[cP]	%
Vistive Oil Based Biodiesel	0	10.0	0.03	7.504	0.1
	100	10.0	0.02	7.568	0.2
	1000	10.0	0.03	8.108	0.2
	2000	10.0	0.03	8.760	0.2
	3000	10.0	0.02	9.440	0.2
	4000	10.0	0.02	10.14	0.2
	5000	10.0	0.02	10.88	0.1
	6000	10.0	0.02	11.67	0.2
	7000	10.0	0.02	12.48	0.1
	8000	10.0	0.01	13.32	0.1
	9000	10.0	0.01	14.19	0.2
	10000	10.0	0.01	15.11	0.1
	10500	10.0	0.01	15.59	0.1

Table A.5.2 Vistive Oil Based Biodiesel, Raw, Uncorrected High Pressure Viscosity Experimental Data at 25 C.					
Vistive Oil Based Biodiesel / 25 Celsius / 50 cP Piston / cdl 473					
Sample	P	T	dT	Raw Viscosity	SD
Name	[psi]	[C]	[C]	[cP]	%
Vistive Oil Based Biodiesel	0	25.0	0.02	4.899	0.2
	100	25.0	0.03	4.955	0.1
	1000	25.0	0.02	5.308	0.2
	2000	25.0	0.02	5.705	0.3
	3000	25.0	0.02	6.106	0.1
	4000	25.0	0.02	6.539	0.2
	5000	25.0	0.02	6.980	0.3
	6000	25.0	0.02	7.430	0.1
	7000	25.0	0.03	7.911	0.1
	8000	25.0	0.03	8.408	0.2
	9000	25.0	0.02	8.928	0.3
	10000	25.0	0.01	9.471	0.1
	11000	25.0	0.01	10.03	0.1
	12000	25.0	0.01	10.62	0.2
	13000	25.0	0.01	11.22	0.1
	14000	25.0	0.02	11.87	0.2
	15000	25.0	0.01	12.54	0.1
	16000	25.0	0.02	13.24	0.2
	17000	25.0	0.01	13.96	0.2
18000	25.0	0.01	14.71	0.2	
19000	25.0	0.01	15.50	0.2	

Table A.5.3 Vistive Oil Based Biodiesel, Raw, Uncorrected High Pressure Viscosity Experimental Data at 40 C.					
Vistive Oil Based Biodiesel / 40 Celsius / 20 cP Piston / cdl 484					
Sample	P	T	dT	Raw Viscosity	SD
Name	[psi]	[C]	[C]	[cP]	%
Vistive Oil Based Biodiesel	0	40.0	0.03	3.450	0.1
	100	40.0	0.03	3.490	0.2
	1000	40.1	0.02	3.721	0.2
	2000	40.0	0.03	3.977	0.1
	3000	39.9	0.01	4.237	0.2
	4000	39.9	0.02	4.505	0.1
	5000	39.9	0.02	4.770	0.2
	6000	40.0	0.02	5.050	0.2
	7000	40.1	0.02	5.335	0.2
	8000	40.1	0.02	5.628	0.2
	9000	40.1	0.02	5.949	0.2
	10000	40.1	0.03	6.293	0.1
	11000	40.0	0.02	6.644	0.3
	12000	40.0	0.02	6.987	0.2
	13000	40.1	0.02	7.342	0.2
	14000	40.1	0.01	7.743	0.1
	15000	40.1	0.02	8.186	0.2
	16000	40.0	0.01	8.658	0.1
	17000	40.0	0.02	9.115	0.1
18000	40.1	0.01	9.564	0.2	
19000	40.1	0.01	10.04	0.1	

Table A.5.4 Vistive Oil Based Biodiesel, Raw, Uncorrected High Pressure Viscosity Experimental Data at 100 C.					
Vistive Oil Based Biodiesel / 100 Celsius / 20 cP Piston / cdl 484					
Sample	P	T	dT	Raw Viscosity	SD
Name	[psi]	[C]	[C]	[cP]	%
Vistive Oil Based Biodiesel	0	100.0	0.05	1.276	0.2
	100	99.9	0.03	1.285	0.2
	1000	99.9	0.03	1.363	0.2
	2000	99.9	0.04	1.448	0.4
	3000	100.0	0.03	1.536	0.3
	4000	99.9	0.06	1.624	0.2
	5000	99.8	0.04	1.713	0.3
	6000	99.8	0.03	1.804	0.2
	7000	99.8	0.04	1.896	0.1
	8000	99.9	0.04	1.986	0.3
	9000	99.9	0.03	2.081	0.2
	10000	99.9	0.04	2.174	0.2
	11000	100.0	0.03	2.272	0.1
	12000	100.0	0.03	2.371	0.2
	13000	100.0	0.04	2.467	0.4
	14000	100.1	0.04	2.565	0.2
	15000	100.1	0.02	2.659	0.2
	16000	100.0	0.04	2.772	0.4
	17000	100.0	0.04	2.880	0.1
18000	99.9	0.03	2.990	0.2	
19000	99.9	0.04	3.103	0.2	

Table A.6.1 No. 2 Diesel, Raw, Uncorrected High Pressure Viscosity Experimental Data at 10 C.					
No. 2 Diesel / 10 Celsius / 50 cP Piston / cdl 473					
Sample	P	T	dT	Raw Viscosity	SD
Name	[psi]	[C]	[C]	[cP]	%
No. 2 Diesel	0	10.0	0.03	4.270	0.3
	100	10.0	0.03	4.344	0.2
	1000	10.0	0.03	4.747	0.3
	2000	10.0	0.03	5.223	0.3
	3000	10.0	0.02	5.738	0.3
	4000	10.0	0.02	6.319	0.3
	5000	10.0	0.02	6.932	0.1
	6000	10.0	0.01	7.611	0.1
	7000	10.0	0.02	8.344	0.1
	8000	10.0	0.01	9.154	0.2
	9000	10.0	0.02	10.03	0.2
	10000	10.0	0.01	10.92	0.2
	11000	10.0	0.01	11.90	0.1
	12000	10.0	0.01	13.01	0.2
	13000	10.0	0.01	14.18	0.2
	14000	10.0	0.01	15.46	0.2
	15000	10.0	0.01	16.79	0.2
	16000	10.0	0.01	18.28	0.2
	17000	10.0	0.01	20.06	0.1
18000	10.0	0.01	22.06	0.2	
19000	10.0	0.01	24.15	0.2	

Table A.6.2 No. 2 Diesel, Raw, Uncorrected High Pressure Viscosity Experimental Data at 25 C.					
No. 2 Diesel / 25 Celsius / 20 cP Piston / cdl 484					
Sample	P	T	dT	Raw Viscosity	SD
Name	[psi]	[C]	[C]	[cP]	%
No. 2 Diesel	0	25.0	0.03	2.756	0.2
	100	25.0	0.02	2.786	0.3
	1000	25.0	0.03	3.011	0.3
	2000	25.0	0.02	3.276	0.2
	3000	25.0	0.02	3.567	0.3
	4000	25.0	0.02	3.874	0.2
	5000	25.0	0.02	4.202	0.1
	6000	25.0	0.01	4.555	0.1
	7000	25.0	0.01	4.930	0.1
	8000	25.0	0.01	5.325	0.1
	9000	25.0	0.01	5.738	0.1
	10000	25.0	0.01	6.196	0.1
	11000	25.0	0.01	6.705	0.1
	12000	25.0	0.01	7.226	0.2
	13000	25.0	0.01	7.827	0.2
	14000	25.0	0.01	8.473	0.1
	15000	25.0	0.01	9.172	0.1
	16000	25.0	0.01	9.918	0.1
	17000	25.0	0.01	10.73	0.2
	18000	25.0	0.01	11.61	0.1
19000	25.0	0.01	12.53	0.1	

Table A.6.3 No. 2 Diesel, Raw, Uncorrected High Pressure Viscosity Experimental Data at 40 C.					
No. 2 Diesel / 40 Celsius / 20 cP Piston / cdl 484					
Sample	P	T	dT	Raw Viscosity	SD
Name	[psi]	[C]	[C]	[cP]	%
No. 2 Diesel	0	40.0	0.03	1.967	0.3
	100	40.0	0.03	1.995	0.1
	1000	40.0	0.03	2.149	0.2
	2000	40.0	0.03	2.331	0.3
	3000	40.0	0.02	2.516	0.2
	4000	40.0	0.03	2.721	0.3
	5000	40.0	0.03	2.932	0.1
	6000	40.0	0.02	3.147	0.2
	7000	40.0	0.02	3.387	0.3
	8000	40.0	0.02	3.643	0.2
	9000	40.0	0.01	3.910	0.2
	10000	40.0	0.02	4.195	0.3
	11000	40.0	0.02	4.496	0.2
	12000	40.0	0.02	4.818	0.2
	13000	40.0	0.02	5.160	0.1
	14000	40.0	0.01	5.497	0.2
	15000	40.0	0.02	5.867	0.3
	16000	40.0	0.02	6.262	0.2
	17000	40.0	0.02	6.664	0.1
	18000	40.0	0.01	7.101	0.1
19000	40.0	0.01	7.604	0.1	

Table A.6.4 No. 2 Diesel, Raw, Uncorrected High Pressure Viscosity Experimental Data at 100 C.					
No. 2 Diesel / 100 Celsius / 5 cP Piston / cdl 470					
Sample	P	T	dT	Raw Viscosity	SD
Name	[psi]	[C]	[C]	[cP]	%
No. 2 Diesel	0	100.0	0.02	0.767	0.2
	100	100.0	0.02	0.775	0.1
	1000	100.0	0.02	0.818	0.2
	2000	100.0	0.03	0.868	0.3
	3000	100.0	0.02	0.919	0.3
	4000	100.0	0.01	0.968	0.2
	5000	100.0	0.04	1.019	0.2
	6000	100.0	0.03	1.070	0.2
	7000	100.0	0.01	1.126	0.2
	8000	100.0	0.02	1.177	0.2
	9000	100.0	0.01	1.227	0.2
	10000	100.0	0.03	1.279	0.2
	11000	100.0	0.01	1.333	0.2
	12000	100.0	0.01	1.386	0.1
	13000	100.0	0.01	1.444	0.3
	14000	100.0	0.01	1.499	0.1
	15000	100.0	0.02	1.559	0.1
	16000	100.0	0.02	1.611	0.1
	17000	100.0	0.01	1.668	0.2
18000	100.0	0.03	1.730	0.2	
19000	100.0	0.02	1.793	0.1	

Table A.7.1 Soybean Oil Based Biodiesel Used in ULSD Blends, Raw, Uncorrected High Pressure Viscosity Experimental Data at 10 C.					
Soybean Oil Based Biodiesel/ Blends / 10 Celsius / 50 cP Piston / cdl 470					
Sample	P	T	dT	Raw Viscosity	SD
Name	[psi]	[C]	[C]	[cP]	%
Soybean Oil Based Biodiesel Used in ULSD Blends	25	10.0	0.02	7.558	0.2
	100	10.0	0.02	7.597	0.1
	1000	10.0	0.03	8.171	0.3
	2000	10.0	0.02	8.799	0.2
	3000	10.0	0.03	9.445	0.1
	4000	10.0	0.02	10.13	0.3
	5000	10.0	0.01	10.86	0.3
	6000	10.0	0.01	11.62	0.2
	7000	10.0	0.01	12.40	0.2
	8000	10.0	0.01	13.26	0.2
9000	10.0	0.01	14.12	0.1	
10000	10.0	0.01	15.06	0.1	

Table A.7.2 Soybean Oil Based Biodiesel Used in ULSD Blends, Raw, Uncorrected High Pressure Viscosity Experimental Data at 25 C.					
Soybean Oil Based Biodiesel/ Blends / 25 Celsius / 50 cP Piston / cdl 470					
Sample	P	T	dT	Raw Viscosity	SD
Name	[psi]	[C]	[C]	[cP]	%
Soybean Oil Based Biodiesel Used in ULSD Blends	11	25.0	0.03	4.914	0.3
	100	25.0	0.02	4.943	0.2
	1000	25.0	0.03	5.284	0.3
	2000	25.0	0.03	5.683	0.3
	3000	25.0	0.02	6.068	0.1
	4000	25.0	0.02	6.466	0.1
	5000	25.0	0.02	6.900	0.2
	6000	25.0	0.01	7.334	0.2
	7000	25.0	0.02	7.813	0.3
	8000	25.0	0.02	8.279	0.1
	9000	25.0	0.02	8.791	0.2
	10000	25.0	0.01	9.342	0.2
	11000	25.0	0.02	9.894	0.1
	12000	25.0	0.01	10.49	0.2
	13000	25.0	0.02	11.09	0.3
	14000	25.0	0.02	11.72	0.2
	15000	25.0	0.01	12.38	0.1
16000	25.0	0.01	13.08	0.1	
17000	25.0	0.01	13.80	0.2	
18000	25.0	0.01	14.52	0.1	
19000	25.0	0.01	15.29	0.1	

Table A.7.3 Soybean Oil Based Biodiesel Used in ULSD Blends, Raw, Uncorrected High Pressure Viscosity Experimental Data at 40 C.					
Soybean Oil Based Biodiesel/ Blends / 40 Celsius / 20 cP Piston / cdl 476					
Sample	P	T	dT	Raw Viscosity	SD
Name	[psi]	[C]	[C]	[cP]	%
Soybean Oil Based Biodiesel Used in ULSD Blends	20	40.0	0.03	3.489	0.2
	100	40.0	0.01	3.503	0.1
	1000	40.0	0.03	3.722	0.1
	2000	40.0	0.03	3.959	0.3
	3000	40.0	0.04	4.203	0.1
	4000	40.0	0.02	4.470	0.3
	5000	40.0	0.02	4.734	0.1
	6000	40.0	0.02	5.016	0.1
	7000	40.0	0.01	5.300	0.1
	8000	40.0	0.01	5.602	0.2
	9000	40.0	0.01	5.898	0.1
	10000	40.0	0.01	6.221	0.1
	11000	40.0	0.01	6.563	0.2
	12000	40.0	0.01	6.891	0.1
	13000	40.0	0.01	7.248	0.4
	14000	40.0	0.02	7.652	0.1
	15000	40.0	0.02	8.049	0.2
	16000	40.0	0.01	8.483	0.2
17000	40.0	0.01	8.934	0.2	
18000	40.0	0.02	9.397	0.1	
19000	40.0	0.01	9.852	0.2	

Table A.7.4 Soybean Oil Based Biodiesel Used in ULSD Blends, Raw, Uncorrected High Pressure Viscosity Experimental Data at 70 C.					
Soybean Oil Based Biodiesel/ Blends / 70 Celsius / 20 cP Piston / cdl 476					
Sample	P	T	dT	Raw Viscosity	SD
Name	[psi]	[C]	[C]	[cP]	%
Soybean Oil Based Biodiesel Used in ULSD Blends	27	70.0	0.03	2.014	0.3
	100	70.0	0.04	2.021	0.3
	1000	70.0	0.04	2.140	0.4
	2000	70.0	0.04	2.275	0.4
	3000	70.0	0.03	2.405	0.2
	4000	70.0	0.02	2.547	0.3
	5000	70.0	0.03	2.693	0.2
	6000	70.0	0.02	2.832	0.1
	7000	70.0	0.02	2.982	0.1
	8000	70.0	0.03	3.136	0.3
	9000	70.0	0.02	3.287	0.2
	10000	70.0	0.02	3.454	0.3
	11000	70.0	0.02	3.616	0.3
	12000	70.0	0.02	3.781	0.3
	13000	70.0	0.02	3.952	0.2
	14000	70.0	0.02	4.122	0.2
	15000	70.0	0.01	4.309	0.3
	16000	70.0	0.02	4.487	0.3
17000	70.0	0.02	4.670	0.1	
18000	70.0	0.02	4.860	0.3	
19000	70.0	0.03	5.046	0.2	

Table A.7.5 Soybean Oil Based Biodiesel Used in ULSD Blends, Raw, Uncorrected High Pressure Viscosity Experimental Data at 100 C.					
Soybean Oil Based Biodiesel/ Blends / 100 Celsius / 5 cP Piston / cdl 466					
Sample	P	T	dT	Raw Viscosity	SD
Name	[psi]	[C]	[C]	[cP]	%
Soybean Oil Based Biodiesel Used in ULSD Blends	25	100.0	0.02	1.274	0.2
	100	100.0	0.02	1.281	0.2
	1000	100.0	0.02	1.339	0.2
	2000	100.0	0.01	1.407	0.3
	3000	100.0	0.02	1.470	0.3
	4000	100.0	0.01	1.530	0.1
	5000	100.0	0.02	1.592	0.1
	6000	100.0	0.02	1.654	0.1
	7000	100.0	0.01	1.717	0.2
	8000	100.0	0.01	1.778	0.1
	9000	100.0	0.01	1.839	0.1
	10000	100.0	0.01	1.906	0.1
	11000	100.0	0.01	1.976	0.2
	12000	100.0	0.01	2.046	0.2
	13000	100.0	0.01	2.114	0.2
	14000	100.0	0.01	2.182	0.2
	15000	100.0	0.02	2.254	0.1
16000	100.0	0.01	2.323	0.1	
17000	100.0	0.01	2.392	0.1	
18000	100.0	0.01	2.461	0.2	
19000	100.0	0.01	2.527	0.2	

Table A.8.1 ULSD Used in Soy Biodiesel/ULSD Blends, Raw, Uncorrected High Pressure Viscosity Experimental Data at 10 C.					
ULSD/ Blends / 10 Celsius / 50 cP Piston / cdl 470					
Sample	P	T	dT	Raw Viscosity	SD
Name	[psi]	[C]	[C]	[cP]	%
ULSD Used in Soy Biodiesel / ULSD Blends	0	10.0	0.03	3.980	0.4
	100	10.0	0.04	4.013	0.2
	1000	10.0	0.04	4.377	0.2
	2000	10.0	0.02	4.816	0.2
	3000	10.0	0.02	5.288	0.3
	4000	10.0	0.02	5.798	0.2
	5000	10.0	0.02	6.341	0.2
	6000	10.0	0.02	6.939	0.3
	7000	10.0	0.03	7.585	0.3
	8000	10.0	0.02	8.282	0.2
	9000	10.0	0.01	9.029	0.3
	10000	10.0	0.02	9.852	0.2
	11000	10.0	0.02	10.70	0.2
	12000	10.0	0.01	11.63	0.1
	13000	10.0	0.01	12.66	0.1
	14000	10.0	0.01	13.73	0.2
	15000	10.0	0.01	14.92	0.2
	16000	10.0	0.01	16.19	0.2
	17000	10.0	0.01	17.58	0.2
18000	10.0	0.01	19.15	0.2	
19000	10.0	0.01	20.98	0.1	

Table A.8.2 ULSD Used in Soy Biodiesel/ULSD Blends, Raw, Uncorrected High Pressure Viscosity Experimental Data at 25 C.					
ULSD/ Blends / 25 Celsius / 50 cP Piston / cdl 470					
Sample	P	T	dT	Raw Viscosity	SD
Name	[psi]	[C]	[C]	[cP]	%
ULSD Used in Soy Biodiesel / ULSD Blends	31	25.0	0.04	2.698	0.1
	100	25.0	0.05	2.712	0.2
	1000	25.0	0.04	2.934	0.2
	2000	25.0	0.04	3.206	0.2
	3000	25.0	0.03	3.489	0.1
	4000	25.0	0.05	3.798	0.2
	5000	25.0	0.02	4.122	0.3
	6000	25.0	0.02	4.455	0.2
	7000	25.0	0.02	4.811	0.2
	8000	25.0	0.03	5.181	0.2
	9000	25.0	0.03	5.592	0.2
	10000	25.0	0.01	6.035	0.2
	11000	25.0	0.02	6.521	0.1
	12000	25.0	0.02	7.031	0.2
	13000	25.0	0.02	7.586	0.2
	14000	25.0	0.01	8.136	0.2
	15000	25.0	0.02	8.759	0.2
	16000	25.0	0.02	9.413	0.1
17000	25.0	0.02	10.14	0.2	
18000	25.0	0.02	10.91	0.1	
19000	25.0	0.01	11.72	0.1	

Table A.8.3 ULSD Used in Soy Biodiesel/ULSD Blends, Raw, Uncorrected High Pressure Viscosity Experimental Data at 40 C.					
ULSD / Blends / 40 Celsius / 20 cP Piston / cdl 476					
Sample	P	T	dT	Raw Viscosity	SD
Name	[psi]	[C]	[C]	[cP]	%
ULSD Used in Soy Biodiesel / ULSD Blends	20	40.0	0.03	1.980	0.3
	100	40.0	0.03	1.994	0.3
	1000	40.0	0.03	2.142	0.2
	2000	40.0	0.03	2.323	0.1
	3000	40.0	0.02	2.518	0.2
	4000	40.0	0.02	2.717	0.2
	5000	40.0	0.02	2.920	0.2
	6000	40.0	0.02	3.137	0.3
	7000	40.0	0.02	3.365	0.2
	8000	40.0	0.01	3.616	0.3
	9000	40.0	0.01	3.813	0.3
	10000	40.0	0.01	4.148	0.3
	11000	40.0	0.01	4.431	0.1
	12000	40.0	0.01	4.740	0.2
	13000	40.0	0.01	5.056	0.1
	14000	40.0	0.01	5.385	0.2
	15000	40.0	0.01	5.741	0.2
16000	40.0	0.02	6.117	0.1	
17000	40.0	0.02	6.517	0.1	
18000	40.0	0.01	6.951	0.1	
19000	40.0	0.02	7.404	0.1	

Table A.8.4 ULSD Used in Soy Biodiesel/ULSD Blends, Raw, Uncorrected High Pressure Viscosity Experimental Data at 70 C.					
ULSD / Blends / 70 Celsius / 20 cP Piston / cdl 476					
Sample	P	T	dT	Raw Viscosity	SD
Name	[psi]	[C]	[C]	[cP]	%
ULSD Used in Soy Biodiesel / ULSD Blends	22	70.0	0.04	1.174	0.2
	100	70.0	0.04	1.184	0.2
	1000	70.0	0.03	1.263	0.2
	2000	70.0	0.03	1.354	0.2
	3000	70.0	0.04	1.452	0.2
	4000	70.0	0.04	1.552	0.2
	5000	70.0	0.04	1.655	0.2
	6000	70.0	0.05	1.764	0.4
	7000	70.0	0.03	1.877	0.2
	8000	70.0	0.03	1.998	0.2
	9000	70.0	0.02	2.120	0.3
	10000	70.0	0.02	2.250	0.3
	11000	70.0	0.03	2.387	0.1
	12000	70.0	0.02	2.523	0.1
	13000	70.0	0.02	2.664	0.3
	14000	70.0	0.02	2.819	0.3
	15000	70.0	0.02	2.979	0.3
	16000	70.0	0.02	3.139	0.2
17000	70.0	0.02	3.311	0.3	
18000	70.0	0.02	3.488	0.2	
19000	70.0	0.02	3.678	0.1	

Table A.8.5 ULSD Used in Soy Biodiesel/ULSD Blends, Raw, Uncorrected High Pressure Viscosity Experimental Data at 100 C.					
ULSD / Blends / 100 Celsius / 5 cP Piston / cdl 466					
Sample	P	T	dT	Raw Viscosity	SD
Name	[psi]	[C]	[C]	[cP]	%
ULSD Used in Soy Biodiesel / ULSD Blends	26	100.0	0.02	0.755	0.2
	100	100.0	0.03	0.764	0.3
	1000	100.0	0.02	0.809	0.3
	2000	100.0	0.03	0.857	0.2
	3000	100.0	0.03	0.905	0.3
	4000	100.0	0.03	0.951	0.1
	5000	100.0	0.02	0.998	0.2
	6000	100.0	0.02	1.047	0.1
	7000	100.0	0.01	1.097	0.3
	8000	100.0	0.02	1.145	0.3
	9000	100.0	0.02	1.195	0.2
	10000	100.0	0.01	1.246	0.3
	11000	100.0	0.01	1.297	0.3
	12000	100.0	0.01	1.348	0.1
	13000	100.0	0.01	1.399	0.1
	14000	100.0	0.01	1.454	0.2
	15000	100.0	0.01	1.506	0.2
	16000	100.0	0.01	1.563	0.1
17000	100.0	0.01	1.620	0.2	
18000	100.0	0.01	1.680	0.2	
19000	100.0	0.01	1.736	0.2	

Table A.9.1 B5 Used in Soy Biodiesel/ULSD Blends, Raw, Uncorrected High Pressure Viscosity Experimental Data at 10 C.					
B5 / Blends / 10 Celsius / 50 cP Piston / cdl 470					
Sample	P	T	dT	Raw Viscosity	SD
Name	[psi]	[C]	[C]	[cP]	%
B5 Blend, Soy Biodiesel / ULSD Blends	18	10.0	0.04	4.216	0.1
	100	10.0	0.04	4.260	0.3
	1000	10.0	0.04	4.634	0.3
	2000	10.0	0.04	5.097	0.4
	3000	10.0	0.03	5.596	0.3
	4000	10.0	0.03	6.124	0.3
	5000	10.0	0.02	6.717	0.3
	6000	10.0	0.02	7.339	0.3
	7000	10.0	0.02	8.023	0.2
	8000	10.0	0.02	8.711	0.2
	9000	10.0	0.01	9.489	0.3
	10000	10.0	0.02	10.33	0.2
	11000	10.0	0.01	11.28	0.3
	12000	10.0	0.01	12.24	0.2
	13000	10.0	0.01	13.32	0.1
	14000	10.0	0.01	14.42	0.1
	15000	10.0	0.01	15.68	0.1
	16000	10.0	0.01	17.02	0.3
17000	10.0	0.01	18.44	0.3	
18000	10.0	0.01	20.20	0.3	
19000	10.0	0.01	22.09	0.4	

Table A.9.2 B5 Used in Soy Biodiesel/ULSD Blends, Raw, Uncorrected High Pressure Viscosity Experimental Data at 25 C.

B5 / Blends / 25 Celsius / 50 cP Piston / cdl 470					
Sample	P	T	dT	Raw Viscosity	SD
Name	[psi]	[C]	[C]	[cP]	%
B5 Blend, Soy Biodiesel / ULSD Blends	30	25.0	0.04	2.819	0.2
	100	25.0	0.05	2.838	0.3
	1000	25.0	0.05	3.069	0.2
	2000	25.0	0.03	3.341	0.4
	3000	25.0	0.03	3.625	0.2
	4000	25.0	0.04	3.930	0.1
	5000	25.0	0.04	4.257	0.3
	6000	25.0	0.02	4.613	0.4
	7000	25.0	0.03	4.984	0.1
	8000	25.0	0.03	5.394	0.2
	9000	25.0	0.02	5.821	0.3
	10000	25.0	0.02	6.284	0.3
	11000	25.0	0.02	6.768	0.3
	12000	25.0	0.02	7.254	0.1
	13000	25.0	0.02	7.823	0.4
	14000	25.0	0.02	8.438	0.3
	15000	25.0	0.01	9.055	0.1
16000	25.0	0.02	9.746	0.2	
17000	25.0	0.01	10.47	0.2	
18000	25.0	0.01	11.21	0.3	
19000	25.0	0.01	12.09	0.3	

Table A.9.3 B5 Used in Soy Biodiesel/ULSD Blends, Raw, Uncorrected High Pressure Viscosity Experimental Data at 40 C.					
B5 / Blends / 40 Celsius / 20 cP Piston / cdl 476					
Sample	P	T	dT	Raw Viscosity	SD
Name	[psi]	[C]	[C]	[cP]	%
B5 Blend, Soy Biodiesel / ULSD Blends	20	40.0	0.04	2.023	0.2
	100	40.0	0.02	2.034	0.2
	1000	40.0	0.04	2.184	0.3
	2000	40.0	0.03	2.359	0.1
	3000	40.0	0.02	2.551	0.2
	4000	40.0	0.02	2.753	0.2
	5000	40.0	0.02	2.970	0.2
	6000	40.0	0.03	3.190	0.2
	7000	40.0	0.02	3.420	0.2
	8000	40.0	0.01	3.668	0.3
	9000	40.0	0.01	3.924	0.2
	10000	40.0	0.01	4.202	0.3
	11000	40.0	0.02	4.495	0.2
	12000	40.0	0.01	4.801	0.2
	13000	40.0	0.01	5.106	0.1
	14000	40.0	0.01	5.450	0.2
	15000	40.0	0.02	5.802	0.1
16000	40.0	0.01	6.176	0.1	
17000	40.0	0.01	6.575	0.2	
18000	40.0	0.01	6.990	0.2	
19000	40.0	0.01	7.446	0.2	

Table A.9.4 B5 Used in Soy Biodiesel/ULSD Blends, Raw, Uncorrected High Pressure Viscosity Experimental Data at 70 C.					
B5 / Blends / 70 Celsius / 20 cP Piston / cdl 476					
Sample	P	T	dT	Raw Viscosity	SD
Name	[psi]	[C]	[C]	[cP]	%
B5 Blend, Soy Biodiesel / ULSD Blends	20	70.0	0.04	1.194	0.04
	100	70.0	0.04	1.199	0.04
	1000	70.0	0.03	1.280	0.03
	2000	70.0	0.04	1.376	0.04
	3000	70.0	0.04	1.477	0.04
	4000	70.0	0.04	1.579	0.04
	5000	70.0	0.03	1.689	0.03
	6000	70.0	0.04	1.805	0.04
	7000	70.0	0.04	1.920	0.04
	8000	70.0	0.03	2.036	0.03
	9000	70.0	0.02	2.163	0.02
	10000	70.0	0.02	2.292	0.02
	11000	70.0	0.02	2.428	0.02
	12000	70.0	0.02	2.567	0.02
	13000	70.0	0.02	2.714	0.02
	14000	70.0	0.02	2.866	0.02
	15000	70.0	0.03	3.023	0.03
	16000	70.0	0.01	3.193	0.01
17000	70.0	0.02	3.354	0.02	
18000	70.0	0.02	3.535	0.02	
19000	70.0	0.02	3.721	0.02	

Table A.9.5 B5 Used in Soy Biodiesel/ULSD Blends, Raw, Uncorrected High Pressure Viscosity Experimental Data at 100 C.					
B5 / Blends / 100 Celsius / 5 cP Piston / cdl 466					
Sample	P	T	dT	Raw Viscosity	SD
Name	[psi]	[C]	[C]	[cP]	%
B5 Blend, Soy Biodiesel / ULSD Blends	14	100.0	0.03	0.802	0.4
	100	100.0	0.03	0.807	0.2
	1000	100.0	0.01	0.849	0.1
	2000	100.0	0.04	0.899	0.2
	3000	100.0	0.03	0.949	0.2
	4000	100.0	0.03	0.998	0.2
	5000	100.0	0.02	1.048	0.4
	6000	100.0	0.01	1.097	0.3
	7000	100.0	0.01	1.146	0.2
	8000	100.0	0.02	1.196	0.2
	9000	100.0	0.01	1.245	0.2
	10000	100.0	0.01	1.296	0.2
	11000	100.0	0.01	1.349	0.2
	12000	100.0	0.01	1.401	0.2
	13000	100.0	0.02	1.455	0.2
	14000	100.0	0.01	1.507	0.2
	15000	100.0	0.01	1.564	0.2
	16000	100.0	0.01	1.620	0.1
17000	100.0	0.01	1.676	0.1	
18000	100.0	0.01	1.736	0.2	
19000	100.0	0.01	1.794	0.1	

Table A.10.1 B10 Used in Soy Biodiesel/ULSD Blends, Raw, Uncorrected High Pressure Viscosity Experimental Data at 10 C.					
B10 / Blends / 10 Celsius / 50 cP Piston / cdl 470					
Sample	P	T	dT	Raw Viscosity	SD
Name	[psi]	[C]	[C]	[cP]	%
B10 Blend, Soy Biodiesel / ULSD Blends	21	10.0	0.04	4.380	0.1
	100	10.0	0.03	4.416	0.3
	1000	10.0	0.04	4.813	0.1
	2000	10.0	0.03	5.286	0.1
	3000	10.0	0.04	5.797	0.2
	4000	10.0	0.02	6.342	0.3
	5000	10.0	0.02	6.934	0.3
	6000	10.0	0.02	7.562	0.1
	7000	10.0	0.02	8.230	0.2
	8000	10.0	0.02	8.930	0.1
	9000	10.0	0.02	9.732	0.3
	10000	10.0	0.01	10.61	0.2
	11000	10.0	0.01	11.50	0.3
	12000	10.0	0.01	12.44	0.1
	13000	10.0	0.01	13.48	0.1
	14000	10.0	0.01	14.66	0.2
	15000	10.0	0.01	15.90	0.2
	16000	10.0	0.01	17.19	0.1
	17000	10.0	0.01	18.68	0.2
18000	10.0	0.01	20.48	0.3	
19000	10.0	0.01	22.40	0.3	

Table A.10.2 B10 Used in Soy Biodiesel/ULSD Blends, Raw, Uncorrected High Pressure Viscosity Experimental Data at 25 C.					
B10 / Blends / 25 Celsius / 50 cP Piston / cdl 470					
Sample	P	T	dT	Raw Viscosity	SD
Name	[psi]	[C]	[C]	[cP]	%
B10 Blend, Soy Biodiesel / ULSD Blends	29	25.0	0.05	2.886	0.2
	100	25.0	0.03	2.912	0.2
	1000	25.0	0.04	3.149	0.3
	2000	25.0	0.04	3.433	0.4
	3000	25.0	0.04	3.726	0.1
	4000	25.0	0.03	4.033	0.3
	5000	25.0	0.03	4.373	0.3
	6000	25.0	0.04	4.723	0.4
	7000	25.0	0.02	5.098	0.2
	8000	25.0	0.03	5.506	0.4
	9000	25.0	0.02	5.922	0.4
	10000	25.0	0.02	6.370	0.2
	11000	25.0	0.02	6.864	0.3
	12000	25.0	0.02	7.356	0.3
	13000	25.0	0.01	7.897	0.3
	14000	25.0	0.02	8.492	0.2
	15000	25.0	0.02	9.107	0.1
	16000	25.0	0.01	9.805	0.2
17000	25.0	0.02	10.53	0.2	
18000	25.0	0.01	11.31	0.3	
19000	25.0	0.01	12.13	0.4	

Table A.10.3 B10 Used in Soy Biodiesel/ULSD Blends, Raw, Uncorrected High Pressure Viscosity Experimental Data at 40 C.					
B10 / Blends / 40 Celsius / 20 cP Piston / cdl 476					
Sample	P	T	dT	Raw Viscosity	SD
Name	[psi]	[C]	[C]	[cP]	%
B10 Blend, Soy Biodiesel / ULSD Blends	21	40.0	0.05	2.105	0.1
	100	40.0	0.03	2.114	0.2
	1000	40.0	0.02	2.267	0.4
	2000	40.0	0.04	2.447	0.4
	3000	40.0	0.03	2.636	0.3
	4000	40.0	0.01	2.837	0.3
	5000	40.0	0.03	3.051	0.3
	6000	40.0	0.03	3.272	0.2
	7000	40.0	0.03	3.513	0.2
	8000	40.0	0.02	3.762	0.1
	9000	40.0	0.02	4.029	0.2
	10000	40.0	0.01	4.307	0.3
	11000	40.0	0.02	4.598	0.1
	12000	40.0	0.01	4.904	0.2
	13000	40.0	0.02	5.223	0.2
	14000	40.0	0.01	5.567	0.1
	15000	40.0	0.01	5.924	0.3
	16000	40.0	0.01	6.296	0.3
17000	40.0	0.02	6.691	0.1	
18000	40.0	0.01	7.116	0.1	
19000	40.0	0.02	7.615	0.3	

Table A.10.4 B10 Used in Soy Biodiesel/ULSD Blends, Raw, Uncorrected High Pressure Viscosity Experimental Data at 70 C.					
B10 / Blends / 70 Celsius / 20 cP Piston / cdl 476					
Sample	P	T	dT	Raw Viscosity	SD
Name	[psi]	[C]	[C]	[cP]	%
B10 Blend, Soy Biodiesel / ULSD Blends	22	70.0	0.04	1.257	0.1
	100	70.0	0.04	1.266	0.2
	1000	70.0	0.04	1.350	0.2
	2000	70.0	0.04	1.449	0.1
	3000	70.0	0.03	1.556	0.1
	4000	70.0	0.03	1.658	0.3
	5000	70.0	0.05	1.773	0.3
	6000	70.0	0.03	1.890	0.3
	7000	70.0	0.03	2.005	0.2
	8000	70.0	0.02	2.128	0.1
	9000	70.0	0.02	2.254	0.3
	10000	70.0	0.03	2.390	0.3
	11000	70.0	0.02	2.531	0.3
	12000	70.0	0.01	2.675	0.3
	13000	70.0	0.02	2.820	0.1
	14000	70.0	0.02	2.981	0.3
	15000	70.0	0.02	3.142	0.3
	16000	70.0	0.02	3.303	0.3
17000	70.0	0.02	3.483	0.4	
18000	70.0	0.02	3.663	0.3	
19000	70.0	0.02	3.855	0.3	

Table A.10.5 B10 Used in Soy Biodiesel/ULSD Blends, Raw, Uncorrected High Pressure Viscosity Experimental Data at 100 C.					
B10 / Blends / 100 Celsius / 5 cP Piston / cdl 466					
Sample	P	T	dT	Raw Viscosity	SD
Name	[psi]	[C]	[C]	[cP]	%
B10 Blend, Soy Biodiesel / ULSD Blends	20	100.0	0.02	0.813	0.2
	100	100.0	0.02	0.817	0.2
	1000	100.0	0.01	0.861	0.3
	2000	100.0	0.02	0.910	0.3
	3000	100.0	0.02	0.958	0.2
	4000	100.0	0.01	1.006	0.1
	5000	100.0	0.02	1.061	0.2
	6000	100.0	0.01	1.108	0.1
	7000	100.0	0.01	1.162	0.1
	8000	100.0	0.01	1.217	0.2
	9000	100.0	0.01	1.278	0.2
	10000	100.0	0.01	1.324	0.3
	11000	100.0	0.01	1.376	0.3
	12000	100.0	0.02	1.427	0.2
	13000	100.0	0.01	1.480	0.2
	14000	100.0	0.01	1.533	0.1
	15000	100.0	0.01	1.590	0.1
	16000	100.0	0.01	1.639	0.3
17000	100.0	0.01	1.706	0.3	
18000	100.0	0.01	1.746	0.2	
19000	100.0	0.01	1.804	0.2	

Table A.11.1 B20 Used in Soy Biodiesel/ULSD Blends, Raw, Uncorrected High Pressure Viscosity Experimental Data at 10 C.					
B20 / Blends / 10 Celsius / 50 cP Piston / cdl 470					
Sample	P	T	dT	Raw Viscosity	SD
Name	[psi]	[C]	[C]	[cP]	%
B20 Blend, Soy Biodiesel / ULSD Blends	28	10.0	0.03	4.525	0.2
	100	10.0	0.02	4.560	0.3
	1000	10.0	0.02	4.964	0.3
	2000	10.0	0.02	5.428	0.3
	3000	10.0	0.02	5.938	0.2
	4000	10.0	0.03	6.471	0.3
	5000	10.0	0.02	7.061	0.2
	6000	10.0	0.02	7.681	0.1
	7000	10.0	0.01	8.354	0.3
	8000	10.0	0.02	9.061	0.2
	9000	10.0	0.01	9.794	0.1
	10000	10.0	0.01	10.62	0.1
	11000	10.0	0.01	11.49	0.3
	12000	10.0	0.01	12.39	0.2
	13000	10.0	0.01	13.38	0.2
	14000	10.0	0.01	14.45	0.1
	15000	10.0	0.01	15.60	0.2
	16000	10.0	0.01	16.87	0.1
17000	10.0	0.01	18.23	0.2	
18000	10.0	0.01	19.84	0.2	
19000	10.0	0.01	21.64	0.3	

Table A.11.2 B20 Used in Soy Biodiesel/ULSD Blends, Raw, Uncorrected High Pressure Viscosity Experimental Data at 25 C.					
B20 / Blends / 25 Celsius / 50 cP Piston / cdl 470					
Sample	P	T	dT	Raw Viscosity	SD
Name	[psi]	[C]	[C]	[cP]	%
B20 Blend, Soy Biodiesel / ULSD Blends	33	25.0	0.04	3.043	0.4
	100	25.0	0.04	3.062	0.4
	1000	25.0	0.04	3.302	0.4
	2000	25.0	0.03	3.588	0.2
	3000	25.0	0.04	3.890	0.4
	4000	25.0	0.04	4.211	0.3
	5000	25.0	0.03	4.549	0.3
	6000	25.0	0.03	4.912	0.4
	7000	25.0	0.02	5.278	0.2
	8000	25.0	0.03	5.684	0.2
	9000	25.0	0.02	6.101	0.1
	10000	25.0	0.02	6.565	0.4
	11000	25.0	0.02	7.030	0.3
	12000	25.0	0.02	7.543	0.4
	13000	25.0	0.02	8.067	0.1
	14000	25.0	0.02	8.658	0.3
	15000	25.0	0.01	9.282	0.2
	16000	25.0	0.01	9.942	0.3
17000	25.0	0.02	10.64	0.2	
18000	25.0	0.01	11.40	0.1	
19000	25.0	0.01	12.24	0.3	

Table A.11.3 B20 Used in Soy Biodiesel/ULSD Blends, Raw, Uncorrected High Pressure Viscosity Experimental Data at 40 C.					
B20 / Blends / 40 Celsius / 20 cP Piston / cdl 476					
Sample	P	T	dT	Raw Viscosity	SD
Name	[psi]	[C]	[C]	[cP]	%
B20 Blend, Soy Biodiesel / ULSD Blends	26	40.0	0.03	2.215	0.3
	100	40.0	0.03	2.226	0.2
	1000	40.0	0.04	2.381	0.3
	2000	40.0	0.03	2.558	0.3
	3000	40.0	0.03	2.763	0.2
	4000	40.0	0.03	2.961	0.3
	5000	40.0	0.02	3.178	0.2
	6000	40.0	0.02	3.409	0.4
	7000	40.0	0.02	3.648	0.1
	8000	40.0	0.02	3.896	0.1
	9000	40.0	0.02	4.172	0.2
	10000	40.0	0.01	4.447	0.1
	11000	40.0	0.02	4.724	0.2
	12000	40.0	0.02	5.028	0.2
	13000	40.0	0.02	5.345	0.2
	14000	40.0	0.02	5.686	0.2
	15000	40.0	0.01	6.045	0.3
	16000	40.0	0.01	6.417	0.3
17000	40.0	0.01	6.808	0.1	
18000	40.0	0.03	7.199	0.3	
19000	40.0	0.02	7.663	0.1	

Table A.11.4 B20 Used in Soy Biodiesel/ULSD Blends, Raw, Uncorrected High Pressure Viscosity Experimental Data at 70 C.					
B20 / Blends / 70 Celsius / 20 cP Piston / cdl 476					
Sample	P	T	dT	Raw Viscosity	SD
Name	[psi]	[C]	[C]	[cP]	%
B20 Blend, Soy Biodiesel / ULSD Blends	31	70.0	0.04	1.298	0.3
	100	70.0	0.04	1.307	0.2
	1000	70.0	0.03	1.394	0.3
	2000	70.0	0.03	1.492	0.3
	3000	70.0	0.03	1.601	0.2
	4000	70.0	0.02	1.704	0.2
	5000	70.0	0.03	1.818	0.2
	6000	70.0	0.03	1.933	0.1
	7000	70.0	0.02	2.053	0.1
	8000	70.0	0.02	2.180	0.3
	9000	70.0	0.03	2.308	0.1
	10000	70.0	0.02	2.442	0.2
	11000	70.0	0.02	2.581	0.2
	12000	70.0	0.01	2.724	0.2
	13000	70.0	0.02	2.871	0.1
	14000	70.0	0.03	3.024	0.1
	15000	70.0	0.02	3.186	0.1
	16000	70.0	0.02	3.353	0.3
17000	70.0	0.02	3.532	0.1	
18000	70.0	0.02	3.715	0.3	
19000	70.0	0.01	3.898	0.2	

Table A.11.5 B20 Used in Soy Biodiesel/ULSD Blends, Raw, Uncorrected High Pressure Viscosity Experimental Data at 100 C.					
B20 / Blends / 100 Celsius / 5 cP Piston / cdl 466					
Sample	P	T	dT	Raw Viscosity	SD
Name	[psi]	[C]	[C]	[cP]	%
B20 Blend, Soy Biodiesel / ULSD Blends	29	100.0	0.02	0.829	0.3
	100	100.0	0.02	0.845	0.3
	1000	100.0	0.01	0.892	0.4
	2000	100.0	0.02	0.944	0.3
	3000	100.0	0.02	0.994	0.2
	4000	100.0	0.02	1.045	0.1
	5000	100.0	0.02	1.098	0.2
	6000	100.0	0.01	1.151	0.3
	7000	100.0	0.01	1.202	0.2
	8000	100.0	0.02	1.257	0.3
	9000	100.0	0.02	1.306	0.1
	10000	100.0	0.01	1.361	0.3
	11000	100.0	0.02	1.412	0.1
	12000	100.0	0.01	1.466	0.2
	13000	100.0	0.02	1.520	0.2
	14000	100.0	0.01	1.573	0.2
	15000	100.0	0.01	1.629	0.1
16000	100.0	0.01	1.686	0.2	
17000	100.0	0.01	1.742	0.2	
18000	100.0	0.01	1.797	0.1	
19000	100.0	0.01	1.858	0.2	

Table A.12.1 B40 Used in Soy Biodiesel/ULSD Blends, Raw, Uncorrected High Pressure Viscosity Experimental Data at 10 C.					
B40 / Blends / 10 Celsius / 50 cP Piston / cdl 470					
Sample	P	T	dT	Raw Viscosity	SD
Name	[psi]	[C]	[C]	[cP]	%
B40 Blend, Soy Biodiesel / ULSD Blends	25	10.0	0.03	5.234	0.4
	100	10.0	0.02	5.257	0.3
	1000	10.0	0.04	5.707	0.4
	2000	10.0	0.03	6.208	0.2
	3000	10.0	0.02	6.773	0.2
	4000	10.0	0.02	7.366	0.4
	5000	10.0	0.02	7.981	0.3
	6000	10.0	0.02	8.650	0.3
	7000	10.0	0.02	9.350	0.2
	8000	10.0	0.02	10.10	0.2
	9000	10.0	0.02	10.92	0.1
	10000	10.0	0.02	11.77	0.3
	11000	10.0	0.01	12.70	0.1
	12000	10.0	0.02	13.68	0.2
	13000	10.0	0.01	14.72	0.2
	14000	10.0	0.02	15.85	0.1
	15000	10.0	0.01	17.05	0.1
16000	10.0	0.01	18.28	0.2	
17000	10.0	0.01	19.77	0.2	
18000	10.0	0.01	21.37	0.2	
19000	10.0	0.01	24.65	0.2	

Table A.12.2 B40 Used in Soy Biodiesel/ULSD Blends, Raw, Uncorrected High Pressure Viscosity Experimental Data at 25 C.

B40 / Blends / 25 Celsius / 50 cP Piston / cdl 470					
Sample	P	T	dT	Raw Viscosity	SD
Name	[psi]	[C]	[C]	[cP]	%
B40 Blend, Soy Biodiesel / ULSD Blends	28	25.0	0.03	3.445	0.2
	100	25.0	0.04	3.466	0.3
	1000	25.0	0.03	3.724	0.4
	2000	25.0	0.04	4.028	0.2
	3000	25.0	0.01	4.348	0.2
	4000	25.0	0.03	4.694	0.2
	5000	25.0	0.03	5.048	0.4
	6000	25.0	0.03	5.431	0.4
	7000	25.0	0.03	5.830	0.2
	8000	25.0	0.02	6.244	0.3
	9000	25.0	0.02	6.678	0.3
	10000	25.0	0.02	7.148	0.2
	11000	25.0	0.02	7.656	0.2
	12000	25.0	0.02	8.141	0.2
	13000	25.0	0.02	8.700	0.3
	14000	25.0	0.02	9.280	0.2
	15000	25.0	0.02	9.933	0.2
	16000	25.0	0.02	10.59	0.2
17000	25.0	0.01	11.31	0.2	
18000	25.0	0.01	12.07	0.3	
19000	25.0	0.02	12.87	0.2	

Table A.12.3 B40 Used in Soy Biodiesel/ULSD Blends, Raw, Uncorrected High Pressure Viscosity Experimental Data at 40 C.					
B40 / Blends / 40 Celsius / 20 cP Piston / cdl 476					
Sample	P	T	dT	Raw Viscosity	SD
Name	[psi]	[C]	[C]	[cP]	%
B40 Blend, Soy Biodiesel / ULSD Blends	24	40.0	0.04	2.450	0.2
	100	40.0	0.03	2.463	0.1
	1000	40.0	0.02	2.640	0.2
	2000	40.0	0.03	2.843	0.2
	3000	40.0	0.03	3.041	0.4
	4000	40.0	0.02	3.262	0.1
	5000	40.0	0.03	3.496	0.1
	6000	40.0	0.02	3.742	0.2
	7000	40.0	0.02	3.988	0.2
	8000	40.0	0.02	4.256	0.2
	9000	40.0	0.02	4.526	0.1
	10000	40.0	0.02	4.811	0.1
	11000	40.0	0.02	5.096	0.4
	12000	40.0	0.01	5.406	0.1
	13000	40.0	0.01	5.734	0.1
	14000	40.0	0.01	6.077	0.2
	15000	40.0	0.01	6.431	0.1
16000	40.0	0.01	6.799	0.2	
17000	40.0	0.01	7.187	0.1	
18000	40.0	0.01	7.619	0.1	
19000	40.0	0.02	8.113	0.2	

Table A.12.4 B40 Used in Soy Biodiesel/ULSD Blends, Raw, Uncorrected High Pressure Viscosity Experimental Data at 70 C.					
B40 / Blends / 70 Celsius / 20 cP Piston / cdl 476					
Sample	P	T	dT	Raw Viscosity	SD
Name	[psi]	[C]	[C]	[cP]	%
B40 Blend, Soy Biodiesel / ULSD Blends	27	70.0	0.05	1.445	0.3
	100	70.0	0.04	1.457	0.3
	1000	70.0	0.04	1.553	0.2
	2000	70.0	0.03	1.656	0.2
	3000	70.0	0.03	1.769	0.2
	4000	70.0	0.03	1.889	0.4
	5000	70.0	0.03	2.008	0.3
	6000	70.0	0.03	2.124	0.2
	7000	70.0	0.02	2.257	0.3
	8000	70.0	0.02	2.386	0.4
	9000	70.0	0.03	2.522	0.2
	10000	70.0	0.03	2.664	0.3
	11000	70.0	0.01	2.811	0.3
	12000	70.0	0.02	2.968	0.4
	13000	70.0	0.02	3.114	0.2
	14000	70.0	0.01	3.272	0.4
	15000	70.0	0.02	3.440	0.1
	16000	70.0	0.02	3.606	0.2
17000	70.0	0.01	3.788	0.2	
18000	70.0	0.02	3.964	0.2	
19000	70.0	0.02	4.154	0.2	

Table A.12.5 B40 Used in Soy Biodiesel/ULSD Blends, Raw, Uncorrected High Pressure Viscosity Experimental Data at 100 C.					
B20 / Blends / 100 Celsius / 5 cP Piston / cdl 466					
Sample	P	T	dT	Raw Viscosity	SD
Name	[psi]	[C]	[C]	[cP]	%
B40 Blend, Soy Biodiesel / ULSD Blends	24	100.0	0.03	0.939	0.3
	100	100.0	0.02	0.943	0.1
	1000	100.0	0.02	0.994	0.1
	2000	100.0	0.02	1.050	0.2
	3000	100.0	0.01	1.105	0.2
	4000	100.0	0.02	1.158	0.2
	5000	100.0	0.02	1.213	0.2
	6000	100.0	0.02	1.266	0.2
	7000	100.0	0.02	1.319	0.2
	8000	100.0	0.01	1.376	0.1
	9000	100.0	0.01	1.428	0.3
	10000	100.0	0.01	1.485	0.3
	11000	100.0	0.01	1.538	0.1
	12000	100.0	0.01	1.593	0.2
	13000	100.0	0.01	1.649	0.2
	14000	100.0	0.01	1.705	0.1
	15000	100.0	0.02	1.761	0.1
16000	100.0	0.01	1.818	0.3	
17000	100.0	0.01	1.880	0.3	
18000	100.0	0.01	1.943	0.2	
19000	100.0	0.01	2.011	0.3	

Table A.13.1 B60 Used in Soy Biodiesel/ULSD Blends, Raw, Uncorrected High Pressure Viscosity Experimental Data at 10 C.					
B60 / Blends / 10 Celsius / 50 cP Piston / cdl 470					
Sample	P	T	dT	Raw Viscosity	SD
Name	[psi]	[C]	[C]	[cP]	%
B60 Blend, Soy Biodiesel / ULSD Blends	21	10.0	0.02	6.026	0.4
	100	10.0	0.02	6.081	0.3
	1000	10.0	0.03	6.530	0.2
	2000	10.0	0.02	7.128	0.3
	3000	10.0	0.02	7.729	0.1
	4000	10.0	0.02	8.371	0.3
	5000	10.0	0.01	9.042	0.2
	6000	10.0	0.02	9.747	0.2
	7000	10.0	0.01	10.50	0.2
	8000	10.0	0.01	11.29	0.3
	9000	10.0	0.01	12.13	0.2
	10000	10.0	0.02	13.02	0.2
	11000	10.0	0.02	13.97	0.2
	12000	10.0	0.01	14.94	0.1
	13000	10.0	0.01	16.01	0.2
	14000	10.0	0.01	17.11	0.1
	15000	10.0	0.01	18.30	0.1
16000	10.0	0.01	19.76	0.2	
16500	10.0	0.01	24.78	0.4	
17000	10.0	0.01	26.40	0.2	

Table A.13.2 B60 Used in Soy Biodiesel/ULSD Blends, Raw, Uncorrected High Pressure Viscosity Experimental Data at 25 C.

B60 / Blends / 25 Celsius / 50 cP Piston / cdl 470					
Sample	P	T	dT	Raw Viscosity	SD
Name	[psi]	[C]	[C]	[cP]	%
B60 Blend, Soy Biodiesel / ULSD Blends	20	25.0	0.03	3.905	0.4
	100	25.0	0.04	3.927	0.3
	1000	25.0	0.02	4.215	0.4
	2000	25.0	0.03	4.554	0.2
	3000	25.0	0.03	4.907	0.3
	4000	25.0	0.02	5.275	0.2
	5000	25.0	0.03	5.667	0.1
	6000	25.0	0.02	6.074	0.2
	7000	25.0	0.02	6.502	0.3
	8000	25.0	0.03	6.952	0.1
	9000	25.0	0.02	7.428	0.2
	10000	25.0	0.02	7.933	0.3
	11000	25.0	0.02	8.441	0.1
	12000	25.0	0.01	9.011	0.2
	13000	25.0	0.02	9.604	0.3
	14000	25.0	0.01	10.19	0.3
	15000	25.0	0.01	10.82	0.2
	16000	25.0	0.02	11.47	0.2
17000	25.0	0.01	12.19	0.2	
18000	25.0	0.01	12.94	0.2	
19000	25.0	0.01	13.71	0.3	

Table A.13.3 B60 Used in Soy Biodiesel/ULSD Blends, Raw, Uncorrected High Pressure Viscosity Experimental Data at 40 C.					
B60 / Blends / 40 Celsius / 20 cP Piston / cdl 476					
Sample	P	T	dT	Raw Viscosity	SD
Name	[psi]	[C]	[C]	[cP]	%
B60 Blend, Soy Biodiesel / ULSD Blends	26	40.0	0.01	2.790	0.1
	100	40.0	0.02	2.805	0.1
	1000	40.0	0.02	2.987	0.1
	2000	40.0	0.02	3.201	0.1
	3000	40.0	0.02	3.427	0.3
	4000	40.0	0.02	3.660	0.2
	5000	40.0	0.02	3.914	0.2
	6000	40.0	0.02	4.173	0.3
	7000	40.0	0.02	4.435	0.2
	8000	40.0	0.01	4.711	0.2
	9000	40.0	0.01	4.994	0.2
	10000	40.0	0.01	5.296	0.2
	11000	40.0	0.01	5.605	0.2
	12000	40.0	0.01	5.922	0.2
	13000	40.0	0.01	6.260	0.1
	14000	40.0	0.01	6.608	0.2
	15000	40.0	0.01	6.975	0.2
	16000	40.0	0.01	7.342	0.2
17000	40.0	0.01	7.784	0.2	
18000	40.0	0.01	8.250	0.2	
19000	40.0	0.01	8.737	0.2	

Table A.13.4 B60 Used in Soy Biodiesel/ULSD Blends, Raw, Uncorrected High Pressure Viscosity Experimental Data at 70 C.					
B60 / Blends / 70 Celsius / 20 cP Piston / cdl 476					
Sample	P	T	dT	Raw Viscosity	SD
Name	[psi]	[C]	[C]	[cP]	%
B60 Blend, Soy Biodiesel / ULSD Blends	29	70.0	0.03	1.645	0.2
	100	70.0	0.04	1.654	0.2
	1000	70.0	0.03	1.756	0.2
	2000	70.0	0.03	1.875	0.1
	3000	70.0	0.02	1.998	0.2
	4000	70.0	0.03	2.122	0.3
	5000	70.0	0.02	2.252	0.2
	6000	70.0	0.02	2.380	0.2
	7000	70.0	0.02	2.520	0.3
	8000	70.0	0.02	2.657	0.2
	9000	70.0	0.02	2.804	0.3
	10000	70.0	0.02	2.949	0.1
	11000	70.0	0.02	3.103	0.2
	12000	70.0	0.02	3.258	0.2
	13000	70.0	0.02	3.421	0.2
	14000	70.0	0.02	3.588	0.1
	15000	70.0	0.02	3.762	0.2
16000	70.0	0.02	3.935	0.2	
17000	70.0	0.01	4.118	0.2	
18000	70.0	0.02	4.309	0.2	
19000	70.0	0.01	4.508	0.2	

Table A.13.5 B60 Used in Soy Biodiesel/ULSD Blends, Raw, Uncorrected High Pressure Viscosity Experimental Data at 100 C.					
B60 / Blends / 100 Celsius / 5 cP Piston / cdl 466					
Sample	P	T	dT	Raw Viscosity	SD
Name	[psi]	[C]	[C]	[cP]	%
B60 Blend, Soy Biodiesel / ULSD Blends	29	100.0	0.03	1.024	0.3
	100	100.0	0.02	1.029	0.2
	1000	100.0	0.02	1.082	0.2
	2000	100.0	0.02	1.140	0.1
	3000	100.0	0.01	1.197	0.2
	4000	100.0	0.02	1.255	0.1
	5000	100.0	0.01	1.316	0.1
	6000	100.0	0.01	1.375	0.2
	7000	100.0	0.01	1.431	0.2
	8000	100.0	0.01	1.487	0.2
	9000	100.0	0.01	1.544	0.2
	10000	100.0	0.01	1.601	0.1
	11000	100.0	0.01	1.657	0.1
	12000	100.0	0.02	1.714	0.2
	13000	100.0	0.01	1.772	0.1
	14000	100.0	0.01	1.824	0.3
	15000	100.0	0.01	1.884	0.2
	16000	100.0	0.01	1.951	0.2
17000	100.0	0.01	2.019	0.1	
18000	100.0	0.01	2.089	0.2	
19000	100.0	0.01	2.154	0.1	

Table A.14.1 B80 Used in Soy Biodiesel/ULSD Blends, Raw, Uncorrected High Pressure Viscosity Experimental Data at 10 C.					
B80 / Blends / 10 Celsius / 50 cP Piston / cdl 470					
Sample	P	T	dT	Raw Viscosity	SD
Name	[psi]	[C]	[C]	[cP]	%
B80 Blend, Soy Biodiesel / ULSD Blends	21	10.0	0.02	6.713	0.3
	100	10.0	0.03	6.765	0.3
	1000	10.0	0.02	7.222	0.1
	2000	10.0	0.02	7.808	0.2
	3000	10.0	0.02	8.438	0.4
	4000	10.0	0.01	9.108	0.2
	5000	10.0	0.02	9.810	0.2
	6000	10.0	0.02	10.54	0.3
	7000	10.0	0.02	11.31	0.3
	8000	10.0	0.02	12.13	0.2
	9000	10.0	0.01	12.98	0.2
	10000	10.0	0.02	13.87	0.1
	11000	10.0	0.01	14.86	0.3
	12000	10.0	0.01	15.87	0.3
	13000	10.0	0.01	16.92	0.3
13500	10.0	0.01	26.14	0.3	

Table A.14.2 B80 Used in Soy Biodiesel/ULSD Blends, Raw, Uncorrected High Pressure Viscosity Experimental Data at 25 C.					
B80 / Blends / 25 Celsius / 50 cP Piston / cdl 470					
Sample	P	T	dT	Raw Viscosity	SD
Name	[psi]	[C]	[C]	[cP]	%
B80 Blend, Soy Biodiesel / ULSD Blends	24	25.0	0.04	4.403	0.3
	100	25.0	0.04	4.412	0.3
	1000	25.0	0.04	4.719	0.3
	2000	25.0	0.04	5.072	0.2
	3000	25.0	0.04	5.460	0.2
	4000	25.0	0.03	5.852	0.2
	5000	25.0	0.03	6.270	0.2
	6000	25.0	0.03	6.700	0.2
	7000	25.0	0.03	7.159	0.1
	8000	25.0	0.02	7.620	0.2
	9000	25.0	0.02	8.125	0.3
	10000	25.0	0.03	8.643	0.2
	11000	25.0	0.02	9.187	0.3
	12000	25.0	0.02	9.721	0.2
	13000	25.0	0.02	10.34	0.2
	14000	25.0	0.02	10.93	0.2
	15000	25.0	0.02	11.56	0.1
	16000	25.0	0.01	12.24	0.2
17000	25.0	0.02	12.96	0.3	
18000	25.0	0.01	13.70	0.3	
19000	25.0	0.01	14.39	0.4	

Table A.14.3 B80 Used in Soy Biodiesel/ULSD Blends, Raw, Uncorrected High Pressure Viscosity Experimental Data at 40 C.					
B80 / Blends / 40 Celsius / 20 cP Piston / cdl 476					
Sample	P	T	dT	Raw Viscosity	SD
Name	[psi]	[C]	[C]	[cP]	%
B80 Blend, Soy Biodiesel / ULSD Blends	34	40.0	0.03	3.192	0.1
	100	40.0	0.02	3.208	0.1
	1000	40.0	0.03	3.409	0.2
	2000	40.0	0.02	3.638	0.4
	3000	40.0	0.02	3.888	0.3
	4000	40.0	0.01	4.139	0.1
	5000	40.0	0.02	4.405	0.2
	6000	40.0	0.01	4.670	0.1
	7000	40.0	0.01	4.951	0.3
	8000	40.0	0.02	5.239	0.1
	9000	40.0	0.01	5.534	0.2
	10000	40.0	0.01	5.861	0.2
	11000	40.0	0.02	6.180	0.1
	12000	40.0	0.02	6.523	0.2
	13000	40.0	0.02	6.853	0.2
	14000	40.0	0.02	7.200	0.1
	15000	40.0	0.01	7.605	0.2
16000	40.0	0.01	8.048	0.3	
17000	40.0	0.01	8.505	0.2	
18000	40.0	0.01	8.987	0.3	
19000	40.0	0.02	9.503	0.2	

Table A.14.4 B80 Used in Soy Biodiesel/ULSD Blends, Raw, Uncorrected High Pressure Viscosity Experimental Data at 70 C.					
B80 / Blends / 70 Celsius / 20 cP Piston / cdl 476					
Sample	P	T	dT	Raw Viscosity	SD
Name	[psi]	[C]	[C]	[cP]	%
B80 Blend, Soy Biodiesel / ULSD Blends	18	70.0	0.03	1.841	0.2
	100	70.0	0.04	1.851	0.1
	1000	70.0	0.02	1.960	0.2
	2000	70.0	0.03	2.082	0.2
	3000	70.0	0.02	2.212	0.2
	4000	70.0	0.02	2.345	0.1
	5000	70.0	0.03	2.484	0.2
	6000	70.0	0.02	2.624	0.2
	7000	70.0	0.02	2.768	0.2
	8000	70.0	0.02	2.921	0.2
	9000	70.0	0.02	3.069	0.2
	10000	70.0	0.02	3.225	0.1
	11000	70.0	0.02	3.385	0.2
	12000	70.0	0.02	3.551	0.1
	13000	70.0	0.02	3.715	0.3
	14000	70.0	0.02	3.890	0.2
	15000	70.0	0.02	4.058	0.2
	16000	70.0	0.02	4.247	0.3
17000	70.0	0.01	4.427	0.2	
18000	70.0	0.01	4.622	0.2	
19000	70.0	0.02	4.816	0.2	

Table A.14.5 B80 Used in Soy Biodiesel/ULSD Blends, Raw, Uncorrected High Pressure Viscosity Experimental Data at 100 C.					
B80 / Blends / 100 Celsius / 5 cP Piston / cdl 466					
Sample	P	T	dT	Raw Viscosity	SD
Name	[psi]	[C]	[C]	[cP]	%
B80 Blend, Soy Biodiesel / ULSD Blends	18	100.0	0.02	1.155	0.1
	100	100.0	0.02	1.161	0.3
	1000	100.0	0.02	1.214	0.2
	2000	100.0	0.02	1.276	0.1
	3000	100.0	0.01	1.337	0.2
	4000	100.0	0.01	1.395	0.2
	5000	100.0	0.01	1.457	0.1
	6000	100.0	0.02	1.517	0.2
	7000	100.0	0.01	1.578	0.2
	8000	100.0	0.01	1.635	0.1
	9000	100.0	0.01	1.695	0.3
	10000	100.0	0.01	1.755	0.1
	11000	100.0	0.01	1.814	0.2
	12000	100.0	0.01	1.875	0.1
	13000	100.0	0.01	1.943	0.2
	14000	100.0	0.01	2.008	0.2
	15000	100.0	0.01	2.076	0.2
	16000	100.0	0.01	2.146	0.2
17000	100.0	0.01	2.211	0.2	
18000	100.0	0.02	2.280	0.2	
19000	100.0	0.01	2.354	0.2	

Table A.15.1 Jatropha Oil Based Biodiesel Used in ULSD Blends, Raw, Uncorrected High Pressure Viscosity Experimental Data at 10 C.					
Jatropha Oil Based Biodiesel / Blends / 10 Celsius / 50 cP Piston / cdl 470					
Sample	P	T	dT	Raw Viscosity	SD
Name	[psi]	[C]	[C]	[cP]	%
Jatropha Oil Based Biodiesel Used in ULSD	21	10.0	0.01	8.388	0.3
	1000	10.0	0.02	9.077	0.3
	2000	10.0	0.02	9.825	0.3
	3000	10.0	0.01	10.58	0.2
	4000	10.0	0.01	11.38	0.2
	5000	10.0	0.01	12.26	0.2

Table A.15.2 Jatropha Oil Based Biodiesel Used in ULSD Blends, Raw, Uncorrected High Pressure Viscosity Experimental Data at 25 C.					
Jatropha Oil Based Biodiesel/ Blends / 25 Celsius / 50 cP Piston / cdl 470					
Sample	P	T	dT	Raw Viscosity	SD
Name	[psi]	[C]	[C]	[cP]	%
Jatropha Oil Based Biodiesel Used in ULSD Blends	28	25.0	0.03	5.315	0.1
	1000	25.0	0.03	5.733	0.3
	2000	25.0	0.02	6.166	0.1
	3000	25.0	0.02	6.625	0.3
	4000	25.0	0.02	7.103	0.2
	5000	25.0	0.02	7.606	0.3
	6000	25.0	0.02	8.122	0.2
	7000	25.0	0.01	8.658	0.2
	8000	25.0	0.01	9.215	0.1
	9000	25.0	0.01	9.814	0.2
	10000	25.0	0.02	10.43	0.1
	11000	25.0	0.01	11.07	0.2
	12000	25.0	0.01	11.74	0.2
	13000	25.0	0.01	12.45	0.2
	14000	25.0	0.01	13.18	0.1
	15000	25.0	0.01	13.98	0.3
	16000	25.0	0.01	14.74	0.2
	17000	25.0	0.01	15.58	0.2
	18000	25.0	0.01	16.44	0.2
19000	25.0	0.01	17.34	0.3	

Table A.15.3 Jatropha Oil Based Biodiesel Used in ULSD Blends, Raw, Uncorrected High Pressure Viscosity Experimental Data at 40 C.					
Jatropha Oil Based Biodiesel/ Blends / 40 Celsius / 20 cP Piston / cdl 476					
Sample	P	T	dT	Raw Viscosity	SD
Name	[psi]	[C]	[C]	[cP]	%
Jatropha Oil Based Biodiesel Used in ULSD Blends	25	40.0	0.02	3.718	0.3
	1000	40.0	0.02	3.978	0.1
	2000	40.0	0.02	4.253	0.3
	3000	40.0	0.02	4.530	0.1
	4000	40.0	0.02	4.823	0.2
	5000	40.0	0.02	5.126	0.2
	6000	40.0	0.01	5.434	0.1
	7000	40.0	0.02	5.770	0.2
	8000	40.0	0.01	6.107	0.2
	9000	40.0	0.02	6.464	0.2
	10000	40.0	0.02	6.807	0.2
	11000	40.0	0.02	7.175	0.2
	12000	40.0	0.01	7.659	0.1
	13000	40.0	0.01	8.117	0.1
	14000	40.0	0.01	8.631	0.2
	15000	40.0	0.01	9.100	0.3
	16000	40.0	0.01	9.548	0.2
17000	40.0	0.01	10.09	0.2	
18000	40.0	0.01	10.62	0.2	
19000	40.0	0.01	11.17	0.1	

Table A.15.4 Jatropha Oil Based Biodiesel Used in ULSD Blends, Raw, Uncorrected High Pressure Viscosity Experimental Data at 70 C.					
Jatropha Oil Based Biodiesel/ Blends / 70 Celsius / 20 cP Piston / cdl 476					
Sample	P	T	dT	Raw Viscosity	SD
Name	[psi]	[C]	[C]	[cP]	%
Jatropha Oil Based Biodiesel Used in ULSD Blends	24	70.0	0.03	2.024	0.3
	1000	70.0	0.03	2.238	0.2
	2000	70.0	0.02	2.390	0.2
	3000	70.0	0.02	2.531	0.2
	4000	70.0	0.03	2.681	0.1
	5000	70.0	0.02	2.842	0.3
	6000	70.0	0.02	2.992	0.1
	7000	70.0	0.04	3.157	0.3
	8000	70.0	0.03	3.328	0.2
	9000	70.0	0.02	3.501	0.2
	10000	70.0	0.02	3.685	0.3
	11000	70.0	0.02	3.857	0.2
	12000	70.0	0.01	4.050	0.3
	13000	70.0	0.02	4.230	0.3
	14000	70.0	0.02	4.423	0.2
	15000	70.0	0.01	4.623	0.3
	16000	70.0	0.02	4.830	0.2
17000	70.0	0.01	5.037	0.2	
18000	70.0	0.01	5.261	0.2	
19000	70.0	0.01	5.480	0.3	

Table A.15.5 Jatropha Oil Based Biodiesel Used in ULSD Blends, Raw, Uncorrected High Pressure Viscosity Experimental Data at 100 C.					
Jatropha Oil Based Biodiesel/ Blends / 100 Celsius / 5 cP Piston / cdl 466					
Sample	P	T	dT	Raw Viscosity	SD
Name	[psi]	[C]	[C]	[cP]	%
Jatropha Oil Based Biodiesel Used in ULSD Blends	25	100.0	0.02	1.258	0.2
	1000	100.0	0.02	1.337	0.2
	2000	100.0	0.02	1.405	0.2
	3000	100.0	0.01	1.472	0.1
	4000	100.0	0.01	1.539	0.1
	5000	100.0	0.01	1.598	0.2
	6000	100.0	0.02	1.663	0.1
	7000	100.0	0.02	1.734	0.2
	8000	100.0	0.01	1.797	0.2
	9000	100.0	0.03	1.859	0.2
	10000	100.0	0.03	1.938	0.2
	11000	100.0	0.02	2.020	0.1
	12000	100.0	0.01	2.093	0.2
	13000	100.0	0.01	2.164	0.2
	14000	100.0	0.01	2.244	0.2
	15000	100.0	0.02	2.316	0.3
	16000	100.0	0.01	2.394	0.3
17000	100.0	0.02	2.471	0.2	
18000	100.0	0.02	2.570	0.3	
19000	100.0	0.01	2.638	0.3	

Table A.16.1 ULSD Used in Jatropha Biodiesel/ULSD Blends, Raw, Uncorrected High Pressure Viscosity Experimental Data at 10 C.

ULSD / Blends / 10 Celsius / 50 cP Piston / cdl 470					
Sample	P	T	dT	Raw Viscosity	SD
Name	[psi]	[C]	[C]	[cP]	%
ULSD Used in Jatropha Biodiesel / ULSD Blends	20	10.0	0.02	4.324	0.2
	1000	10.0	0.04	4.791	0.3
	2000	10.0	0.03	5.284	0.1
	3000	10.0	0.02	5.816	0.3
	4000	10.0	0.02	6.397	0.3
	5000	10.0	0.03	7.004	0.2
	6000	10.0	0.02	7.665	0.1
	7000	10.0	0.03	8.384	0.1
	8000	10.0	0.02	9.158	0.2
	9000	10.0	0.02	9.996	0.1
	10000	10.0	0.02	10.91	0.1
	11000	10.0	0.02	11.89	0.1
	12000	10.0	0.01	12.98	0.2
	13000	10.0	0.01	14.11	0.2
	14000	10.0	0.01	15.36	0.2
	15000	10.0	0.01	16.76	0.2
	16000	10.0	0.01	18.18	0.1
17000	10.0	0.01	19.97	0.2	
18000	10.0	0.01	21.95	0.2	
19000	10.0	0.00	26.95	0.2	

Table A.16.2 ULSD Used in Jatropha Biodiesel/ULSD Blends, Raw, Uncorrected High Pressure Viscosity Experimental Data at 25 C.

ULSD / Blends / 25 Celsius / 50 cP Piston / cdl 470					
Sample	P	T	dT	Raw Viscosity	SD
Name	[psi]	[C]	[C]	[cP]	%
ULSD Used in Jatropha Biodiesel / ULSD Blends	26	25.0	0.05	2.870	0.3
	1000	25.0	0.05	3.122	0.1
	2000	25.0	0.05	3.411	0.2
	3000	25.0	0.04	3.726	0.2
	4000	25.0	0.04	4.065	0.3
	5000	25.0	0.04	4.393	0.2
	6000	25.0	0.03	4.770	0.3
	7000	25.0	0.02	5.160	0.3
	8000	25.0	0.02	5.571	0.1
	9000	25.0	0.01	6.055	0.3
	10000	25.0	0.02	6.524	0.1
	11000	25.0	0.01	7.024	0.3
	12000	25.0	0.02	7.561	0.1
	13000	25.0	0.01	8.197	0.2
	14000	25.0	0.01	8.835	0.2
	15000	25.0	0.01	9.537	0.2
	16000	25.0	0.01	10.26	0.2
17000	25.0	0.01	11.04	0.2	
18000	25.0	0.01	11.86	0.2	
19000	25.0	0.01	12.78	0.2	

Table A.16.3 ULSD Used in Jatropha Biodiesel/ULSD Blends, Raw, Uncorrected High Pressure Viscosity Experimental Data at 40 C.					
ULSD / Blends / 40 Celsius / 20 cP Piston / cdl 476					
Sample	P	T	dT	Raw Viscosity	SD
Name	[psi]	[C]	[C]	[cP]	%
ULSD Used in Jatropha Biodiesel / ULSD Blends	33	40.0	0.04	2.096	0.2
	1000	40.0	0.03	2.267	0.1
	2000	40.0	0.03	2.460	0.3
	3000	40.0	0.02	2.666	0.3
	4000	40.0	0.03	2.878	0.2
	5000	40.0	0.03	3.099	0.2
	6000	40.0	0.02	3.338	0.1
	7000	40.0	0.01	3.600	0.2
	8000	40.0	0.02	3.865	0.2
	9000	40.0	0.02	4.145	0.3
	10000	40.0	0.02	4.437	0.1
	11000	40.0	0.01	4.753	0.2
	12000	40.0	0.02	5.085	0.1
	13000	40.0	0.02	5.441	0.2
	14000	40.0	0.01	5.808	0.1
	15000	40.0	0.02	6.219	0.3
	16000	40.0	0.01	6.652	0.3
	17000	40.0	0.01	7.092	0.2
18000	40.0	0.01	7.556	0.1	
19000	40.0	0.01	8.101	0.2	

Table A.16.4 ULSD Used in Jatropha Biodiesel/ULSD Blends, Raw, Uncorrected High Pressure Viscosity Experimental Data at 70 C.					
ULSD / Blends / 70 Celsius / 20 cP Piston / cdl 476					
Sample	P	T	dT	Raw Viscosity	SD
Name	[psi]	[C]	[C]	[cP]	%
ULSD Used in Jatropha Biodiesel / ULSD Blends	27	70.0	0.04	1.215	0.3
	1000	70.0	0.05	1.312	0.3
	2000	70.0	0.04	1.406	0.2
	3000	70.0	0.04	1.508	0.2
	4000	70.0	0.03	1.613	0.1
	5000	70.0	0.04	1.724	0.2
	6000	70.0	0.03	1.843	0.3
	7000	70.0	0.04	1.963	0.3
	8000	70.0	0.03	2.097	0.3
	9000	70.0	0.03	2.224	0.3
	10000	70.0	0.03	2.364	0.3
	11000	70.0	0.02	2.508	0.2
	12000	70.0	0.02	2.664	0.2
	13000	70.0	0.03	2.828	0.3
	14000	70.0	0.01	2.987	0.1
	15000	70.0	0.02	3.159	0.2
	16000	70.0	0.02	3.347	0.3
17000	70.0	0.02	3.542	0.1	
18000	70.0	0.01	3.737	0.2	
19000	70.0	0.02	3.938	0.3	

Table A.16.5 ULSD Used in Jatropha Biodiesel/ULSD Blends, Raw, Uncorrected High Pressure Viscosity Experimental Data at 100 C.					
ULSD / Blends / 100 Celsius / 5 cP Piston / cdl 466					
Sample	P	T	dT	Raw Viscosity	SD
Name	[psi]	[C]	[C]	[cP]	%
ULSD Used in Jatropha Biodiesel / ULSD Blends	21	100.0	0.03	0.788	0.1
	1000	100.0	0.02	0.836	0.1
	2000	100.0	0.02	0.891	0.2
	3000	100.0	0.03	0.944	0.1
	4000	100.0	0.02	0.998	0.2
	5000	100.0	0.01	1.049	0.2
	6000	100.0	0.01	1.101	0.1
	7000	100.0	0.01	1.154	0.1
	8000	100.0	0.01	1.206	0.1
	9000	100.0	0.01	1.258	0.1
	10000	100.0	0.02	1.314	0.1
	11000	100.0	0.01	1.368	0.2
	12000	100.0	0.02	1.429	0.2
	13000	100.0	0.01	1.484	0.2
	14000	100.0	0.01	1.548	0.2
	15000	100.0	0.01	1.607	0.2
	16000	100.0	0.01	1.665	0.1
	17000	100.0	0.01	1.728	0.1
18000	100.0	0.01	1.793	0.1	
19000	100.0	0.01	1.859	0.1	

Table A.17.1 B5 Used in Jatropha Biodiesel/ULSD Blends, Raw, Uncorrected High Pressure Viscosity Experimental Data at 10 C.					
B5 / Blends / 10 Celsius / 50 cP Piston / cdl 470					
Sample	P	T	dT	Raw Viscosity	SD
Name	[psi]	[C]	[C]	[cP]	%
B5 Blend, Jatropha Biodiesel / ULSD Blends	40	10.0	0.04	4.468	0.3
	1000	10.0	0.02	4.905	0.2
	2000	10.0	0.04	5.404	0.1
	3000	10.0	0.04	5.938	0.3
	4000	10.0	0.02	6.504	0.3
	5000	10.0	0.02	7.124	0.2
	6000	10.0	0.02	7.804	0.2
	7000	10.0	0.02	8.513	0.1
	8000	10.0	0.01	9.303	0.3
	9000	10.0	0.02	10.12	0.2
	10000	10.0	0.02	11.06	0.3
	11000	10.0	0.01	12.03	0.1
	12000	10.0	0.02	13.10	0.2
	13000	10.0	0.01	14.26	0.1
	14000	10.0	0.01	15.53	0.2
	15000	10.0	0.01	16.92	0.2
	16000	10.0	0.01	18.54	0.2
17000	10.0	0.01	20.32	0.3	
18000	10.0	0.01	23.32	0.3	
19000	10.0	0.02	26.61	0.2	

Table A.17.2 B5 Used in Jatropha Biodiesel/ULSD Blends, Raw, Uncorrected High Pressure Viscosity Experimental Data at 25 C.

B5 / Blends / 25 Celsius / 50 cP Piston / cdl 470					
Sample	P	T	dT	Raw Viscosity	SD
Name	[psi]	[C]	[C]	[cP]	%
B5 Blend, Jatropha Biodiesel / ULSD Blends	52	25.0	0.03	2.945	0.2
	1000	25.0	0.03	3.203	0.2
	2000	25.0	0.04	3.491	0.2
	3000	25.0	0.03	3.803	0.2
	4000	25.0	0.04	4.134	0.3
	5000	25.0	0.03	4.483	0.2
	6000	25.0	0.03	4.851	0.1
	7000	25.0	0.03	5.247	0.1
	8000	25.0	0.03	5.680	0.3
	9000	25.0	0.03	6.136	0.3
	10000	25.0	0.03	6.629	0.2
	11000	25.0	0.02	7.147	0.3
	12000	25.0	0.02	7.694	0.2
	13000	25.0	0.02	8.270	0.2
	14000	25.0	0.02	8.900	0.2
	15000	25.0	0.01	9.580	0.1
	16000	25.0	0.01	10.36	0.3
17000	25.0	0.01	11.13	0.3	
18000	25.0	0.01	11.97	0.3	
19000	25.0	0.01	12.88	0.3	

Table A.17.3 B5 Used in Jatropha Biodiesel/ULSD Blends, Raw, Uncorrected High Pressure Viscosity Experimental Data at 40 C.					
B5 / Blends / 40 Celsius / 20 cP Piston / cdl 476					
Sample	P	T	dT	Raw Viscosity	SD
Name	[psi]	[C]	[C]	[cP]	%
B5 Blend, Jatropha Biodiesel / ULSD Blends	24	40.0	0.03	2.146	0.1
	1000	40.0	0.03	2.327	0.3
	2000	40.0	0.03	2.520	0.3
	3000	40.0	0.03	2.719	0.2
	4000	40.0	0.03	2.933	0.1
	5000	40.0	0.02	3.161	0.2
	6000	40.0	0.02	3.396	0.2
	7000	40.0	0.02	3.657	0.3
	8000	40.0	0.02	3.921	0.1
	9000	40.0	0.01	4.210	0.2
	10000	40.0	0.02	4.501	0.1
	11000	40.0	0.02	4.817	0.3
	12000	40.0	0.01	5.141	0.2
	13000	40.0	0.01	5.494	0.2
	14000	40.0	0.01	5.871	0.2
	15000	40.0	0.02	6.255	0.2
	16000	40.0	0.01	6.667	0.2
17000	40.0	0.01	7.116	0.3	
18000	40.0	0.01	7.600	0.3	
19000	40.0	0.01	8.136	0.3	

Table A.17.4A B5 Used in Jatropha Biodiesel/ULSD Blends, Raw, Uncorrected High Pressure Viscosity Experimental Data at 70 C.					
B5 / Blends / 70 Celsius / 20 cP Piston / cdl 476					
Sample	P	T	dT	Raw Viscosity	SD
Name	[psi]	[C]	[C]	[cP]	%
B5 Blend, Jatropha Biodiesel / ULSD Blends	24	70.0	0.05	1.256	0.2
	1000	70.0	0.05	1.354	0.2
	2000	70.0	0.04	1.454	0.3
	3000	70.0	0.03	1.559	0.3
	4000	70.0	0.05	1.666	0.2
	5000	70.0	0.04	1.784	0.3
	6000	70.0	0.04	1.899	0.3
	7000	70.0	0.02	2.024	0.1
	8000	70.0	0.04	2.150	0.3
	9000	70.0	0.03	2.289	0.3
	10000	70.0	0.02	2.434	0.3
	11000	70.0	0.02	2.578	0.2
	12000	70.0	0.02	2.731	0.2
	13000	70.0	0.03	2.883	0.1
	14000	70.0	0.02	3.044	0.2
	15000	70.0	0.02	3.214	0.2
	16000	70.0	0.03	3.408	0.3
17000	70.0	0.02	3.599	0.3	
18000	70.0	0.02	3.791	0.3	
19000	70.0	0.02	3.985	0.2	

Table A.17.4B B5 Used in Jatropha Biodiesel/ULSD Blends, Raw, Uncorrected High Pressure Viscosity Experimental Data at 70 C.					
B5 / Blends / 70 Celsius / 5 cP Piston / cdl 466					
Sample	P	T	dT	Raw Viscosity	SD
Name	[psi]	[C]	[C]	[cP]	%
B5 Blend, Jatropha Biodiesel / ULSD Blends	26	70.0	0.02	1.190	0.2
	1000	70.0	0.02	1.263	0.1
	2000	70.0	0.02	1.354	0.3
	3000	70.0	0.01	1.429	0.2
	4000	70.0	0.01	1.513	0.1
	5000	70.0	0.01	1.600	0.2
	6000	70.0	0.01	1.684	0.2
	7000	70.0	0.02	1.772	0.1
	8000	70.0	0.01	1.866	0.2
	9000	70.0	0.01	1.966	0.1
	10000	70.0	0.01	2.071	0.1
	11000	70.0	0.01	2.178	0.2
	12000	70.0	0.01	2.294	0.1
	13000	70.0	0.01	2.416	0.2
	14000	70.0	0.02	2.532	0.2
	15000	70.0	0.01	2.653	0.1
	16000	70.0	0.01	2.781	0.2
17000	70.0	0.02	2.915	0.2	
18000	70.0	0.01	3.058	0.2	
19000	70.0	0.01	3.195	0.1	

Table A.17.5 B5 Used in Jatropha Biodiesel/ULSD Blends, Raw, Uncorrected High Pressure Viscosity Experimental Data at 100 C.					
B5 / Blends / 100 Celsius / 5 cP Piston / cdl 466					
Sample	P	T	dT	Raw Viscosity	SD
Name	[psi]	[C]	[C]	[cP]	%
B5 Blend, Jatropha Biodiesel / ULSD Blends	28	100.0	0.03	0.805	0.3
	1000	100.0	0.03	0.854	0.2
	2000	100.0	0.02	0.905	0.3
	3000	100.0	0.01	0.956	0.2
	4000	100.0	0.02	1.007	0.2
	5000	100.0	0.02	1.064	0.2
	6000	100.0	0.02	1.116	0.2
	7000	100.0	0.02	1.168	0.2
	8000	100.0	0.02	1.219	0.2
	9000	100.0	0.01	1.271	0.2
	10000	100.0	0.01	1.325	0.2
	11000	100.0	0.01	1.378	0.1
	12000	100.0	0.01	1.438	0.2
	13000	100.0	0.01	1.497	0.3
	14000	100.0	0.01	1.552	0.1
	15000	100.0	0.01	1.611	0.1
	16000	100.0	0.01	1.668	0.1
	17000	100.0	0.01	1.729	0.2
18000	100.0	0.01	1.796	0.2	
19000	100.0	0.01	1.862	0.2	

Table A.18.1 B10 Used in Jatropha Biodiesel/ULSD Blends, Raw, Uncorrected High Pressure Viscosity Experimental Data at 10 C.					
B10 / Blends / 10 Celsius / 50 cP Piston / cdl 470					
Sample	P	T	dT	Raw Viscosity	SD
Name	[psi]	[C]	[C]	[cP]	%
B10 Blend, Jatropha Biodiesel / ULSD Blends	26	10.0	0.04	4.602	0.2
	1000	10.0	0.03	5.066	0.2
	2000	10.0	0.02	5.573	0.2
	3000	10.0	0.02	6.115	0.2
	4000	10.0	0.02	6.708	0.2
	5000	10.0	0.01	7.340	0.2
	6000	10.0	0.02	8.037	0.3
	7000	10.0	0.02	8.747	0.2
	8000	10.0	0.02	9.545	0.2
	9000	10.0	0.02	10.38	0.1
	10000	10.0	0.01	11.31	0.2
	11000	10.0	0.01	12.30	0.2
	12000	10.0	0.01	13.39	0.2
	13000	10.0	0.01	14.58	0.1
	14000	10.0	0.01	15.86	0.2
	15000	10.0	0.01	17.24	0.2
	16000	10.0	0.01	18.77	0.2
17000	10.0	0.01	20.69	0.2	
18000	10.0	0.01	25.38	0.2	
19000	10.0	0.00	29.74	0.2	

Table A.18.2 B10 Used in Jatropha Biodiesel/ULSD Blends, Raw, Uncorrected High Pressure Viscosity Experimental Data at 25 C.

B10 / Blends / 25 Celsius / 50 cP Piston / cdl 470					
Sample	P	T	dT	Raw Viscosity	SD
Name	[psi]	[C]	[C]	[cP]	%
B10 Blend, Jatropha Biodiesel / ULSD Blends	27	25.0	0.05	2.996	0.3
	1000	25.0	0.03	3.253	0.3
	2000	25.0	0.03	3.535	0.2
	3000	25.0	0.03	3.853	0.3
	4000	25.0	0.03	4.190	0.2
	5000	25.0	0.03	4.545	0.3
	6000	25.0	0.04	4.924	0.1
	7000	25.0	0.03	5.333	0.3
	8000	25.0	0.03	5.761	0.1
	9000	25.0	0.04	6.231	0.1
	10000	25.0	0.03	6.711	0.2
	11000	25.0	0.02	7.208	0.2
	12000	25.0	0.01	7.742	0.2
	13000	25.0	0.02	8.334	0.3
	14000	25.0	0.02	8.950	0.2
	15000	25.0	0.02	9.630	0.2
	16000	25.0	0.02	10.34	0.2
17000	25.0	0.01	11.14	0.2	
18000	25.0	0.01	12.00	0.2	
19000	25.0	0.01	12.84	0.3	

Table A.18.3 B10 Used in Jatropha Biodiesel/ULSD Blends, Raw, Uncorrected High Pressure Viscosity Experimental Data at 40 C.					
B10 / Blends / 40 Celsius / 20 cP Piston / cdl 476					
Sample	P	T	dT	Raw Viscosity	SD
Name	[psi]	[C]	[C]	[cP]	%
B10 Blend, Jatropha Biodiesel / ULSD Blends	25	40.0	0.03	2.185	0.1
	1000	40.0	0.02	2.364	0.1
	2000	40.0	0.03	2.555	0.2
	3000	40.0	0.03	2.762	0.2
	4000	40.0	0.02	2.980	0.3
	5000	40.0	0.02	3.198	0.1
	6000	40.0	0.02	3.432	0.1
	7000	40.0	0.01	3.703	0.3
	8000	40.0	0.02	3.964	0.3
	9000	40.0	0.02	4.250	0.2
	10000	40.0	0.01	4.540	0.3
	11000	40.0	0.01	4.847	0.2
	12000	40.0	0.01	5.173	0.1
	13000	40.0	0.01	5.516	0.2
	14000	40.0	0.01	5.882	0.2
	15000	40.0	0.01	6.260	0.1
	16000	40.0	0.01	6.675	0.2
17000	40.0	0.01	7.118	0.3	
18000	40.0	0.01	7.585	0.2	
19000	40.0	0.01	8.093	0.3	

Table A.18.4A B10 Used in Jatropha Biodiesel/ULSD Blends, Raw, Uncorrected High Pressure Viscosity Experimental Data at 70 C.					
B10 / Blends / 70 Celsius / 20 cP Piston / cdl 476					
Sample	P	T	dT	Raw Viscosity	SD
Name	[psi]	[C]	[C]	[cP]	%
B10 Blend, Jatropha Biodiesel / ULSD Blends	24	70.0	0.05	1.278	0.2
	1000	70.0	0.04	1.372	0.2
	2000	70.0	0.03	1.477	0.3
	3000	70.0	0.03	1.584	0.3
	4000	70.0	0.04	1.698	0.2
	5000	70.0	0.04	1.813	0.1
	6000	70.0	0.04	1.934	0.3
	7000	70.0	0.03	2.063	0.3
	8000	70.0	0.01	2.190	0.2
	9000	70.0	0.02	2.329	0.2
	10000	70.0	0.03	2.465	0.2
	11000	70.0	0.04	2.615	0.3
	12000	70.0	0.03	2.762	0.2
	13000	70.0	0.02	2.925	0.2
	14000	70.0	0.02	3.095	0.2
	15000	70.0	0.02	3.277	0.2
	16000	70.0	0.02	3.457	0.2
17000	70.0	0.01	3.643	0.2	
18000	70.0	0.02	3.840	0.3	
19000	70.0	0.02	4.038	0.3	

Table A.18.4B B10 Used in Jatropha Biodiesel/ULSD Blends, Raw, Uncorrected High Pressure Viscosity Experimental Data at 70 C.					
B10 / Blends / 70 Celsius / 5 cP Piston / cdl 466					
Sample	P	T	dT	Raw Viscosity	SD
Name	[psi]	[C]	[C]	[cP]	%
B10 Blend, Jatropha Biodiesel / ULSD Blends	25	70.0	0.02	1.222	0.2
	1000	70.0	0.01	1.297	0.3
	2000	70.0	0.02	1.377	0.1
	3000	70.0	0.02	1.461	0.2
	4000	70.0	0.01	1.544	0.2
	5000	70.0	0.01	1.628	0.2
	6000	70.0	0.02	1.722	0.1
	7000	70.0	0.02	1.812	0.2
	8000	70.0	0.01	1.908	0.1
	9000	70.0	0.01	2.010	0.1
	10000	70.0	0.01	2.116	0.1
	11000	70.0	0.01	2.225	0.1
	12000	70.0	0.01	2.338	0.2
	13000	70.0	0.01	2.458	0.1
	14000	70.0	0.00	2.585	0.1
	15000	70.0	0.01	2.702	0.2
	16000	70.0	0.01	2.827	0.1
17000	70.0	0.01	2.959	0.1	
18000	70.0	0.00	3.102	0.2	
19000	70.0	0.00	3.240	0.3	

Table A.18.5 B10 Used in Jatropha Biodiesel/ULSD Blends, Raw, Uncorrected High Pressure Viscosity Experimental Data at 100 C.					
B10 / Blends / 100 Celsius / 5 cP Piston / cdl 466					
Sample	P	T	dT	Raw Viscosity	SD
Name	[psi]	[C]	[C]	[cP]	%
B10 Blend, Jatropha Biodiesel / ULSD Blends	26	100.0	0.02	0.828	0.3
	1000	100.0	0.02	0.873	0.2
	2000	100.0	0.01	0.926	0.3
	3000	100.0	0.03	0.977	0.3
	4000	100.0	0.02	1.031	0.1
	5000	100.0	0.01	1.086	0.1
	6000	100.0	0.02	1.138	0.2
	7000	100.0	0.02	1.190	0.1
	8000	100.0	0.01	1.243	0.1
	9000	100.0	0.01	1.296	0.1
	10000	100.0	0.01	1.351	0.1
	11000	100.0	0.02	1.408	0.3
	12000	100.0	0.02	1.468	0.2
	13000	100.0	0.01	1.518	0.2
	14000	100.0	0.01	1.574	0.2
	15000	100.0	0.01	1.636	0.2
	16000	100.0	0.01	1.699	0.1
17000	100.0	0.01	1.761	0.3	
18000	100.0	0.01	1.822	0.2	
19000	100.0	0.01	1.892	0.2	

Table A.19.1 B20 Used in Jatropha Biodiesel/ULSD Blends, Raw, Uncorrected High Pressure Viscosity Experimental Data at 10 C.					
B20 / Blends / 10 Celsius / 50 cP Piston / cdl 470					
Sample	P	T	dT	Raw Viscosity	SD
Name	[psi]	[C]	[C]	[cP]	%
B20 Blend, Jatropha Biodiesel / ULSD Blends	24	10.0	0.04	4.904	0.3
	1000	10.0	0.03	5.364	0.3
	2000	10.0	0.04	5.870	0.2
	3000	10.0	0.02	6.437	0.2
	4000	10.0	0.02	7.040	0.1
	5000	10.0	0.02	7.686	0.1
	6000	10.0	0.02	8.396	0.2
	7000	10.0	0.02	9.125	0.2
	8000	10.0	0.02	9.957	0.3
	9000	10.0	0.02	10.79	0.2
	10000	10.0	0.02	11.73	0.1
	11000	10.0	0.02	12.78	0.2
	12000	10.0	0.01	13.91	0.2
	13000	10.0	0.01	15.12	0.1
	14000	10.0	0.01	16.39	0.1
	15000	10.0	0.01	17.80	0.2
	16000	10.0	0.01	19.44	0.2
17000	10.0	0.01	21.38	0.2	
18000	10.0	0.00	30.33	0.2	
18250	10.0	0.01	31.18	0.3	

Table A.19.2 B20 Used in Jatropha Biodiesel/ULSD Blends, Raw, Uncorrected High Pressure Viscosity Experimental Data at 25 C.

B20 / Blends / 25 Celsius / 50 cP Piston / cdl 470					
Sample	P	T	dT	Raw Viscosity	SD
Name	[psi]	[C]	[C]	[cP]	%
B20 Blend, Jatropha Biodiesel / ULSD Blends	23	25.0	0.04	3.231	0.2
	1000	25.0	0.03	3.522	0.2
	2000	25.0	0.04	3.831	0.2
	3000	25.0	0.04	4.166	0.1
	4000	25.0	0.04	4.515	0.3
	5000	25.0	0.02	4.895	0.2
	6000	25.0	0.02	5.270	0.2
	7000	25.0	0.02	5.697	0.3
	8000	25.0	0.02	6.136	0.2
	9000	25.0	0.02	6.616	0.2
	10000	25.0	0.02	7.137	0.2
	11000	25.0	0.01	7.673	0.1
	12000	25.0	0.01	8.248	0.2
	13000	25.0	0.02	8.851	0.2
	14000	25.0	0.02	9.519	0.3
	15000	25.0	0.02	10.200	0.2
	16000	25.0	0.01	10.940	0.3
17000	25.0	0.01	11.750	0.2	
18000	25.0	0.01	12.660	0.2	
19000	25.0	0.01	13.490	0.2	

Table A.19.3 B20 Used in Jatropha Biodiesel/ULSD Blends, Raw, Uncorrected High Pressure Viscosity Experimental Data at 40 C.					
B20 / Blends / 40 Celsius / 20 cP Piston / cdl 476					
Sample	P	T	dT	Raw Viscosity	SD
Name	[psi]	[C]	[C]	[cP]	%
B20 Blend, Jatropha Biodiesel / ULSD Blends	23	40.0	0.03	2.324	0.2
	1000	40.0	0.03	2.502	0.3
	2000	40.0	0.01	2.702	0.2
	3000	40.0	0.02	2.916	0.2
	4000	40.0	0.03	3.142	0.3
	5000	40.0	0.02	3.369	0.2
	6000	40.0	0.01	3.616	0.3
	7000	40.0	0.02	3.870	0.1
	8000	40.0	0.02	4.150	0.1
	9000	40.0	0.01	4.438	0.2
	10000	40.0	0.01	4.740	0.1
	11000	40.0	0.02	5.060	0.1
	12000	40.0	0.01	5.391	0.2
	13000	40.0	0.01	5.736	0.1
	14000	40.0	0.01	6.112	0.1
	15000	40.0	0.01	6.493	0.2
	16000	40.0	0.01	6.919	0.1
17000	40.0	0.01	7.363	0.2	
18000	40.0	0.01	7.902	0.3	
19000	40.0	0.01	8.406	0.2	

Table A.19.4A B20 Used in Jatropha Biodiesel/ULSD Blends, Raw, Uncorrected High Pressure Viscosity Experimental Data at 70 C.					
B20 / Blends / 70 Celsius / 20 cP Piston / cdl 476					
Sample	P	T	dT	Raw Viscosity	SD
Name	[psi]	[C]	[C]	[cP]	%
B20 Blend, Jatropha Biodiesel / ULSD Blends	24	70.0	0.04	1.338	0.2
	1000	70.0	0.03	1.439	0.2
	2000	70.0	0.04	1.544	0.2
	3000	70.0	0.03	1.656	0.3
	4000	70.0	0.04	1.772	0.2
	5000	70.0	0.03	1.893	0.1
	6000	70.0	0.03	2.022	0.3
	7000	70.0	0.03	2.147	0.2
	8000	70.0	0.03	2.280	0.2
	9000	70.0	0.04	2.413	0.1
	10000	70.0	0.03	2.561	0.2
	11000	70.0	0.02	2.709	0.1
	12000	70.0	0.02	2.865	0.2
	13000	70.0	0.02	3.025	0.1
	14000	70.0	0.02	3.198	0.3
	15000	70.0	0.02	3.384	0.2
	16000	70.0	0.02	3.557	0.3
17000	70.0	0.02	3.748	0.2	
18000	70.0	0.01	3.951	0.3	
19000	70.0	0.01	4.155	0.2	

Table A.19.4B B20 Used in Jatropha Biodiesel/ULSD Blends, Raw, Uncorrected High Pressure Viscosity Experimental Data at 70 C.					
B20 / Blends / 70 Celsius / 5 cP Piston / cdl 466					
Sample	P	T	dT	Raw Viscosity	SD
Name	[psi]	[C]	[C]	[cP]	%
B20 Blend, Jatropha Biodiesel / ULSD Blends	26	70.0	0.03	1.280	0.1
	1000	70.0	0.02	1.358	0.2
	2000	70.0	0.02	1.443	0.2
	3000	70.0	0.01	1.530	0.2
	4000	70.0	0.01	1.616	0.2
	5000	70.0	0.01	1.702	0.1
	6000	70.0	0.01	1.791	0.1
	7000	70.0	0.01	1.885	0.2
	8000	70.0	0.01	1.990	0.1
	9000	70.0	0.01	2.096	0.2
	10000	70.0	0.01	2.204	0.2
	11000	70.0	0.00	2.313	0.1
	12000	70.0	0.01	2.429	0.2
	13000	70.0	0.01	2.548	0.1
	14000	70.0	0.01	2.673	0.1
	15000	70.0	0.01	2.803	0.2
	16000	70.0	0.01	2.925	0.2
17000	70.0	0.01	3.056	0.2	
18000	70.0	0.00	3.193	0.2	
19000	70.0	0.01	3.337	0.2	

Table A.19.5 B20 Used in Jatropha Biodiesel/ULSD Blends, Raw, Uncorrected High Pressure Viscosity Experimental Data at 100 C.					
B20 / Blends / 100 Celsius / 5 cP Piston / cdl 466					
Sample	P	T	dT	Raw Viscosity	SD
Name	[psi]	[C]	[C]	[cP]	%
B20 Blend, Jatropha Biodiesel / ULSD Blends	25	100.0	0.03	0.854	0.2
	1000	100.0	0.02	0.906	0.2
	2000	100.0	0.01	0.963	0.2
	3000	100.0	0.02	1.013	0.3
	4000	100.0	0.02	1.066	0.2
	5000	100.0	0.02	1.123	0.2
	6000	100.0	0.02	1.178	0.2
	7000	100.0	0.01	1.232	0.2
	8000	100.0	0.01	1.285	0.1
	9000	100.0	0.01	1.340	0.1
	10000	100.0	0.01	1.397	0.2
	11000	100.0	0.01	1.453	0.2
	12000	100.0	0.01	1.508	0.2
	13000	100.0	0.01	1.566	0.1
	14000	100.0	0.01	1.625	0.1
	15000	100.0	0.01	1.689	0.1
	16000	100.0	0.01	1.748	0.1
17000	100.0	0.01	1.808	0.1	
18000	100.0	0.01	1.872	0.1	
19000	100.0	0.01	1.946	0.2	

Table A.20.1 ULSD Used in Palm & Tallow Biodiesel/ULSD Blends, Raw, Uncorrected High Pressure Viscosity Experimental Data at 5 C.					
ULSD / Blends / 5 Celsius / 50 cP Piston / cdl 470					
Sample	P	T	dT	Raw Viscosity	SD
Name	[psi]	[C]	[C]	[cP]	%
ULSD Used in Palm & Tallow Biodiesel / ULSD Blends	41	5.0	0.03	4.880	0.3
	1000	5.0	0.04	5.370	0.3
	2000	5.0	0.02	5.931	0.3
	3000	5.0	0.02	6.600	0.3
	4000	5.0	0.03	7.247	0.3
	5000	5.0	0.02	7.980	0.3
	6000	5.0	0.01	8.819	0.2
	7000	5.0	0.02	9.643	0.3
	8000	5.0	0.01	10.48	0.2
	9000	5.0	0.02	11.45	0.3
	10000	5.0	0.01	12.57	0.3
	11000	5.0	0.01	13.78	0.2
	12000	5.0	0.01	15.08	0.3
	13000	5.0	0.01	16.45	0.2
	14000	5.0	0.01	17.94	0.3
	15000	5.0	0.01	19.69	0.1
	16000	5.0	0.01	22.52	0.3
17000	5.0	0.01	25.28	0.3	
18000	5.0	0.01	28.26	0.3	
19000	5.0	0.04	31.89	0.5	

Table A.20.2 ULSD Used in Palm & Tallow Biodiesel/ULSD Blends, Raw, Uncorrected High Pressure Viscosity Experimental Data at 10 C.					
ULSD / Blends / 10 Celsius / 50 cP Piston / cdl 470					
Sample	P	T	dT	Raw Viscosity	SD
Name	[psi]	[C]	[C]	[cP]	%
ULSD Used in Palm & Tallow Biodiesel / ULSD Blends	25	10.0	0.05	4.101	0.3
	1000	10.0	0.03	4.506	0.2
	2000	10.0	0.03	4.954	0.1
	3000	10.0	0.03	5.448	0.2
	4000	10.0	0.03	5.982	0.3
	5000	10.0	0.03	6.559	0.1
	6000	10.0	0.02	7.200	0.2
	7000	10.0	0.02	7.898	0.2
	8000	10.0	0.02	8.610	0.2
	9000	10.0	0.02	9.444	0.3
	10000	10.0	0.01	10.30	0.3
	11000	10.0	0.01	11.19	0.2
	12000	10.0	0.01	12.18	0.3
	13000	10.0	0.01	13.21	0.3
	14000	10.0	0.01	14.34	0.2
	15000	10.0	0.01	15.58	0.2
	16000	10.0	0.01	16.93	0.3
17000	10.0	0.01	18.36	0.2	
18000	10.0	0.01	20.13	0.1	
19000	10.0	0.01	22.08	0.2	

Table A.20.3 ULSD Used in Palm & Tallow Biodiesel/ULSD Blends, Raw, Uncorrected High Pressure Viscosity Experimental Data at 20 C.					
ULSD / Blends / 20 Celsius / 50 cP Piston / cdl 470					
Sample	P	T	dT	Raw Viscosity	SD
Name	[psi]	[C]	[C]	[cP]	%
ULSD Used in Palm & Tallow Biodiesel / ULSD Blends	15	20.0	0.03	3.087	0.3
	1000	20.0	0.03	3.406	0.3
	2000	20.0	0.03	3.689	0.2
	3000	20.0	0.04	4.028	0.2
	4000	20.0	0.04	4.374	0.2
	5000	20.0	0.04	4.760	0.2
	6000	20.0	0.03	5.177	0.3
	7000	20.0	0.03	5.621	0.2
	8000	20.0	0.02	6.080	0.2
	9000	20.0	0.02	6.598	0.3
	10000	20.0	0.02	7.151	0.3
	11000	20.0	0.02	7.807	0.2
	12000	20.0	0.02	8.446	0.3
	13000	20.0	0.02	9.205	0.2
	14000	20.0	0.02	10.05	0.3
	15000	20.0	0.02	10.79	0.3
	16000	20.0	0.01	11.87	0.3
	17000	20.0	0.01	12.54	0.3
18000	20.0	0.01	13.45	0.3	
19000	20.0	0.02	14.45	0.3	

Table A.20.4 ULSD Used in Palm & Tallow Biodiesel/ULSD Blends, Raw, Uncorrected High Pressure Viscosity Experimental Data at 25 C.

ULSD / Blends / 25 Celsius / 50 cP Piston / cdl 470					
Sample	P	T	dT	Raw Viscosity	SD
Name	[psi]	[C]	[C]	[cP]	%
ULSD Used in Palm & Tallow Biodiesel / ULSD Blends	33	25.0	0.05	2.757	0.2
	1000	25.0	0.05	3.011	0.2
	2000	25.0	0.05	3.273	0.3
	3000	25.0	0.03	3.561	0.1
	4000	25.0	0.01	3.862	0.2
	5000	25.0	0.02	4.204	0.1
	6000	25.0	0.01	4.523	0.1
	7000	25.0	0.03	4.905	0.2
	8000	25.0	0.03	5.295	0.2
	9000	25.0	0.03	5.733	0.1
	10000	25.0	0.02	6.192	0.2
	11000	25.0	0.03	6.670	0.2
	12000	25.0	0.01	7.182	0.1
	13000	25.0	0.02	7.748	0.2
	14000	25.0	0.01	8.339	0.3
	15000	25.0	0.02	8.971	0.2
	16000	25.0	0.02	9.654	0.2
17000	25.0	0.01	10.38	0.2	
18000	25.0	0.01	11.14	0.1	
19000	25.0	0.01	11.98	0.2	

Table A.20.5 ULSD Used in Palm & Tallow Biodiesel/ULSD Blends, Raw, Uncorrected High Pressure Viscosity Experimental Data at 40 C.					
ULSD / Blends / 40 Celsius / 20 cP Piston / cdl 476					
Sample	P	T	dT	Raw Viscosity	SD
Name	[psi]	[C]	[C]	[cP]	%
ULSD Used in Palm & Tallow Biodiesel / ULSD Blends	33	40.0	0.04	1.993	0.2
	1000	40.0	0.03	2.162	0.3
	2000	40.0	0.02	2.353	0.3
	3000	40.0	0.03	2.548	0.3
	4000	40.0	0.03	2.745	0.3
	5000	40.0	0.03	2.969	0.3
	6000	40.0	0.01	3.200	0.3
	7000	40.0	0.02	3.432	0.3
	8000	40.0	0.02	3.676	0.2
	9000	40.0	0.01	3.947	0.3
	10000	40.0	0.02	4.240	0.1
	11000	40.0	0.02	4.545	0.3
	12000	40.0	0.01	4.858	0.2
	13000	40.0	0.02	5.176	0.2
	14000	40.0	0.02	5.527	0.2
	15000	40.0	0.01	5.877	0.2
	16000	40.0	0.01	6.267	0.3
17000	40.0	0.02	6.655	0.2	
18000	40.0	0.01	7.091	0.2	
19000	40.0	0.01	7.563	0.2	

Table A.20.6 ULSD Used in Palm & Tallow Biodiesel/ULSD Blends, Raw, Uncorrected High Pressure Viscosity Experimental Data at 70 C.					
ULSD / Blends / 70 Celsius / 20 cP Piston / cdl 476					
Sample	P	T	dT	Raw Viscosity	SD
Name	[psi]	[C]	[C]	[cP]	%
ULSD Used in Palm & Tallow Biodiesel / ULSD Blends	44	70.0	0.02	1.205	0.1
	1000	70.0	0.05	1.289	0.3
	2000	70.0	0.04	1.396	0.2
	3000	70.0	0.04	1.486	0.3
	4000	70.0	0.04	1.592	0.3
	5000	70.0	0.04	1.699	0.2
	6000	70.0	0.03	1.813	0.3
	7000	70.0	0.05	1.921	0.3
	8000	70.0	0.04	2.046	0.3
	9000	70.0	0.03	2.165	0.2
	10000	70.0	0.03	2.301	0.2
	11000	70.0	0.02	2.437	0.2
	12000	70.0	0.03	2.577	0.3
	13000	70.0	0.01	2.742	0.2
	14000	70.0	0.02	2.891	0.3
	15000	70.0	0.02	3.044	0.1
	16000	70.0	0.02	3.218	0.3
17000	70.0	0.03	3.397	0.3	
18000	70.0	0.02	3.566	0.2	
19000	70.0	0.02	3.752	0.2	

Table A.20.7 ULSD Used in Palm & Tallow Biodiesel/ULSD Blends, Raw, Uncorrected High Pressure Viscosity Experimental Data at 100 C.					
ULSD / Blends / 100 Celsius / 5 cP Piston / cdl 466					
Sample	P	T	dT	Raw Viscosity	SD
Name	[psi]	[C]	[C]	[cP]	%
ULSD Used in Palm & Tallow Biodiesel / ULSD Blends	29	100.0	0.02	0.805	0.3
	1000	100.0	0.03	0.853	0.1
	2000	100.0	0.04	0.905	0.3
	3000	100.0	0.02	0.950	0.2
	4000	100.0	0.02	1.000	0.2
	5000	100.0	0.03	1.055	0.3
	6000	100.0	0.02	1.101	0.3
	7000	100.0	0.01	1.148	0.1
	8000	100.0	0.01	1.210	0.2
	9000	100.0	0.01	1.255	0.3
	10000	100.0	0.02	1.303	0.3
	11000	100.0	0.02	1.356	0.2
	12000	100.0	0.02	1.403	0.2
	13000	100.0	0.01	1.464	0.3
	14000	100.0	0.02	1.516	0.3
	15000	100.0	0.01	1.572	0.2
	16000	100.0	0.01	1.632	0.2
17000	100.0	0.01	1.687	0.3	
18000	100.0	0.01	1.750	0.2	
19000	100.0	0.01	1.806	0.2	

Table A.21.1 B5, Palm Biodiesel/ULSD Blends, Raw, Uncorrected High Pressure Viscosity Experimental Data at 5 C.					
B5 / Blends / 5 Celsius / 50 cP Piston / cdl 470					
Sample	P	T	dT	Raw Viscosity	SD
Name	[psi]	[C]	[C]	[cP]	%
B5 Blend Palm Biodiesel / ULSD Blends	8	5.0	0.04	4.953	0.2
	1000	5.0	0.02	5.474	0.3
	2000	5.0	0.02	6.035	0.2
	3000	5.0	0.02	6.628	0.1
	4000	5.0	0.01	7.275	0.2
	5000	--	--	--	--
	6000	5.0	0.02	8.812	0.3
	7000	5.0	0.02	9.635	0.2
	8000	5.0	0.01	10.52	0.3
	9000	5.0	0.01	11.50	0.3
	10000	5.0	0.02	12.56	0.2
	11000	5.0	0.01	13.69	0.2
	12000	5.0	0.01	14.89	0.1
	13000	5.0	0.01	16.19	0.2
	14000	5.0	0.03	17.79	0.2
	15000	5.0	0.01	19.54	0.3
	16000	5.0	0.01	24.19	0.3
	17000	5.0	0.01	28.69	0.3
18000	--	--	--	--	
19000	5.0	0.01	45.01	0.9	

Table A.21.2 B5, Palm Biodiesel/ULSD Blends, Raw, Uncorrected High Pressure Viscosity Experimental Data at 10 C.					
B5 / Blends / 10 Celsius / 50 cP Piston / cdl 470					
Sample	P	T	dT	Raw Viscosity	SD
Name	[psi]	[C]	[C]	[cP]	%
B5 Blend Palm Biodiesel / ULSD Blends	17	10.0	0.03	4.215	0.3
	1000	10.0	0.04	4.643	0.3
	2000	10.0	0.03	5.113	0.3
	3000	10.0	0.04	5.615	0.2
	4000	10.0	0.02	6.147	0.3
	5000	10.0	0.02	6.723	0.2
	6000	10.0	0.02	7.321	0.1
	7000	10.0	0.01	7.989	0.3
	8000	10.0	0.02	8.669	0.3
	9000	10.0	0.02	9.453	0.2
	10000	10.0	0.02	10.32	0.3
	11000	10.0	0.02	11.23	0.2
	12000	10.0	0.02	12.23	0.2
	13000	10.0	0.01	13.32	0.2
	14000	10.0	0.02	14.47	0.2
	15000	10.0	0.02	15.69	0.2
	16000	10.0	0.02	17.03	0.2
17000	10.0	0.01	18.52	0.2	
18000	10.0	0.01	20.22	0.1	
19000	10.0	0.01	22.08	0.2	

Table A.21.3 B5, Palm Biodiesel/ULSD Blends, Raw, Uncorrected High Pressure Viscosity Experimental Data at 15 C.					
B5 / Blends / 15 Celsius / 50 cP Piston / cdl 470					
Sample	P	T	dT	Raw Viscosity	SD
Name	[psi]	[C]	[C]	[cP]	%
B5 Blend Palm Biodiesel / ULSD Blends	13	15.0	0.05	3.655	0.3
	1000	15.0	0.04	4.015	0.2
	2000	15.0	0.04	4.401	0.2
	3000	15.0	0.03	4.817	0.3
	4000	15.0	0.04	5.281	0.2
	5000	15.0	0.03	5.713	0.2
	6000	15.0	0.03	6.252	0.3
	7000	15.0	0.02	6.800	0.3
	8000	15.0	0.01	7.357	0.3
	9000	15.0	0.02	7.996	0.2
	10000	15.0	0.01	8.657	0.3
	11000	15.0	0.02	9.348	0.2
	12000	15.0	0.01	10.12	0.3
	13000	15.0	0.01	10.92	0.2
	14000	15.0	0.01	11.80	0.2
	15000	15.0	0.01	12.82	0.2
	16000	15.0	0.01	13.89	0.3
17000	15.0	0.01	14.97	0.3	
18000	15.0	0.01	16.16	0.2	
19000	15.0	0.01	17.42	0.2	

Table A.21.4 B5, Palm Biodiesel/ULSD Blends, Raw, Uncorrected High Pressure Viscosity Experimental Data at 20 C.					
B5 / Blends / 20 Celsius / 50 cP Piston / cdl 470					
Sample	P	T	dT	Raw Viscosity	SD
Name	[psi]	[C]	[C]	[cP]	%
B5 Blend Palm Biodiesel / ULSD Blends	19	20.0	0.03	3.216	0.3
	1000	20.0	0.05	3.512	0.2
	2000	20.0	0.04	3.879	0.2
	3000	20.0	0.03	4.235	0.2
	4000	20.0	0.03	4.611	0.3
	5000	20.0	0.02	5.016	0.3
	6000	20.0	0.03	5.444	0.2
	7000	20.0	0.04	5.907	0.3
	8000	20.0	0.02	6.400	0.2
	9000	20.0	0.02	6.942	0.3
	10000	20.0	0.02	7.499	0.3
	11000	20.0	0.01	8.096	0.3
	12000	20.0	0.01	8.749	0.3
	13000	20.0	0.02	9.442	0.2
	14000	20.0	0.01	10.19	0.2
	15000	20.0	0.01	10.99	0.3
	16000	20.0	0.01	11.82	0.2
17000	20.0	0.02	12.72	0.2	
18000	20.0	0.01	13.68	0.2	
19000	20.0	0.01	14.77	0.3	

Table A.21.5 B5, Palm Biodiesel/ULSD Blends, Raw, Uncorrected High Pressure Viscosity Experimental Data at 25 C.					
B5 / Blends / 25 Celsius / 50 cP Piston / cdl 470					
Sample	P	T	dT	Raw Viscosity	SD
Name	[psi]	[C]	[C]	[cP]	%
B5 Blend Palm Biodiesel / ULSD Blends	27	25.0	0.05	2.786	0.1
	1000	25.0	0.05	3.049	0.3
	2000	25.0	0.04	3.309	0.3
	3000	25.0	0.03	3.598	0.3
	4000	25.0	0.04	3.909	0.2
	5000	25.0	0.04	4.231	0.3
	6000	25.0	0.03	4.587	0.1
	7000	25.0	0.03	4.968	0.3
	8000	25.0	0.04	5.373	0.3
	9000	25.0	0.03	5.815	0.3
	10000	25.0	0.02	6.234	0.1
	11000	25.0	0.02	6.727	0.3
	12000	25.0	0.02	7.222	0.2
	13000	25.0	0.02	7.786	0.2
	14000	25.0	0.02	8.383	0.2
	15000	25.0	0.01	9.023	0.3
	16000	25.0	0.02	9.692	0.3
	17000	25.0	0.01	10.40	0.3
18000	25.0	0.01	11.18	0.3	
19000	25.0	0.02	11.99	0.2	

Table A.22.1 B10, Palm Biodiesel/ULSD Blends, Raw, Uncorrected High Pressure Viscosity Experimental Data at 5 C.					
B10 / Blends / 5 Celsius / 50 cP Piston / cdl 470					
Sample	P	T	dT	Raw Viscosity	SD
Name	[psi]	[C]	[C]	[cP]	%
B10 Blend Palm Biodiesel / ULSD Blends	21	5.0	0.02	5.074	0.2
	1000	5.0	0.03	5.598	0.3
	2000	5.0	0.02	6.108	0.3
	3000	5.0	0.02	6.723	0.3
	4000	5.0	0.03	7.353	0.3
	5000	5.0	0.03	8.067	0.3
	6000	5.0	0.02	8.816	0.3
	7000	5.0	0.02	9.628	0.2
	8000	5.0	0.01	10.55	0.2
	9000	5.0	0.01	11.49	0.2
	10000	5.0	0.01	12.52	0.2
	11000	5.0	0.01	13.67	0.3
	12000	5.0	0.01	14.85	0.1
	13000	5.0	0.02	16.18	0.3
	14000	5.0	0.01	17.60	0.3
	15000	5.0	0.01	19.25	0.2
	16000	5.0	0.01	27.69	0.3
17000	5.0	0.01	36.91	0.6	
18000	5.0	0.0	49.86	1.0	
19000	5.0	0.0	66.00	2.5	

Table A.22.2 B10, Palm Biodiesel/ULSD Blends, Raw, Uncorrected High Pressure Viscosity Experimental Data at 10 C.					
B10 / Blends / 10 Celsius / 50 cP Piston / cdl 470					
Sample	P	T	dT	Raw Viscosity	SD
Name	[psi]	[C]	[C]	[cP]	%
B10 Blend Palm Biodiesel / ULSD Blends	17	10.0	0.04	4.359	0.2
	1000	10.0	0.04	4.800	0.3
	2000	10.0	0.02	5.266	0.3
	3000	10.0	0.03	5.793	0.3
	4000	10.0	0.02	6.348	0.2
	5000	10.0	0.02	6.923	0.1
	6000	10.0	0.03	7.562	0.3
	7000	10.0	0.02	8.240	0.3
	8000	10.0	0.02	8.953	0.2
	9000	10.0	0.02	9.756	0.3
	10000	10.0	0.01	10.59	0.1
	11000	10.0	0.02	11.48	0.2
	12000	10.0	0.01	12.46	0.1
	13000	10.0	0.02	13.53	0.2
	14000	10.0	0.02	14.67	0.3
	15000	10.0	0.01	15.84	0.1
	16000	10.0	0.01	17.17	0.3
17000	10.0	0.01	18.54	0.3	
18000	10.0	0.01	20.24	0.3	
19000	10.0	0.01	22.07	0.3	

Table A.22.3 B10, Palm Biodiesel/ULSD Blends, Raw, Uncorrected High Pressure Viscosity Experimental Data at 15 C.					
B10 / Blends / 15 Celsius / 50 cP Piston / cdl 470					
Sample	P	T	dT	Raw Viscosity	SD
Name	[psi]	[C]	[C]	[cP]	%
B10 Blend Palm Biodiesel / ULSD Blends	6	15.0	0.04	3.799	0.2
	1000	15.0	0.03	4.183	0.3
	2000	15.0	0.03	4.599	0.3
	3000	15.0	0.03	5.020	0.3
	4000	15.0	0.02	5.483	0.3
	5000	15.0	0.02	5.986	0.3
	6000	15.0	0.02	6.497	0.3
	7000	15.0	0.03	7.169	0.3
	8000	15.0	0.03	7.679	0.2
	9000	15.0	0.01	8.290	0.2
	10000	15.0	0.02	8.964	0.1
	11000	15.0	0.02	9.701	0.2
	12000	15.0	0.02	10.52	0.2
	13000	15.0	0.02	11.36	0.2
	14000	15.0	0.02	12.30	0.2
	15000	15.0	0.01	13.28	0.3
	16000	15.0	0.01	14.36	0.3
17000	15.0	0.01	15.49	0.2	
18000	15.0	0.01	16.64	0.3	
19000	15.0	0.01	17.86	0.3	

Table A.22.4 B10, Palm Biodiesel/ULSD Blends, Raw, Uncorrected High Pressure Viscosity Experimental Data at 20 C.					
B10 / Blends / 20 Celsius / 50 cP Piston / cdl 470					
Sample	P	T	dT	Raw Viscosity	SD
Name	[psi]	[C]	[C]	[cP]	%
B10 Blend Palm Biodiesel / ULSD Blends	3	20.0	0.05	3.296	0.3
	1000	20.0	0.05	3.596	0.1
	2000	20.0	0.04	3.915	0.3
	3000	20.0	0.04	4.276	0.3
	4000	20.0	0.02	4.637	0.2
	5000	20.0	0.03	5.029	0.3
	6000	20.0	0.03	5.449	0.2
	7000	20.0	0.03	5.899	0.3
	8000	20.0	0.02	6.388	0.3
	9000	20.0	0.02	6.916	0.2
	10000	20.0	0.02	7.458	0.3
	11000	20.0	0.02	8.074	0.2
	12000	20.0	0.02	8.783	0.1
	13000	20.0	0.01	9.405	0.2
	14000	20.0	0.01	10.12	0.3
	15000	20.0	0.02	10.90	0.2
	16000	20.0	0.01	11.72	0.2
17000	20.0	0.01	12.62	0.2	
18000	20.0	0.01	13.60	0.2	
19000	20.0	0.01	14.60	0.1	

Table A.22.5 B10, Palm Biodiesel/ULSD Blends, Raw, Uncorrected High Pressure Viscosity Experimental Data at 25 C.					
B10 / Blends / 25 Celsius / 50 cP Piston / cdl 470					
Sample	P	T	dT	Raw Viscosity	SD
Name	[psi]	[C]	[C]	[cP]	%
B10 Blend Palm Biodiesel / ULSD Blends	27	25.0	0.05	2.854	0.3
	1000	25.0	0.02	3.080	0.3
	2000	25.0	0.04	3.357	0.1
	3000	25.0	0.04	3.628	0.3
	4000	25.0	0.04	3.926	0.1
	5000	25.0	0.04	4.255	0.2
	6000	25.0	0.02	4.593	0.3
	7000	25.0	0.03	4.943	0.3
	8000	25.0	0.03	5.325	0.2
	9000	25.0	0.02	5.741	0.2
	10000	25.0	0.02	6.185	0.3
	11000	25.0	0.03	6.653	0.1
	12000	25.0	0.02	7.174	0.3
	13000	25.0	0.03	7.699	0.3
	14000	25.0	0.03	8.251	0.3
	15000	25.0	0.02	8.873	0.3
	16000	25.0	0.03	9.514	0.3
17000	25.0	0.02	10.22	0.3	
18000	25.0	0.02	10.94	0.3	
19000	25.0	0.02	11.70	0.3	

Table A.23.1 B20, Palm Biodiesel/ULSD Blends, Raw, Uncorrected High Pressure Viscosity Experimental Data at 5 C.					
B20 / Blends / 5 Celsius / 50 cP Piston / cdl 470					
Sample	P	T	dT	Raw Viscosity	SD
Name	[psi]	[C]	[C]	[cP]	%
B20 Blend Palm Biodiesel / ULSD Blends	13	5.0	0.03	5.436	0.3
	1000	5.0	0.03	5.962	0.2
	2000	5.0	0.02	6.556	0.3
	3000	5.0	0.03	7.191	0.2
	4000	5.0	0.02	7.892	0.1
	5000	5.0	0.02	8.629	0.3
	6000	5.0	0.01	9.433	0.2
	7000	5.0	0.01	10.30	0.2
	8000	5.0	0.01	11.24	0.3
	9000	5.0	0.02	12.23	0.3
	10000	5.0	0.01	13.29	0.1
	11000	5.0	0.01	14.43	0.2
	12000	5.0	0.01	15.67	0.2
13000	5.0	0.01	16.99	0.2	

Table A.23.2 B20, Palm Biodiesel/ULSD Blends, Raw, Uncorrected High Pressure Viscosity Experimental Data at 10 C.					
B20 / Blends / 10 Celsius / 50 cP Piston / cdl 470					
Sample	P	T	dT	Raw Viscosity	SD
Name	[psi]	[C]	[C]	[cP]	%
B20 Blend Palm Biodiesel / ULSD Blends	17	10.0	0.02	4.694	0.2
	1000	10.0	0.03	5.163	0.3
	2000	10.0	0.02	5.652	0.2
	3000	10.0	0.03	6.186	0.3
	4000	10.0	0.03	6.763	0.2
	5000	10.0	0.03	7.366	0.3
	6000	10.0	0.02	8.023	0.1
	7000	10.0	0.03	8.733	0.3
	8000	10.0	0.02	9.474	0.2
	9000	10.0	0.02	10.28	0.3
	10000	10.0	0.02	11.15	0.1
	11000	10.0	0.02	12.11	0.2
	12000	10.0	0.01	13.12	0.3
	13000	10.0	0.01	14.22	0.2
	14000	10.0	0.02	15.37	0.3
	15000	10.0	0.01	16.57	0.2
16000	10.0	0.01	17.89	0.1	
17000	10.0	0.01	19.49	0.1	
18000	10.0	0.01	21.26	0.3	

Table A.23.3 B20, Palm Biodiesel/ULSD Blends, Raw, Uncorrected High Pressure Viscosity Experimental Data at 15 C.					
B20 / Blends / 15 Celsius / 50 cP Piston / cdl 470					
Sample	P	T	dT	Raw Viscosity	SD
Name	[psi]	[C]	[C]	[cP]	%
B20 Blend Palm Biodiesel / ULSD Blends	8	15.0	0.05	4.026	0.2
	1000	15.0	0.05	4.461	0.3
	2000	15.0	0.03	4.819	0.3
	3000	15.0	0.03	5.260	0.3
	4000	15.0	0.03	5.730	0.1
	5000	15.0	0.03	6.191	0.3
	6000	15.0	0.02	6.711	0.3
	7000	15.0	0.03	7.266	0.1
	8000	15.0	0.02	7.869	0.2
	9000	15.0	0.02	8.520	0.2
	10000	15.0	0.02	9.220	0.3
	11000	15.0	0.03	9.987	0.3
	12000	15.0	0.02	10.81	0.1
	13000	15.0	0.02	11.67	0.1
	14000	15.0	0.01	12.61	0.3
	15000	15.0	0.02	13.59	0.2
	16000	15.0	0.01	14.60	0.2
17000	15.0	0.01	15.72	0.2	
18000	15.0	0.01	16.98	0.3	
19000	15.0	0.01	18.24	0.2	

Table A.23.4 B20, Palm Biodiesel/ULSD Blends, Raw, Uncorrected High Pressure Viscosity Experimental Data at 20 C.					
B20 / Blends / 20 Celsius / 50 cP Piston / cdl 470					
Sample	P	T	dT	Raw Viscosity	SD
Name	[psi]	[C]	[C]	[cP]	%
B20 Blend Palm Biodiesel / ULSD Blends	17	20.0	0.02	3.501	0.2
	1000	20.0	0.04	3.818	0.2
	2000	20.0	0.04	4.169	0.2
	3000	20.0	0.04	4.534	0.2
	4000	20.0	0.02	4.933	0.1
	5000	20.0	0.04	5.356	0.1
	6000	20.0	0.03	5.815	0.3
	7000	20.0	0.03	6.303	0.3
	8000	20.0	0.02	6.804	0.2
	9000	20.0	0.02	7.354	0.3
	10000	20.0	0.03	7.959	0.3
	11000	20.0	0.02	8.530	0.3
	12000	20.0	0.02	9.214	0.3
	13000	20.0	0.02	9.830	0.3
	14000	20.0	0.01	10.57	0.2
	15000	20.0	0.01	11.35	0.2
16000	20.0	0.01	12.23	0.3	
17000	20.0	0.02	13.13	0.2	
18000	20.0	0.01	14.15	0.3	
19000	20.0	0.01	15.15	0.2	

Table A.23.5 B20, Palm Biodiesel/ULSD Blends, Raw, Uncorrected High Pressure Viscosity Experimental Data at 25 C.					
B20 / Blends / 25 Celsius / 50 cP Piston / cdl 470					
Sample	P	T	dT	Raw Viscosity	SD
Name	[psi]	[C]	[C]	[cP]	%
B20 Blend Palm Biodiesel / ULSD Blends	22	25.0	0.05	2.995	0.3
	1000	25.0	0.04	3.276	0.3
	2000	25.0	0.04	3.566	0.2
	3000	25.0	0.04	3.884	0.3
	4000	25.0	0.03	4.197	0.3
	5000	25.0	0.03	4.538	0.2
	6000	25.0	0.02	4.905	0.2
	7000	25.0	0.03	5.295	0.3
	8000	25.0	0.03	5.702	0.3
	9000	25.0	0.03	6.126	0.1
	10000	25.0	0.02	6.592	0.2
	11000	25.0	0.03	7.074	0.3
	12000	25.0	0.02	7.589	0.1
	13000	25.0	0.02	8.139	0.2
	14000	25.0	0.02	8.750	0.3
	15000	25.0	0.02	9.365	0.2
	16000	25.0	0.02	10.02	0.1
17000	25.0	0.02	10.72	0.2	
18000	25.0	0.01	11.47	0.2	
19000	25.0	0.01	12.26	0.3	

Table A.24.1A B5, Tallow Biodiesel/ULSD Blends, Raw, Uncorrected High Pressure Viscosity Experimental Data at 5 C.					
B5 / Blends / 5 Celsius / 50 cP Piston / cdl 470					
Sample	P	T	dT	Raw Viscosity	SD
Name	[psi]	[C]	[C]	[cP]	%
B5 Blend Tallow Biodiesel / ULSD Blends	17	5.0	0.03	5.078	0.3
	1000	5.0	0.02	5.586	0.1
	2000	5.0	0.01	6.155	0.1
	3000	5.0	0.02	6.784	0.3
	4000	5.0	0.01	7.453	0.2
	5000	5.0	0.01	8.197	0.3
	6000	5.0	0.02	8.972	0.2
	7000	5.0	0.02	9.841	0.3
	8000	5.0	0.01	10.77	0.2
	9000	5.0	0.02	11.79	0.2
	10000	5.0	0.01	12.90	0.1
	11000	5.0	0.01	14.09	0.2
	12000	5.0	0.02	15.32	0.1
	13000	5.0	0.01	16.72	0.2
	14000	5.0	0.01	18.17	0.2
	15000	5.0	0.01	21.72	0.3
	16000	5.0	0.01	27.46	0.3
17000	5.0	0.00	34.40	0.3	
18000	5.0	--	43.00	7.8	

Table A.24.1B B5, Tallow Biodiesel/ULSD Blends, Raw, Uncorrected High Pressure Viscosity Experimental Data at 5 C.					
B5 / Blends / 5 Celsius / 50 cP Piston / cdl 470					
Sample Name	P [psi]	T [C]	dT [C]	Raw Viscosity [cP]	SD %
B5 Blend Tallow Biodiesel / ULSD Blends	14	5.0	0.03	5.221	0.3
	1000	5.0	0.03	5.762	0.2
	2000	5.0	0.04	6.367	0.2
	3000	5.0	0.02	7.031	0.2
	4000	5.0	0.02	7.683	0.2
	5000	5.0	0.02	8.411	0.1
	6000	5.0	0.02	9.246	0.3
	7000	5.0	0.01	10.12	0.2
	8000	5.0	0.01	11.07	0.3
	9000	5.0	0.01	12.08	0.2
	10000	5.0	0.01	13.21	0.2
	11000	5.0	0.02	14.42	0.3
	12000	5.0	0.01	15.68	0.2
	13000	5.0	0.01	17.08	0.1
	14000	5.0	0.01	18.62	0.2
	15000	5.0	0.01	22.12	0.3
	16000	5.0	0.01	27.34	0.3
17000	5.0	0.01	33.12	0.8	
18000	5.0	0.0	39.17	0.3	
19000	5.0	0.0	47.19	0.4	

Table A.24.2 B5, Palm Biodiesel/ULSD Blends, Raw, Uncorrected High Pressure Viscosity Experimental Data at 10 C.					
B5 / Blends / 10 Celsius / 50 cP Piston / cdl 470					
Sample	P	T	dT	Raw Viscosity	SD
Name	[psi]	[C]	[C]	[cP]	%
B5 Blend Tallow Biodiesel / ULSD Blends	53	10.0	0.05	4.245	0.3
	1000	10.0	0.02	4.624	0.2
	2000	10.0	0.03	5.093	0.2
	3000	10.0	0.03	5.603	0.3
	4000	10.0	0.02	6.131	0.2
	5000	10.0	0.01	6.721	0.3
	6000	10.0	0.03	7.358	0.2
	7000	10.0	0.02	8.043	0.2
	8000	10.0	0.03	8.801	0.3
	9000	10.0	0.02	9.538	0.2
	10000	10.0	0.02	10.41	0.1
	11000	10.0	0.01	11.33	0.2
	12000	10.0	0.02	12.28	0.2
	13000	10.0	0.01	13.46	0.3
	14000	10.0	0.01	14.56	0.3
	15000	10.0	0.01	15.73	0.2
	16000	10.0	0.01	17.22	0.3
17000	10.0	0.01	18.62	0.2	
18000	10.0	0.01	20.34	0.3	
19000	10.0	0.01	22.35	0.3	

Table A.24.3 B5, Palm Biodiesel/ULSD Blends, Raw, Uncorrected High Pressure Viscosity Experimental Data at 15 C.					
B5 / Blends / 15 Celsius / 50 cP Piston / cdl 470					
Sample	P	T	dT	Raw Viscosity	SD
Name	[psi]	[C]	[C]	[cP]	%
B5 Blend Tallow Biodiesel / ULSD Blends	19	15.0	0.03	3.691	0.3
	1000	15.0	0.04	4.034	0.3
	2000	15.0	0.03	4.413	0.2
	3000	15.0	0.03	4.807	0.1
	4000	15.0	0.03	5.246	0.2
	5000	15.0	0.03	5.713	0.1
	6000	15.0	0.03	6.255	0.1
	7000	15.0	0.02	6.832	0.3
	8000	15.0	0.02	7.448	0.2
	9000	15.0	0.03	8.133	0.3
	10000	15.0	0.02	8.820	0.3
	11000	15.0	0.02	9.526	0.3
	12000	15.0	0.02	10.28	0.2
	13000	15.0	0.02	11.12	0.2
	14000	15.0	0.01	12.02	0.2
	15000	15.0	0.02	12.99	0.2
	16000	15.0	0.01	14.07	0.1
17000	15.0	0.01	15.23	0.2	
18000	15.0	0.01	16.44	0.1	
19000	15.0	0.01	17.76	0.2	

Table A.24.4 B5, Palm Biodiesel/ULSD Blends, Raw, Uncorrected High Pressure Viscosity Experimental Data at 20 C.					
B5 / Blends / 20 Celsius / 50 cP Piston / cdl 470					
Sample	P	T	dT	Raw Viscosity	SD
Name	[psi]	[C]	[C]	[cP]	%
B5 Blend Tallow Biodiesel / ULSD Blends	23	20.0	0.05	3.318	0.3
	1000	20.0	0.05	3.620	0.1
	2000	20.0	0.02	3.958	0.2
	3000	20.0	0.03	4.299	0.2
	4000	20.0	0.03	4.664	0.3
	5000	20.0	0.04	5.069	0.3
	6000	20.0	0.03	5.448	0.3
	7000	20.0	0.02	5.844	0.2
	8000	20.0	0.03	6.325	0.3
	9000	20.0	0.03	6.842	0.2
	10000	20.0	0.02	7.412	0.2
	11000	20.0	0.02	7.994	0.2
	12000	20.0	0.01	8.639	0.3
	13000	20.0	0.02	9.303	0.2
	14000	20.0	0.01	10.03	0.3
	15000	20.0	0.01	10.83	0.3
16000	20.0	0.01	11.63	0.3	
17000	20.0	0.01	12.52	0.3	
18000	20.0	0.01	13.50	0.3	
19000	20.0	0.02	14.55	0.2	

Table A.24.5 B5, Palm Biodiesel/ULSD Blends, Raw, Uncorrected High Pressure Viscosity Experimental Data at 25 C.					
B5 / Blends / 25 Celsius / 50 cP Piston / cdl 470					
Sample	P	T	dT	Raw Viscosity	SD
Name	[psi]	[C]	[C]	[cP]	%
B5 Blend Tallow Biodiesel / ULSD Blends	22	25.0	0.04	2.857	0.2
	1000	25.0	0.05	3.114	0.1
	2000	25.0	0.03	3.395	0.2
	3000	25.0	0.03	3.680	0.2
	4000	25.0	0.05	3.968	0.3
	5000	25.0	0.03	4.310	0.2
	6000	25.0	0.03	4.661	0.1
	7000	25.0	0.04	5.034	0.3
	8000	25.0	0.01	5.429	0.1
	9000	25.0	0.02	5.876	0.1
	10000	25.0	0.03	6.327	0.3
	11000	25.0	0.02	6.817	0.3
	12000	25.0	0.02	7.324	0.3
	13000	25.0	0.02	7.884	0.2
	14000	25.0	0.01	8.443	0.2
	15000	25.0	0.01	9.067	0.3
	16000	25.0	0.02	9.747	0.3
17000	25.0	0.01	10.46	0.2	
18000	25.0	0.01	11.30	0.2	
19000	25.0	0.01	12.14	0.2	

Table A.25.1 B20, Tallow Biodiesel/ULSD Blends, Raw, Uncorrected
High Pressure Viscosity Experimental Data at 5 C.

B20 / Blends / 5 Celsius / 50 cP Piston / cdl 470					
Sample	P	T	dT	Raw Viscosity	SD
Name	[psi]	[C]	[C]	[cP]	%
B20 Blend Tallow Biodiesel / ULSD Blends	56	5.0	0.03	6.090	0.3
	1000	5.0	0.02	6.443	0.2
	2000	5.0	0.02	7.077	0.3
	3000	5.0	0.02	7.824	0.2
	4000	5.0	0.02	8.449	0.3
	5000	5.0	0.02	9.170	0.2
	6000	5.0	0.02	10.05	0.3
	7000	5.0	0.01	10.96	0.2
	8000	5.0	0.01	11.92	0.2
	9000	5.0	0.02	12.92	0.1
	10000	5.0	0.02	15.58	0.3
	11000	5.0	0.01	20.58	0.3
	12000	5.0	0.01	29.52	1.3
	13000	5.0	0.00	35.25	1.6
	14000	5.0	0.00	39.82	0.8
15000	5.0	0.00	46.31	1.4	
16000	5.0	0.00	57.65	1.3	

Table A.25.2 B20, Tallow Biodiesel/ULSD Blends, Raw, Uncorrected
High Pressure Viscosity Experimental Data at 10 C.

B20 / Blends / 10 Celsius / 50 cP Piston / cdl 470					
Sample	P	T	dT	Raw Viscosity	SD
Name	[psi]	[C]	[C]	[cP]	%
B20 Blend Tallow Biodiesel / ULSD Blends	29	10.0	0.04	5.244	0.3
	1000	10.0	0.01	5.494	0.3
	2000	10.0	0.04	6.143	0.3
	3000	10.0	0.03	6.677	0.3
	4000	10.0	0.03	7.231	0.3
	5000	10.0	0.02	7.832	0.1
	6000	10.0	0.02	8.556	0.2
	7000	10.0	0.02	9.350	0.2
	8000	10.0	0.02	10.16	0.1
	9000	10.0	0.02	11.04	0.2
	10000	10.0	0.01	11.91	0.1
	11000	10.0	0.01	12.91	0.3
	12000	10.0	0.01	14.04	0.2
	13000	10.0	0.01	15.16	0.2
	14000	10.0	0.01	16.38	0.1
15000	10.0	0.01	24.12	1.1	

Table A.25.3 B20, Tallow Biodiesel/ULSD Blends, Raw, Uncorrected High Pressure Viscosity Experimental Data at 15 C.					
B20 / Blends / 15 Celsius / 50 cP Piston / cdl 470					
Sample	P	T	dT	Raw Viscosity	SD
Name	[psi]	[C]	[C]	[cP]	%
B20 Blend Tallow Biodiesel / ULSD Blends	55	15.0	0.04	4.268	0.2
	1000	15.0	0.04	4.670	0.3
	2000	15.0	0.04	5.126	0.2
	3000	15.0	0.03	5.629	0.2
	4000	15.0	0.03	6.188	0.3
	5000	15.0	0.03	6.734	0.3
	6000	15.0	0.02	7.331	0.3
	7000	15.0	0.02	7.960	0.2
	8000	15.0	0.02	8.659	0.2
	9000	15.0	0.02	9.390	0.2
	10000	15.0	0.02	10.18	0.2
	11000	15.0	0.02	11.07	0.2
	12000	15.0	0.02	11.96	0.1
	13000	15.0	0.01	13.02	0.2
	14000	15.0	0.01	14.04	0.2
	15000	15.0	0.01	15.13	0.2
	16000	15.0	0.01	16.27	0.2
17000	15.0	0.01	17.51	0.2	
18000	15.0	0.01	18.87	0.1	
19000	15.0	0.01	20.48	0.2	

Table A.25.4 B20, Tallow Biodiesel/ULSD Blends, Raw, Uncorrected High Pressure Viscosity Experimental Data at 20 C.					
B20 / Blends / 20 Celsius / 50 cP Piston / cdl 470					
Sample	P	T	dT	Raw Viscosity	SD
Name	[psi]	[C]	[C]	[cP]	%
B20 Blend Tallow Biodiesel / ULSD Blends	67	20.0	0.04	3.721	0.2
	1000	20.0	0.04	4.020	0.3
	2000	20.0	0.03	4.311	0.2
	3000	20.0	0.03	4.655	0.1
	4000	20.0	0.03	5.040	0.3
	5000	20.0	0.03	5.482	0.1
	6000	20.0	0.03	5.981	0.2
	7000	20.0	0.02	6.474	0.2
	8000	20.0	0.01	6.987	0.3
	9000	20.0	0.02	7.534	0.2
	10000	20.0	0.02	8.138	0.2
	11000	20.0	0.02	8.785	0.3
	12000	20.0	0.02	9.474	0.3
	13000	20.0	0.01	10.21	0.1
	14000	20.0	0.01	10.98	0.3
	15000	20.0	0.01	11.80	0.1
	16000	20.0	0.02	12.66	0.2
17000	20.0	0.01	13.61	0.2	
18000	20.0	0.01	14.62	0.3	
19000	20.0	0.01	15.77	0.2	

Table A.25.5 B20, Tallow Biodiesel/ULSD Blends, Raw, Uncorrected High Pressure Viscosity Experimental Data at 25 C.					
B20 / Blends / 25 Celsius / 50 cP Piston / cdl 470					
Sample	P	T	dT	Raw Viscosity	SD
Name	[psi]	[C]	[C]	[cP]	%
B20 Blend Tallow Biodiesel / ULSD Blends	60	25.0	0.05	3.175	0.1
	1000	25.0	0.04	3.438	0.3
	2000	25.0	0.02	3.728	0.2
	3000	25.0	0.02	4.047	0.2
	4000	25.0	0.02	4.413	0.2
	5000	25.0	0.04	4.762	0.2
	6000	25.0	0.02	5.159	0.1
	7000	25.0	0.03	5.546	0.2
	8000	25.0	0.05	5.964	0.3
	9000	25.0	0.02	6.403	0.2
	10000	25.0	0.02	6.895	0.3
	11000	25.0	0.02	7.422	0.2
	12000	25.0	0.02	7.967	0.2
	13000	25.0	0.02	8.557	0.3
	14000	25.0	0.01	9.175	0.3
	15000	25.0	0.02	9.830	0.2
	16000	25.0	0.02	10.55	0.1
17000	25.0	0.02	11.32	0.2	
18000	25.0	0.01	12.16	0.3	
19000	25.0	0.01	13.01	0.2	

Table A.26.1A Soy / Coconut Biodiesel Blend, Raw, Uncorrected High Pressure Viscosity Experimental Data at 10 C.					
Soy / Coconut Oil Biodiesel / Blends / 10 Celsius / 50 cP Piston / cdl 470					
Sample	P	T	dT	Raw Viscosity	SD
Name	[psi]	[C]	[C]	[cP]	%
Soy / Coconut Oil Based Biodiesel 50 / 50 by Mass Blend	18	10.0	0.02	5.867	0.1
	1000	10.0	0.03	6.341	0.2
	3000	10.0	0.03	7.379	0.3
	5000	10.0	0.02	8.468	0.3
	7000	10.0	0.02	9.696	0.2
	9000	10.0	0.02	11.04	0.3
	10000	10.0	0.01	11.75	0.2
	11000	10.0	0.01	12.48	0.2
	12000	10.0	0.01	13.23	0.2
Table A.26.1B Soy / Coconut Biodiesel Blend, Raw, Uncorrected High Pressure Viscosity Experimental Data at 10 C.					
Soy / Coconut Oil Biodiesel / Blends / 10 Celsius / 50 cP Piston / cdl 470					
Sample	P	T	dT	Raw Viscosity	SD
Name	[psi]	[C]	[C]	[cP]	%
Soy / Coconut Oil Based Biodiesel 50 / 50 by Mass Blend	18	10.0	0.03	5.795	0.1
	1000	10.0	0.03	6.265	0.3
	3000	10.0	0.03	7.252	0.1
	5000	10.0	0.02	8.351	0.3
	7000	10.0	0.02	9.548	0.2
	9000	10.0	0.02	10.87	0.3
	10000	10.0	0.01	11.57	0.3
	11000	10.0	0.01	12.30	0.2
	12000	10.0	0.01	13.05	0.2

Table A.26.2A Soy / Coconut Biodiesel Blend, Raw, Uncorrected High Pressure Viscosity Experimental Data at 25 C.					
Soy / Coconut Oil Biodiesel / Blends / 25 Celsius / 50 cP Piston / cdl 470					
Sample	P	T	dT	Raw Viscosity	SD
Name	[psi]	[C]	[C]	[cP]	%
Soy / Coconut Oil Based Biodiesel 50 / 50 by Mass Blend	23	25.0	0.05	3.859	0.3
	1000	25.0	0.04	4.134	0.2
	3000	25.0	0.02	4.741	0.1
	5000	25.0	0.02	5.400	0.1
	7000	25.0	0.03	6.125	0.2
	9000	25.0	0.02	6.889	0.3
	11000	25.0	0.03	7.721	0.2
	13000	25.0	0.02	8.636	0.3
	15000	25.0	0.02	9.622	0.1
	17000	25.0	0.02	10.69	0.2
19000	25.0	0.02	11.87	0.1	

Table A.26.2B Soy / Coconut Biodiesel Blend, Raw, Uncorrected High Pressure Viscosity Experimental Data at 25 C.					
Soy / Coconut Oil Biodiesel / Blends / 25 Celsius / 50 cP Piston / cdl 470					
Sample	P	T	dT	Raw Viscosity	SD
Name	[psi]	[C]	[C]	[cP]	%
Soy / Coconut Oil Based Biodiesel 50 / 50 by Mass Blend	24	25.0	0.03	3.819	0.3
	1000	25.0	0.03	4.101	0.2
	3000	25.0	0.03	4.710	0.2
	5000	25.0	0.03	5.374	0.3
	7000	25.0	0.03	6.072	0.1
	9000	25.0	0.02	6.863	0.3
	11000	25.0	0.02	7.697	0.1
	13000	25.0	0.02	8.614	0.3
	15000	25.0	0.02	9.624	0.2
	17000	25.0	0.02	10.69	0.3
19000	25.0	0.01	11.85	0.2	

Table A.26.3A Soy / Coconut Biodiesel Blend, Raw, Uncorrected High Pressure Viscosity Experimental Data at 40 C.					
Soy / Coconut Oil Biodiesel / Blends / 40 Celsius / 20 cP Piston / cdl 476					
Sample	P	T	dT	Raw Viscosity	SD
Name	[psi]	[C]	[C]	[cP]	%
Soy / Coconut Oil Based Biodiesel 50 / 50 by Mass Blend	30	40.0	0.03	2.790	0.3
	1000	40.0	0.05	2.959	0.2
	3000	40.0	0.02	3.364	0.2
	5000	40.0	0.03	3.787	0.1
	7000	40.0	0.02	4.237	0.1
	9000	40.0	0.02	4.721	0.2
	11000	40.0	0.03	5.237	0.1
	13000	40.0	0.02	5.798	0.1
	15000	40.0	0.01	6.391	0.2
	17000	40.0	0.02	7.026	0.2
19000	40.0	0.01	7.708	0.1	

Table A.26.3B Soy / Coconut Biodiesel Blend, Raw, Uncorrected High Pressure Viscosity Experimental Data at 40 C.					
Soy / Coconut Oil Biodiesel / Blends / 40 Celsius / 20 cP Piston / cdl 476					
Sample	P	T	dT	Raw Viscosity	SD
Name	[psi]	[C]	[C]	[cP]	%
Soy / Coconut Oil Based Biodiesel 50 / 50 by Mass Blend	24	40.0	0.04	2.803	0.3
	1000	40.0	0.03	2.977	0.1
	3000	40.0	0.03	3.382	0.2
	5000	40.0	0.03	3.800	0.1
	7000	40.0	0.03	4.262	0.1
	9000	40.0	0.02	4.753	0.2
	11000	40.0	0.02	5.262	0.2
	13000	40.0	0.01	5.818	0.1
	15000	40.0	0.01	6.402	0.2
	17000	40.0	0.01	7.026	0.1
19000	40.0	0.02	7.737	0.2	

Table A.26.4A Soy / Coconut Biodiesel Blend, Raw, Uncorrected High Pressure Viscosity Experimental Data at 70 C.					
Soy / Coconut Oil Biodiesel / Blends / 70 Celsius / 20 cP Piston / cdl 476					
Sample Name	P [psi]	T [C]	dT [C]	Raw Viscosity [cP]	SD %
Soy / Coconut Oil Based Biodiesel 50 / 50 by Mass Blend	33	70.0	0.04	1.629	0.2
	1000	70.0	0.03	1.730	0.3
	3000	70.0	0.04	1.947	0.3
	5000	70.0	0.02	2.174	0.1
	7000	70.0	0.02	2.412	0.3
	9000	70.0	0.02	2.660	0.2
	11000	70.0	0.02	2.922	0.1
	13000	70.0	0.03	3.199	0.3
	15000	70.0	0.02	3.483	0.1
	17000	70.0	0.02	3.781	0.2
19000	70.0	0.03	4.091	0.2	

Table A.26.4B Soy / Coconut Biodiesel Blend, Raw, Uncorrected High Pressure Viscosity Experimental Data at 70 C.					
Soy / Coconut Oil Biodiesel / Blends / 70 Celsius / 20 cP Piston / cdl 476					
Sample Name	P [psi]	T [C]	dT [C]	Raw Viscosity [cP]	SD %
Soy / Coconut Oil Based Biodiesel 50 / 50 by Mass Blend	27	70.0	0.04	1.627	0.2
	1000	70.0	0.03	1.729	0.2
	3000	70.0	0.04	1.949	0.1
	5000	70.0	0.03	2.178	0.1
	7000	70.0	0.02	2.417	0.3
	9000	70.0	0.03	2.666	0.3
	11000	70.0	0.03	2.928	0.2
	13000	70.0	0.03	3.209	0.1
	15000	70.0	0.02	3.495	0.3
	17000	70.0	0.02	3.794	0.3
19000	70.0	0.02	4.101	0.2	

Table A.26.5A Soy / Coconut Biodiesel Blend, Raw, Uncorrected High Pressure Viscosity Experimental Data at 100 C.					
Soy / Coconut Oil Biodiesel / Blends / 100 Celsius / 5 cP Piston / cdl 466					
Sample	P	T	dT	Raw Viscosity	SD
Name	[psi]	[C]	[C]	[cP]	%
Soy / Coconut Oil Based Biodiesel 50 / 50 by Mass Blend	18	100.0	0.02	1.028	0.3
	1000	100.0	0.02	1.080	0.1
	3000	100.0	0.01	1.186	0.1
	5000	100.0	0.03	1.293	0.2
	7000	100.0	0.02	1.393	0.2
	9000	100.0	0.02	1.495	0.2
	11000	100.0	0.01	1.599	0.1
	13000	100.0	0.01	1.698	0.1
	15000	100.0	0.01	1.797	0.2
	17000	100.0	0.01	1.902	0.2
19000	100.0	0.01	2.015	0.2	

Table A.26.5B Soy / Coconut Biodiesel Blend, Raw, Uncorrected High Pressure Viscosity Experimental Data at 100 C.					
Soy / Coconut Oil Biodiesel / Blends / 100 Celsius / 5 cP Piston / cdl 466					
Sample	P	T	dT	Raw Viscosity	SD
Name	[psi]	[C]	[C]	[cP]	%
Soy / Coconut Oil Based Biodiesel 50 / 50 by Mass Blend	20	100.0	0.03	1.028	0.3
	1000	100.0	0.02	1.083	0.1
	3000	100.0	0.02	1.191	0.2
	5000	100.0	0.02	1.295	0.1
	7000	100.0	0.01	1.398	0.1
	9000	100.0	0.02	1.500	0.1
	11000	100.0	0.02	1.600	0.2
	13000	100.0	0.01	1.698	0.1
	15000	100.0	0.02	1.798	0.1
	17000	100.0	0.01	1.903	0.1
	19000	100.0	0.01	2.017	0.1

Appendix B

High-Pressure Viscometer Consistency, Precision, and Comparison to Literature Data

The consistency, repeatability and estimated uncertainty of the viscometer apparatus were determined. Determining the consistency of the apparatus over time for each of the three pistons used in this work is important in evaluating whether applying the same temperature and pressure corrections to the entire data set is valid. The repeatability or precision of the apparatus was determined by repeating isotherms at ambient and high-pressure using biodiesels and normal alkanes. The largest sources of uncertainty in the high-pressure experimentation are from the repeatability of the instrument and the corrections that are required for temperature and elevated pressure. The corrections required for temperature and elevated pressure were developed relative to a well-known and referenced literature source for normal dodecane. Correction parameters were regressed using a Gauss-Newton non-linear regression method. ***Data that is used in the repeatability analysis or elsewhere described as “raw” data, has not been adjusted for temperature and pressure.*** Calibration standard S6 from Cannon Instrument Company and Reagent Plus dodecane and pentadecane with purities greater than 99% from Sigma Aldrich were used in the analysis. The purity of the dodecane and pentadecane were further analyzed by GCMS in house, and were found to have peak areas of 99.8 and 99.5 percent of the total.

The measured viscosities of dodecane were found to be similar regardless of experimental date. The repeatability of the instrument was found to be 1.2% on average with 95% of the data

within 3.3% of repeated measurements. Ambient viscosity repeatability was found to be greater than high-pressure repeatability, and on average approximately 2%, although this value is based on a much smaller data set of 27 points compared to approximately 350 data points at high pressure. The temperature and pressure corrections derived were found to give corrected viscosities within the mutual uncertainty of the data in this work and the literature data cited.

B.1 Viscometer Consistency

The data was taken over multiple years using the same general set up described in Chapter 3. Dodecane ambient and high-pressure measurements were taken several times throughout the collection period as shown in Figures B.1 to B.4.

B.1.1 5 cP Piston Consistency

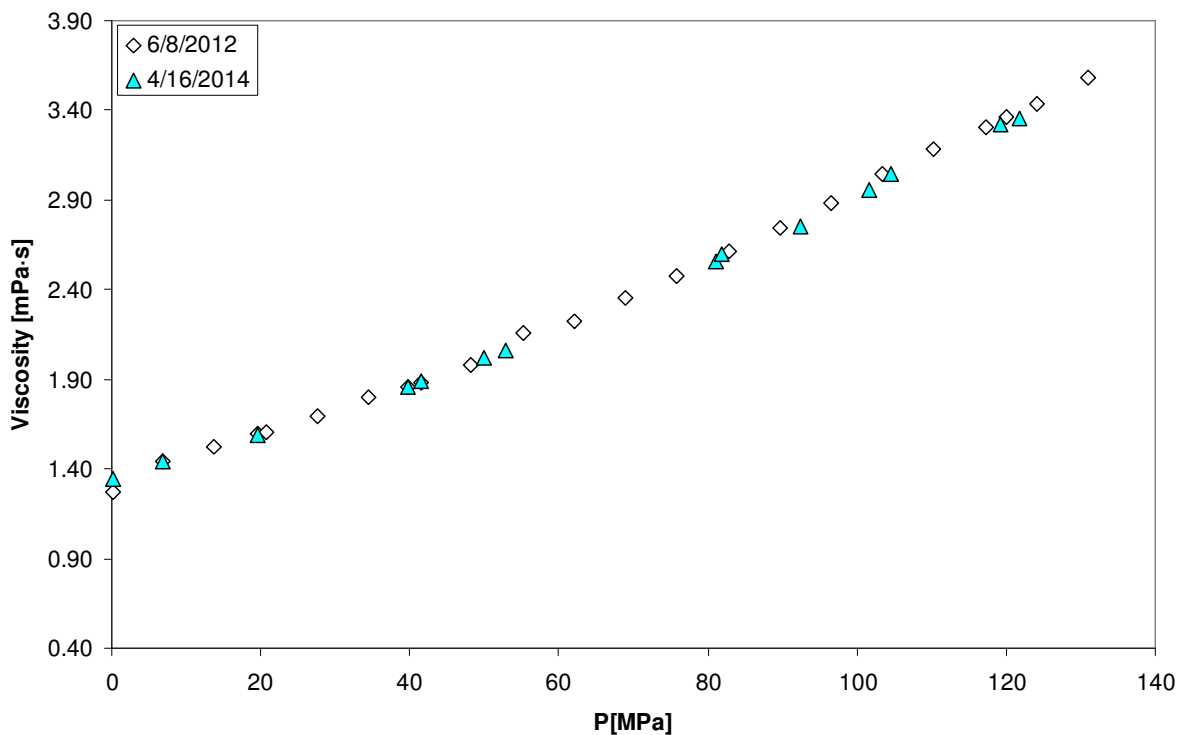


Figure B.1. Raw, uncorrected viscosity of dodecane at 25 C using the 5 cP piston.

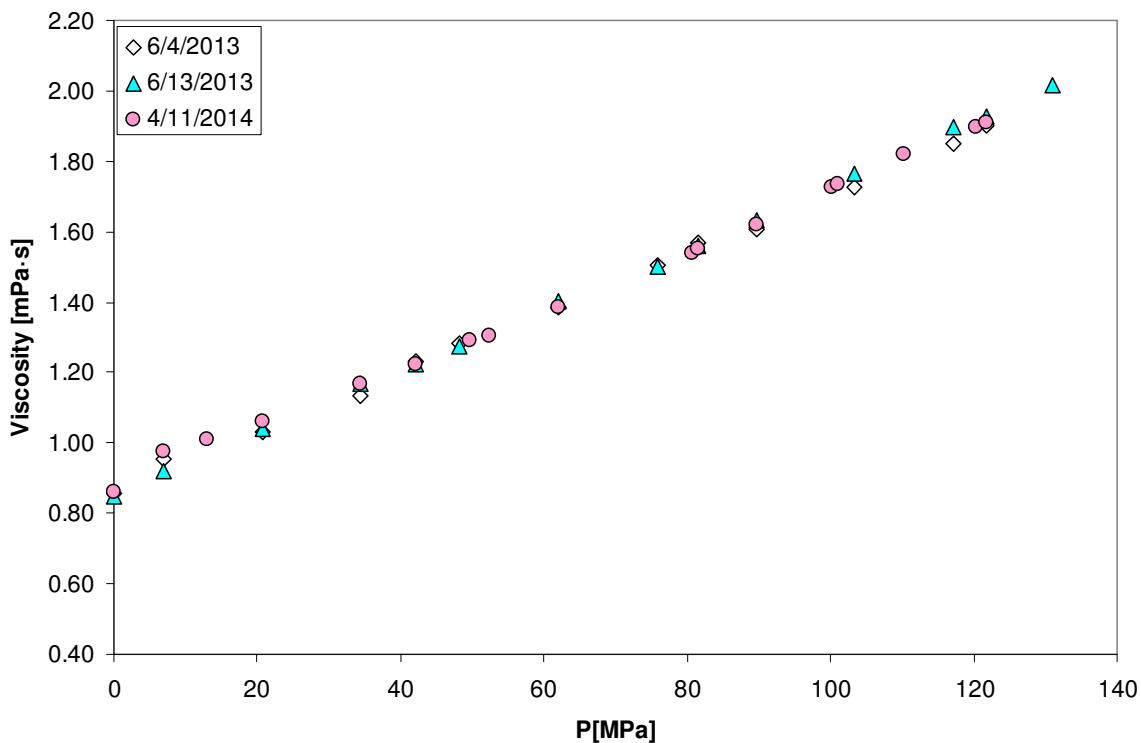


Figure B.2. Raw, uncorrected viscosity of dodecane at 50 C using the 5 cP piston.

B.1.2 20 cP Piston Consistency

The absolute average relative deviation (AARD) between runs for the 20 cP piston at 298.15 K in July 2012 compared to runs in April 2014 and June 2014 are less than 2 percent with a maximum deviation at high pressure of 3.3%. The AARD between the two runs in 2014 was also less than 2% with a maximum deviation of 3.6%. These results do not indicate a difference with respect to experiment date.

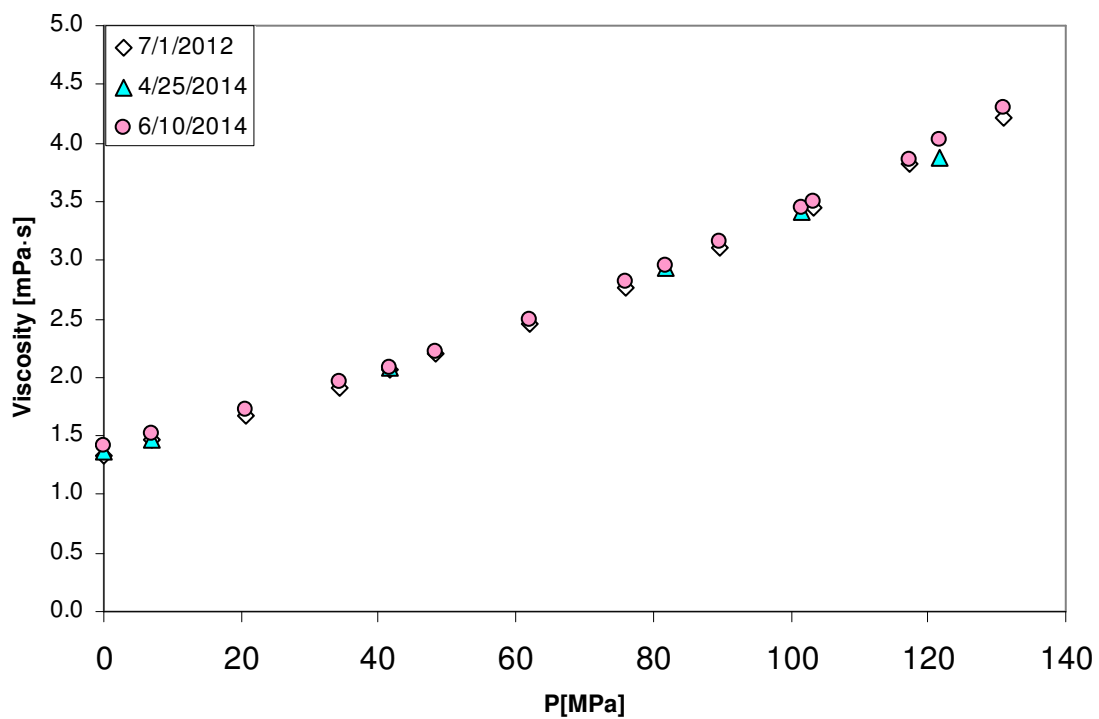


Figure B.3. Raw, uncorrected viscosity of dodecane at 298.15 K using the 20 cP piston in July 2012, April 2014, and June 2014.

B.1.3 50 cP Piston Consistency

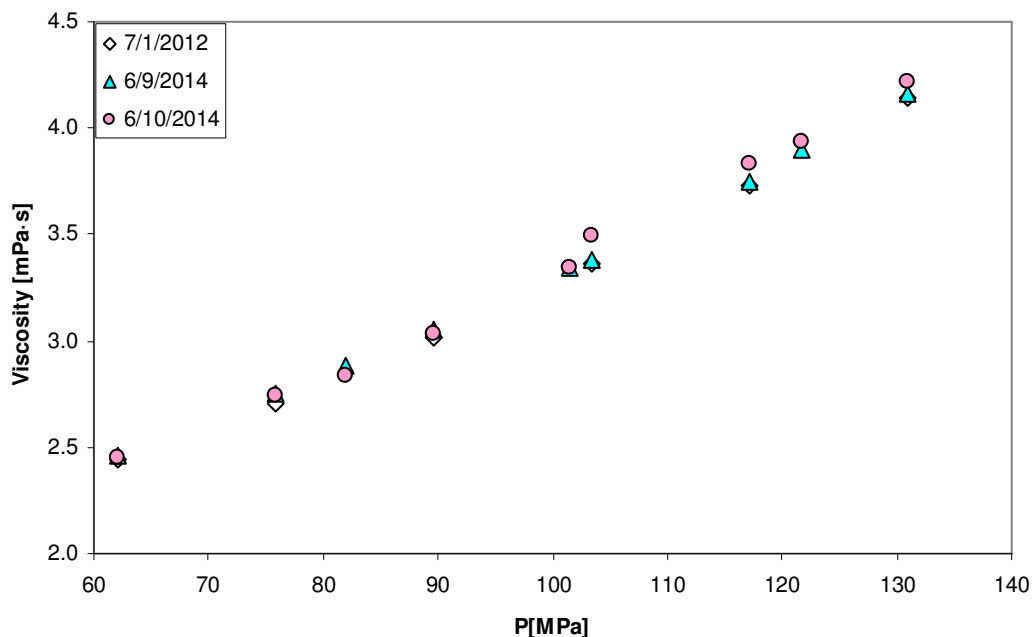


Figure B.4. Raw, uncorrected viscosity of dodecane at 298.15 K using the 50 cP piston.

The largest relative deviation at 103 MPa of less than 4 % occurs between runs that were within one day of each other. Experiments performed years apart did not yield significantly different results from those performed days or months apart for any of the three pistons.

B.2 Viscometer Repeatability at Higher than Ambient Pressure

Pentadecane, dodecane and two types of biodiesel were measured in duplicate and triplicate for a wide range of pressures and temperatures to find the average apparatus repeatability. Those data performed in triplicate would generate three relative deviation values, while those performed in duplicate would generate just one. High-pressure viscosity measurements were repeated for several temperatures of 283.15 up to 373.15 K and pressures up to 131 MPa. The

repeatability of the viscometer was evaluated as a function of pressure, percentage of maximum piston viscosity, temperature and piston type, as shown in Figures B.5 to B.21. ***There did not appear to be any significant association between absolute relative deviation (ARD) and any of the variables tested at high pressure.*** However, higher pressure measurements were typically less likely to have large ARDs, especially when compared to ambient pressure measurements, discussed later in this Appendix. Biodiesel, dodecane, and pentadecane had AARDs of 0.5, 1.5, and 1.0 percent respectively. At high pressure, 352 repeated data points had an AARD of 1.2 % with 95% of values having an ARD of less than 3.3%, shown in Figure B.5. When examining the repeatability of the viscometer for the temperature/piston pairs tested in the biodiesel, and the biodiesel-diesel blend studies (for example the 5 cP piston has repeated measurements at 298.15, 323.15, 348.15 and 373.15 K, but is only used for 373.15 K for all biodiesel and biodiesel diesel blend data) there are 232 repeated data points with an AARD of less than 1.0 %.

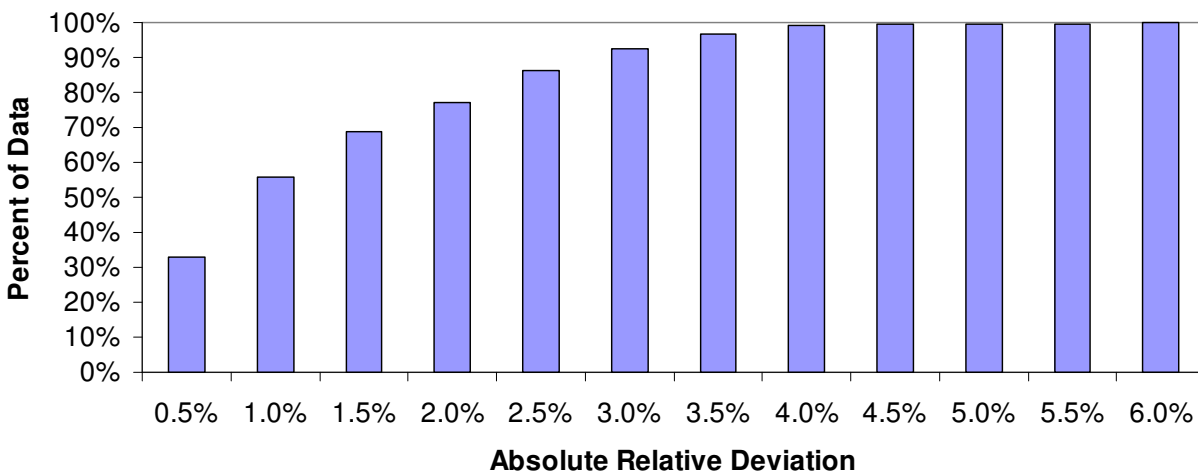


Figure B.5. Histogram of repeated data at higher than ambient pressure. Less than one percent of all repeated measurements had an ARD greater than 4 percent.

The ARD can be seen as a function of pressure in Figure B.6. There is no significant effect of pressure on ARD for the data set as a whole.

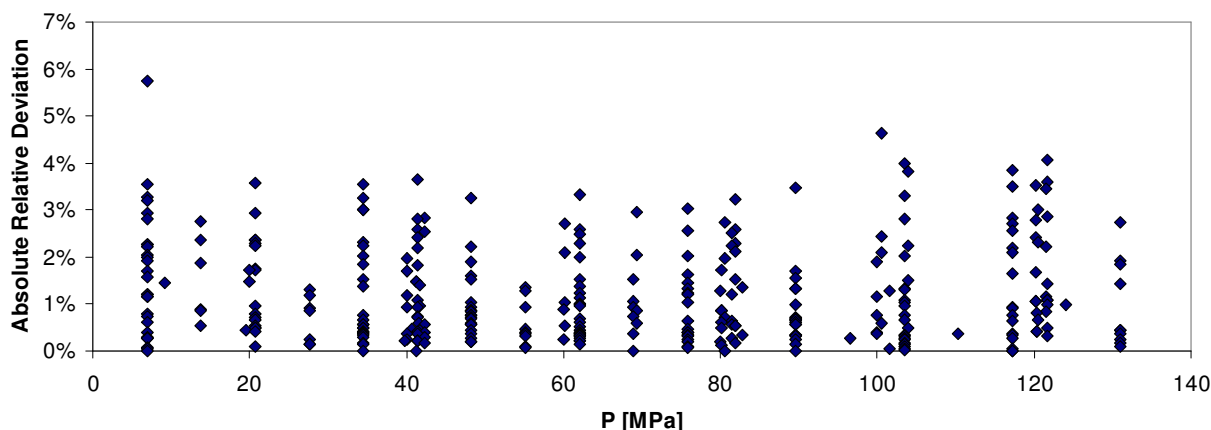


Figure B.6. Absolute relative deviation of 352 repeated points as function of pressure.

B.2.1 Overall ARD and Percentage of Maximum Piston Viscosity

Each piston has a nominal range of use, for example, the uncorrected maximum viscosity for the 5 cP piston is 5 cP or 5 mPa·s. The percentage of raw viscosity / piston maximum was calculated by using the average of the two measurements used to calculate the ARD and dividing that value by the uncorrected piston maximum 5, 20 or 50 mPa·s. It was considered that the center of the piston range might give more reliable measurements than those on the edges. There were no repeated measurements for viscosities greater than 51.2% of piston maximum. The result in Figure B.7 indicates there may be a relationship between absolute relative deviation and piston maximum, but this may simply be an artifact caused by the biodiesel data, which had a low ARD regardless of viscosity magnitude. Biodiesel comprised the majority of the set beyond 30% piston maximum as seen in Figure B.8.

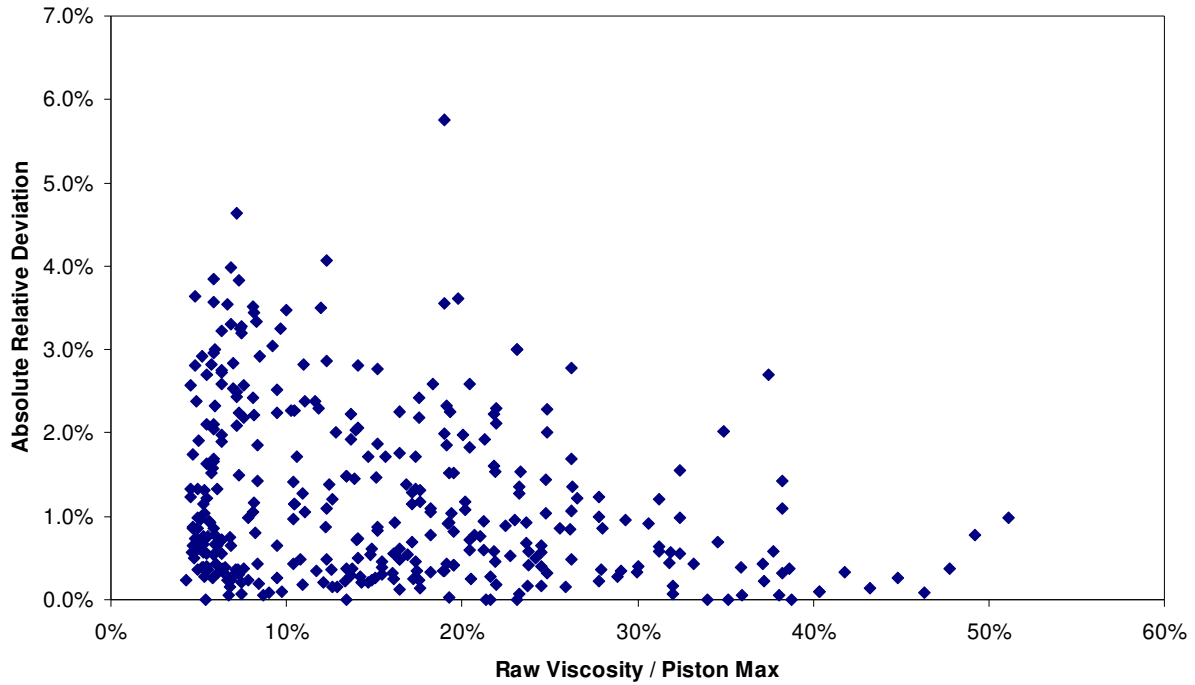


Figure B.7. Absolute relative deviation as a function of percent of piston maximum viscosity.

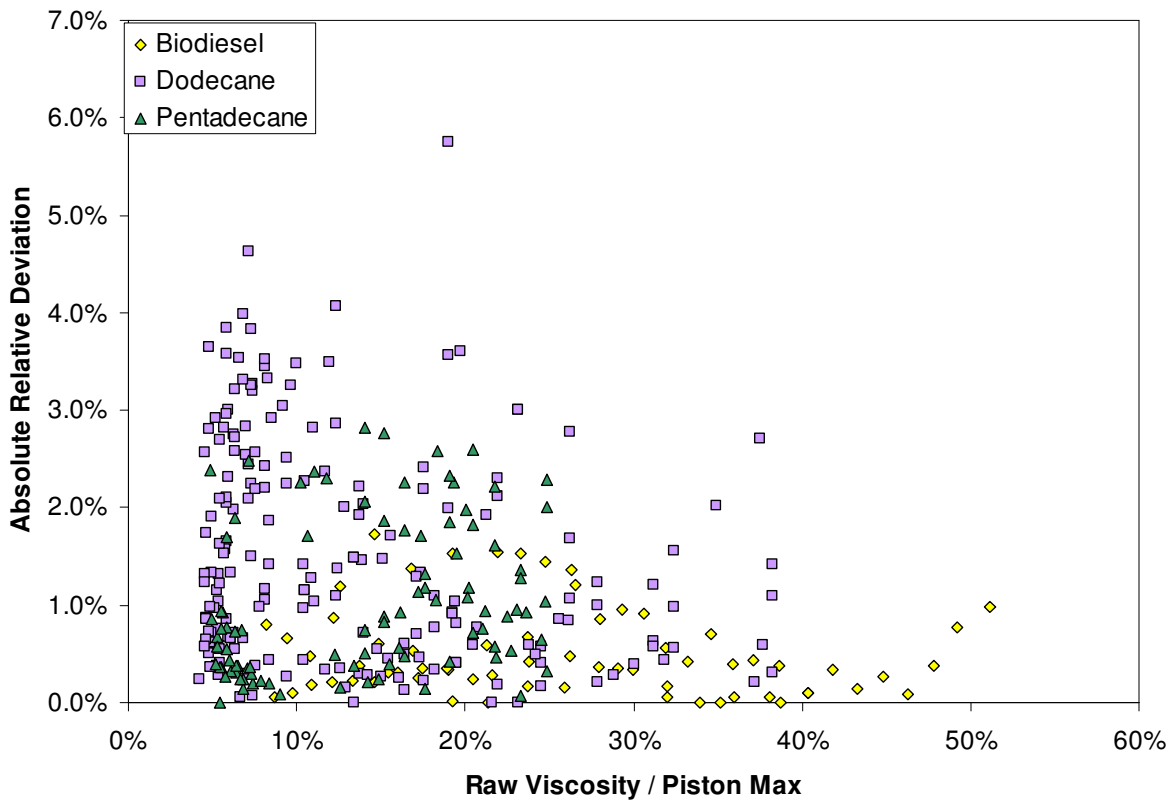


Figure B.8. Absolute relative deviation as a function of percent of piston maximum viscosity by sample type.

The distribution of ARD was very similar across the temperature range tested as seen in Figure B.9.

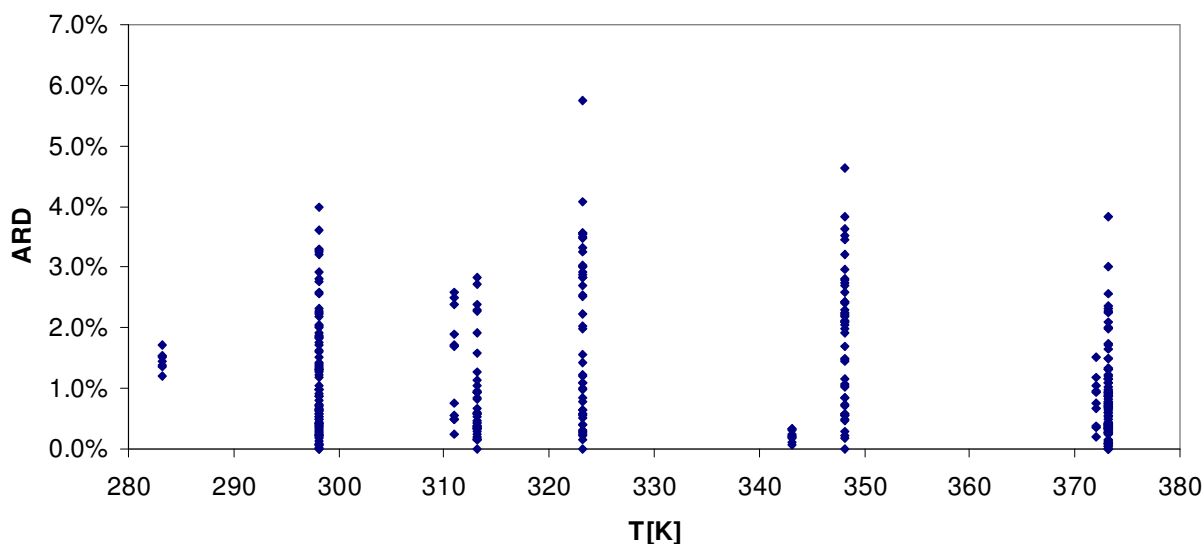


Figure B.9. Absolute relative deviation as a function of temperature for high-pressure measurements.

Separating data into groups of low, medium, and high-temperature measurements yielded AARDs of 1.23, 1.43, and 0.84%, respectively. The differences are associated with the percent of biodiesel data in each group, and are not believed to be related to system bias.

B.2.2 Low-Viscosity Piston in Range of Use

The 0.25-5 cP (5 cP) piston was used for the majority of high-temperature measurements. Specifically, the 5 cP piston was used for the 373.15 K isotherm in all biodiesel-diesel blend studies, and for coconut biodiesel and diesel fuels presented in Chapter 4. The ARD for repeated measurements given in Figures B.10 to B.12 indicate precision that is lower at 100 C (where it was used in this work) than was found overall.

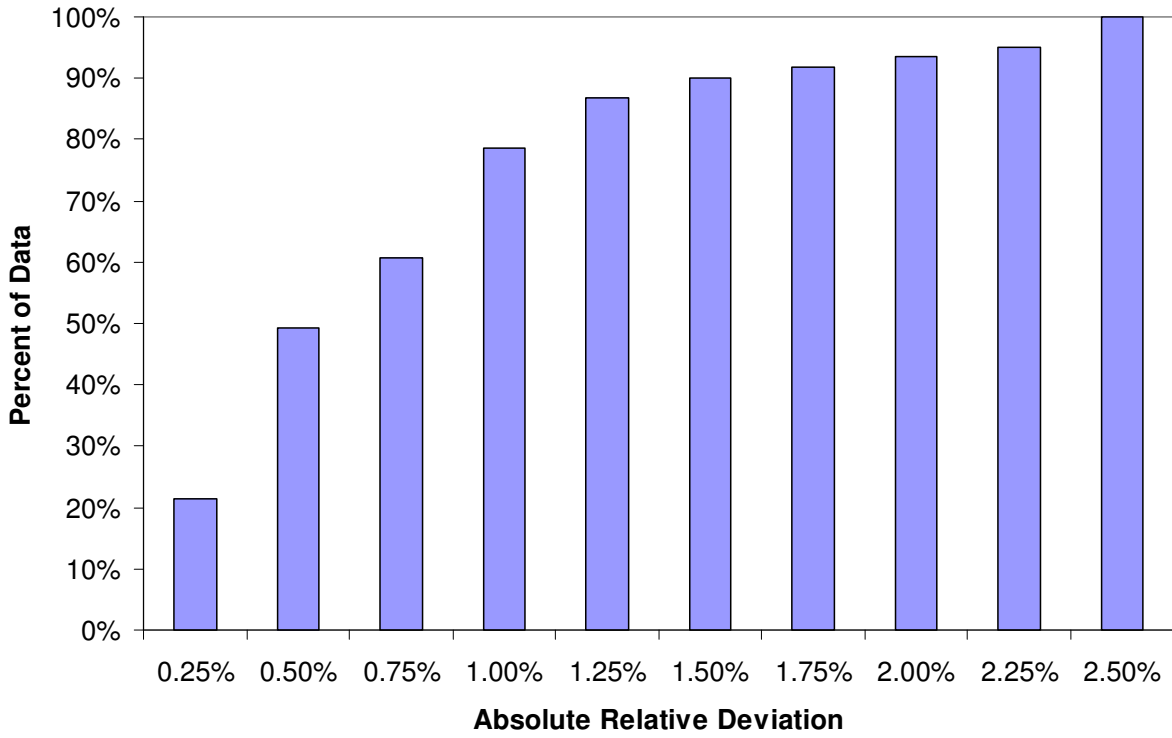


Figure B.10. Histogram of repeated data at higher than ambient pressure for 5 cP piston at 100

C.

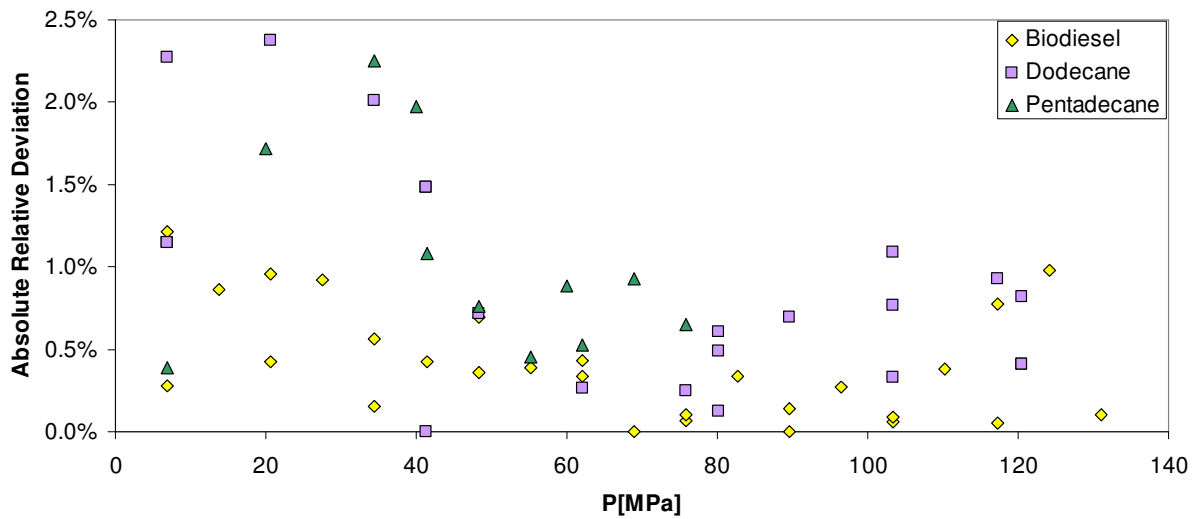


Figure B.11. Absolute relative deviation for the 5 cP piston at 100 C as a function of pressure.

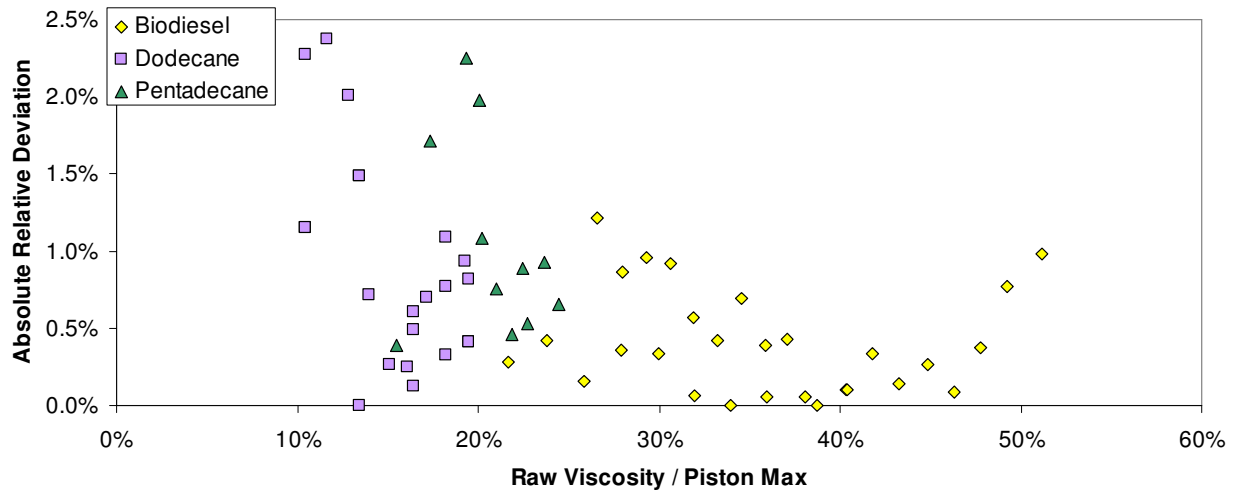


Figure B.12. Absolute relative deviation for the 5 cP piston at 100 C as a function of nominal piston capacity.

B.2.3 Mid-range Viscosity Piston in Range of Use

The 1-20 cP (20 cP) piston's use spanned the largest temperature range of the three pistons—298.15 to 373.15 K. The 20 cP piston was used for all 313.15 and 343.15 K isotherms in the biodiesel-diesel blend studies. The 20 cP piston was also used for several isotherms in the feedstock study; diesel at 298.15 and 313.15 K, coconut at 313.15 K, Vistive and soybean at 313.15 and 373.15 K, and used canola and canola at 373.15 K. The repeatability of the piston shown in Figures B.13 to B.15 was greater on average than for the 5 cP piston, but most of the data was within the 3.3% estimated uncertainty.

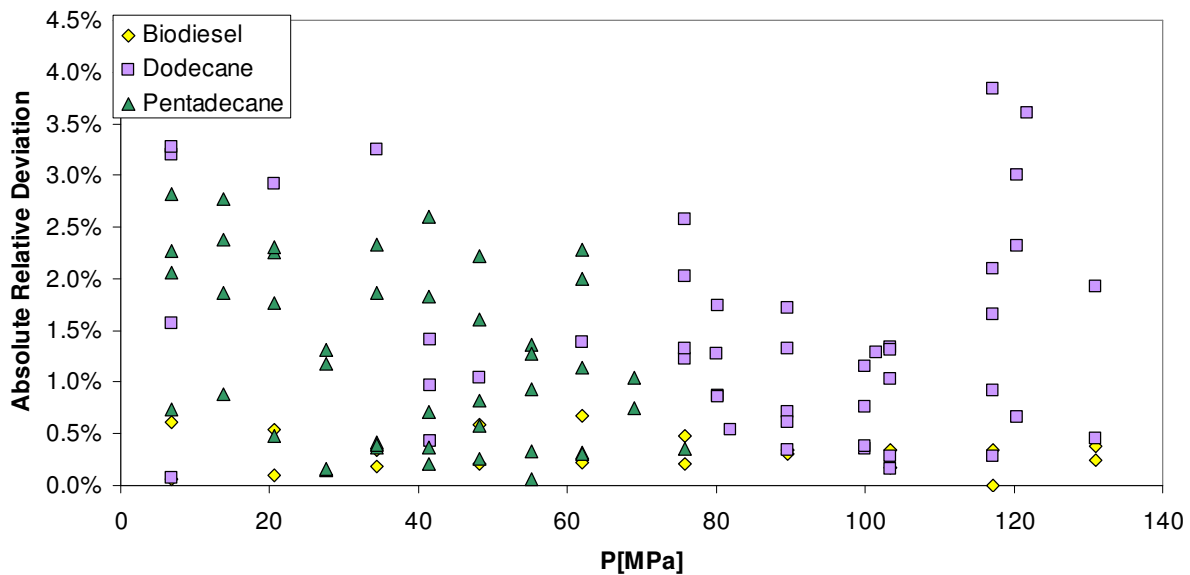


Figure B.13. Absolute relative deviation as a function of pressure for 20 cP piston at 25, 40, 70 and 100 C.

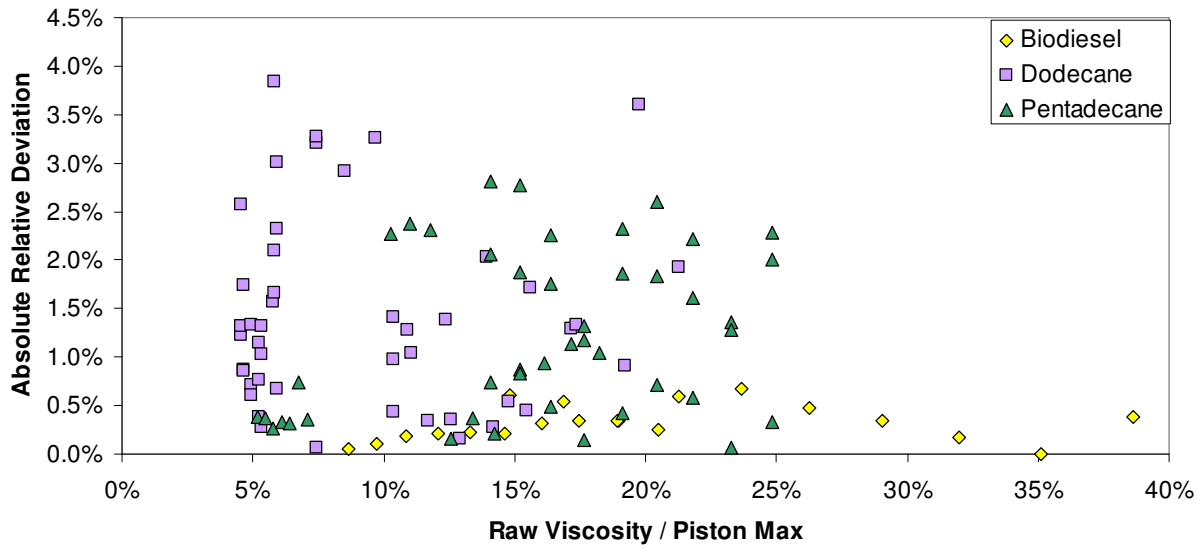


Figure B.14. Absolute relative deviation as a function of percent piston capacity for 20 cP piston and 25, 40, 70 and 100 C.

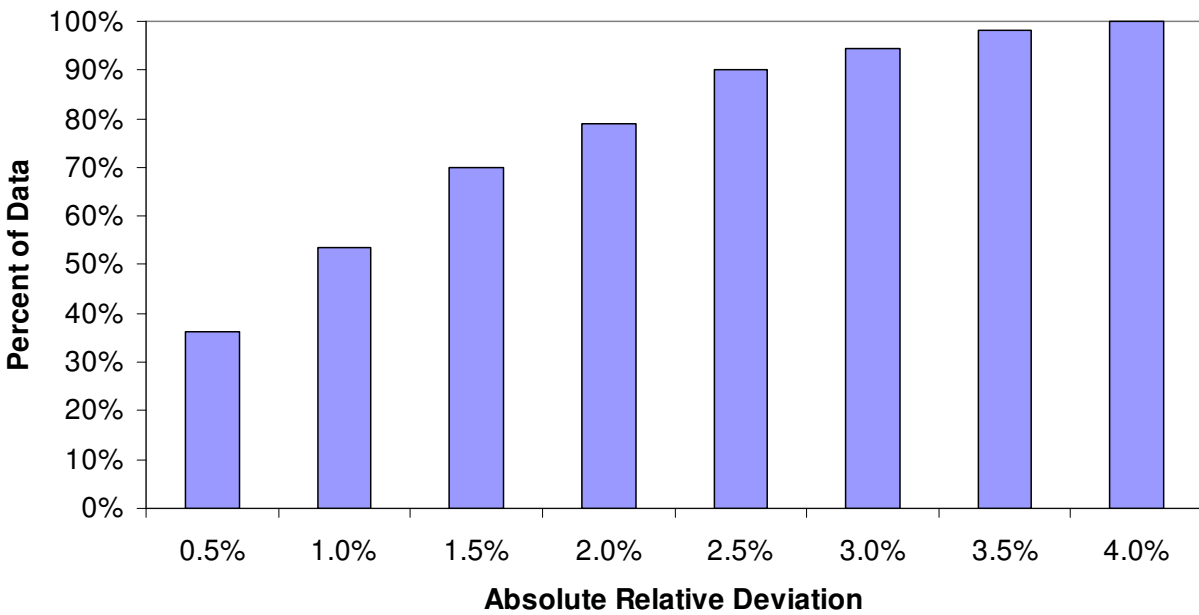


Figure B.15. Histogram of repeated data at higher than ambient pressure for 20 cP piston at 25, 40, 70 and 100 C.

B.2.4 High-Viscosity Piston in Range of Use

The 2.5-50 cP (50 cP) piston was used for all 283.15 and 298.15 K isotherms in the biodiesel-diesel blend studies. In the feedstock study, the 50 cP piston was used for diesel at 283.15 K, coconut, Vistive, and soybean at 283.15 and 298.15 K, and used canola and canola at 283.15, 298.15, and 313.15 K. Therefore, this section contains repeated data at 283.15, 298.15, and 313.15 K. The repeatability of this piston shown in Figures B.16 to B.18 was comparable to the 20 cP piston, and the majority of data within the 3.3% estimated uncertainty.

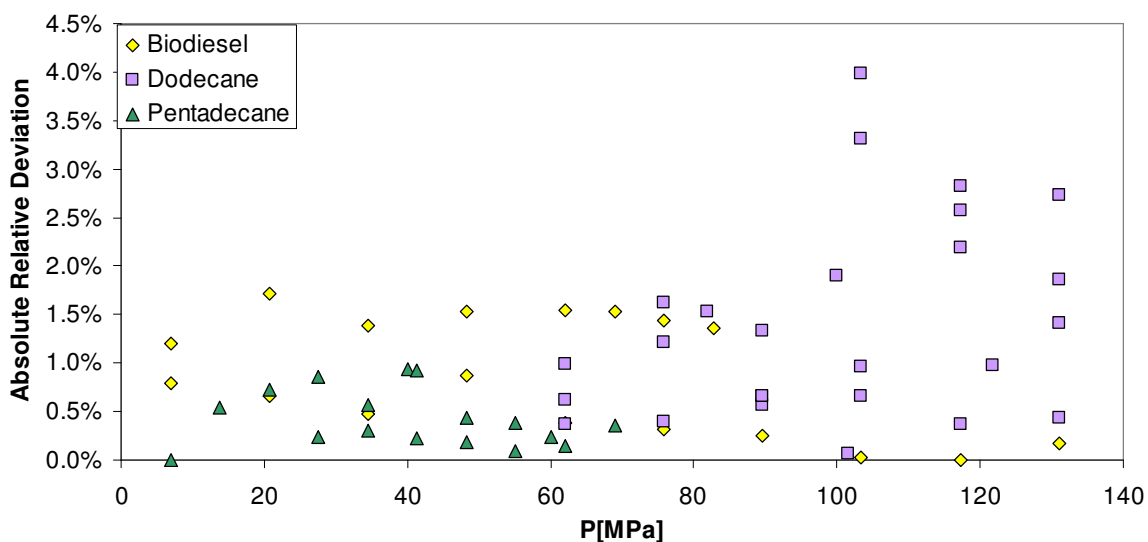


Figure B.16. Absolute relative deviation as a function of pressure for the 50 cP piston at 10, 25 and 40 C isotherms.

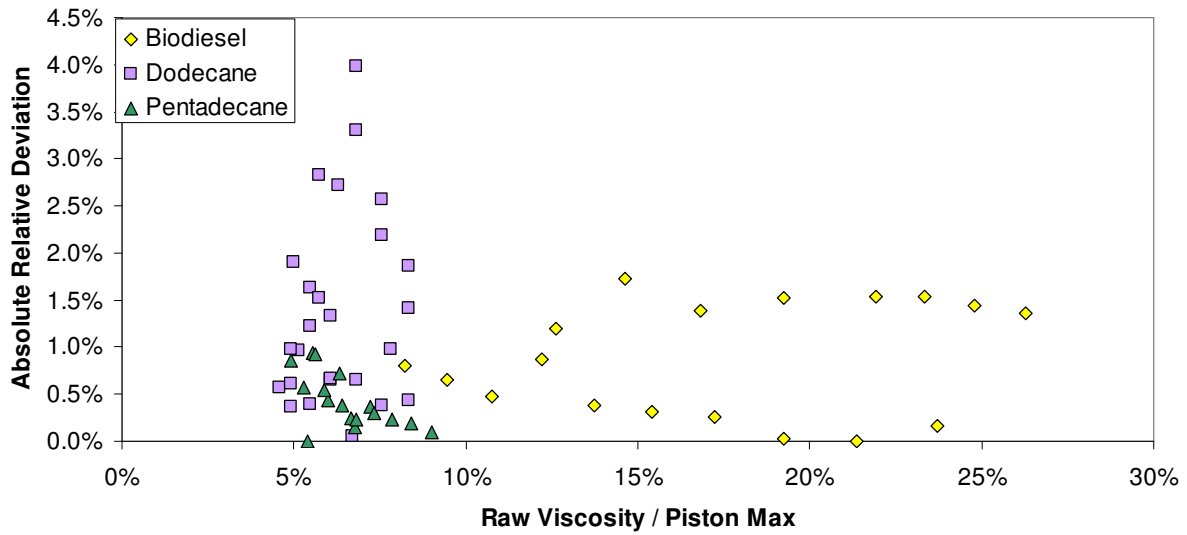


Figure B.17. Absolute relative deviation as a function of percent piston capacity for 50 cP piston at 10, 25, and 40 C.

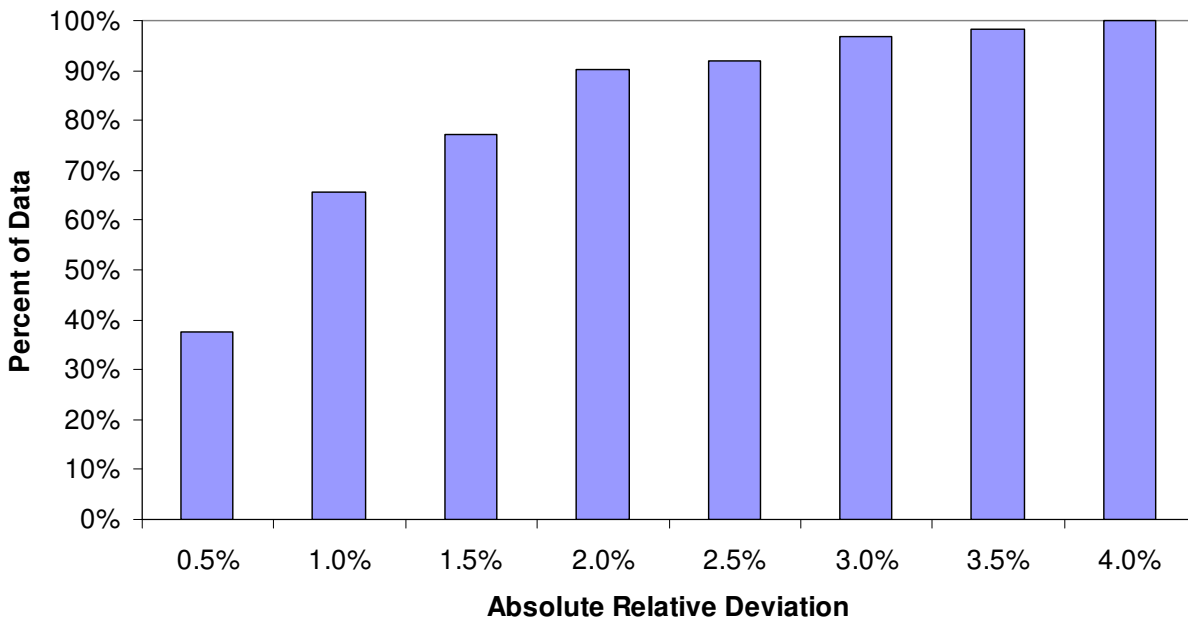


Figure B.18. Histogram of repeated data at higher than ambient pressure for 50 cP piston at 10, 25 and 40 C.

B.3 Viscometer Repeatability at Ambient Pressure

The repeatability of viscosity measurements at ambient pressure was greater than for those at elevated pressures. The AARD for repeatability was 2.2% for 27 repeated data points, with 25 of the 27 data points having an ARD of 4% or less. A distribution is given in Figure B.19 below.

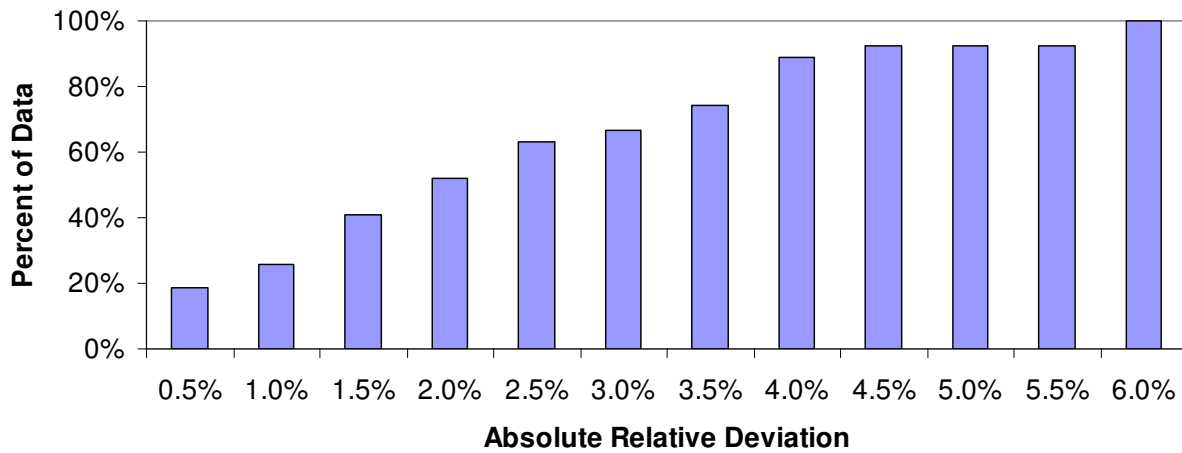


Figure B.19. Histogram for ambient pressure viscosity measurements absolute relative deviations.

Percent of piston capacity and temperature were not strongly correlated with ARD as seen in Figure B.20 and Figure B.21.

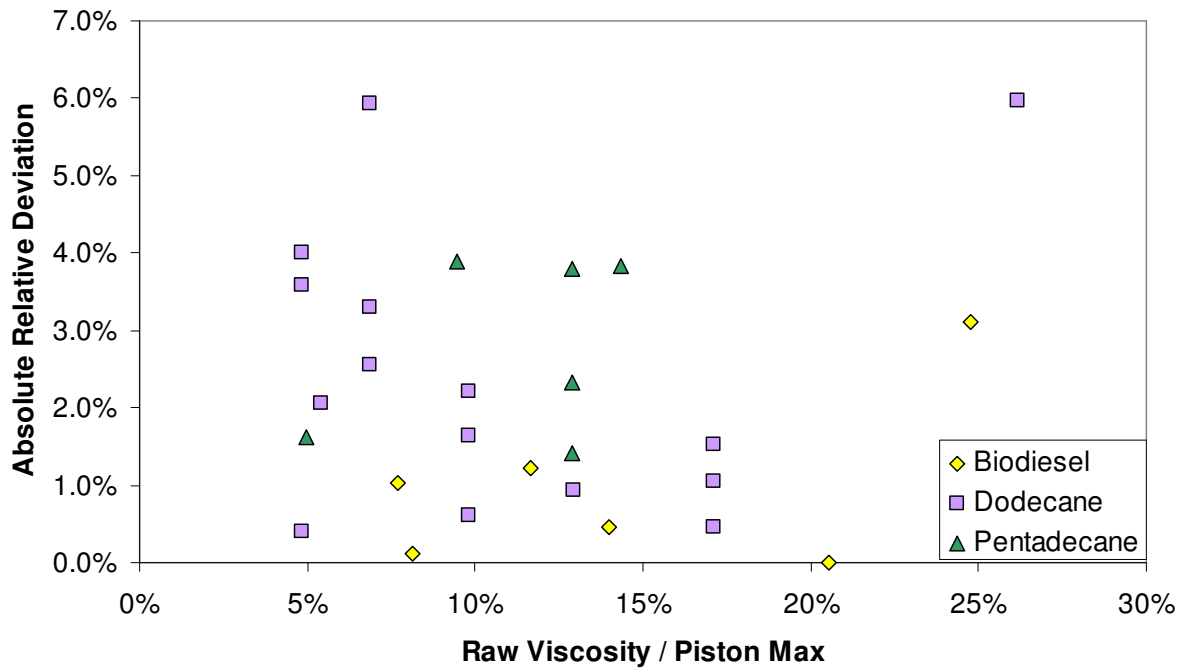


Figure B.20. Absolute relative deviation as a function of percent maximum piston capacity for ambient pressure viscosity measurements.

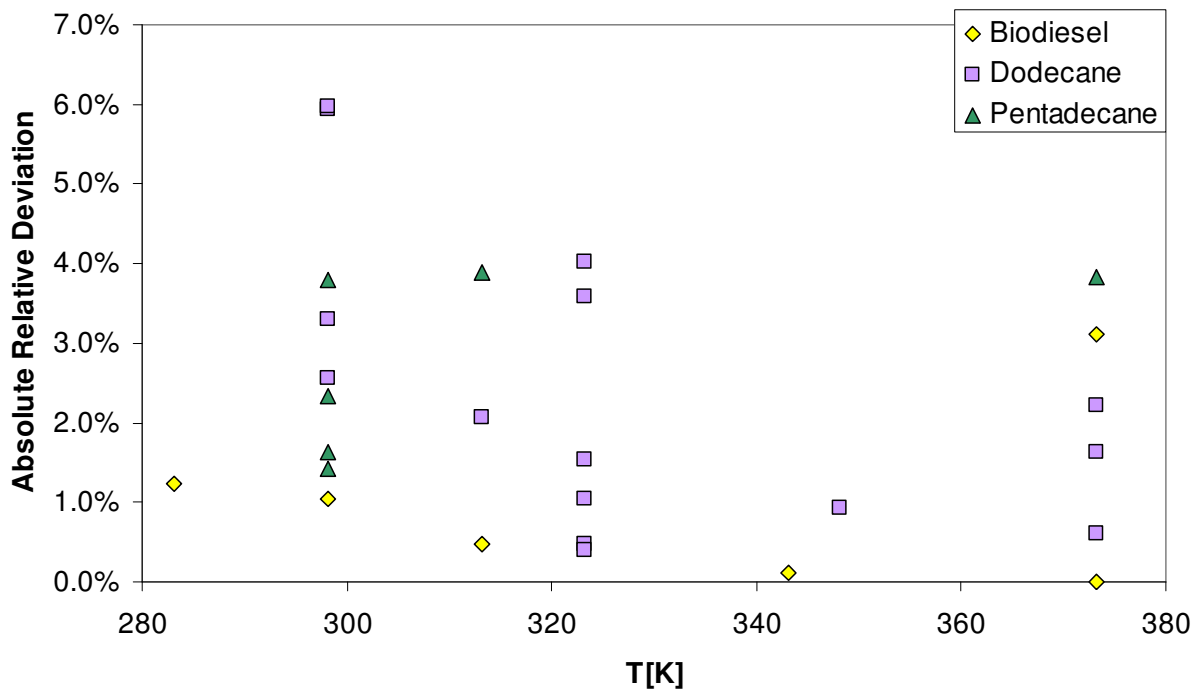


Figure B.21. Absolute relative deviation as a function of temperature for ambient pressure viscosity measurements.

After comparing the many permutations of data that may cause a lowering or an increase in the perceived repeatability it was determined that adjustments to the uncertainty based on piston type, temperature, or pressure are not justified or necessary. Using alternate equipment to verify ambient viscosity measurements is recommended based on the higher ambient viscosity repeatability. A conservative estimate would be to use the uncertainty for the entire data set, 3.3%, for high pressure.

B.4 Viscosity Correction Due to Elevated Temperature and Pressure

The calibration standard S6 was used for all three pistons for ambient-pressure calibrations between 293.15 and 373.15 K. Dodecane was a suitable choice for all three pistons at high pressure as its viscosity from 298.15 to 373.15 K spanned all three piston ranges used in the biodiesel and biodiesel-diesel blends studies. High-pressure viscosity of dodecane as measured by Caudwell et al.¹ is used as a calibration standard in numerous works and it includes an extensive evaluation of data sets from literature. The Caudwell et al. work was included by researchers at NIST² in the development of their dodecane viscosity correlation. At regions of low pressure and high temperature for which dodecane's viscosity is too low for the specified piston viscosity range, pentadecane was used.

The annular spacing of the viscometer varies with the temperature and pressure of the system. Increasing temperature or pressure causes the inner chamber diameter to expand. When the

temperature or pressure increases beyond ambient conditions, a correction is required. The pressure correction factor is 1.0 at ambient pressure and has a maximum of 1.46 at 131 MPa for the 5 cP piston. The manufacturer supplied pressure and temperature compensation equations for each piston. Temperature and pressure compensation factor equations used a combination of expansion correlations for the viscometer chamber and experimental data relative to reported literature values for more accurate data reporting. These data were collected from both company personnel and viscometer users. High-purity alkanes and viscosity standards were used to verify and enhance the accuracy of the corrections.

B.4.1 Temperature Correction at Ambient Pressure

A parameter called the cdl (described in Chapter 3) was changed for all pistons after the initial feedstock study. The cdl can be altered using a computer interface in order to adjust the displayed viscosity. This is done to calibrate a piston without necessarily using a temperature correction. The temperature correction factor, T_{Corr} , was expected to be linear with temperature where the correction factor is given by:

$$T_{\text{Corr}} = \text{Literature Viscosity} / \text{Raw Viscosity} \quad \text{Eqn. [1]}$$

It was observed that regardless of the cdl selected, the temperature correction was linear as a function of temperature. Each linear correction factor equation's slope was nearly identical to those of other cdl values for the same piston using the S6 calibration fluid for which this was tested.

A temperature correction was found to be approximately linear for calibration fluid S6 and pentadecane through the temperature range tested, although this range varied based on piston

type as shown in Figures B.22 to B.27. See Figure B.22 to Figure B.27 for ambient temperature correction equations and residuals for these corrections, and a summary of all slopes and intercepts used to correct for temperature in Table B.1.

The ambient viscosity of dodecane from Caudwell et al. was similar to those found in other works^{3, 4}. The temperature compensation slope for dodecane was found to increase between 25 and 40 C, but decrease between approximately 40 or 50 and 100 C for the two pistons tested, 5 and 20 cP. These results are similar to the manufacturer's findings of a divergence in temperature correction.

Due to the non-linear behavior of the dodecane, calibration standard S6 and pentadecane were the only fluids used in determining the temperature correction equation at ambient pressure. The calibration standard and pentadecane are more similar in terms of viscosity range to the biodiesel, diesel, and biodiesel blends studied in this work, and gave similar correction equations to each other. It is not clear what might account for the difference in dodecane's more bell-shaped temperature correction factor. Possible non-newtonian behavior at high-shear rates was considered. The maximum shear rate for any piston used is less than 50,000 s⁻¹—well below that which might affect a Newtonian fluid like dodecane⁵. Also considered was the possibility that a narrowing of the distance between the piston and chamber wall might create a distance that gives viscosity characteristics seen when fluids are restricted to only a few molecular layers. Under these conditions the viscosity can be greater than in the bulk until substantial shear rates are reached⁵, which would require a lower compensation factor. In one study with dodecane between alumina, bulk viscosities were observed at distances greater than

5 nm;⁶ the calculated distance between the piston and viscometer chamber should be on the order of 10s of microns, most likely eliminating this phenomenon as the cause. The viscosity of unfamiliar samples should be verified with high-accuracy ambient-pressure measurement to ensure a valid temperature correction factor is used.

Table B.1. Recommended temperature correction factors as a function of temperature in Celsius for particular calibration values for 5, 20, and 50 cP piston.

Piston cP	cdl #	Fluids Used for Calibration Name	Linear Constants, $T_{comp}=m \cdot T[C]+b$		AARD %	Max. Deviation %
			$m \cdot 10^4$	b		
5	466	nC15, S6	7.876	1.01840	1.0	2.0
	464	S6	8.000	1.00857	0.6	1.0
	466	S6	8.000	1.01783	0.6	1.0
	468	S6	8.140	1.02642	0.5	0.9
	470	S6	8.220	1.03492	0.4	0.8
20	476	nC15, S6	7.640	0.97466	1.5	4.6
	476	S6	6.151	0.97457	0.1	0.1
	478	S6	5.924	0.98493	0.6	0.9
	480	S6	6.062	0.99288	0.0	0.0
	484	S6	6.116	1.01071	0.1	0.2
50	470	nC15, S6	1.165	1.01630	0.4	1.1
	462	S6	0.870	0.97631	0.5	1.1
	466	S6	1.476	0.99466	0.4	0.7
	470	S6	1.970	1.01230	0.2	0.4
	472	S6	1.500	1.02462	0.0	0.1
	473	S6	0.640	1.03041	0.4	0.8

5 cP Piston Ambient Correction Equation

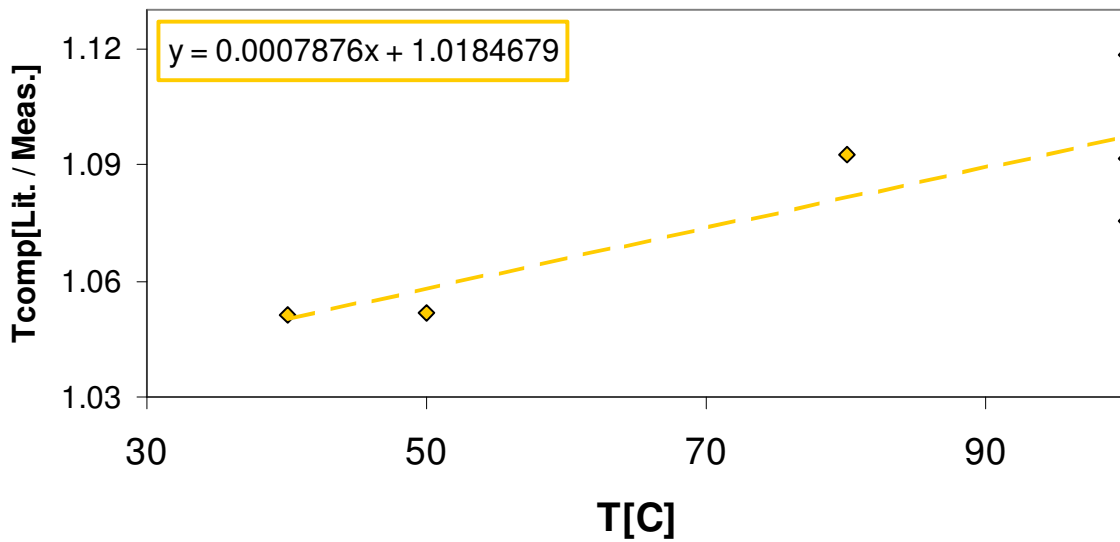


Figure B.22. Ambient-pressure temperature correction factor as a function of temperature for 5 cP piston using S6 and pentadecane as calibration fluids.

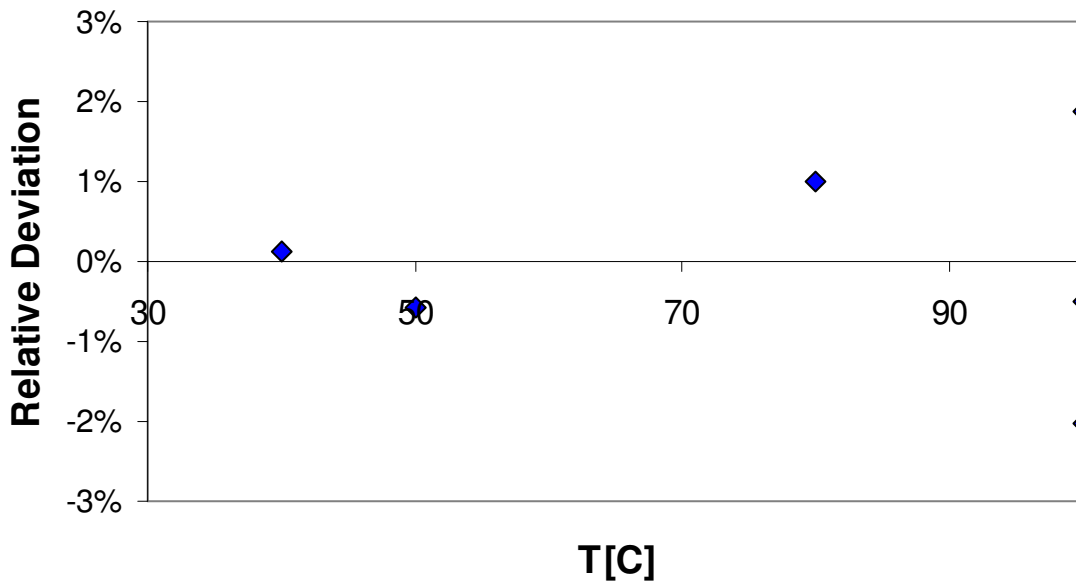


Figure B.23. Ambient-pressure temperature correction factor deviations as a function of temperature for 20 cP piston using S6 and pentadecane as calibration fluids.

20 cP Piston Ambient Correction Equation

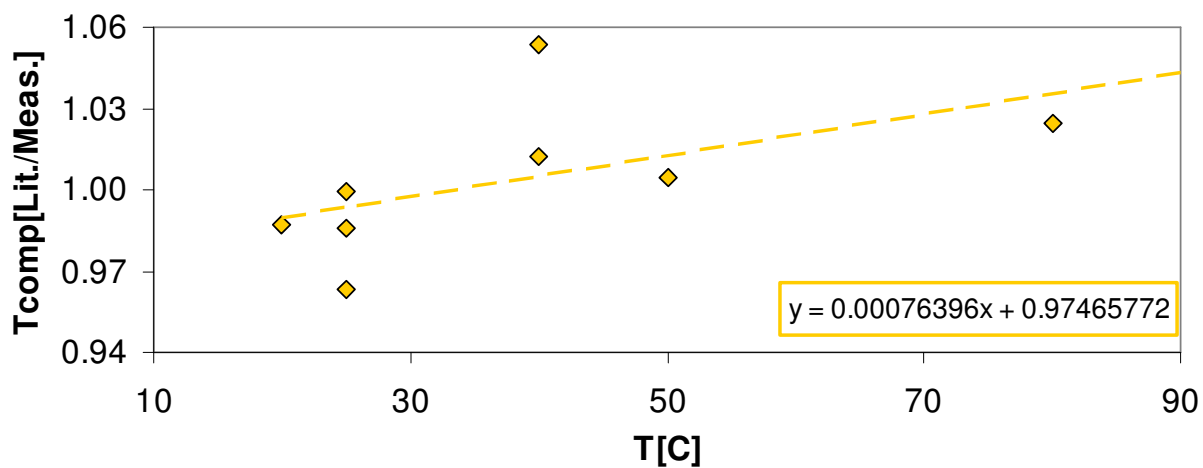


Figure B.24. Ambient-pressure temperature correction factor as a function of temperature for 20 cP piston using S6 and pentadecane as calibration fluids.

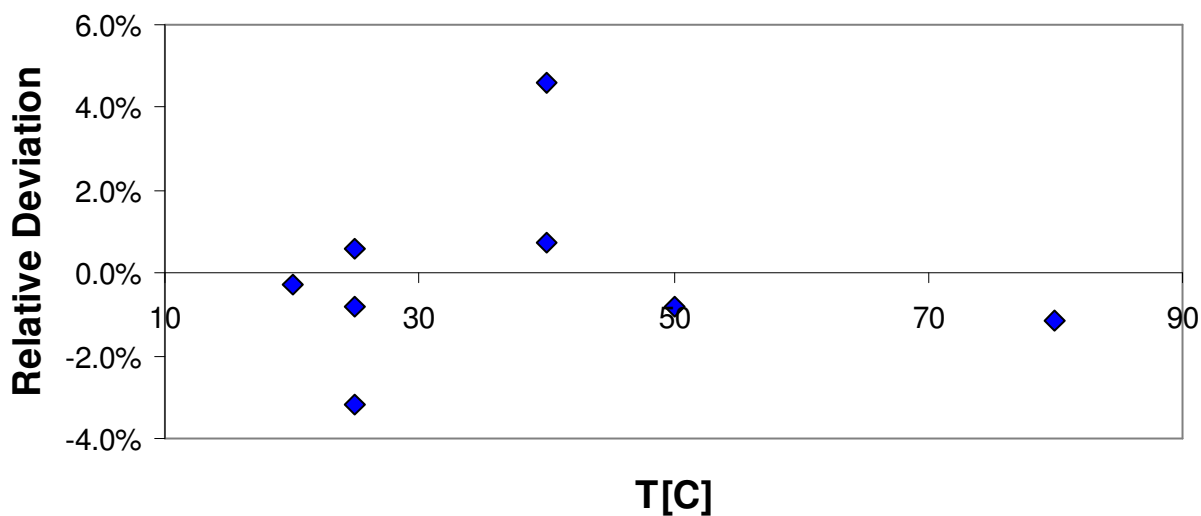


Figure B.25. Ambient-pressure temperature correction factor deviations as a function of temperature for 20 cP piston using S6 and pentadecane as calibration fluids.

50 cP Piston Ambient Correction Equation

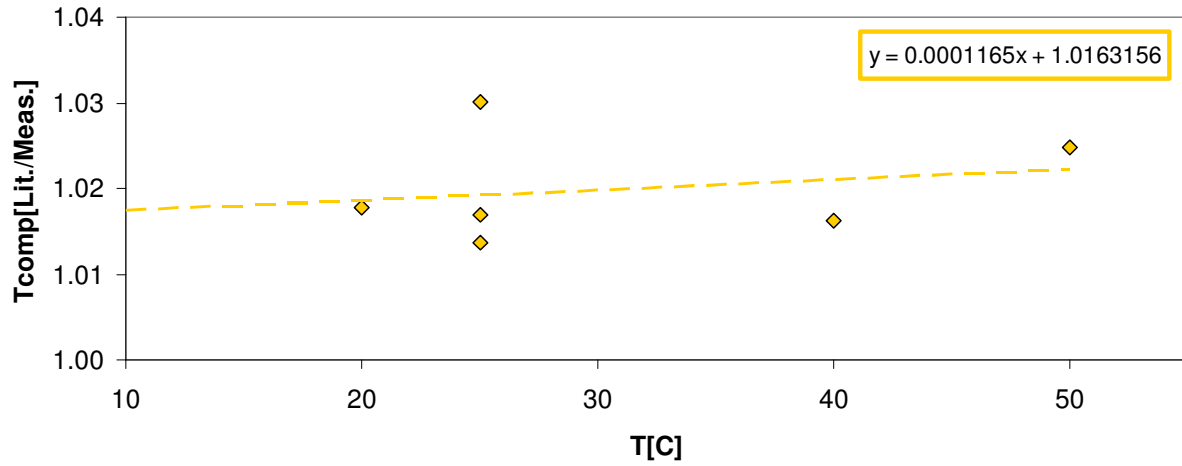


Figure B.26. Ambient-pressure, temperature correction factor as a function of temperature for 50 cP piston using S6 and pentadecane as calibration fluids.

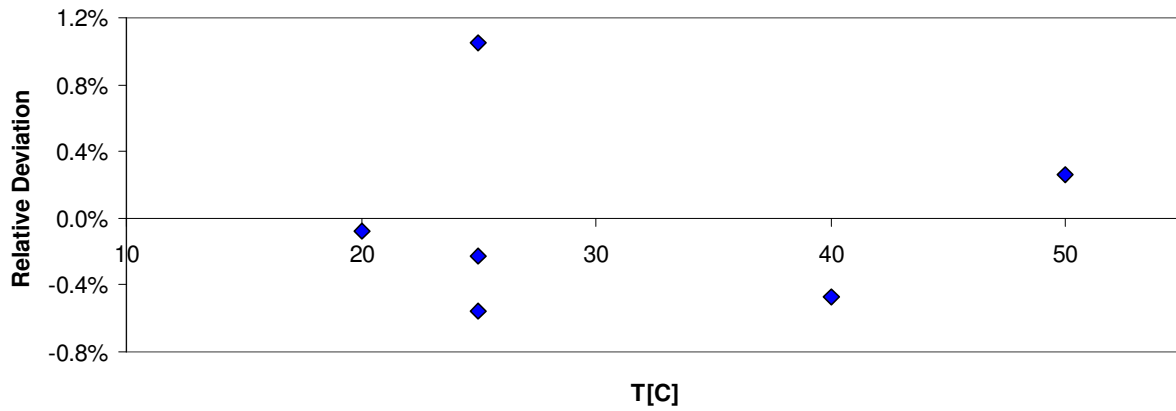


Figure B.27. Ambient-pressure, temperature correction factor deviations as a function of temperature for 50 cP piston using S6 and pentadecane as calibration fluids.

B.4.2 Viscosity Corrections due to Pressure and Temperature

As stated in the previous section, the slope of dodecane is in contrast to the slopes of higher viscosity calibration fluids for the ambient-pressure temperature correction. Instead of using the ambient-pressure linear correction for temperature just developed, ambient-pressure viscosity measurements were performed in duplicates or triplicates for each isotherm so that the average could be “zeroed” to literature values at ambient pressure. To clarify, “zeroed” simply means that the temperature correction factor is adjusted to give a 0.0% relative deviation at ambient pressure. The pressure correction was calculated at each temperature and pressure by:

$$P_{corr} = \text{Literature Viscosity}[T,P] / (\text{Raw Viscosity}[T,P] * T_{corr}) \quad \text{Eqn. [2]}$$

The pressure correction can then be calculated as a function of pressure. It was discovered that for the 5 cP piston the pressure correction values were dependent on temperature as well as pressure as seen in Figure B.28. The increase in pressure compensation factor required at a specific temperature was also seen by the manufacturer.

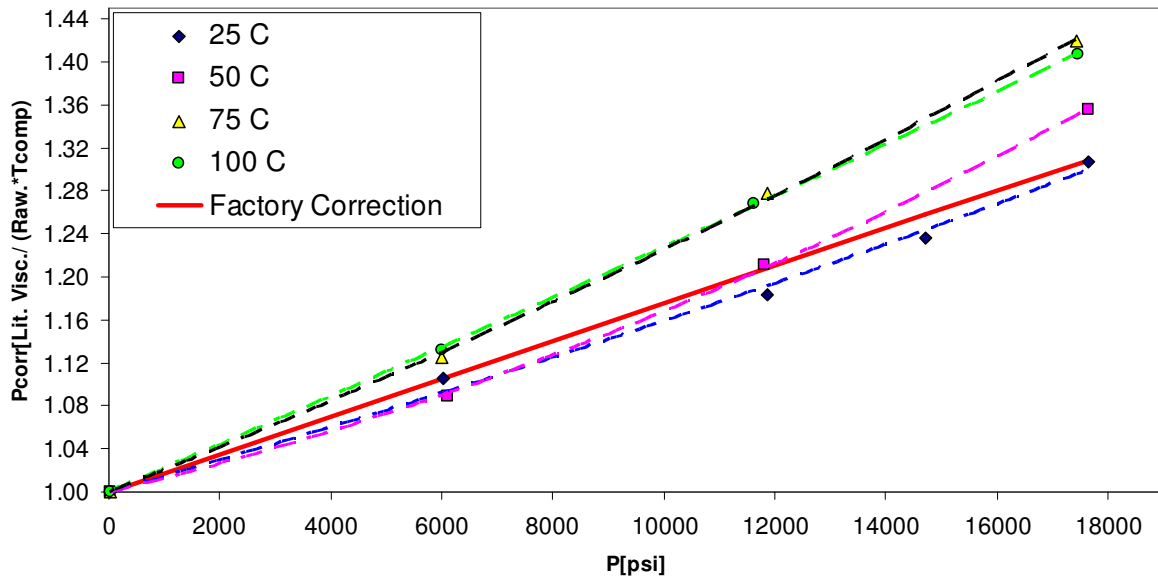


Figure B.28. Pressure correction, P_{corr} as a function of pressure in psi for dodecane compared to Caudwell et al. data. The dashed lines are second order equations with a y intercept of 1.

The literature data to which the 5 cP piston is calibrated contained three general pressure ranges, 6000-6120, 11600-11900, and 17400-17650 psi for each isotherm. The pressure correction as a function of temperature was found to be approximately linear at each pressure range as seen in Figure B.29.

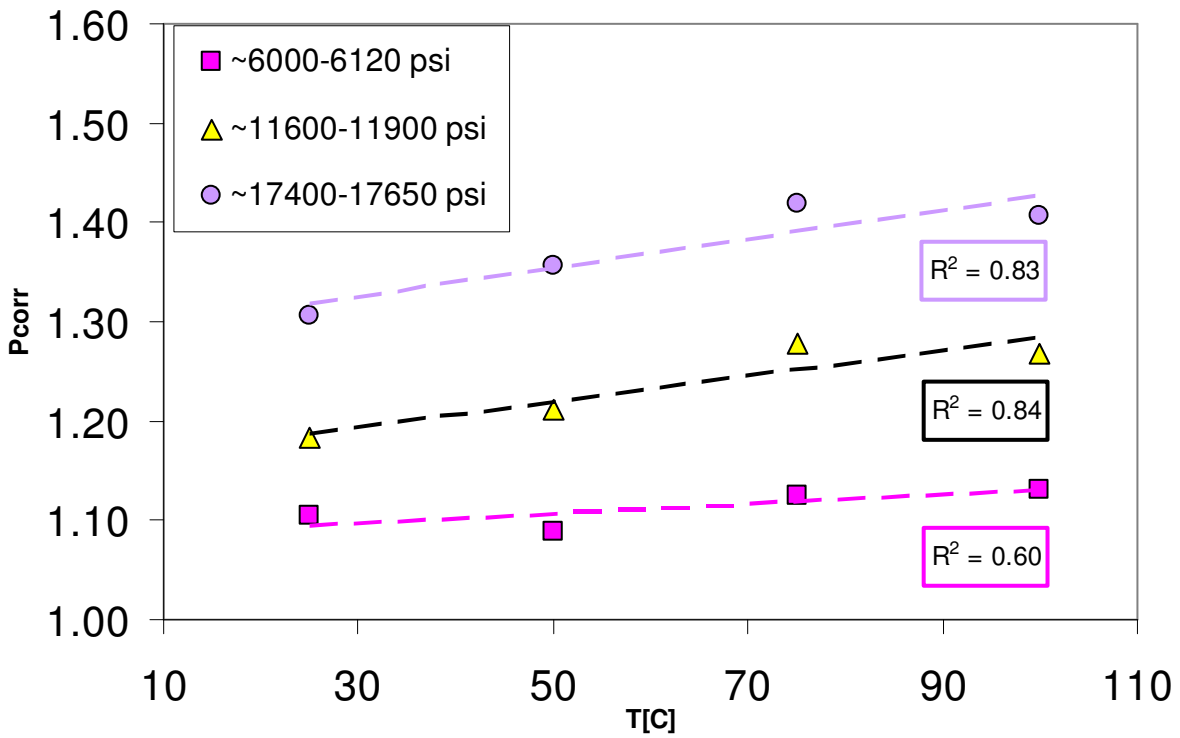


Figure B.29. Pressure correction required as a function of temperature at constant pressure for dodecane using the 5 cP piston when compared to literature.

The rate at which the pressure correction, as a function of temperature, changes with increasing pressure was found to be approximately linear as shown in Figure B.30.

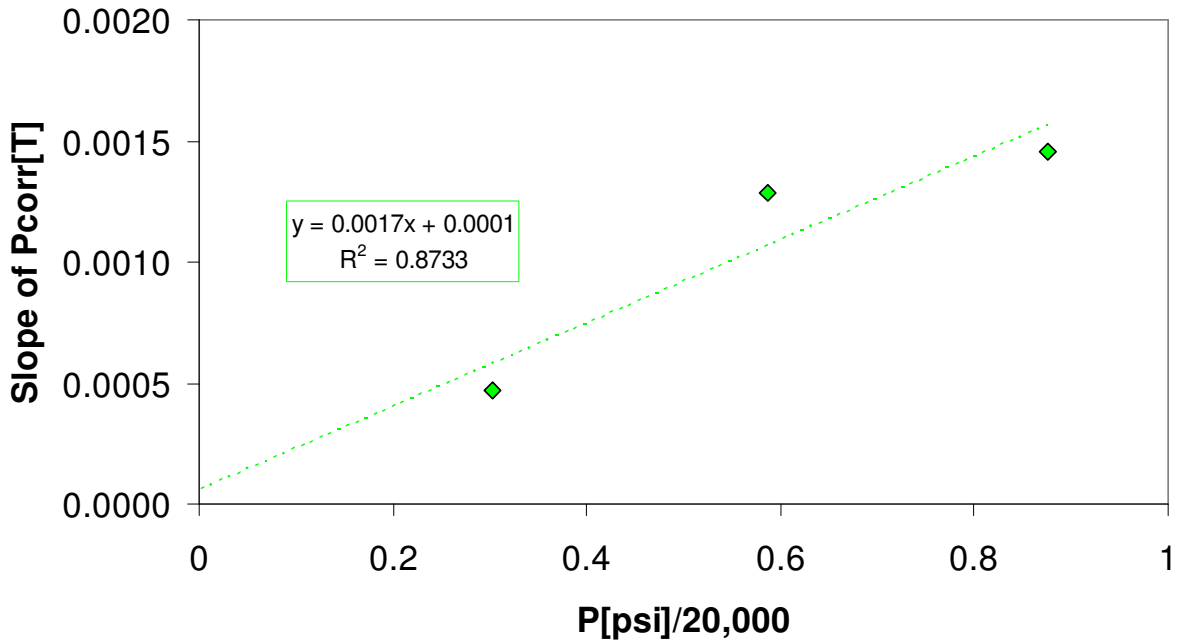


Figure B.30. Slope of the pressure correction (a function of temperature), as a function of pressure in psi divided by 20,000 psi.

The relationship between temperature, pressure and correction factor in the figures above provide the justification for the overall correction of the form described in Eqn. 3.

$$\eta_{corrected} = \eta_{raw} \cdot T_{corr}[C] \cdot P_{corr,P} [psi] \cdot P_{corr,T,P} [C,psi] \quad Eqn. [3]$$

η_{raw} is the measured viscosity without adjustment for annulus expansion, $T_{corr}[C]$ is a linear equation that accounts for annulus expansion at low pressures as derived in the previous section, $P_{corr,P} [psi]$ is a second order expression that compensates for pressure's effect on the annulus expansion at a particular pressure,

$$P_{corr,P} [psi] = 1 + X1 \cdot (P[psi]/20,000) + X2 \cdot (P[psi]/20,000)^2 \quad Eqn.[4]$$

where X1 and X2 are regressed parameters, and $P_{corr,T,P}[C,psi]$ is a first ordered expression that compensates for the combined temperature and pressure effect at higher pressure demonstrated in Figure B.29 and Figure B.30:

$$P_{corr,T,P} [C,psi]=M \cdot (P[psi] / 20,000) \cdot T[C]+1 \quad Eqn.[5]$$

Where M is a regressed parameter.

In order to provide a range of options for future users, parameters have been regressed for multiple forms of the correction equation and for various temperature ranges for each piston, given in Table B.2, Table B.3 and Table B.4. Gauss-Newton non-linear regression was used to calculate parameters X1, X2, and M. Line 5 on Table B.2 was used for all high-pressure biodiesel and diesel data for the 5 cP piston. Line 1 for 343.15 and 373.15 K, and Line 10 for 298.15 and 313.15 K were used for the 20 cP piston. Line 4 was used for all isotherms of the 50 cP piston.

Table B.2. Regressed parameters for 5 cP piston.

5 cP Piston				
Line #	T [C]	Regressed Parameters		
		X1	X2	M
1	100	0.44104	0.02892	0
2	75	0.41056	0.08210	0
3	50	0.25040	0.17313	0
4	25	0.26200	0.09254	0
5	100&75	0.421966	0.062429	0
6	75&50	0.306485	0.135913	0
7	50&25	0.249709	0.121897	0
8A	100-25	0.216211	0.083702	0.001756
8B	100-25	0.259018	0.064443	0.001428
8C	100-50	0.222876	0.088964	0.001632
Cambridge	All	0.35	0	0

Table B.3. Regressed parameters for the 20 cP piston.

20 cP Piston				
Line	T	Regressed Parameters		
#	[C]	X1	X2	M
1	70	0.15725	0.08064	0
2	50	0.28640	-0.07531	0
3	40	0.04101	0.18399	0
4	25	0.11709	0.05712	0
5	50&40	0.122036	0.102334	0
6	40&25	0.122612	0.052244	0
7	50&25	0.14842	0.033775	0
8	50,40,25	0.137804	0.046415	0
9	50,40,25	0.07163	0.05260	0.00179
10	50,25	0.09036	0.01670	0.00220
11	40,25	0.10272	0.05967	0.00046
12	70,50,25	0.11365	0.02833	0.00117
13	100,70,50,25	0.10111	0.03828	0.00122
Cambridge	All	0.23	0	0

Table B.4. Regressed parameters for 50 cP piston.

50 cP Piston				
Line	T	Regressed Parameters		
#	[C]	X1	X2	M
1	25	0.14456	-0.00924	--
2	40	0.21020	-0.06663	--
3	25 & 40	0.17377	-0.03556	--
4	40&25	0.13926	-0.03641	0.001096
Cambridge	All	0.13123	0	0

Temperature and pressure corrections for additional pistons may be developed in a similar fashion with well known fluids, for example, the 0.2-2 cP piston could be calibrated using dodecane in the upper temperature range, and normal hexane in the lower temperature range. While the 3 parameter regressed correction works well for the 5 cP piston data set, all of the biodiesel and biodiesel blend data set for which the 5 cP piston is used are for higher temperatures—373.15 K. The 2 parameter correction for 70 & 100 gives a lower absolute

relative deviation for dodecane when compared to literature at these higher temperatures at the highest pressure tested.

B.4.3 High Pressure Viscosity Calibration and Literature Comparison

As stated previously, data were regressed to high pressure viscosity measurements of dodecane from Caudwell et al¹. to improve pressure correction parameters supplied by the viscometer manufacturer for our apparatus's specific arrangement. The 5 cP piston covers the entirety of the dodecane set, up to our apparatus's maximum pressure. The literature data ranges from 0.503 mPa·s at 373.15 K and ambient pressure to 4.497 mPa·s at 298.15 K and 121 MPa. After developing 2 and 3 parameter pressure corrections, high-pressure pentadecane data were used to verify their validity.

Data from Ducoulombier et al⁷. is included in the dodecane evaluation to show the similarities between the Caudwell et al. data and to give an idea of the integrity of their instrument for the pentadecane for further literature comparison. Pentadecane data from Hogenboom et al⁸. is also compared to data generated using all three pistons. Parameters were developed for the 20 and 50 cP pistons by fitting isotherms to literature data or to piston data that has already been regressed to literature data. There is uncertainty associated with the ambient-pressure correction, even for data used for the correlation. To find the least amount of error among pistons, the ambient pressure measurements were averaged and then a temperature correction was calculated that would make the difference between literature and experimental data 0.0%. This temperature correction was used for the entirety of the isotherm. For dodecane experiments at high temperatures this is especially important due to the decreasing

temperature correction above 313.15 K discussed earlier. Due to the expansive nature of the 20 cP data set, which ranged from 298.15 to 373.15 K, two correction equations were used. One equation for data between 298.15 and 313.15 K, and one equation for data between and including 343.15 and 373.15 K. The overall results for dodecane and pentadecane at elevated temperature and pressure are shown Figures B.31 to B.35 for dodecane and Figures B.36 to B.39 for pentadecane with results summarized in Table B.5. The 50 cP piston uses the temperature correction linear equation for both dodecane and pentadecane data sets. The 5 cP and 20 cP pistons use the temperature correction linear equation for pentadecane data and are ‘zeroed’ for the dodecane data.

Table B.5. High-pressure viscosity comparison to literature values.

Piston	Dodecane				Pentadecane			
	Caudwell et al.		Ducoulombier et al.		Hogenboom et al.		Ducoulombier et al.	
	AARD	Max ARD	AARD	Max	AARD	Max	AARD	Max
5	0.8%	1.8%	1.2%	1.2%	0.4%	0.7%	1.0%	2.1%
20	0.9%	2.5%	1.9%	2.4%	1.4%	2.0%	2.6%	2.6%
50	0.6%	1.0%	1.1%	1.1%	2.2%	2.2%	1.8%	2.1%
	No ambient deviations included in calculations				Ambient deviations included in calculations			

B.4.3.1 Dodecane Viscosity Comparison to Literature

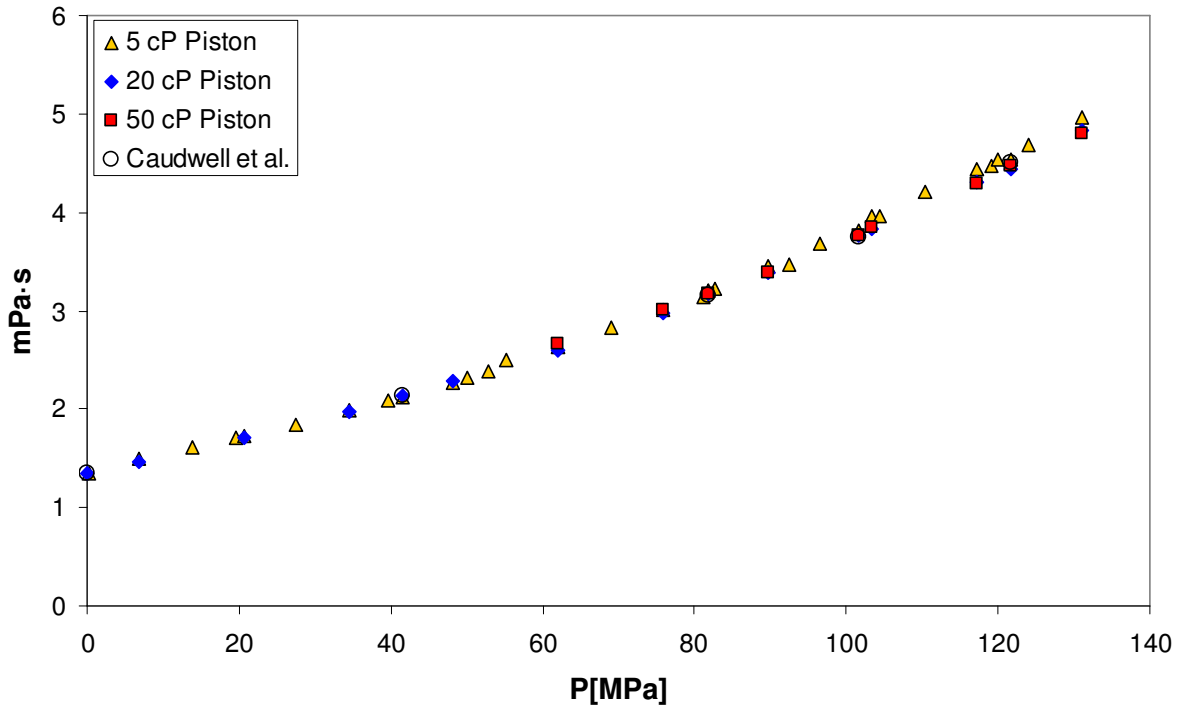


Figure B.31. High-pressure viscosity of dodecane at 298.15 K.

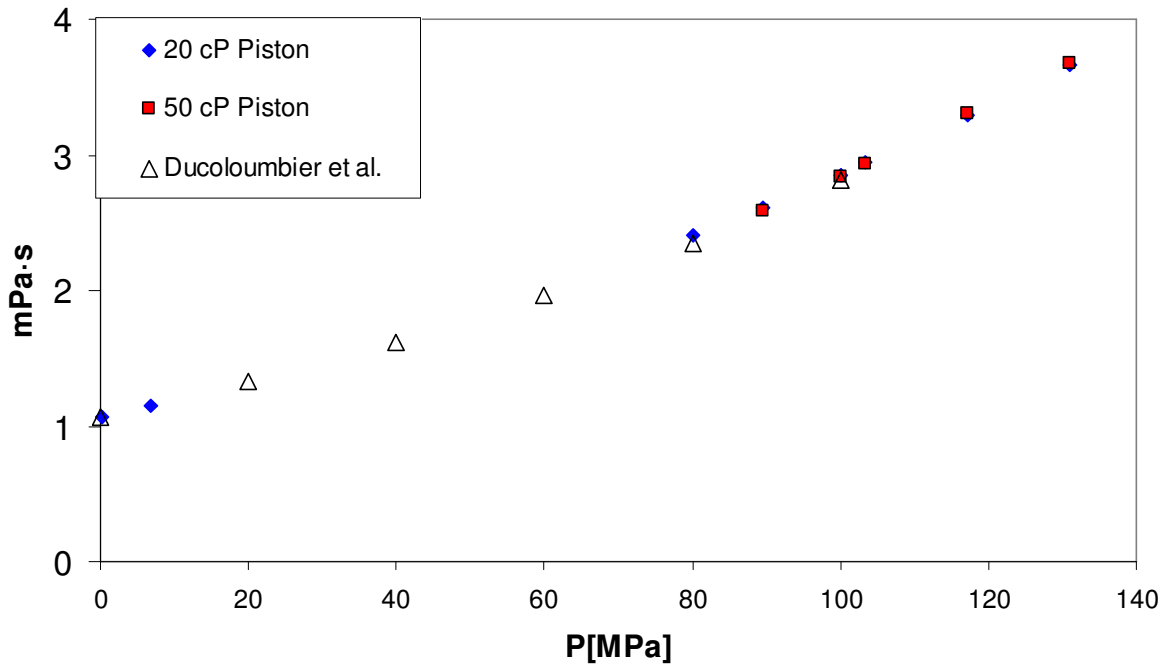


Figure B.32. High-pressure viscosity of dodecane at 313.15 K.

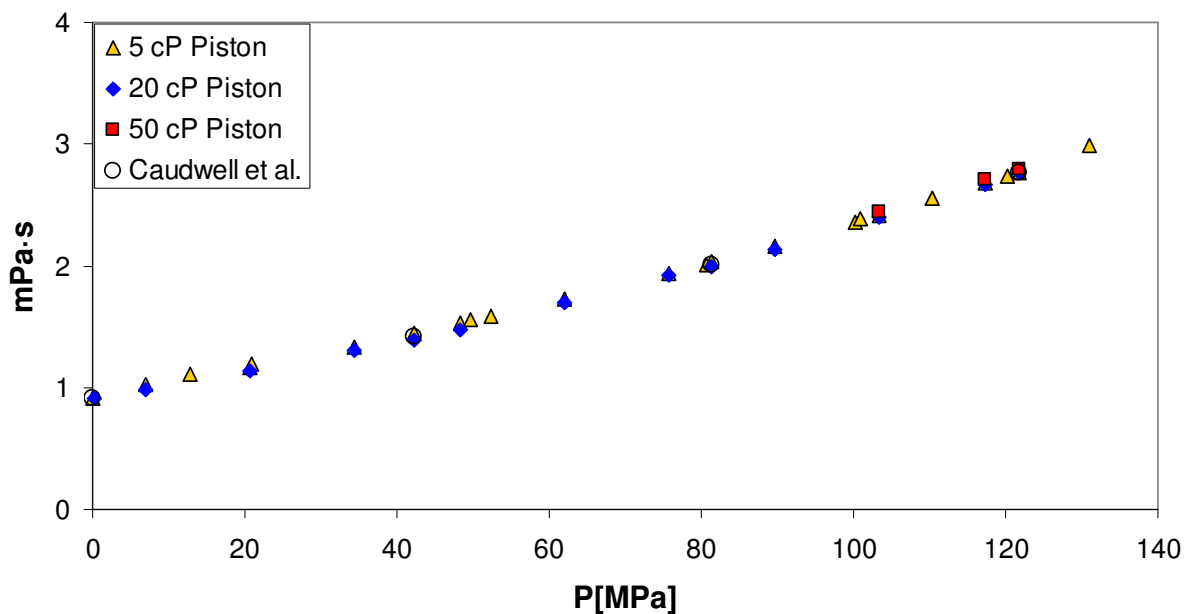


Figure B.33. High-pressure viscosity of dodecane at 323.15 K.

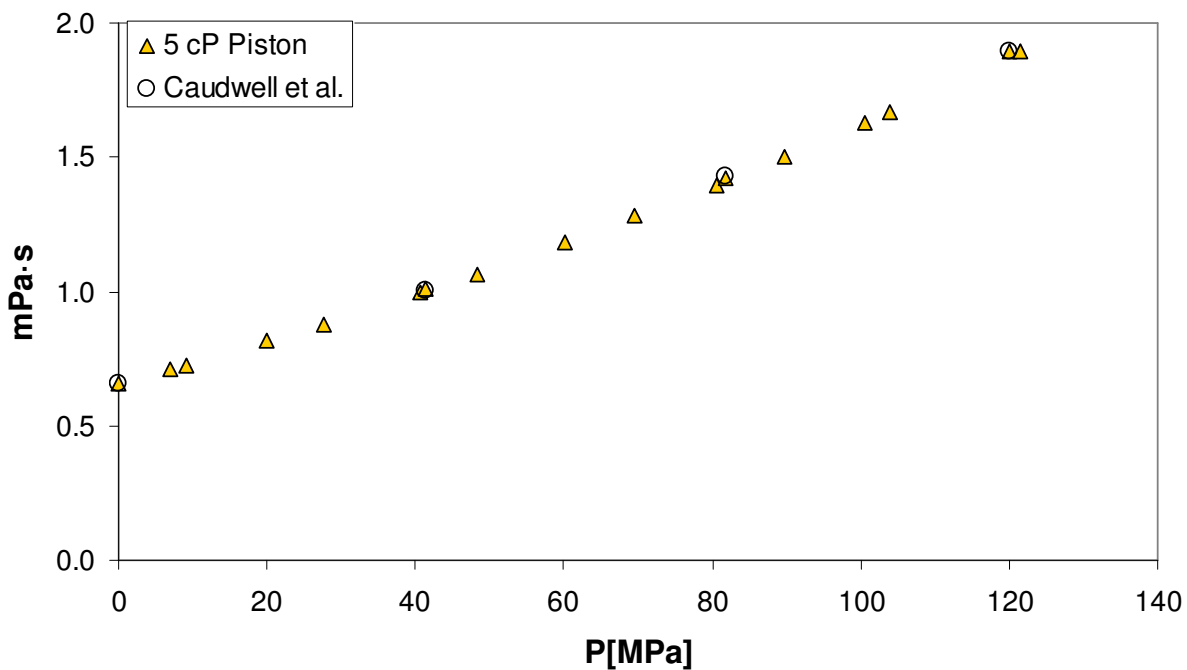


Figure B.34. High-pressure viscosity of dodecane at 348.15 K.

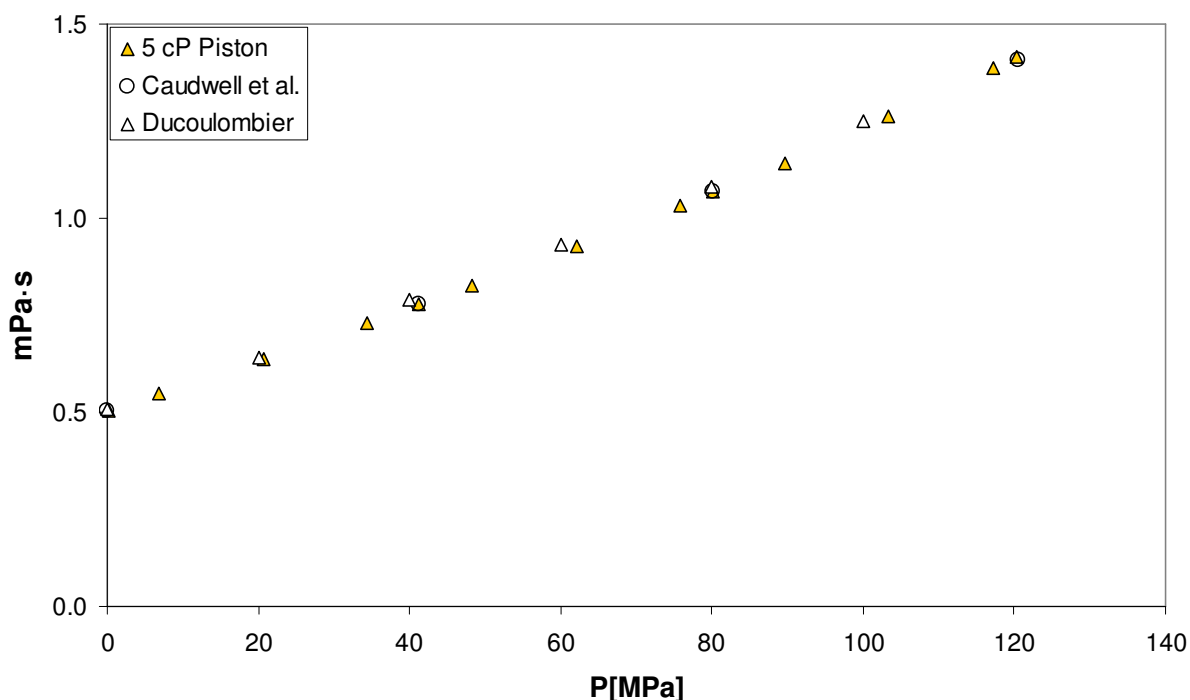


Figure B.35. High-pressure viscosity of dodecane at 373.15 K.

B.4.3.2 Pentadecane Comparison to Literature

All comparisons to pentadecane viscosity literature values are performed with the ambient viscosity linear corrections that used pentadecane and calibration fluid S6 in their determination. Due to pressure freezing, which would occur in the high-pressure tubing outside of the oven, pressure measurements above 80 MPa were not possible. An attempt was made to add temperature-controlled heating rope to exposed areas. The heating rope would operate at temperatures of approximately 10-15 K above ambient. The addition of the external heating supply was able to increase measurements between 10 and 15 MPa.

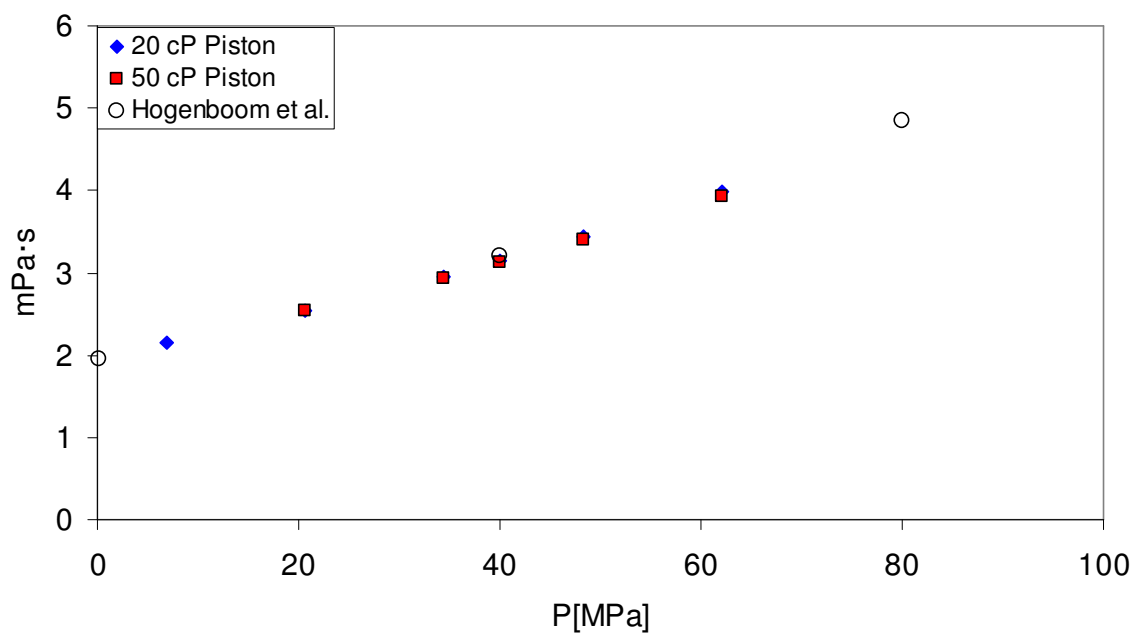


Figure B.36. High-pressure viscosity of pentadecane at 310.95 K.

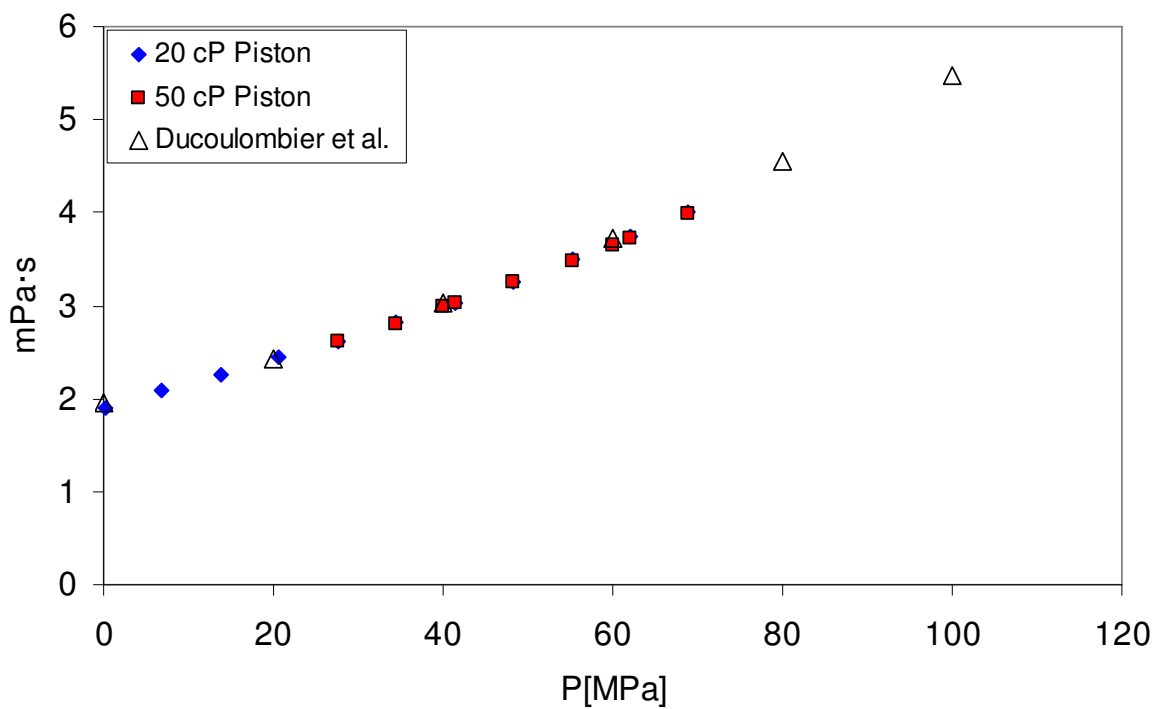


Figure B.37. High-pressure viscosity of pentadecane at 313.15 K.

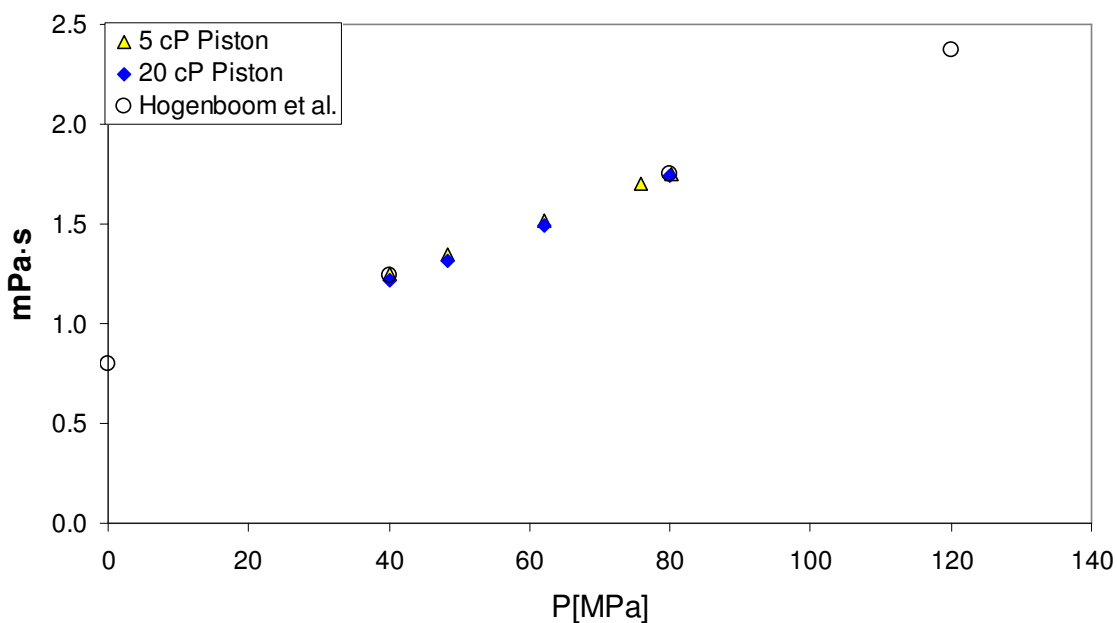


Figure B.38. High-pressure viscosity of pentadecane at 372.05 K.

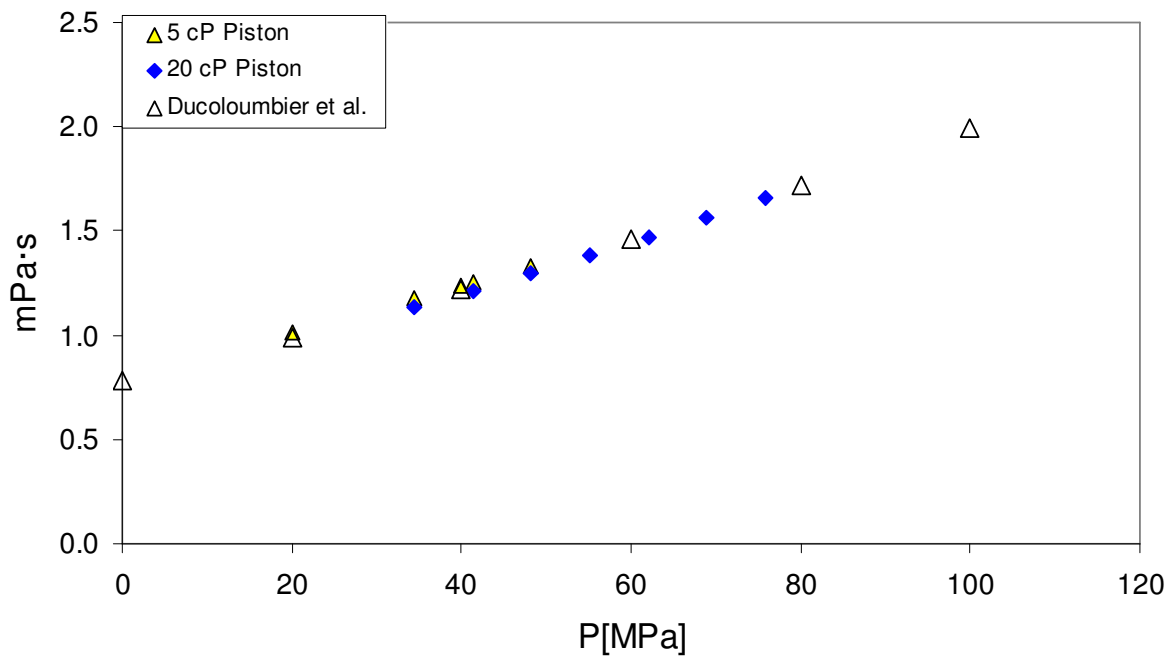


Figure B.39. High-pressure viscosity of pentadecane at 373.15 K.

B.5 Overlapping Pistons

For the majority of work, each isotherm was studied using a single piston. Fuel temperatures of 283.15 and 298.15 K were measured using the 50 cP piston, fuel temperatures of 313.15 and 343.15 K were measured using the 20 cP piston, and for fuels at 373.15 K the 5 cP piston was used. Approximately 5% of the data sets recorded used an alternate piston. In the entirety of the work, isotherms for which multiple pistons were used include 298.15, 313.15, and 373.15 K. The 20 and 50 cP piston were used for both 298.15 and 313.15K and the 20 cP piston and 5 cP were both used for 373.15 K.

B.5.1 298.15 K Overlap

Figure B.40 shows that isotherms at 298.15 K are within the mutual uncertainty of the 20 and 50 cP pistons used as indicated in Figure B.41. The 20 cP piston has a viscosity that is approximately one percent larger than the 50 cP piston throughout the pressure range. The AARD is 1.14% with a maximum deviation of 2.06 at 131 MPa.

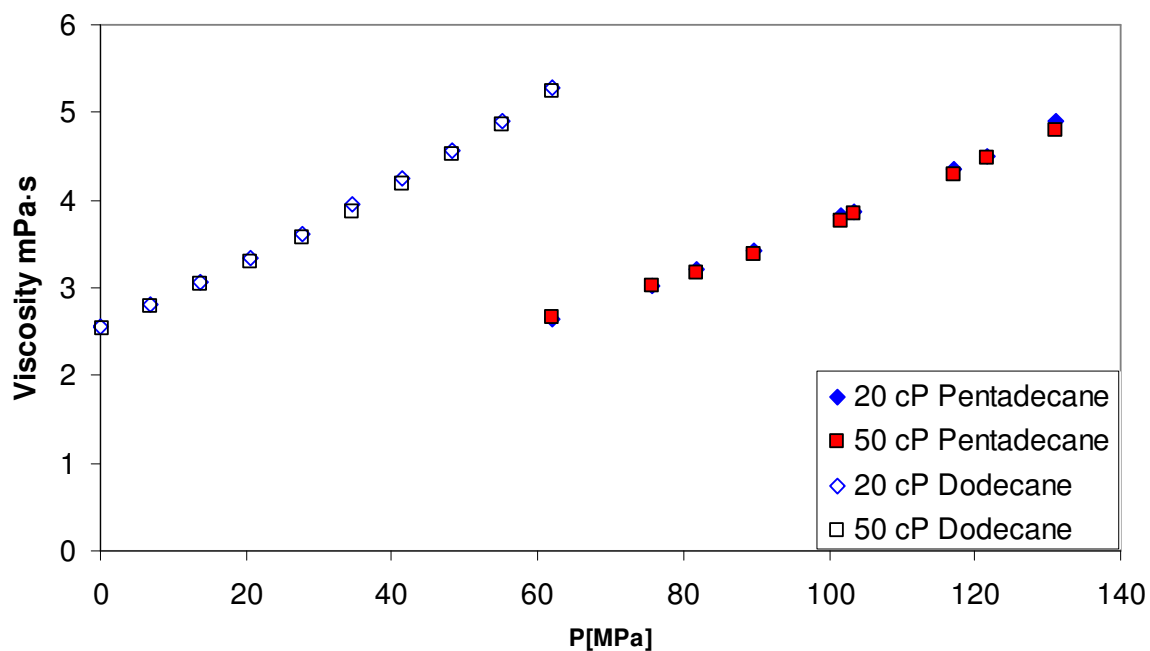


Figure B.40. High-pressure viscosity of dodecane and pentadecane at 298.15 K overlapping measurements using the 20 and 50 cP pistons.

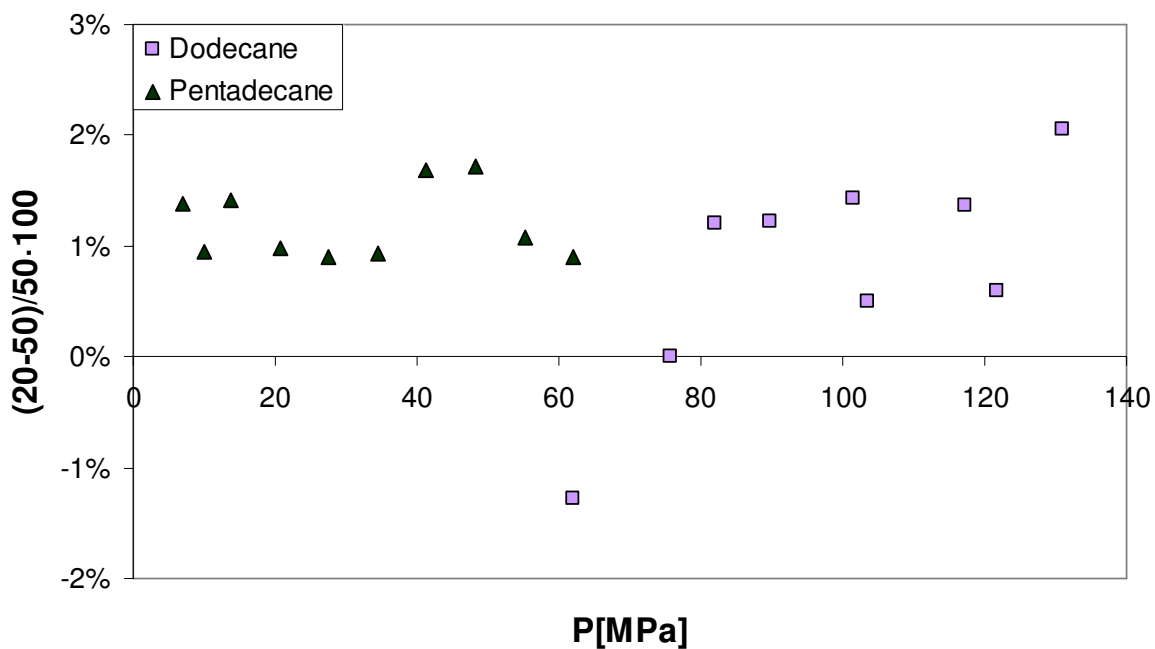


Figure B.41. High-pressure viscosity deviations of dodecane and pentadecane at 298.15 K and overlapping measurements using the 20 and 50 cP pistons.

B.5.2 313.15 K Overlap

Figure B.42 indicates that isotherms at 313.15 K are within the mutual uncertainty of the 20 and 50 cP pistons as shown explicitly in Figure B.43. Like the 298.15 K isotherms, the 20 cP piston has a viscosity that is approximately one percent larger than the 50 cP piston throughout the pressure range. The AARD is 0.78% with a maximum deviation of 2.26% at approximately 90 MPa.

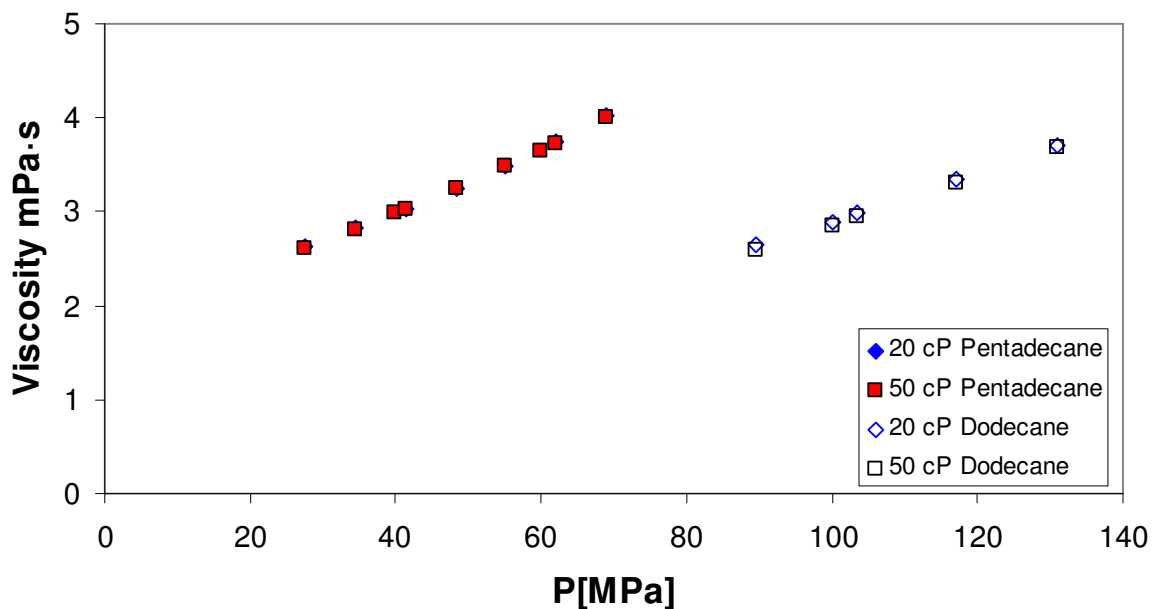


Figure B.42. High-pressure viscosity of dodecane and pentadecane at 313.15 K overlapping measurements using the 20 and 50 cP pistons.

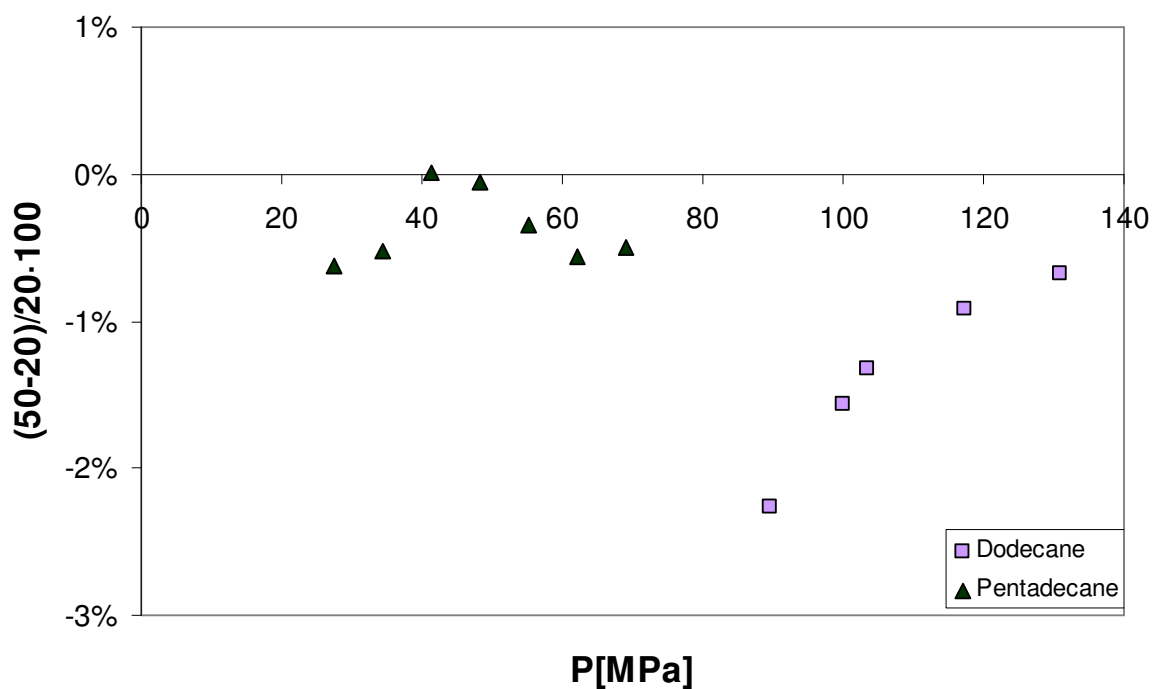


Figure B.43. High-pressure viscosity deviations of dodecane and pentadecane at 313.15 K and overlapping measurements using the 20 and 50 cP pistons.

B.5.3 373.15 K Overlap

The 20 and 5 cP pistons share the 373.15 K isotherm for some data. Overlapping data for comparison is available for pentadecane at approximately 372.05 K and 373.15 K, for jatropha biodiesel blends, and soybean biodiesel. The relative deviations of these overlapping pistons are given in Figure B.44.

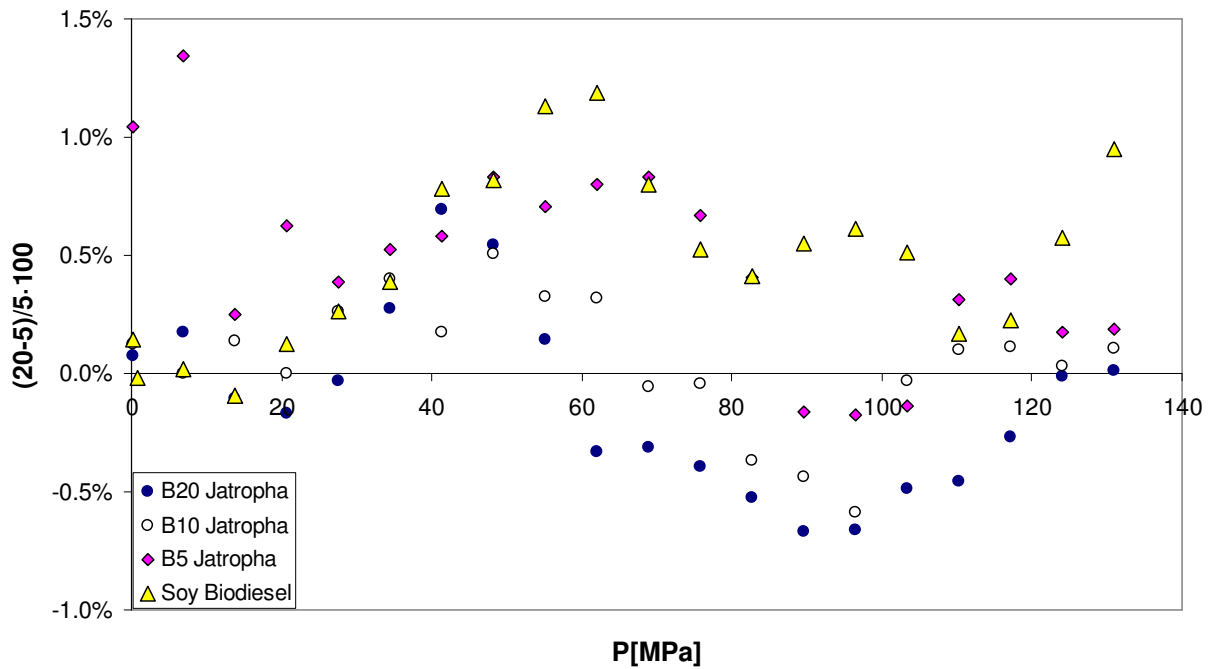


Figure B.44. Deviations for Jatropha biodiesel blends and soybean biodiesel. The jatropha blends are the same fuel sample, while the soybean biodiesel is from different fuels, but the oil producer and biodiesel production methods were used.

As discussed earlier, it was found that a 2 parameter model was the best fit for the 5 cP piston at 348.15 and 373.15 K and high pressure when compared to the dodecane data. Jatropha biodiesel blends B5, B10, and B20 were tested at 343.15 K using both the 20 and 5 cP piston for the purpose of piston overlap evaluation and used to regress a 2 parameter model at 70 C for the 20 cP piston, given in Table B.3. The AARD% for the jatropha blends between the 20 and 5 cP piston was 0.35 %, while the AARD between the two soy bean biodiesels, Chapter 4 and Chapter 5 soy biodiesels, was 0.49%. The soybean biodiesel appears to show a similar trend as the jatropha blend fuels.

While pentadecane isotherm piston overlaps are available, they only show data for a narrow pressure range. The trend at 98.9 and 100 shows the high pressure data to be within 1% of reported literature values at 80 MPa. The two high pressure measurements of 40 and 80 MPa for the 372.05 K data have an AARD of 0.4% for the 5 cP piston while the 20 cP piston has an AARD of 1.1%; the AARD of their overlap is 2.0% due to how they straddle the literature data. The maximum difference at 373.15 K is approximately 3.5% at the lowest pressure tested decreasing to 1.5% at approximately 76 MPa.

References for Appendix B

1. Caudwell, D.; Trusler, J.; Vesovic, V.; Wakeham, W., The viscosity and density of n-dodecane and n-octadecane at pressures up to 200 MPa and temperatures up to 473 K. *International Journal of Thermophysics* 2004, 25, (5), 1339-1352.
2. Huber, M. L.; Laesecke, A.; Perkins, R., Transport properties of n-dodecane. *Energy & Fuels* 2004, 18, (4), 968-975.
3. Dymond, J.; Robertson, J.; Isdale, J., Transport properties of nonelectrolyte liquid mixtures—III. Viscosity coefficients for n-octane, n-dodecane, and equimolar mixtures of n-octane+ n-dodecane and n-hexane+ n-dodecane from 25 to 100° C at pressures up to the freezing pressure or 500 MPa. *International Journal of Thermophysics* 1981, 2, (2), 133-154.
4. Tanaka, Y.; Hosokawa, H.; Kubota, H.; Makita, T., Viscosity and density of binary mixtures of cyclohexane with n-octane, n-dodecane, and n-hexadecane under high pressures. *International Journal of Thermophysics* 1991, 12, (2), 245-264.
5. Cui, S.; McCabe, C.; Cummings, P.; Cochran, H., Molecular dynamics study of the nano-rheology of n-dodecane confined between planar surfaces. *The Journal of Chemical Physics* 2003, 118, (19), 8941-8944.
6. Tonck, A.; Georges, J.; Loubet, J., Measurements of intermolecular forces and the rheology of dodecane between alumina surfaces. *Journal of colloid and interface science* 1988, 126, (1), 150-163.
7. Ducoulombier, D.; Zhou, H.; Boned, C.; Peyrelasse, J.; Saint-Guirons, H.; Xans, P., Pressure (1-1000 bars) and temperature (20-100. degree. C) dependence of the viscosity of liquid hydrocarbons. *The Journal of Physical Chemistry* 1986, 90, (8), 1692-1700.

8. Hogenboom, D. L.; Webb, W.; Dixon, J. A., Viscosity of several liquid hydrocarbons as a function of temperature, pressure, and free volume. *The Journal of Chemical Physics* 1967, 46, (7), 2586-2598.

Appendix C

Corrected High-Pressure Data for Biodiesel, Diesel and Biodiesel-Diesel Blends

Below are the high-pressure viscosities of biodiesel, diesel, and biodiesel-diesel blends after the corrections developed in Appendix B have been applied. A superscript 'b' denotes the final pressure prior to a potential freezing point pressure, and a subscript 'c' denotes that while the data point has been included, the standard deviation of the sample is larger than the typical 0.3% standard used in this work. Table C.0 below gives the page number for each fuel's corrected data table included in this appendix. Tables C.24 and C.25 contain data for beef tallow biodiesel blends with diesel 4 (C.20), and due to some irregularities during testing need to be verified.

Table C.0 Table of Contents for Appendix C								
Table	Sample	Page #	Table	Sample	Page #	Table	Sample	Page #
C.1	Canola	323	C.10	Soy B10	332	C.19	Jatropha B20	341
C.2	Used Car	324	C.11	Soy B20	333	C.20	Diesel4	342
C.3	Coconut	325	C.12	Soy B40	334	C.21	Palm B5	343
C.4	Soy1	326	C.13	Soy B60	335	C.22	Palm B10	344
C.5	Vistive	327	C.14	Soy B80	336	C.23	Palm B20	345
C.6	Diesel1	328	C.15	Jatropha	337	C.24	Tallow B5	346
C.7	Soy2	329	C.16	Diesel3	338	C.25	Tallow B20	347
C.8	Diesel2	330	C.17	Jatropha	339	C.26	Soy-Coconut	348
C.9	Soy B5	331	C.18	Jatropha	340			

Table C.1 High-Pressure Viscosity of Canola Biodiesel				
P	η [mPa·s]			
[MPa]	283.15 K	298.15 K	313.15 K	373.15 K
0.0	8.60	5.59	3.88	1.45
0.7	8.64	5.63	3.92	1.47
6.9	9.39	6.07	4.22	1.56
13.8	10.25	6.60	4.56	1.67
20.7	11.13	7.14	4.92	1.79
27.6	12.09	7.70	5.29	1.91
34.5	13.05	8.30	5.68	2.03
41.4	14.13	8.91	6.09	2.16
48.3	15.23	9.55	6.50	2.29
55.2	16.41	10.24	6.92	2.44
62.1	17.68	10.94	7.37	2.59
68.9	19.03	11.65	7.84	2.74
75.8	20.35	12.44	8.34	2.90
82.7	22.23 ^b	13.23	8.86	3.05
89.6		14.10	9.39	3.23
96.5		15.00	9.97	3.40
103.4		15.99	10.58	3.58
110.3		16.99	11.21	3.76
117.2		18.06	11.86	3.95
124.1		19.19	12.51	4.16
131.0		20.34	13.21	4.35

Table C.2 High-Pressure Viscosity of Used Canola Biodiesel				
P	η [mPa·s]			
[MPa]	283.15 K	298.15 K	313.15 K	373.15 K
0.0	8.64	5.55	3.90	1.46
0.7	8.73	5.60	3.94	1.47
6.9	9.47	6.03	4.24	1.57
13.8	10.26	6.54	4.58	1.68
20.7	11.10	7.08	4.95	1.80
27.6	12.03	7.63	5.31	1.92
34.5	13.02	8.21	5.68	2.05
41.4	14.05	8.84	6.09	2.17
48.3	15.20	9.50	6.51	2.30
55.2	16.37	10.16	6.96	2.45
62.1	17.59	10.89	7.43	2.59
68.9	18.90	11.64	7.91	2.74
75.8	20.28	12.45	8.41	2.90
82.7	21.93 ^b	13.24	8.93	3.06
89.6		14.08	9.49	3.23
96.5		14.96	10.06	3.41
103.4		15.90	10.65	3.58
110.3		16.90	11.29	3.77
117.2		17.93	11.93	3.97
124.1		18.98	12.59	4.18
131.0		20.18	13.30	4.39

Table C.3 High-Pressure Viscosity of Coconut Biodiesel				
P	η [mPa·s]			
[MPa]	283.15 K	298.15 K	313.15 K	373.15 K
0.0	4.87	3.27	2.18	0.89
0.7	4.91	3.29	2.24	0.94
6.9	5.29	3.54	2.40	1.01
13.8	5.73	3.85	2.59	1.09
20.7	6.21	4.14	2.78	1.16
27.6	6.70	4.46	2.97	1.23
34.5	7.22	4.79	3.19	1.31
41.4	7.77	5.11	3.40	1.39
48.3	8.34	5.46	3.62	1.47
55.2	8.94	5.84	3.86	1.56
62.1	9.56	6.21	4.11	1.65
68.9	10.20	6.60	4.37	1.74
75.8	10.88	7.03	4.65	1.84
82.7	11.58	7.47	4.94	1.93
89.6	12.35	7.91	5.23	2.03
96.5	13.13b	8.37	5.56	2.13
103.4		8.88	5.87	2.23
110.3		9.40	6.19	2.33
117.2		9.95	6.54	2.44
124.1		10.52	6.91	2.55
131.0		11.12	7.29	2.68

Table C.4 High-Pressure Viscosity of Soy Biodiesel (Soy 1)				
P	η [mPa·s]			
[MPa]	283.15 K	298.15 K	313.15 K	373.15 K
0.0	7.44	5.03	3.52	1.40
0.7	7.56	5.07	3.56	1.41
6.9	8.16	5.47	3.81	1.50
13.8	8.87	5.91	4.11	1.61
20.7	9.62	6.38	4.41	1.72
27.6	10.41	6.87	4.72	1.83
34.5	11.24	7.39	5.03	1.95
41.4	12.12	7.90	5.38	2.07
48.3	13.02	8.47	5.74	2.19
55.2	14.00	9.07	6.13	2.33
62.1	15.02	9.69	6.55	2.46
68.9	16.16 ^b	10.33	6.96	2.59
75.8		10.99	7.39	2.73
82.7		11.72	7.86	2.88
89.6		12.45	8.34	3.03
96.5		13.21	8.88	3.19
103.4		14.10	9.45	3.36
110.3		14.95	10.04	3.52
117.2		15.83	10.65	3.69
124.1		16.79	11.34	3.88
131.0		17.74	12.08	4.08

Table C.5 High-Pressure Viscosity of Vistive Biodiesel				
P	η [mPa·s]			
[MPa]	283.15 K	298.15 K	313.15 K	373.15 K
0.0	7.76	5.07	3.59	1.39
0.7	7.83	5.13	3.64	1.40
6.9	8.45	5.53	3.91	1.49
13.8	9.19	6.00	4.22	1.60
20.7	9.98	6.47	4.53	1.71
27.6	10.79	6.98	4.86	1.83
34.5	11.65	7.50	5.20	1.95
41.4	12.58	8.04	5.55	2.07
48.3	13.53	8.62	5.92	2.20
55.2	14.53	9.23	6.30	2.32
62.1	15.56	9.86	6.72	2.46
68.9	16.67	10.53	7.18	2.60
72.4	17.24b			
75.8		11.22	7.65	2.74
82.7		11.95	8.12	2.90
89.6		12.70	8.61	3.05
96.5		13.51	9.17	3.21
103.4		14.34	9.79	3.36
110.3		15.22	10.45	3.55
117.2		16.13	11.11	3.73
124.1		17.08	11.77	3.92
131.0		18.08	12.47	4.12

Table C.6 High-Pressure Viscosity of Diesel (Diesel 1)				
P	η [mPa·s]			
[MPa]	283.15 K	298.15 K	313.15 K	373.15 K
0.0	4.42	2.84	2.05	0.86
0.7	4.50	2.87	2.08	0.87
6.9	4.95	3.12	2.26	0.93
13.8	5.48	3.42	2.47	1.01
20.7	6.06	3.76	2.69	1.09
27.6	6.72	4.11	2.94	1.17
34.5	7.42	4.49	3.19	1.26
41.4	8.20	4.91	3.46	1.35
48.3	9.05	5.35	3.76	1.45
55.2	9.98	5.82	4.08	1.55
62.1	11.00	6.32	4.42	1.65
68.9	12.04	6.88	4.79	1.75
75.8	13.19	7.50	5.18	1.86
82.7	14.50	8.15	5.60	1.97
89.6	15.88	8.90	6.05	2.10
96.5	17.40	9.71	6.51	2.22
103.4	18.98	10.59	7.02	2.35
110.3	20.75	11.55	7.56	2.48
117.2	22.87	12.60	8.12	2.61
124.1	25.25	13.74	8.74	2.76
131.0	27.75	14.95	9.45	2.92

Table C.7 High-Pressure Viscosity of Soy Biodiesel (Soy 2)

P	η [mPa·s]				
	[MPa]	283.15 K	298.15 K	313.15 K	343.15 K
0.1	7.69	5.01	3.51	2.07	1.40
0.7	7.74	5.04	3.52	2.08	1.41
6.9	8.38	5.43	3.77	2.22	1.50
13.8	9.08	5.89	4.05	2.38	1.61
20.7	9.82	6.33	4.34	2.54	1.72
27.6	10.60	6.80	4.66	2.71	1.82
34.5	11.44	7.31	4.98	2.89	1.94
41.4	12.32	7.83	5.32	3.07	2.05
48.3	13.23	8.40	5.68	3.26	2.18
55.2	14.23	8.96	6.06	3.47	2.30
62.1	15.24	9.57	6.43	3.67	2.43
68.9	16.34b	10.24	6.85	3.90	2.57
75.8		10.91	7.29	4.13	2.71
82.7		11.63	7.73	4.37	2.86
89.6		12.37	8.21	4.62	3.02
96.5		13.14	8.75	4.87	3.17
103.4		13.96	9.29	5.15	3.34
110.3		14.82	9.88	5.43	3.51
117.2		15.72	10.51	5.72	3.68
124.1		16.62	11.16	6.03	3.86
131.0		17.58	11.81	6.34	4.04

Table C.8 High-Pressure Viscosity of ULSD (diesel 2)					
P	η [mPa·s]				
[MPa]	283.15 K	298.15 K	313.15 K	343.15 K	373.15 K
0.1	4.05	2.75	1.99	1.21	0.83
0.7	4.09	2.77	2.01	1.22	0.84
6.9	4.49	3.02	2.17	1.31	0.91
13.8	4.97	3.32	2.38	1.42	0.98
20.7	5.50	3.64	2.60	1.53	1.06
27.6	6.07	3.99	2.83	1.65	1.13
34.5	6.68	4.37	3.07	1.78	1.21
41.4	7.36	4.75	3.33	1.91	1.30
48.3	8.09	5.17	3.60	2.06	1.39
55.2	8.89	5.60	3.91	2.21	1.48
62.1	9.74	6.09	4.16	2.37	1.58
68.9	10.69	6.61	4.57	2.54	1.68
75.8	11.67	7.19	4.93	2.73	1.78
82.7	12.75	7.80	5.32	2.91	1.89
89.6	13.95	8.46	5.73	3.11	2.00
96.5	15.20	9.12	6.16	3.33	2.12
103.4	16.59	9.88	6.63	3.56	2.23
110.3	18.08	10.67	7.13	3.80	2.36
117.2	19.72	11.55	7.67	4.06	2.50
124.1	21.56	12.49	8.25	4.33	2.64
131.0	23.71	13.47	8.88	4.62	2.78

Table C.9 High-Pressure Viscosity of Soy B5					
P	η [mPa·s]				
[MPa]	283.15 K	298.15 K	313.15 K	343.15 K	373.15 K
0.1	4.29	2.87	2.03	1.23	0.88
0.7	4.34	2.89	2.05	1.23	0.89
6.9	4.75	3.15	2.22	1.33	0.95
13.8	5.26	3.46	2.41	1.44	1.03
20.7	5.82	3.78	2.63	1.56	1.11
27.6	6.41	4.13	2.87	1.68	1.19
34.5	7.08	4.51	3.12	1.81	1.28
41.4	7.78	4.92	3.39	1.96	1.36
48.3	8.56	5.36	3.66	2.10	1.45
55.2	9.35	5.84	3.96	2.25	1.55
62.1	10.24	6.34	4.28	2.42	1.64
68.9	11.21	6.89	4.63	2.59	1.74
75.8	12.30	7.46	5.00	2.77	1.85
82.7	13.42	8.04	5.39	2.96	1.96
89.6	14.67	8.73	5.78	3.17	2.08
96.5	15.96	9.46	6.23	3.39	2.19
103.4	17.44	10.21	6.70	3.62	2.32
110.3	19.01	11.05	7.20	3.87	2.45
117.2	20.68	11.93	7.73	4.11	2.58
124.1	22.74	12.83	8.30	4.39	2.72
131.0	24.97	13.90	8.93	4.68	2.87

Table C.10 High-Pressure Viscosity of Soy B10					
P	η [mPa·s]				
[MPa]	283.15 K	298.15 K	313.15 K	343.15 K	373.15 K
0.1	4.46	2.94	2.12	1.29	0.89
0.7	4.50	2.97	2.13	1.30	0.90
6.9	4.93	3.24	2.30	1.40	0.96
13.8	5.46	3.56	2.50	1.51	1.04
20.7	6.03	3.89	2.72	1.64	1.12
27.6	6.64	4.24	2.96	1.76	1.20
34.5	7.30	4.63	3.21	1.90	1.29
41.4	8.02	5.04	3.47	2.05	1.38
48.3	8.78	5.48	3.76	2.20	1.47
55.2	9.58	5.96	4.07	2.35	1.57
62.1	10.50	6.45	4.40	2.52	1.69
68.9	11.51	6.98	4.74	2.70	1.78
75.8	12.54	7.57	5.11	2.89	1.89
82.7	13.64	8.16	5.50	3.09	2.00
89.6	14.85	8.81	5.92	3.29	2.11
96.5	16.23	9.52	6.36	3.52	2.23
103.4	17.68	10.27	6.84	3.76	2.36
110.3	19.20	11.11	7.34	4.00	2.48
117.2	20.95	11.99	7.87	4.27	2.63
124.1	23.06	12.94	8.45	4.55	2.74
131.0	25.32	13.95	9.13	4.84	2.88

Table C.11 High-Pressure Viscosity of Soy B20					
P	η [mPa·s]				
[MPa]	283.15 K	298.15 K	313.15 K	343.15 K	373.15 K
0.1	4.60	3.10	2.23	1.33	0.91
0.7	4.64	3.12	2.24	1.34	0.93
6.9	5.09	3.39	2.41	1.44	1.00
13.8	5.60	3.72	2.62	1.56	1.08
20.7	6.17	4.06	2.85	1.69	1.16
27.6	6.77	4.43	3.09	1.81	1.25
34.5	7.44	4.82	3.34	1.95	1.34
41.4	8.14	5.24	3.62	2.10	1.43
48.3	8.91	5.67	3.91	2.25	1.52
55.2	9.72	6.15	4.21	2.41	1.63
62.1	10.57	6.64	4.55	2.58	1.72
68.9	11.52	7.19	4.90	2.76	1.83
75.8	12.53	7.75	5.25	2.95	1.94
82.7	13.58	8.36	5.64	3.15	2.05
89.6	14.74	9.00	6.05	3.35	2.17
96.5	16.00	9.71	6.50	3.57	2.29
103.4	17.35	10.47	6.98	3.81	2.42
110.3	18.84	11.27	7.48	4.06	2.55
117.2	20.44	12.12	8.01	4.33	2.68
124.1	22.34	13.05	8.55	4.61	2.82
131.0	24.46	14.07	9.19	4.90	2.97

Table C.12 High-Pressure Viscosity of Soy B40					
P	η [mPa·s]				
[MPa]	283.15 K	298.15 K	313.15 K	343.15 K	373.15 K
0.1	5.33	3.51	2.46	1.49	1.03
0.7	5.35	3.54	2.48	1.50	1.04
6.9	5.85	3.83	2.68	1.61	1.11
13.8	6.41	4.17	2.91	1.73	1.20
20.7	7.04	4.54	3.14	1.86	1.29
27.6	7.71	4.94	3.40	2.01	1.38
34.5	8.41	5.35	3.68	2.16	1.48
41.4	9.17	5.80	3.97	2.30	1.57
48.3	9.97	6.26	4.27	2.47	1.67
55.2	10.84	6.75	4.60	2.64	1.78
62.1	11.78	7.27	4.94	2.82	1.88
68.9	12.77	7.83	5.30	3.01	2.00
75.8	13.85	8.44	5.66	3.21	2.11
82.7	15.00	9.03	6.07	3.43	2.23
89.6	16.22	9.70	6.49	3.64	2.35
96.5	17.54	10.41	6.95	3.87	2.48
103.4	18.96	11.20	7.42	4.11	2.61
110.3	20.42	12.00	7.92	4.37	2.75
117.2	22.17	12.88	8.45	4.64	2.90
124.1	24.06	13.81	9.05	4.92	3.05
131.0	27.86 ^b	14.80	9.73	5.22	3.22

Table C.13 High-Pressure Viscosity of Soy B60					
P	η [mPa·s]				
[MPa]	283.15 K	298.15 K	313.15 K	343.15 K	373.15 K
0.1	6.13	3.98	2.85	1.69	1.12
0.7	6.19	4.01	2.87	1.70	1.13
6.9	6.69	4.33	3.08	1.82	1.21
13.8	7.36	4.72	3.33	1.96	1.30
20.7	8.03	5.12	3.59	2.11	1.40
27.6	8.76	5.55	3.87	2.26	1.50
34.5	9.53	6.00	4.18	2.42	1.60
41.4	10.33	6.48	4.50	2.58	1.71
48.3	11.20	6.99	4.82	2.76	1.81
55.2	12.11	7.52	5.17	2.94	1.92
62.1	13.09	8.09	5.53	3.13	2.04
68.9	14.13	8.69	5.92	3.33	2.15
75.8	15.24	9.31	6.33	3.54	2.27
82.7	16.38	9.99	6.75	3.76	2.40
89.6	17.64	10.71	7.20	4.00	2.53
96.5	18.94	11.43	7.67	4.24	2.65
103.4	20.35	12.20	8.18	4.50	2.79
110.3	22.07	13.00	8.69	4.76	2.95
113.8	27.73				
117.2	29.61 ^b	13.88	9.30	5.05	3.11
124.1		14.81	9.95	5.35	3.28
131.0		15.76	10.64	5.66	3.44

Table C.14 High-Pressure Viscosity of Soy B80					
P	η [mPa·s]				
[MPa]	283.15 K	298.15 K	313.15 K	343.15 K	373.15 K
0.1	6.83	4.49	3.21	1.89	1.27
0.7	6.89	4.50	3.23	1.90	1.28
6.9	7.40	4.85	3.46	2.03	1.36
13.8	8.06	5.25	3.72	2.18	1.46
20.7	8.77	5.70	4.01	2.33	1.56
27.6	9.53	6.16	4.31	2.49	1.66
34.5	10.33	6.64	4.63	2.67	1.77
41.4	11.17	7.15	4.96	2.84	1.88
48.3	12.06	7.69	5.30	3.03	2.00
55.2	13.01	8.24	5.66	3.23	2.11
62.1	14.01	8.85	6.04	3.43	2.24
68.9	15.05	9.47	6.45	3.64	2.36
75.8	16.21	10.13	6.87	3.87	2.49
82.7	17.40	10.78	7.32	4.10	2.62
89.6	18.64	11.53	7.76	4.34	2.77
96.5	28.87 ^b	12.26	8.23	4.60	2.92
103.4		13.03	8.78	4.85	3.08
110.3		13.87	9.38	5.14	3.24
117.2		14.76	10.00	5.43	3.41
124.1		15.68	10.67	5.73	3.58
131.0		16.54	11.39	6.05	3.76

Table C.15 High-Pressure Viscosity of Jatropha Biodiesel

P	η [mPa·s]				
	[MPa]	283.15 K	298.15 K	313.15 K	343.15 K
0.1	8.54	5.42	3.74	2.08	1.38
6.9	9.30	5.89	4.03	2.32	1.50
13.8	10.14	6.39	4.35	2.50	1.61
20.7	11.00	6.92	4.68	2.67	1.72
27.6	11.91	7.47	5.03	2.85	1.84
34.5	12.92 ^b	8.06	5.39	3.05	1.95
41.4		8.67	5.77	3.24	2.07
48.3		9.30	6.18	3.46	2.20
55.2		9.97	6.60	3.68	2.32
62.1		10.69	7.05	3.91	2.45
68.9		11.43	7.50	4.16	2.61
75.8		12.20	7.97	4.41	2.77
82.7		13.02	8.59	4.68	2.93
89.6		13.89	9.19	4.94	3.09
96.5		14.78	9.87	5.23	3.26
103.4		15.76	10.50	5.53	3.43
110.3		16.71	11.12	5.85	3.62
117.2		17.75	11.87	6.17	3.81
124.1		18.81	12.61	6.53	4.03
131.0		19.94	13.39	6.89	4.22

Table C.16 High-Pressure Viscosity of ULSD (diesel 3)

P	η [mPa·s]				
	[MPa]	283.15 K	298.15 K	313.15 K	343.15 K
0.1	4.40	2.93	2.11	1.25	0.86
6.9	4.91	3.21	2.30	1.36	0.94
13.8	5.46	3.53	2.52	1.47	1.02
20.7	6.05	3.89	2.75	1.59	1.10
27.6	6.70	4.28	3.00	1.72	1.19
34.5	7.38	4.65	3.26	1.85	1.28
41.4	8.13	5.09	3.54	2.00	1.37
48.3	8.94	5.54	3.86	2.15	1.46
55.2	9.83	6.03	4.18	2.32	1.56
62.1	10.79	6.59	4.52	2.49	1.66
68.9	11.84	7.15	4.89	2.67	1.77
75.8	12.97	7.74	5.28	2.86	1.88
82.7	14.23	8.38	5.71	3.08	2.00
89.6	15.55	9.14	6.16	3.30	2.12
96.5	17.00	9.91	6.64	3.53	2.25
103.4	18.64	10.75	7.18	3.78	2.38
110.3	20.30	11.63	7.75	4.05	2.52
117.2	22.40	12.57	8.34	4.34	2.66
124.1	24.72	13.57	8.97	4.64	2.81
131.0	30.46	14.69	9.71	4.95	2.97

Table C.17 High-Pressure Viscosity of Jatropha B5					
P	η [mPa·s]				
[MPa]	283.15 K	298.15 K	313.15 K	343.15 K	373.15 K
0.1	4.55	3.00	2.16	1.29	0.88
6.9	5.03	3.29	2.36	1.40	0.96
13.8	5.58	3.62	2.58	1.52	1.04
20.7	6.17	3.97	2.81	1.64	1.12
27.6	6.81	4.35	3.06	1.77	1.20
34.5	7.50	4.75	3.32	1.92	1.30
41.4	8.27	5.18	3.60	2.06	1.39
48.3	9.08	5.64	3.92	2.22	1.48
55.2	9.98	6.14	4.24	2.38	1.58
62.1	10.92	6.68	4.59	2.56	1.68
68.9	12.00	7.26	4.96	2.75	1.78
75.8	13.12	7.88	5.35	2.94	1.89
82.7	14.36	8.53	5.77	3.15	2.01
89.6	15.71	9.22	6.22	3.37	2.14
96.5	17.19	9.98	6.71	3.60	2.26
103.4	18.81	10.80	7.22	3.84	2.39
110.3	20.71	11.74	7.77	4.13	2.52
117.2	22.79	12.68	8.37	4.41	2.66
124.1	26.26	13.70	9.03	4.70	2.82
131.0	30.08	14.81	9.76	5.01	2.98

Table C.18 High-Pressure Viscosity of Jatropha B10

P	η [mPa·s]				
	[MPa]	283.15 K	298.15 K	313.15 K	343.15 K
0.1	4.68	3.05	2.20	1.31	0.91
6.9	5.19	3.34	2.40	1.42	0.98
13.8	5.75	3.66	2.61	1.54	1.06
20.7	6.36	4.02	2.85	1.67	1.14
27.6	7.02	4.41	3.11	1.81	1.23
34.5	7.73	4.82	3.36	1.95	1.32
41.4	8.52	5.25	3.64	2.10	1.41
48.3	9.33	5.73	3.97	2.26	1.51
55.2	10.24	6.23	4.28	2.42	1.61
62.1	11.20	6.78	4.64	2.60	1.71
68.9	12.27	7.35	5.00	2.78	1.82
75.8	13.42	7.95	5.39	2.99	1.93
82.7	14.68	8.59	5.80	3.19	2.05
89.6	16.06	9.29	6.25	3.42	2.17
96.5	17.56	10.04	6.72	3.66	2.29
103.4	19.17	10.86	7.22	3.92	2.43
110.3	20.96	11.72	7.78	4.18	2.57
117.2	23.20	12.69	8.37	4.46	2.71
124.1	28.58	13.73	9.01	4.76	2.86
131.0	33.61	14.76	9.70	5.07	3.02

Table C.19 High-Pressure Viscosity of Jatropha B20

P	η [mPa·s]				
	[MPa]	283.15 K	298.15 K	313.15 K	343.15 K
0.1	4.99	3.29	2.34	1.38	0.94
6.9	5.50	3.62	2.54	1.49	1.02
13.8	6.06	3.97	2.77	1.61	1.10
20.7	6.69	4.35	3.01	1.75	1.18
27.6	7.37	4.75	3.27	1.89	1.27
34.5	8.10	5.19	3.54	2.03	1.37
41.4	8.90	5.62	3.84	2.19	1.46
48.3	9.73	6.12	4.14	2.35	1.56
55.2	10.68	6.64	4.49	2.52	1.66
62.1	11.64	7.20	4.84	2.70	1.77
68.9	12.73	7.82	5.22	2.89	1.88
75.8	13.94	8.46	5.62	3.09	1.99
82.7	15.25	9.15	6.05	3.31	2.11
89.6	16.66	9.87	6.50	3.53	2.23
96.5	18.14	10.68	6.99	3.78	2.36
103.4	19.79	11.50	7.49	4.05	2.50
110.3	21.71	12.40	8.06	4.31	2.64
117.2	23.98	13.38	8.66	4.59	2.78
124.1	34.15	14.49	9.38	4.90	2.94
125.8	35.14 ^b				
131.0		15.51	10.08	5.22	3.11

Table C.20 High-Pressure Viscosity of ULSD (diesel 4)

P	η [mPa·s]						
	[MPa]	278.15 K	283.15 K	293.15 K	298.15 K	313.15 K	343.15 K
0.1	4.96	4.17	3.14	2.81	2.00	1.24	0.88
6.9	5.50	4.62	3.50	3.09	2.19	1.34	0.96
13.8	6.12	5.11	3.82	3.39	2.41	1.46	1.04
20.7	6.85	5.66	4.20	3.72	2.63	1.57	1.11
27.6	7.57	6.26	4.59	4.06	2.86	1.69	1.19
34.5	8.39	6.91	5.03	4.45	3.12	1.82	1.28
41.4	9.33	7.63	5.51	4.83	3.40	1.97	1.37
48.3	10.26	8.42	6.03	5.27	3.68	2.10	1.46
55.2	11.21	9.24	6.56	5.73	3.97	2.26	1.56
62.1	12.32	10.19	7.16	6.24	4.31	2.42	1.66
68.9	13.59	11.18	7.81	6.78	4.67	2.60	1.75
75.8	14.98	12.21	8.58	7.35	5.05	2.78	1.86
82.7	16.47	13.35	9.33	7.96	5.45	2.98	1.96
89.6	18.05	14.55	10.22	8.64	5.86	3.20	2.09
96.5	19.77	15.87	11.22	9.35	6.32	3.42	2.21
103.4	21.79	17.32	12.11	10.11	6.78	3.64	2.33
110.3	25.03	18.91	13.39	10.94	7.30	3.90	2.47
117.2	28.20	20.59	14.21	11.82	7.83	4.16	2.60
124.1	31.65	22.67	15.31	12.75	8.42	4.42	2.75
131.0	35.84	24.96	16.52	13.77	9.07	4.71	2.89

Table C.21 High-Pressure Viscosity of Palm B5					
P	η [mPa·s]				
[MPa]	278.15	283.15	288.15	293.15	298.15
0.1	5.04	4.29	3.72	3.28	2.84
6.9	5.61	4.76	4.12	3.61	3.13
13.8	6.22	5.28	4.55	4.01	3.43
20.7	6.88	5.83	5.01	4.41	3.76
27.6	7.60	6.43	5.54	4.84	4.11
34.5	--	7.07	6.03	5.30	4.48
41.4	9.32	7.75	6.64	5.80	4.90
48.3	10.25	8.50	7.27	6.33	5.34
55.2	11.26	9.28	7.92	6.90	5.81
62.1	12.37	10.17	8.65	7.54	6.33
68.9	13.58	11.17	9.42	8.19	6.83
75.8	14.88	12.21	10.23	8.89	7.42
82.7	16.26	13.36	11.14	9.67	8.01
89.6	17.76	14.62	12.08	10.49	8.68
96.5	19.61	15.96	13.12	11.38	9.40
103.4	21.63	17.38	14.32	12.33	10.17
110.3	26.88	18.94	15.59	13.33	10.98
117.2	32.01	20.67	16.88	14.41	11.85
124.1	--	22.66	18.30	15.57	12.79
131.0	50.58 ^c	24.83	19.80	16.89	13.79

Table C.22 High-Pressure Viscosity of Palm B10					
P	η [mPa·s]				
[MPa]	278.15	283.15	288.15	293.15	298.15
0.1	5.16	4.44	3.87	3.36	2.91
6.9	5.73	4.92	4.29	3.69	3.17
13.8	6.30	5.44	4.75	4.05	3.48
20.7	6.98	6.02	5.23	4.46	3.79
27.6	7.68	6.64	5.75	4.87	4.13
34.5	8.48	7.29	6.32	5.32	4.51
41.4	9.33	8.02	6.90	5.80	4.90
48.3	10.24	8.79	7.67	6.32	5.31
55.2	11.29	9.61	8.26	6.89	5.76
62.1	12.36	10.53	8.97	7.51	6.25
68.9	13.54	11.49	9.76	8.15	6.78
75.8	14.86	12.52	10.62	8.87	7.33
82.7	16.22	13.66	11.58	9.70	7.96
89.6	17.75	14.91	12.57	10.45	8.59
96.5	19.40	16.24	13.67	11.30	9.25
103.4	21.31	17.61	14.84	12.23	10.00
110.3	30.77	19.18	16.12	13.22	10.78
117.2	41.18 ^c	20.79	17.46	14.30	11.64
124.1	55.83 ^c	22.79	18.84	15.48	12.52
131.0	74.17 ^c	24.95	20.30	16.69	13.45

Table C.23 High-Pressure Viscosity of Palm B20					
P	η [mPa·s]				
[MPa]	278.15	283.15	288.15	293.15	298.15
0.1	5.53	4.78	4.10	3.57	3.05
6.9	6.11	5.29	4.58	3.92	3.37
13.8	6.76	5.84	4.98	4.31	3.69
20.7	7.47	6.43	5.48	4.73	4.05
27.6	8.25	7.08	6.01	5.18	4.41
34.5	9.07	7.76	6.53	5.66	4.81
41.4	9.98	8.51	7.13	6.19	5.23
48.3	10.96	9.31	7.77	6.76	5.69
55.2	12.03	10.16	8.47	7.34	6.17
62.1	13.16	11.09	9.22	7.98	6.67
68.9	14.37	12.10	10.04	8.69	7.22
75.8	15.68	13.21	10.93	9.37	7.80
82.7	17.11	14.38	11.90	10.18	8.42
89.6	18.64 ^b	15.67	12.91	10.92	9.08
96.5		17.01	14.02	11.80	9.81
103.4		18.43	15.18	12.74	10.56
110.3		19.98	16.39	13.79	11.36
117.2		21.86	17.72	14.88	12.21
124.1		23.94 ^b	19.22	16.11	13.13
131.0			20.73	17.32	14.10

Table C.24 High-Pressure Viscosity of Beef Tallow B5						
P	η [mPa·s]					
[MPa]	278.15	278.15	283.15	288.15	293.15	298.15
0.1	5.16	5.31	4.32	3.76	3.38	2.91
6.9	5.72	5.90	4.74	4.14	3.72	3.20
13.8	6.35	6.57	5.26	4.56	4.10	3.52
20.7	7.04	7.30	5.82	5.00	4.48	3.84
27.6	7.79	8.03	6.42	5.50	4.90	4.17
34.5	8.62	8.84	7.08	6.03	5.36	4.57
41.4	9.49	9.78	7.80	6.65	5.80	4.97
48.3	10.47	10.77	8.58	7.31	6.26	5.41
55.2	11.52	11.84	9.44	8.01	6.82	5.87
62.1	12.68	13.00	10.29	8.80	7.43	6.40
68.9	13.95	14.29	11.29	9.60	8.09	6.93
75.8	15.31	15.67	12.36	10.43	8.78	7.52
82.7	16.73	17.12	13.46	11.31	9.54	8.12
89.6	18.34	18.74	14.83	12.30	10.33	8.79
96.5	20.02	20.52	16.12	13.36	11.20	9.47
103.4	24.04	24.48	17.49	14.51	12.15	10.22
110.3	30.52	30.38	19.23	15.79	13.12	11.05
117.2	38.38	36.95 ^c	20.88	17.17	14.19	11.91
124.1	48.15 ^c	43.86	22.90	18.61	15.37	12.93
131.0		53.03 ^c	25.26	20.19	16.63	13.96

Table C.25 High-Pressure Viscosity of Beef Tallow B20

P	η [mPa·s]				
	[MPa]	278.15	283.15	288.15	293.15
0.1	6.20	5.34	4.35	3.79	3.24
6.9	6.60	5.63	4.79	4.13	3.53
13.8	7.30	6.34	5.30	4.46	3.86
20.7	8.12	6.94	5.86	4.85	4.22
27.6	8.83	7.57	6.49	5.29	4.64
34.5	9.64	8.25	7.11	5.80	5.05
41.4	10.63	9.07	7.79	6.37	5.51
48.3	11.66	9.97	8.51	6.94	5.96
55.2	12.75	10.90	9.32	7.54	6.45
62.1	13.90	11.91	10.16	8.18	6.97
68.9	16.85	12.92	11.08	8.89	7.55
75.8	22.37	14.08	12.12	9.65	8.18
82.7	32.24 ^c	15.39	13.16	10.47	8.84
89.6	38.68 ^c	16.70	14.40	11.34	9.54
96.5	43.88 ^c	18.13	15.61	12.26	10.29
103.4	51.26 ^c	26.82 ^b	16.90	13.24	11.08
110.3	64.07 ^c		18.26	14.28	11.96
117.2			19.74	15.42	12.89
124.1			21.36	16.64	13.92
131.0			23.28	18.03	14.96

Table C.26 High-Pressure Viscosity of Soybean-Coconut 50:50 by Mass Biodiesel					
P	η [mPa·s]				
[MPa]	283.15 K	298.15 K	313.15 K	343.15 K	373.15 K
0.1	5.93	3.91	2.81	1.67	1.13
6.9	6.46	4.23	3.01	1.79	1.21
20.7	7.61	4.93	3.48	2.05	1.39
34.5	8.86	5.71	3.99	2.34	1.58
48.3	10.26	6.55	4.55	2.64	1.77
62.1	11.82	7.49	5.17	2.98	1.98
68.9	12.65				
75.8	13.51	8.50	5.83	3.34	2.20
82.7	14.41 ^b				
89.6		9.62	6.58	3.74	2.42
103.4		10.85	7.38	4.17	2.67
117.2		12.18	8.26	4.64	2.93
131.0		13.64	9.26	5.15	3.22